Bioprocess development for aliphatic alcohol oxidation and alkyl glycoside purification using biocatalysis

Alice Jeannine Catherine Wahart

A thesis in fulfilment for the degree of Doctor of Philosophy

Under the supervision of Prof Gavin J Miller, Dr Sebastian Cosgrove and Dr Jessica Staniland

June 2024

Keele University

Table of contents

Acknowledgement

I would like to express my sincere gratitude to my supervisory team, Prof Gavin Miller, Dr Sebastian Cosgrove and Dr Jessica Staniland for the opportunity to work for them on such interesting projects. I'm extremely grateful for their expertise, guidance, patience and humour during the roller coaster of this PhD. Due to their expert guidance, I also had the opportunity to work with Prof Rob Field and his team at the Manchester Institute of Biotechnology (MIB). I also wish to thank the Process Innovation Team at Croda (Widnes) for their welcome and the opportunity to work with them: Dr Emma Parks, Dr Rachel Scullion, Dr James Birbeck, Dr Steven Brewer, Jack Vincent and Adam Crennell.

I would like to extend my sincere thanks to the technical staff of Keele University: Dr Drijfhout, JC, Dave, Sian, Neil, Leanne and Aisling. They always heard my many last-minute requests with a smile. Special thanks to Leanne who was always ready to test my dirty samples and for her help with the GC instrument (specifically Rapunzel). Thank you for teaching me how to use the instrument with such care.

I had the chance to meet all the fantastic members of the Miller Group (Laura, Elleni, Sanaz, Aisling, Meenakshi, Tapasi, Peter, Cæcilie, Ren, Jonathan, Sian, Jack, Conor, Hannah, Sean, Thibault, Lauren, Liam and Jacob) and Cosgrove group (Simon and Tom). Every interaction was unparalleled to everything I've known. Your personalities, opinions and backgrounds made me feel like a little piece of the giant jigsaw puzzle of R&D we all belong to. To the newly formed Cosgrove group, your weirdness and professionalism make you a dream team I wished I'd met earlier. I gratefully acknowledge the incredible assistance of Dr Jonathan Dolan and Dr Simon Anderson since they started at Keele. Your guidance and honest corrections were always accepted.

This thesis wouldn't have been created without the inspirations given over the years by all the comrades I have met during my Master and PhD, in France (University of Orléans), in Scotland (University of St Andrews) and in England (University of Keele): Dr Pierre, Dr Mélanie, future-Dr

Eléonore, Dr Justina, future-Dr Louis, Dr Martin, Dr Van, Dr Alan, Juba, Dr Ryan, Dr Nina, Dr Megan, Dr Nikoletta, Dr Rebecca, Dr Yohan, Dr Laura, Andrea, Dr Chrystelle, Vali...

I am incredibly grateful to Maureen and Richard for letting me stay in their B&B for three months. I will always be grateful for their time and interest in books and jigsaw puzzles. My free time wouldn't have been possible without Diane of the Lavender Cattery and her husband who took great care of my talkative cat during every holiday.

I am also grateful to everyone who gave a new definition to the expression "C'est la vie!" and who loves my hobbies: Z first official furry cat living in my heart, future Dr Tom Roberts ("I am not a weirdo, but weirdo love me and refuse to leave!"), Dr Laura Latham (Critical role, and so much more), future Dr Hannah Wootton (jigsaw puzzle supporter and amazing cat mom), Dr Pierre Buisson & Dr Mélanie Cimorelli (the "sugar team" is always ready to play games and to kill zombies), the wise Margaux Bertin (Sims 4 and +10 years of friendship), my friends from Poitiers and my family (food and more). And finally thank you Maman for continuing to love me even when you don't understand me.

Publications by the author

1 A. J. C. Wahart, J. P. Dolan, S. D. Anderson, A. Ní Cheallaigh, J. Staniland, M. A. Lima, M. A. Skidmore, G. J. Miller and S. C. Cosgrove, Harnessing a biocatalyst to bioremediate the purification of alkylglycosides, *ChemBioChem*, 2023, 10.1002/cbic.202300625.

2 J. P. Dolan, S. Ahmadipour, A. J. C. Wahart, A. Ní Cheallaigh, S. Sari, C. Eurtivong M. A. Lima, M. A. Skidmore, K. P. Volcho, J. Reynisson, R. A. Field and G. J. Miller, Virtual screening, identification and *in vitro* validation of small molecule GDP-mannose dehydrogenase inhibitors, *RSC Chem Biol,* 2023, **4**, 865.

3 T. Keenan, N. Hatton, J. Porter, J.-B. Vendeville, D. Wheatley, M. Ghirardello, A. J. C. Wahart, S. Ahmadipour, J. Walton, C. Galan, B. Linclau, G. J. Miller and M. A. Fascione, Reverse thiophosphorylase activity of a glycoside phosphorylase in the synthesis of an unnatural Man-β-1,4-GlcNac library, *Chem Sci,* 2023, **14**, 11638.

4 S. Ahmadipour, A. J. C. Wahart, J. P. Dolan, L. Beswick, C. S. Hawes, R. A. Field and G. J. Miller, Synthesis of C6-modified mannose 1-phosphates and evaluation of derived sugar nucleotides against GDP-mannose dehydrogenase, *Beilstein J. Org. Chem.,* 2022, **18**, 1379.

5 A. J. C. Wahart, J. Staniland, G. J. Miller and S. C. Cosgrove, Oxidase enzymes as sustainable oxidation catalysts, *RSocOpenSci*, 2022, **9**, 211572.

Abstract

The detergents and skin care products are composed of surfactants that decrease interfacial tension between two phases (i.e. oil and water).[1] Before the ecological dangers issued from non-renewable sources surfactants (pollution of aqueous environments and their aqueous lives), biosurfactants conceived from renewable feedstocks are favoured : glycolipids, lipopeptides, fatty acids, sucrose esters, sorbitan esters, alkyl glucamides, methyl glucoside esters, alkyl polyglycosides (APGs).[2] In a world where the market of APG biosurfactants reached US$ 1,024 million in 2019,[3] the concerns to enhance production of APG biosurfactants and chemical reactions in accord to green chemistry principles are evolving daily.[4]

In the interest of furthering sustainable approaches, this work will focused on the bioprocess development of aliphatic chain compounds with oxidases, firstly, for an alternative to distillation of biosurfactant APGs and, secondly, for the formation of unsaturated carbon-carbon double bond in mild conditions via Wittig olefination in aqueous media. To this purpose, a process purification for APGs using oxidases-mediated bio-oxidation followed by sequestration solid-supported was investigated pre- and post-distillation from analytical scale to gram scale. Many challenges were encountered to cover the design of the process and the application to gram scale on manufacture APG biosurfactant. Finally, the work of Bergdahl and coworkers[5] inspired a novel cascade reaction performed in deionised water, which combined enzymatic oxidation and Wittig olefination on functionalised alkyl alcohols. From fourteen alkyl alcohols, ten vinyl ester were successfully afforded using the novel cascade with a stabilised ylide.

Abbreviations

4-AAP	4-aminoantipyrine
6-HDNO	6-hydroxy-D-nicotidine
AAO	Aryl-alcohol oxidase
ABTS	2,2'-azino-bis(3-ethylbenzothiazoline-6-sulfonic acid)
Ac	Acetate
AcCO	Choline oxidase from *Arthrobacter cholorphenolicus*
ACS	American Chemical Society
ADH	Alcohol dehydrogenase
AgCO	Choline oxidase from *Arthrobacter globiformis*
AIM	Auto-induction media
AMG	Alkyl monoglucosides
APG	Alkyl PolyGlycoside
BCA	Bicinchoninic acid assay
BSA	Bovin serum albumine
CAGR	Compound Annual Growth Rate
CaLB	*C. antartica* lipase B
CAR	Carboxylic acid reductase
CFE	Cell free extract
CIR	Cosmetic Ingredient Review
CLEA	Cross-linked enzyme aggregates
CLEC	Cross-linked enzyme crystals
CMC	Critical micellar concentration
CRO-AOx	Copper radical alcohol oxidase
CSTR	Continuously Stirred Tank Reactor
D5	Decamethylcyclopentasiloxane
DCM	Dichloromethane
DMF	*N*,*N*-Dimethylformamide
DMP	Dess–Martin periodinane
DMSO	Dimethyl sulfoxide
DP	Degree of polymerisation
DVB	Divinylbenzene
EC	Enzyme Commission

EDG	Electron donating group
EDTA	Ethylenediaminetetraacetic acid
Et	Ethyl
EWG	Electron-withdrawing group
FAD-AOx	Flavin dependent alcohol oxidase
FALDH	aldehyde dehydrogenase
FAME	Fatty acid methyl ester
FID	Flame Ionization Detector
FTIR	Fourier-transform infrared spectroscopy
GC	Gas chromatography
GCI	Green Chemistry Institute
GDH	Glucose dehydrogenase
Goase	Galactose oxidase
HBL	Hydrophilic Lipophilic Balance
HHDH	Halohydrin dehalogenase
HRMS	High resolution mass spectrometry
HRP	Horseradish peroxidase
HW	Wittig-Horner
HWE	Horner-Wadsworth-Emmons
IPTG	isopropyl-β-D-thiogalactopyranoside
JLR	Jet Loop Reactor
KPi	Potassium phosphate
KRED	Ketoreductase
LCA	Life Cycle Assessment
LCAO	Long chain alcohol oxidases
Lip	Lipase
MOF	Metal organic framework
MSA	Methanesulfonic acid
n.a.	Not available
n.d.	Not detected
NAD(P)	Nicotinamide
NMGAs	*N*-methylglucamides
NMR	Nuclear Magnetic Resonance
NP	Nonylphenol

NPE	Nonylphenol ethoxylate
P&G	Procter & Gamble Company
PEG	Polyethylene glycol
Pet. Ether	Petroleum ether
PFSA	Perfluorosulfonic acid
PR	Pharmaceutical Roundtable
PS	Polystyrene
PS-DVB	Polystyrene-divinylbenzene
R&D	Research&Development
RBR	Rotating bed reactor
RoR	Rate of return
Rt	Retention time
rt	Room temperature
SD	Standard deviation
SDS-PAGE	sodium dodecyl sulfate–polyacrylamide gel electrophoresis
SN	nucleophilic substitution
SPPS	Solid-phase peptide synthesis
TBHBA	2,4,6-tribromo-3-hydroxybenzoic acid
TEMPO	(2,2,6,6-Tetramethylpiperidin-1-yl)oxy
TFSA	Trifluoromethanesulfonic acid
Tris	Tris(hydroxymethyl)aminomethane
UV-Vis	UV–visible spectroscopy
VRA	Viscosity reducing agent
WT	Wild type
α-DOX	α-dioxygenase

Chapter 1 - Industrial backgrounds on alkyl polyglucoside and enzymatic catalysis

1.1 Alkylpolyglycoside (APG) as surfactant

1.1.1 Definitions of surfactant and biosurfactant

1.1.1.1 Definition of Surfactant

Surfactants decrease interfacial tension, which makes them popular ingredients in formulation. To this purpose, surfactants facilitate interactions between two phases (liquid-liquid, liquid-gas, liquid-solid) at the interface by inducing physico-chemical properties such as auto-organisation (Figure 1).[1] They are characterised by an amphiphilic structure with a polar head (cationic, anionic, zwitterionic, neutral) and a lipophilic tail (Figure 1).[6] Surfactants are differentiated into multiple categories such as polarity, number of lipophilic chains (monobicatenary, bicatenary or tricatenary surfactants), and hydrophilic lipophilic balance (HLB). The HLB is a physico-chemical parameter defined by assessing the size of the polar head compared to the number and the length of the hydrocarbon chain(s). The higher the HLB value, the bigger the size of the polar head and the higher the water solubility of the surfactant. Consequently, the stabilisation of mixtures occurs with surfactants such as oil in water (o/w) emulsion, water in oil (w/o) emulsion, poly(ethylene oxide)-based surfactants and metal alkoxides,[7] micelles to dissolve lipophilic raw material in aqueous solution or liposomes for the encapsulation of DNA for instance.[8,9]

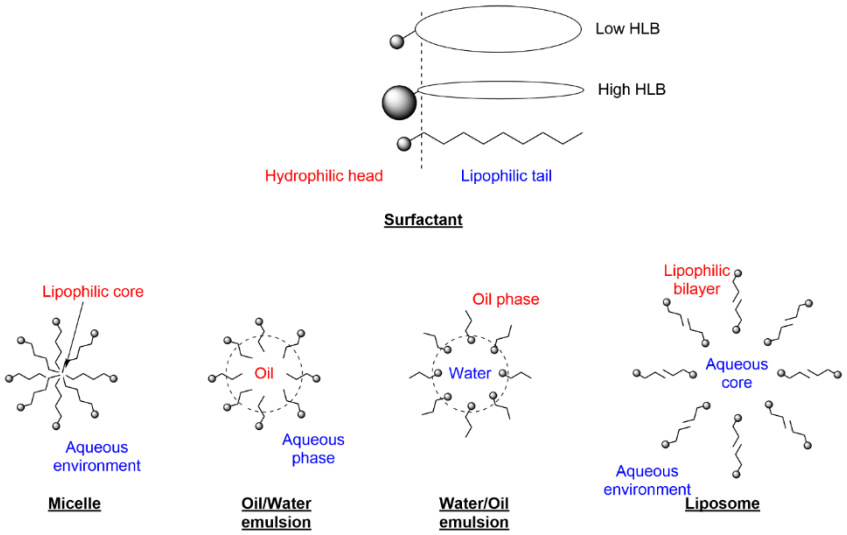

Figure 1 - Scheme of the biosurfactants and auto-organisation of surfactant between two phases[1]

Surfactants are compounds that can be derived from either petroleum-based sources or microbial/plant origins (Figure 2).[2] Synthetic surfactants derived from petroleum-based sources are known to cause severe ecological damage, such as the persistence of chemical foams in rivers and lakes that inhibit photosynthesis,[10] increase the persistence of phosphate in soils, which contribute to the growth of plants (eutrophication)[11] and to harm aquatic species.[12] Therefore, ecological alternatives are crucial to maintain environmental sustainability. The interest in surfactants from microbial/plant origins has been growing to develop biosurfactants, which offer high biodegradability and lower toxicity than synthetic surfactants. For this reason, biosurfactants are also known as “green surfactants”.

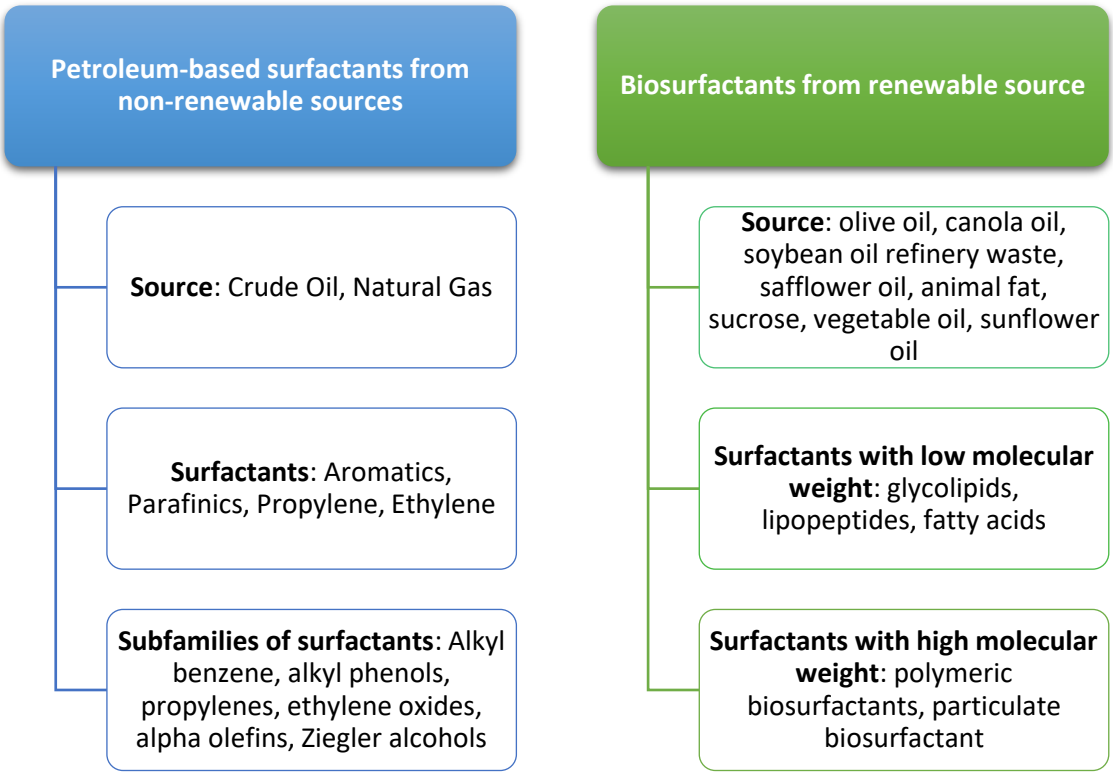

Figure 2 – Classification of common surfactants.[2]

1.1.1.2 Definition of Bio-based Surfactant

Bio-based surfactants are a subclass made from biological feedstock (vegetable origin), such as sorbitan ester, sucrose esters, and APG.[2] These surfactants have several advantages over petroleum-based surfactants, including biodegradability and biocompatibility.[2,13] The production of bio-surfactants can be done using chemical, enzymatic or cell factory methods. A review compared the advantages of green surfactants to petroleum surfactants, categorising them by nature, solubility, feedstock, applications, limitation, production methods, and market.[2] The review has also presented the industrial challenges of bio-based surfactants.[2]

Sugar-based surfactants are becoming more attractive because carbohydrates are the most abundant organic compound worldwide. These biosurfactants are classified into subclasses, including sorbitan ester, sucrose ester, APG, alkyl glucamides, and methyl glucoside esters (Table 1). APGs are molecules with a hydrophilic moiety from D-glucose, harvested from wheat bran, corn starch or potatoes. The lipophilic tail of APGs is a side-product issue arising from either the petrochemical industry (fatty alcohols C_{12}-C_{14} carbon chain) or from saturated vegetable oils

such as palm (fatty alcohols C_{16}-C_{18}) or soybean.[14] The process of extracting fatty alcohols from organic sources has yet to be developed fully for industrial use.[15,16] However, the recipes for APGs with long chains (> C_{14}) derived from 100 % renewable plant-based sources are growing, which raises concerns about deforestation.[16,17]

Table 1 – Subclasses of sugar-based biosurfactant.[2]

Name	Composition	Applications	Production	Ref.
APG	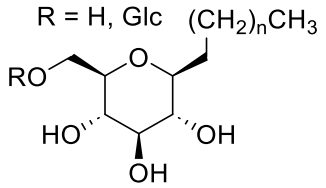	Detergent, dishwashing agent, personal care products, agrochemicals, emulsifiers, etc…	Glycosylation between D-glucose and fatty alcohol,[18] enzymatically with *C. antartica* lipase[19]	10,18,19
Fatty acid glucamides or *N*-methylglucamides (NMGAs)	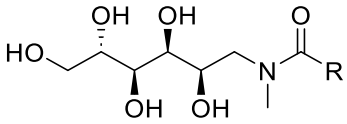 R = C_{12},C_{18}, $C_{18:1}$	Liquid dishwashing agents and powdered and liquid detergent by The Procter & Gamble Company (P&G)	Glycosylation of D-glucose with methylamine followed by addition of fatty acid methyl ester ($C_{12}/_{14}$ and $C_{16}/_{18}$)	20,21
Sorbitan esters (Span)	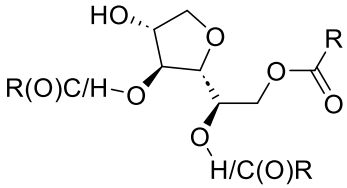 R = C_{12},C_{18}, $C_{18:1}$	Water-in-oil emulsions, emulsifiers, solubilisers, food, cosmetic, medicinal	Dehydration of sorbitol followed by esterification with fatty acids	22–25
Sucrose esters	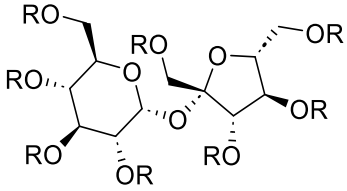 R = R'COO, H R' = C_{12},C_{14}, C_{18}, $C_{18:1}$	Personal care products, cosmetic care applications, food emulsifiers, detergent	Transesterification between sucrose and fatty acid ester	18,26

1.1.1.3 Synthesis of sugar-based surfactant

- **Alkyl polyglucoside (APG) and alkyl monoglucoside (AMG)**

Reaction pathways for the chemical production of APGs rely on Fischer glycosylation between D-glucose **1** and fatty alcohols **2** (Scheme 1).[14,18] Because the hydroxyl positions of D-glucose are unprotected, side reactions occur to afford mixtures of alkyl glucoside with multiple degrees of polymerisation (*n*). The lowest degree of polymerisation (*n* = 0) consists of one unit of D-glucose and is named an alkyl monoglucoside **3** (AMG). More complex polymerisations (*n* ≥ 1) afford alkyl polyglucoside **4** (APG).

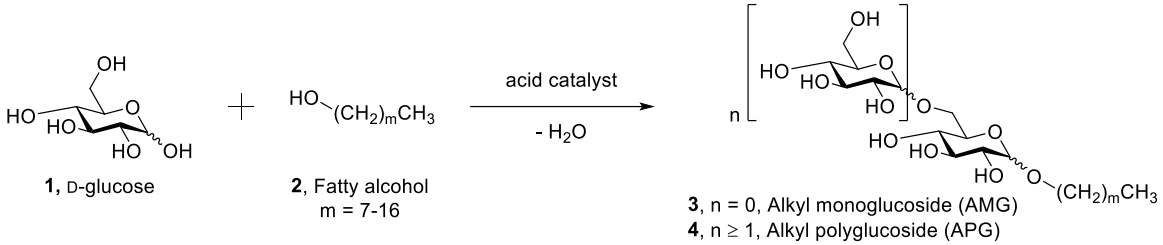

Scheme 1 – Simplified scheme of chemical synthesis of AMG and APG via Fischer glycosylation

- **Fatty acid glucamides or *N*-methylglucamides (NMGAs)**

N-methylglucamides (NMGAs) **6** are afforded by reductive amination of D-glucose with methylamine followed by condensation with fatty acid methyl ester (FAME, Scheme 2).

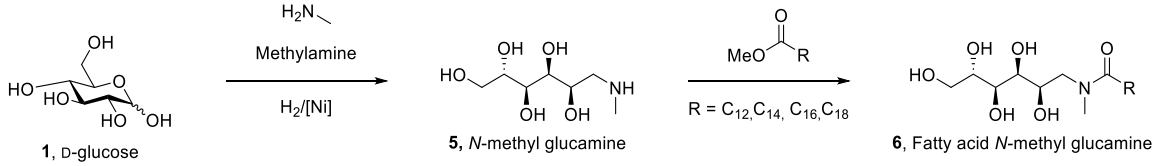

Scheme 2 – Two steps synthesis of fatty acid N-methyl glucamine[14]

- **Sorbitan esters (Spans)**

Sorbitan esters (Spans) **9** are anhydro sorbitol, derived from sorbitol **7** dehydration and cyclisation to sorbitan intermediate **8** (Scheme 3). Industrial routes to Spans involved high temperature transesterification (200-250 °C) and acid catalysts (H3PO2, H3PO3, *p*TosOH).[14,27–29] The harsh reaction conditions are energy-consuming and not considered sustainable chemistry.

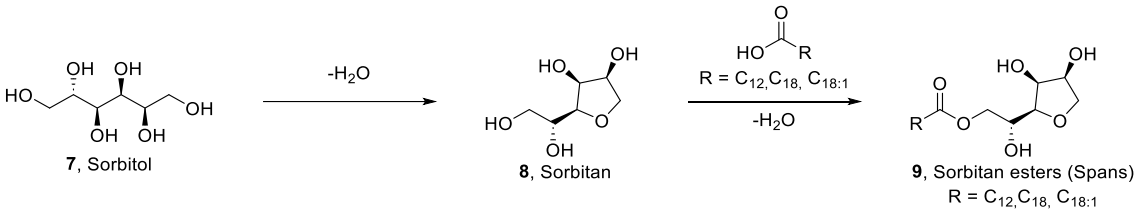

Scheme 3 – Synthesis of sorbitan esters by intramolecular dehydration of sorbitol in the presence of acid [14,22–25]

- **Sucrose esters**

The synthesis of sucrose esters is broadly investigated because of the difficulty of predicting the reactivity of the eight hydroxyl group unprotected of the starting material sucrose **10**.[14] As shown in Scheme 4, several approaches has been investigated to afford sucrose esters **11-14** by controlling the selectivity with the utilisation of organic aprotic solvent[30,31] and by chemoenzymatic regioselective approaches.[32,33] Despite the presented non-green synthesis, sucrose esters have the potential of biosurfactant because they are made from renewable sources (cane, beets, fait or oil triglycerides) and are biodegradable.

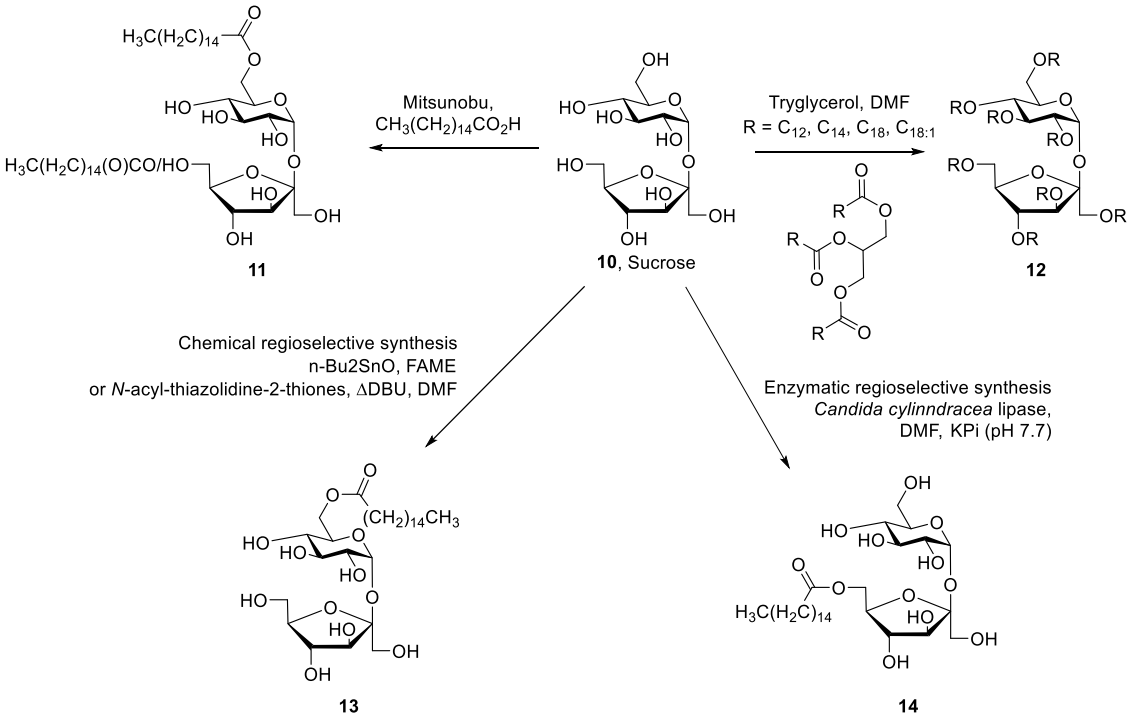

Scheme 4 – Possible routes to afford commercial sucrose.[30–33]

1.1.1.4 Decomposition of AMG surfactant

The environmental impact of sugar-based surfactants is considered negligible. For instance, the decomposition of APGs **3** is based on two possible pathways: glucosidic bond cleavage and ω-oxidation (Figure 3).[34] The degradation by ω-oxidation starts with the oxidation of the alkyl chain to carboxylic acids **15**. These are further degraded by β-oxidation, releasing acetyl-CoA. The cleavage of glucosidic bonds led to D-glucose **1** and fatty alcohol **2**. Glucose is metabolised via pyruvate to pyruvic acid **16** and decomposes into carbon dioxide and water. The remaining fatty alcohol **2** is oxidised to the corresponding fatty acid **18** and degraded via the β-oxidation mechanism.

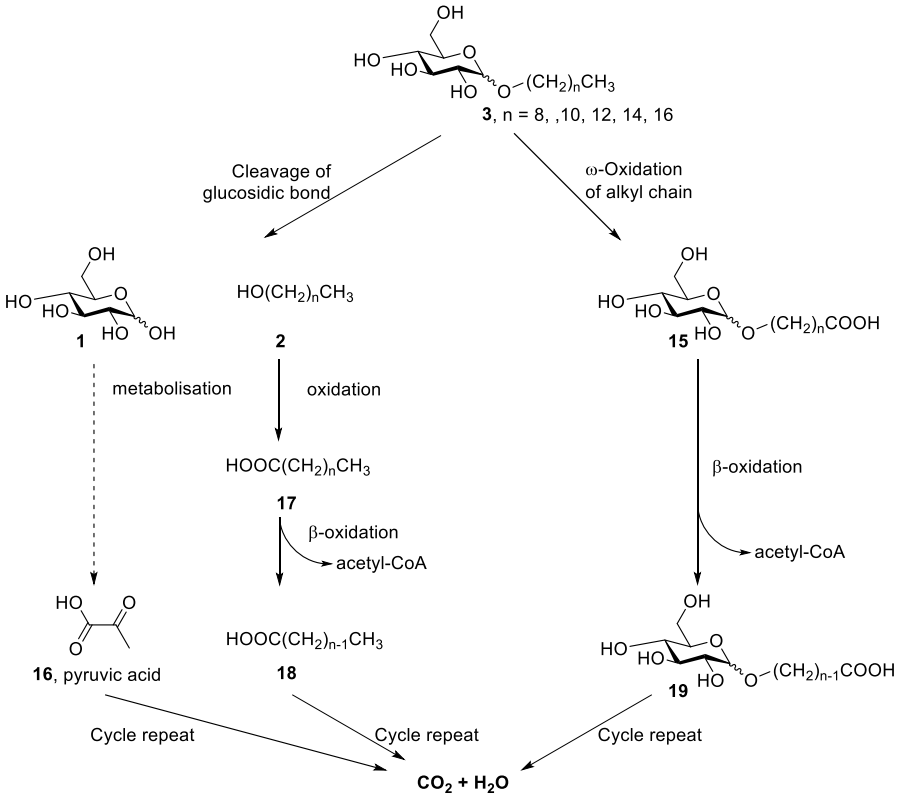

Figure 3 - Biodegradation pathways for APGs[34]

1.1.2 APG: market and applications

1.1.2.1 Market of bio-based surfactant

The first company to commercialise APGs was Henkel, with their patent published in 1995.[35] Since then, the biosurfactants market has been growing. Online market researchers, such as Polaris Market Research, Grand View Research, and Mordor Intelligence, have noticed a decline in petroleum-based surfactants for the benefit of biodegradable surfactants and sulphate-free surfactants. The main reason to abandon petroleum surfactants is the negative environmental impacts of petroleum-based surfactants, as opposed to non-toxic surfactants. This radical shift to more sustainable and non-toxic surfactants is approved by the growing demand for home care and personal care products and their industries (Croda International PLC, BASF SE, Huntsman Corporation, Dow Chemical Company, Akzo Nobel NV, SEPPIC S.A., LG Household&Health Care Ltd., Galaxy Surfactants, Pilot Chemical Company, Shanghai Fine Chemical Co Ltd.).

Before the COVID-19 pandemic, a financial report (Figure 4) stated that the bio-based surfactant APG market was primarily located in North America, Europe, and Asia-Pacific. In 2019, the global market reached US$1,024 million and was expected to grow at a compound annual growth rate (CAGR) of 7.8 % annually until 2027. CAGR is the rate of return (RoR) invested over a period of time. When the rate reached 10-15 %, the CAGR is considered impressive. If the CAGR value remains above 7 %, the APG market should continue to remain competitive for a few more decades. However, since this report was published, the market has been impacted by the COVID-19 pandemic and the Ukraine-Russia war.

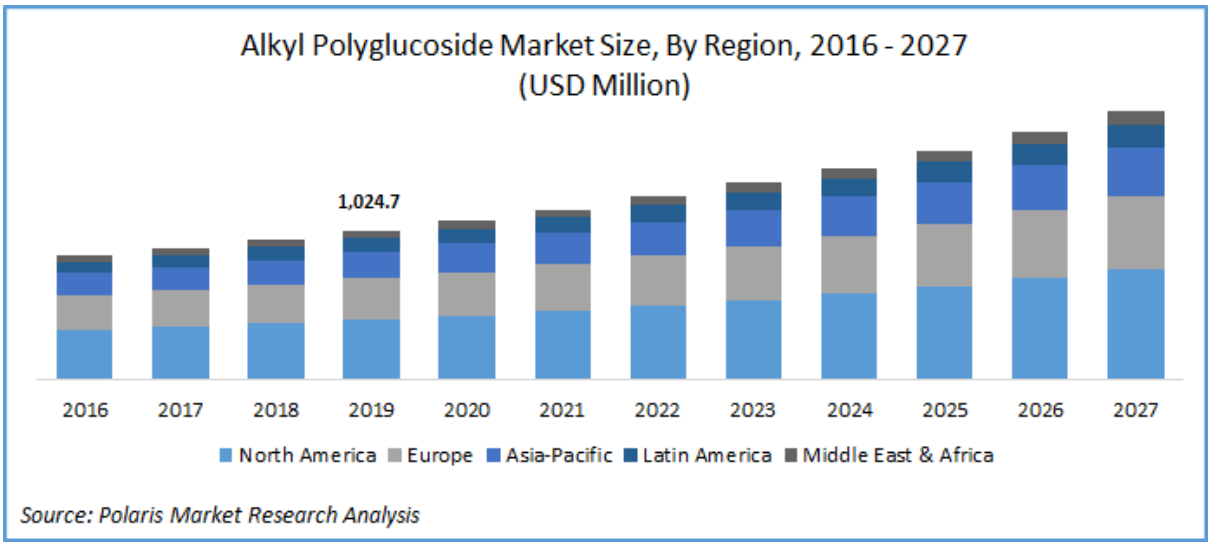

Figure 4 - Alkyl polyglucoside market size, by region, 2016-2027, simulated before COVID-19 pandemic. Source: Polaris Market Research Analysis

Despite international conflicts and health challenges, the demand for cosmetics, personal care, home care products, detergents, and hand sanitisers increased significantly in the APG market until 2020, particularly in Europe and North America. Since the COVID-19 pandemic, there has been a growing interest in understanding sustainability for "green beauty" and its impact on international relations, as noticed by companies such as Accenture and its managing director, Oliver Wright.[36] Due to these reasons, the development of APG as a biosurfactant is crucial for the planet and its people.

1.1.2.2 Application of APG as Biosurfactant

APG surfactants find use in a wide range of products, from cosmetics to fuel extraction as drilling lubricants.[37] This section introduces only three applications of APG surfactants: detergents, dyeing agents, and emulsifiers for cosmetic products.

1.1.2.2.1 Surfactant APG as detergent

Detergents are cleaning agents that dissolve in water and improve the removal of surface impurities. Previously, nonylphenol ethoxylate (NPE) was a popular surfactant due to its effectiveness and affordability. However, NPE is not biodegradable and degrades into nonylphenol (NP), a synthetic compound classified as a harmful endocrine disruptor and can cause neurological damage.[38–40] APGs have been suggested as more sustainable alternative surfactants to NPE in detergents.[40] Detergents containing APGs have been found to have better surface tension (>25 %), a lower critical micellar concentration (CMC) (2.5 times lower) and lower viscosity than detergent containing NPE. These benefits make APGs a more desirable choice for detergent production.

1.1.2.2.2 Surfactant APG as a dyeing agent for clothes

The initial dyeing process for pure cotton has limitations such as poor dye fixation, poor colour yield and a considerable amount of dye residue. To overcome these issues, bifunctional dye systems are introduced[41] with the combination of nonionic polyethylene glycol (PEG)-based surfactant and decamethylcyclopentasiloxane (D5) as organic solvent. The dyeing system creates a reverse micelle where the dye (PEG) is encapsulated by the D5 solvent (Figure 5). D5 is a siloxane-based solvent that is odourless, colourless, reusable, and harmless to human health and the environment.[42,43] However, PEG-based solvents are not biodegradable. Therefore, researches have been conducted to replace (PEG)-based surfactant in bifunctional dye systems with APG surfactant because of its better biodegradability.[44]

Commonly, APGs are used as tensioactive in the action model of a micelle (Figure 5). In this model, the hydrophobic element, such as soap, is encapsulated in an APG-based micelle with its APG hydrophilic head in contact with an aqueous solvent. In the context of dyeing agents for the textile industry, the bifunctional dye system relies on the HLB relationship between D5-siloxane surfactant and APG-surfactant to create an APG-based reverse micelle (Figure 5). The APG head is hydrophilic and contains the water-based dye inside the micelle, while the D5 hydrophobic solvent faces the APG hydrophobic tail.

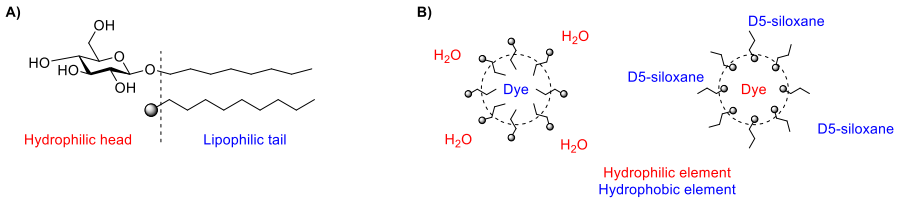

Figure 5 – A) APG biosurfactant, B) APG-based micelle in aqueous media (left) and reverse micelle APG-based micelle in siloxane (right)

1.1.2.2.3 Surfactant APG in cosmetic formulation

APGs, which are ingredients with short (< C_5), average (C_5-C_{14}) or long (> C_{14}) lipophilic chains, are demonstrated to be popular and invisible ingredients in our daily lives for cosmetics, personal care products, baby products, and hair-conditioning agents. Cosmetics are products that aim to enhance a person's appearance. The Cosmetic Ingredient Review (CIR) Expert Panel conducted safety assessments of APGs for the consumer and the environment.[45] Their main concern is the effect of human hydrolase on decomposing APGs and releasing fatty alcohols and D-glucose on the skin. Individual alcohols show low risks of toxicity to human and animal health and are considered safe to use. However, the risk remains in spray bottles when droplets of cosmetic-containing APG are sprayed in contact with mucoid (eyes, mouth) and inhaled by the nose, lungs, or mouth. Therefore, caution signs are written on cosmetic spray bottles of hair dyeing spray and deodorant spray.

1.1.3 Manufacturing and purification of APG

In 1893, Emil Fischer, a German chemist, developed the first synthesis process for APG and was later awarded the Nobel Prize in 1902.[46–48] A century later, the company Henkel successfully designed an industrial production process for APGs following a costly and complex research & development (R&D) effort. Since, APGs are commercialised worldwide. Their synthetic routes are being investigated chemically and enzymatically to decrease costs and improve large-scale production (Table 2).

Table 2 – Advantages and disadvantages of each APG synthetic process. Source: Croda internal report (2014).

Type of synthesis	Synthetic route	Advantages	Disadvantages
Chemical	Fischer glycosylation	• Virtually emission-free technology • High yield • Control of average degree of polymerisation (DP) over a wide range to determine end-use properties • Oligomerisation equilibria • Direct reaction	• Corrosive or toxic acid catalyst • High generation of waste product • Require careful pressure management during reaction to limit by-product • Give an undesirable coloured product
	Koenigs-Knorr Halogenoses Chloride/Bromide	• Stereospecific (alkyl-β-glucosides)	• Half the waste consist of acetic acid
	Schmidt (Trichloroacetamide)	• Stereospecific • Stereoselective • Direct 1-*O*-alkylation	• Complex reaction • Palladium metal toxicity • Expensive
	Base-catalysed alkylation	• Use of unprotected saccharides • One-step synthesis	• NaH 'nasty' reagent • Limited stereoselectivity • Alkyl sulphate is waste product
	Lewis-acid catalysation	• Convenient for producing APGs with defined DP • Use different Lewis acid	• Limited stereoselectivity • DCM 'nasty' reagent • Ratio of anomers depends on reaction time
	Helferich mechanism	• Stereospecific (alkyl-β-glucosides)	• HgCN toxic • CN waste stream
Enzymatic	Enzymatic glycosylation (β-glycosidase)	• Only waste products are sugars (5-fold less waste) • Cleaner process • Function naturally at ambient temperature • 15 fold higher space-time yield	• Lower % product yield • Further work needed to optimise conditions • Plant scale bioreactors have high capital cost • Expensive method • May require the use of genetically modified enzyme

1.1.3.1 Synthetic process for APG biosurfactant

In Table 2, it is shown that various chemical processes have been used to produce APGs, including Fischer glycosylation, Koenigs-Knorr Halogenoses Chloride/Bromide, Schmidt, Base-catalysed alkylation, Lewis-acid catalysation, and Helferich mechanism. However, these processes employ toxic reagents, such as palladium, sodium hydride, mercury (II) cyanide, dichloromethane, and produce undesirable waste products, such as acetic acid and cyanide stream. On the other hand, enzymatic glycosylation, affording APGs, is a sustainable and clean process that can be carried out at ambient temperature. However, the low yield production and the high financial cost for the required equipment, such as the plant-scale bioreactor and the equipment for the design of genetically modified enzymes, have yet to convince industries to invest further in enzymatic glycosylation.

Most industries value the formation of APG via Fischer glycosylation. This process permits a high yield (69-85 %) with minimum chemicals (Scheme 5).[49–51] The Fischer reaction relies on the glycosylation of free sugars **1** with fatty alcohol solvents **2** to form mixtures of α and β substituted glycosides **3**. Although β-anomer is less hindered, the α-anomer is thermodynamically preferred and predominates at more prolonged reaction times.[52]

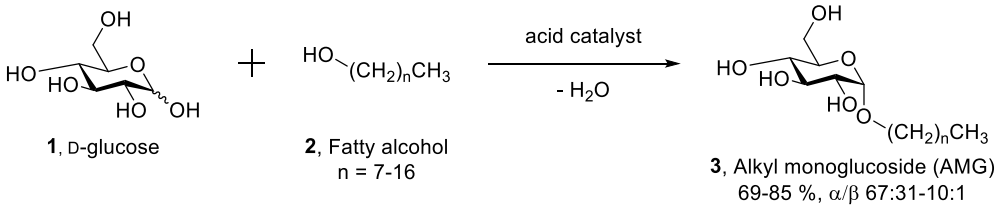

Scheme 5 – Simplified scheme of direct chemical synthesis of AMG via Fischer glycosylation[49–51,53]

1.1.3.2 Industrial production of biosurfactant

- **Chemical reaction for APG biosurfactant**

Fischer glycosylation is currently the favourite method for synthesising tonne-scale amounts of APG to answer the worldwide demands for APG biosurfactant. However, this method requires

severe reaction conditions to afford experimentally 15 g APGs (Scheme 6), such as high temperature (110-230 °C), high pressure (50-550 mbar), the use of strong acid (*p*-TsOH, pKa -2.8) and utilisation of excess alcohol solvent (48 %*w/w*). Additionally, the removal of water molecules by-product requires distillation at high pressure (100 mbar).[54] Unfortunately, these conditions are not suited economically and energetically for industries.

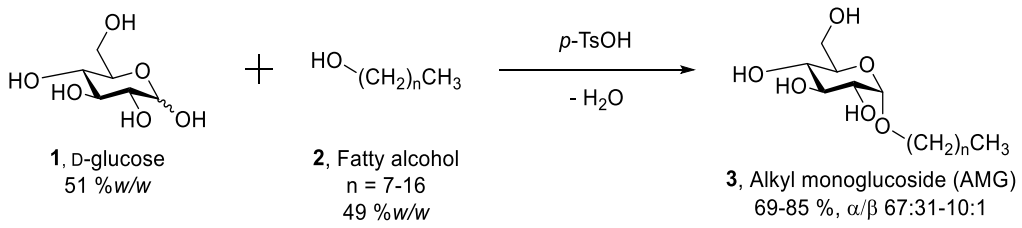

Scheme 6 – Simplified scheme of Fischer glycosylation to form AMG

For these previous reasons, R&D departments strive to achieve sustainable biobased surfactant production in mild conditions. For example, the use of acids, such as superacid Aquivion perfluorosulfonic acid (PFSA),[54,55] concentrated sulfuric acid and phosphorus acid[56] instead of sulfonic acid have improved the APG-C_{12} glycosylation from 50 % yield to 100 % and 92 % respectively. The use of superacids like TFSA has made it possible to perform the glycosylation of APGs to a lower temperature of 90 °C compared to a higher temperature of 110 °C when using weak acid methanesulfonic acid (MSA).[53] As an alternative to chemical processes, R&D are exploring new cost-friendly technologies to improve the enzymatic production of biobased surfactants on an industrial scale. These include using a membrane bioreactor to separate water by-product production and alcohol after reaction by adsorption technique,[57] protein immobilisation to purify and reuse protein,[58–61] and absorption-desorption.

- **Physical side effects of sugar-based biosurfactant reaction**

During the production process of biosurfactants, extensive foaming occurs. To reduce the foam amount, antifoaming agents can be added or mechanical foam breakers can be employed. However, mechanical foam breakers require a lot of energy. Recently, a new membrane technology

that uses a stirrer system to enable foam-free biosurfactant production by redistributing dioxygen gas in the medium has been designed.[62] This technology allied a mechanical solution for foam-free reactions and chemical purposes for gas distribution. Eventually, this technology could help with water by-product sequestration, homogeneous heat distribution, and media mixing by enzymatic or biologic biosurfactant production.

- **Equipment's consideration**

The APG glycosylation at tonne-scale depends on choosing the appropriate reaction reactor, which mainly depends on the ratio of alcohol to sugar and the agitation efficiency.[53] In industrial processes, Continuous Stirred Tank Reactors (CSTR) are commonly used. These reactors feature a large tank with constant stirring. During glycosylation, the mechanical flow of the reactor helps the water molecules and side-products to be removed more easily. However, the viscosity of the APG product can limit the flow created by the stirrer.

- **Quench and purification of APG**

After glycosylation of free sugar **1** with fatty alcohol **2** (Scheme 7), the resulting mixture of APG surfactant is quenched with triethylamine and then subjected to distillation *in vacuo* to extract the excess alcohol from APG syrup. The distillation method is an established technology that is more cost-effective on a kilo/tonne-scale and allows the recycling of the distillate alkyl alcohols. However, after distillation, APG syrup usually has 5-10 %*w/w* of residual alcohol. The incomplete removal of fatty alcohols is due to the viscosity of APG, which slows down the distillation process. As a result, more energy and mechanical power are required, along with a lower vacuum, to produce a commercial APG product with 5-10 %*w/w* alcohol residue.

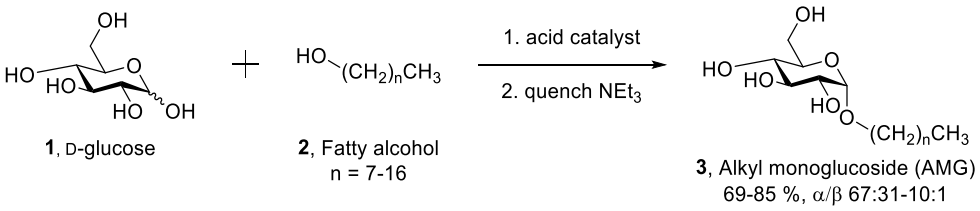

Scheme 7 – Direct chemical synthesis of AMG via Fischer glycosylation

- **APG surfactant appearance**

Industries are interested in producing biosurfactants with low colouration to meet consumer preferences. However, the manufacturing process of APGs significantly affects the colour of the product (Figure 6). The colour of the surfactant is measured using Gardner colourimetry, which ranges from 0 to 18. After the glycosylation and quenching, the reaction mixture is observed as an orange syrup (5 G). Once the mixture is distilled, the bright colour darkens to a black APG syrup, which cannot be measured by colourimetry.

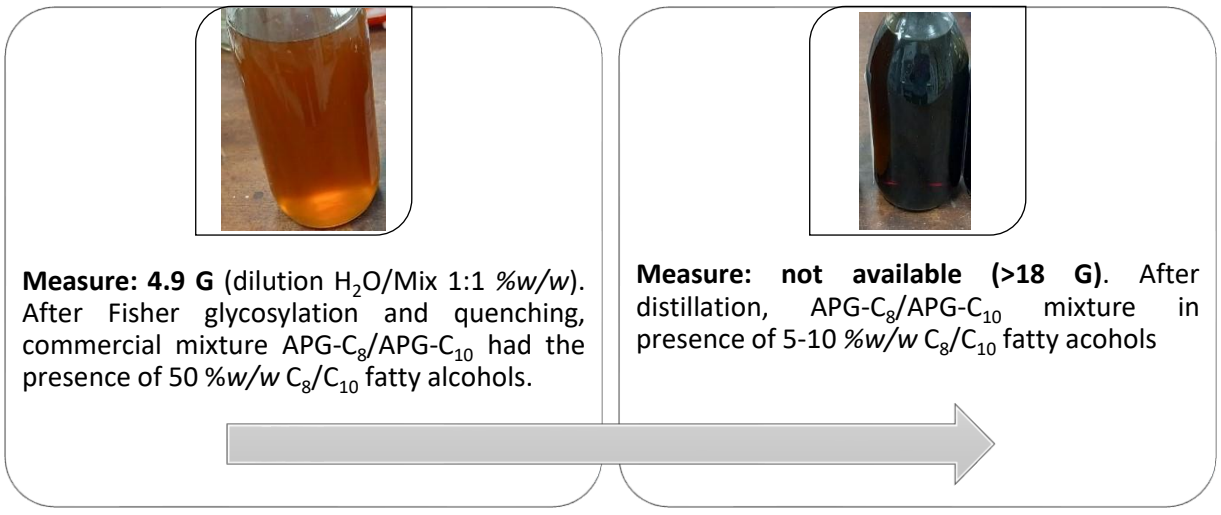

Figure 6 - Evaluation colorimetric of APG sample manufacture

Because of the benefits of sugar-based surfactants, this thesis explored a novel eco-friendly purification process of APG surfactant by exploiting the potential of enzymes (section 1.2).

1.2 Enzyme as catalyst for industry

Chemical industries are adopting new tools to minimise environmental impact, such as photochemistry, biocatalysis, computational synthesis planning, lab automation, molecular design expertise, chemical biology.[63] This thesis focuses on biocatalysis, which uses natural substances (enzymes) from biological sources.

1.2.1 Introduction to enzyme

Enzymes are proteins made by living organisms that catalyse biochemical reactions. They consist of linear polypeptide chains of L-amino acids and are classified according to the type of reaction they catalyse, using the Enzyme Commission number (EC number, Table 3). Enzymes have several advantages: fast activity, high catalytic efficiency, strong specificity, mild reaction conditions, and the ability to express activity in aqueous and inorganic solvents. They have many applications in drug discovery[64–69] and crop reagents.[70–77]

Table 3 - Classification of enzyme by function

Enzyme name	EC number	Catalytic function
Oxidoreductase	EC 1	Redox reaction
Transferase	EC 2	Transfer of specific functional group to one molecule to another
Hydrolase	EC 3	Break a chemical bond with a water molecule
Lyase	EC 4	Break a chemical bond
Isomerase	EC 5	Convert a molecule from one isomer to another
Ligase	EC 6	Form a new chemical bond
Translocase	EC 7	Influence transmembrane transport

It is worth noting that a limited range of enzymes is available in the market, including carbohydrases, proteases, lipases, and alcohol dehydrogenases (ADH), which are commercialised

by a few producers.[78] Unfortunately, these enzymes cover only limited fields of research. Enzyme evolution studies aim to modify a protein's DNA sequence and afford a mutant enzyme with a novel amino acid sequence with a suitable chemical screen.[79–84] For instance, five engineered mutants of choline oxidase from *Arthrobacter cholorphenolicus* have higher catalytic efficiency than the wild type (WT) towards the oxidation of substrate 1-hexanol.[70] Variant E350L/E352D of 6-hydroxy-D-nicotidine (6-HDNO) is active for a broader scope than the WT, with nineteen substrates for the variant against eight for the WT.[83] Cholesterol oxidase variants oxidise cyclohexanol to corresponding ketone with >86 % conversion, whereas WT has less than <1 % conversion.[82] However, protein engineering has limits, and sometimes, the mutants have less activity than the WT, such as variants of protein esterase (EstC) that showed ×10-100 less activity.[81]

Most enzymes have a limited robustness and are denatured at high temperatures. Nevertheless, some robust enzymes, like amylases, lipases, laccases, and cellulases, are used in detergent and industrial processes. Generally, they come from microorganisms capable of surviving in extreme environments (extremophiles) like glucoamylases, amylases which survive at 100 °C.[85,86]

One of the challenges posed by biocatalytic reactions is the recovery of the used biocatalyst. One solution is to increase the biocatalyst's value by immobilising the enzyme of interest on a solid support that can be recovered and reused until the inactivation of the protein (see section 1.2.4.1).

Biocatalysts are considered to be an environmentally friendly and sustainable technology due to several reasons. Firstly, they exhibit a wide range of possible reactions and can be mutated to suit specific requirements. Secondly, they are reactive under a wide range of reaction conditions. Thirdly, they leverage reusable solid technology. As a result, biocatalysts satisfy 10 out of the 12 principles of green chemistry and sustainable technology (Table 4).[4,87–89]

Table 4 - Green Chemistry and Biocatalysis.[4]

N°	Green chemistry principles	Biocatalysis
1	Waste prevention	Significantly reduce waste
2	Atom economy	More atom-and step-economical
3	Less hazardous synthesis	Generally low toxicity
4	Design for safer products	Not relevant (product not process)
5	Safer solvents and auxiliaries	Usually performed in water
6	Energy efficiency	Mild conditions/energy-efficient
7	Renewable feedstocks	Enzymes are renewable
8	Reduced derivatisation	Avoids protection/deprotection steps
9	Catalysis	Enzymes are catalysts
10	Design for degradation	Not relevant (product not process)
11	Real-time analysis	Applicability to biocatalytic processes
12	Inherently safer processes	Mild and safe conditions

Chemical companies producing crop care products or personal care products are struggling to develop white biotechnologies (use of microorganism and protein to manufacture a chemical product) to reduce their environmental impact.[90,91]

1.2.2 Interest of biocatalysts in cosmetics

The cosmetic market in the United States reached $379.7 billion in 2022.[92] In front of this lucrative market and the growing trend for “natural” cosmetics, it is in the manufacturer's interest to reduce the use of unsustainable reagents and to enhance white biotechnologies. This shift towards more sustainable practices will not only reduce environmental impact but also qualify products as "natural".

Cosmetics are substances that aim to enhance the skin's appearance and smell.[93] To this purpose, fragrances and flavour compounds are popular in the Western hemisphere and belong to families of well-known compounds: terpene/terpenoids, alcohols/aldehydes/esters or lactose/ketones. Enzymatic synthesis for these compound families are of interest, and aldehydes, in particular, are fascinating because they provide popular floral, orange, and citrus fragrances.[77,94] They can be synthesised enzymatically by oxidoreduction from the corresponding alcohols or carboxylic acids using oxidoreductase enzyme (EC 1. : alcohol oxidase, alcohol dehydrogenase, laccase, carboxylic acid reductase). Some enzymatic processes for the manufacture of scent molecules are in the early stages (entries 1, 2 and 4), others are ready to scale up to 5-250 mg (entries 3, 5 and 6), and the optimisation challenges will be related to scale-up and equipment.

Table 5 - Enzymes capable to synthesise fragrance molecules

Entry	Compounds (Family)	Enzyme	Molecule produced	Scent	Scale	Ref.
1	1-hexanol (alcohol) 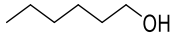	Choline oxidase AcCO6	Hexanal 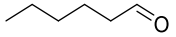	Orange	1 mg, > 99 % conversion	84,95
2	Isovanillyl alcohol (alcohol) 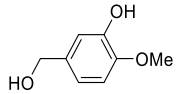	Aryl-alcohol oxidase 2 from *Pleurotus eryngii Pe*AAO2	Isovanillylin 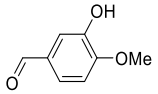	Vanilla	245.7 % specific activity	71
3	*Trans*-2-hexen-1-ol (alcohol) 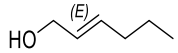	Aryl-alcohol oxidase from *Pleurotus eryngii Pe*AAO	*Trans*-2-hexenal 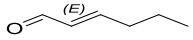	Green notes (apples)	• 6 mg, 31 % conversion in two-liquid-phase-system approach • 250 mg in continuous flow reactor 90 % conversion, 81 % isolated yield	72,96
4	Octanoic acid (acid) 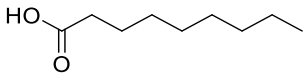	Carboxylic acid reductase (CARs)s from five microorganism sources	Octanal 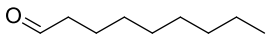	Orange	High kinetic efficiencies (29-1350 $min^{-1}.mM^{-1}$)	97
5	Tertiary allylic alcohol (alcohol) 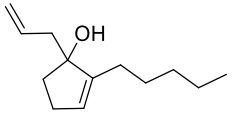	Laccase from *Trametes versicolor* with $TEMPO^{+}BF_4^{-}$	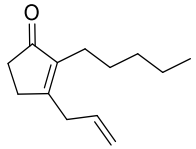	Intermediate for jasmin (*trans*/*cis*-Magnolione)	194 mg, > 99 % yield,	98
6	Margaroleic acid (lipid) from fungus *Mortierella hyaline* 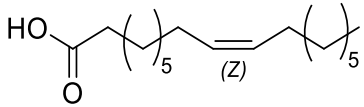	Lipase from *Candida rugosa* α-dioxygenase (α-DOX) and aldehyde dehydrogenase (FALDH)	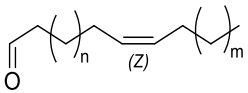 **20**, n = 4, m = 5 **21**, n = 3, m = 5 **22**, n = 2, m = 5 **23**, n = 1, m = 5	green, citrus-like, soapy, waxy, cooked meat	5 mg of lipid, yield: **20** 54 $mg.g^{-1}$, **21** 128 $mg.g^{-1}$, **22** 1 $mg.g^{-1}$, **23** 8 $mg.g^{-1}$.	99

1.2.3 Introduction to oxidase

Enzymatic oxidoreduction involves various subfamilies of oxidoreductase (EC 1.). These subfamilies involve laccase (EC 1.10.3.2), alcohol dehydrogenase (EC 1.1.1.1), alcohol oxidase (EC 1.1.3.13).[100] Oxidases are enzymes that catalyse the oxidation of alcohol and amines. They are four categories of oxidases (EC 1.), which are mostly oxygen-dependent, such as dehydrogenases, oxidases, monooxygenases, or peroxygenases (Scheme 8).[101] presents. Oxidases permit an irreversible reaction with an economy of atoms because of the constant presence of oxygen in the air and the absence of external agents.

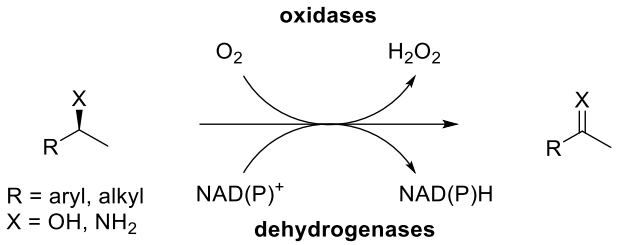

Scheme 8 – Biocatalytic approaches to oxidation with oxidases or dehydrogenases.

There are multiple classes of alcohol oxidases (AOx) that can oxidise primary alcohol, which sometimes require the participation of cofactors. In Scheme 8, dehydrogenases depend on the cofactor nicotinamide $NAD(P)^+$. Similarly, laccases are metal-dependent and require an external oxidating agent, such as TEMPO. Conversely, alcohol oxidases (AOx) do not require the addition of external organic cofactors. Cofactors are usually co-expressed with oxidases, where the enzyme slowly folds around the cofactor and binds to it. Copper radical alcohol oxidase (CRO-AOx) and flavin-dependent alcohol oxidase (FAD-AOx) have to be in the presence of their substrate and oxygen to catalyse the oxidation of alcohols to the corresponding aldehydes or acids. The by-product of the reaction is hydrogen peroxide.

Table 6 - Classes of enzymes capable of alcohol oxidations

Name	EC Number	Co-factor	Ref
Laccase	EC 1.10.3.2	Copper, TEMPO	[102]
Alcohol dehydrogenase (ADH)	EC 1.1.1.1	NAD(P)H	[101]
Copper radical alcohol oxidase (CRO-AOx)	EC 1.1.3.13	Copper dependent	[94,103–105]
Flavin dependent alcohol oxidase (FAD-AOx)	EC 1.1.3.13	Flavin dependent	[106–108]

- **Copper radical alcohol oxidase (CRO-AOx)**

The CRO-AOx is known to oxidise primary alcohols into their corresponding aldehydes via a mechanism involving two consecutive single-electron transfer steps. This process rarely leads to over-oxidation to the acid oxidation level (Scheme 9).[104] After years of investigations, the scientific community has extensively studied the CRO-OAx oxidation mechanism. It has been agreed that the mechanism relies on two consecutive single-electron transfer steps via the transition of metal copper and the reduction of oxygen to hydrogen peroxide.[104,105,109–112] The most famous example of this mechanism was noticed in galactose oxidase (GOase).[113]

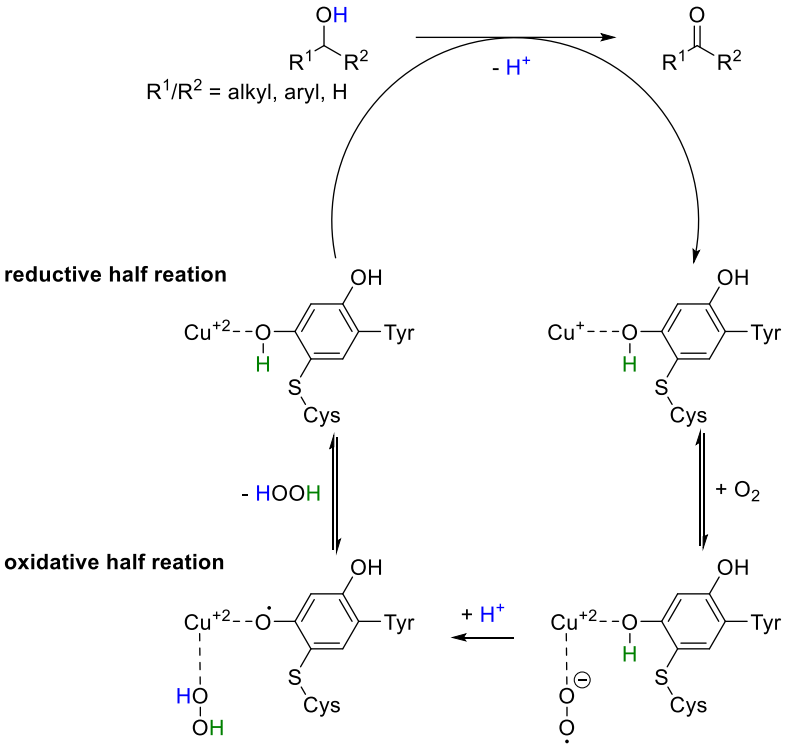

Scheme 9 - Catalytic cycle of copper-containing oxidase[73,100]

- **Flavin dependent alcohol oxidase (FAD-AOx)**

FAD-AOx enzymes are made up of multimeric subunits and contain a flavin cofactor that can be either covalently bound (vanillyl-alcohol oxidase flavoprotein family) or rest within a flavin-binding domain (glucose–methanol–choline flavoprotein family). The flavin cofactor can exist in two forms – flavin adenine dinucleotide (FAD) or flavin mononucleotide (FMN), as shown in Figure 7.[114]

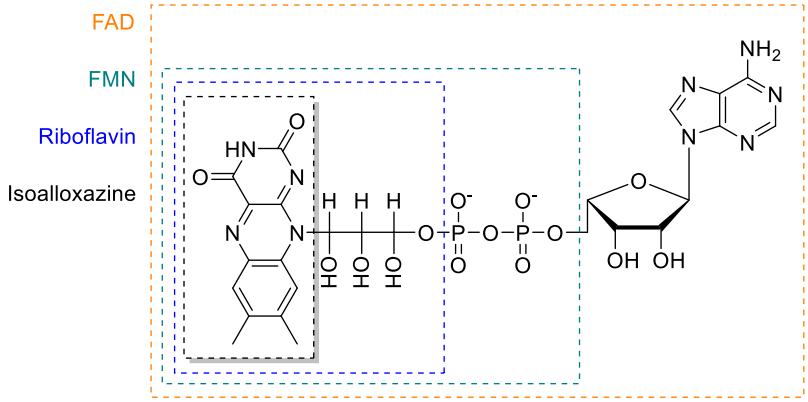

Figure 7 – Structure of cofactor in flavin-dependent oxidoreductases [115]

The oxidation using AOx containing flavin is localised on the isoalloxazine ring. The reaction occurs via two half-reactions, where the alcohol is initially oxidised through a two-electron transfer, leading to reduced flavin (Scheme 10).[73,116,117] Secondly, the flavin cofactor is recycled to its oxidised flavin state by reducing oxygen to hydrogen peroxide.

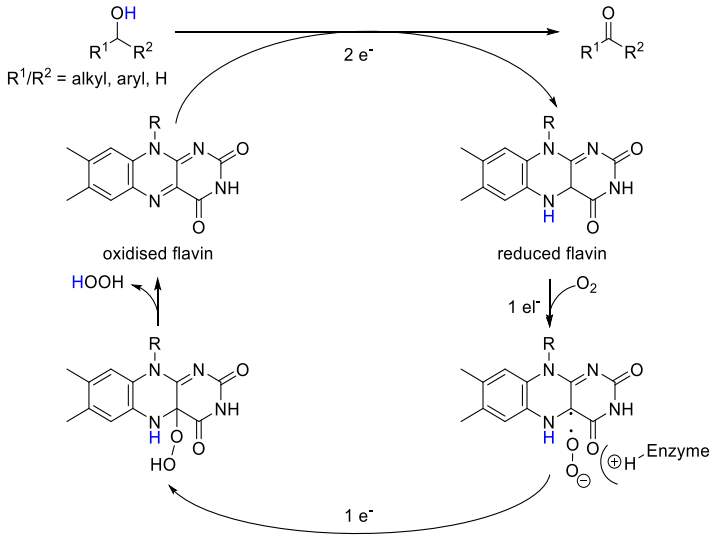

Scheme 10 - Catalytic cycle of flavin containing AOx[73]

The oxidation of primary alcohol catalysed by FAD-AOx mostly results in an aldehyde oxidation level. However, in some cases, flavoprotein oxidase can cause the formation of acid oxidation levels.[118,119] This second oxidation occurs via the aldehyde hydrate (*gem*-diol). The over-oxidation occurs because of the natural properties of the aldehyde hydrate in aqueous solution[118] or because the aldehyde hydrate is also the substrate of the AOx (Scheme 11).[118] However, not all FAD-AOx oxidise primary alcohol to carboxylic acid state.[73]

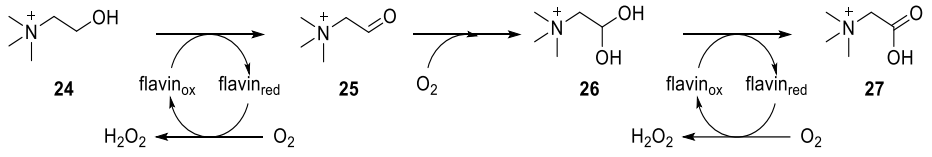

*Scheme 11 – Over-oxidation of choline **24** with choline oxidase AcCO via aldehyde hydrate **26** yielding betaine **27***[118]

This thesis explores the potential of a variant of FAD-AOx, known as choline oxidase AcCO6, which has shown to catalyse a range of substrates.[70] This enzyme can participate in multi-enzyme cascades and has been successfully used in combination with a reductive aminase to convert alcohols to *N*-substituted amines.[120]

1.2.4 Industrial perspective of enzyme as biocatalyst

Many industries are now focusing on promoting the recycling of catalysts and improving green chemistry processes. In this regard, the use of biocatalysts has led to the development of new technologies such as the immobilisation of proteins on solid support (section 1.2.4.1) and the use of rotating bed reactors (RBR) from Spinchem® (section 1.2.4.3).

1.2.4.1 Protein immobilisation to recycle biocatalyst

Since the 1990s, protein/enzyme immobilisation has been extensively discussed in the literature.[58,61,121–129] This method involves stabilising an enzyme by attaching it to a solid carrier, which aims to improve its lifetime, reaction conditions (pH, temperature, and organic solvent) and maximum reusability up to 20 cycles with enzymatic activity retained at ≥50 %.[130] Because of this stabilisation on solid carriers, the immobilised biocatalyst can be used with good relative activity multiple times.

Immobilised proteins have restricted mobility but can be shaped into a recoverable and reusable heterogeneous catalyst. One example is the immobilisation of alcohol dehydrogenase (YADH) from *S. cerevisiae* on glyoxyl agarose beads, which catalyses the oxidation of long-chain fatty alcohol (C24) and other aliphatic alcohols.[131] YADH activity toward aliphatic alcohols was achieved due to the stabilisation of YADH by immobilisation. Another example is the immobilisation of galactose oxidase (GOase) on Purolite epoxybutyl methacrylate beads (ECR8285). When compared to free GOase, immobilised GOase has superior fundamental properties, including a 21-fold increase in half-life, 3.8 times higher thermal activity, 3.8 times longer thermal stability, and better organic solvent tolerance.[95]

Enzyme immobilisation is a process used in industrial applications that can be costly because of the cost of protein expression, protein immobilisation processes, support carriers and the training necessary. However, investing in protein immobilisation can be profitable over time. In biomedicine, immobilised genipin is preferred over free genipin because it has lower toxicity despite a higher cost.[109,126,132–135]

1.2.4.1.1 Types of immobilisation

Proteins can be immobilised through cross-linking, encapsulation/entrapment in organic or inorganic polymer matrices, or binding to a prefabricated carrier.

- **Immobilisation by cross-linking**

Cross-linking is an immobilisation method where enzymes are compacted into aggregates or crystals without carrier. This cost-effective method results in highly concentrated enzyme activity and better stability in the catalyst. For instance, the pharmaceutical industry uses glutaraldehyde to create cross-linked enzyme crystals (CLECs).[136,137] However, the crystallisation of enzyme for CLECS is a laborious process. Salt can be added to an aqueous protein solution to counterbalance, causing protein precipitation and stable conformation through non-covalent bonding. This process is called cross-linked enzyme aggregates (CLEA). The first CLEA was created using penicillin G amidase to synthesise ampicillin.[137,138]

- **Immobilisation by entrapment**

Entrapment via inclusion of an enzyme within an aerogel is possible by polymerisation such as silica sol-gel. For instance, lipase from *Burkholderia cepacian* immobilised in silica aerogel improved the esterification reaction rate (*Vmax*) of lauric acid with 1-octanol with a factor 10.[139] In past decade, metal organic framework (MOF) has displayed interesting abilities for enzyme encapsulation (enzyme@MOF). The combination between MOFs-metal node and environmentally friendly buffers (sodium acetate, potassium phosphate, Tris-HCl) has successfully retained lipase

(Lip@MOF).[140] Similarly, the laccase immobilisation on MOF has shown a sustainable interest, as lipase permits the degradation of environmental pollutants like phenolic synthetic dyes.[141]

- **Immobilisation by support binding**

The immobilisation by support binding involves the creation of bonds: physical (van der Waals interaction, hydrophobic), ionic or covalent (Scheme 12). The risk of enzyme leaching decreases as the bonding strength increases from weak ionic interaction to strong covalent bonding. Enzyme leaching can cause irreversible inactivation of this method. Therefore, carriers should be chemically inert, durable, economically viable and regenerable. Synthetic polymeric resins, such as mesoporous silica or zeolite, are often used as carriers. For example, acrylic resin Eupergit® C is a microporous copolymer with multi-point attachment for biding to penicillin amidase,[142] while microporous acrylic resin Novozyme 435 can serve as a carrier for enzyme *C. antartica* lipase B (CaLB).[143]

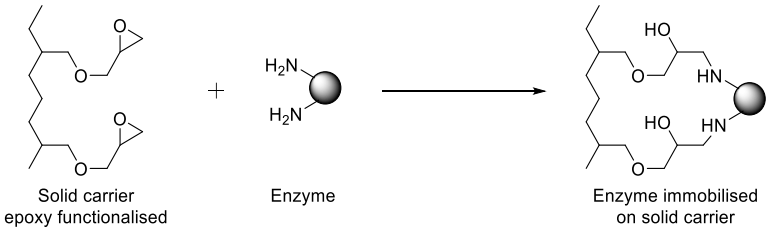

Scheme 12 - Immobilisation of enzyme on solid support by covalent binding

1.2.4.1.2 Current immobilisation methods

Strategies for protein immobilisation are designed to separate a specific enzyme from an impure proteinic mixture. One approach is to immobilise His-Tag protein by metal affinity between the enzyme and a carrier. With this approach, multiple enzymes of interest can be co-immobilised (ketoreductase and glucose dehydrogenase)[144] on one polymer, EziG™, with Fe(III) ions chelation.[130,145,146] Some studies have found that stabilisers, such as glycerol, can enhance the stability of immobilised enzymes, including laccase, catalase, and glutaraldehyde-chymotrypsin. The concentration of glycerol used depends on the pH value.[147] Usually, these procedures require purification of the protein before immobilisation.

Immobilisation protocols aim to simplify support fabrication through combining purification and immobilisation of his-tagged enzymes directly from impurified cell lysate. For instance, Ma et.al. used an amorphous cobalt phosphate for the treatment of his-tagged β-glucosidase.[148]

1.2.4.2 Three types of carriers for protein immobilisation

The performance of an immobilised enzyme depends on the properties of the carrier material used. This thesis examines three types of carriers: covalent attachment on Purolite® epoxy butylmethacrylate resin, covalent attachment on Purolite® amino methacrylate resin, and non-covalent attachment.

- **Purolite® epoxy butylmethacrylate resin**

Purolite® offers a range of enzyme carriers called Lifetech™ ECR (Figure 8). They are resins composed of methacrylic or styrene with different degrees of hydrophobicity and porosity.

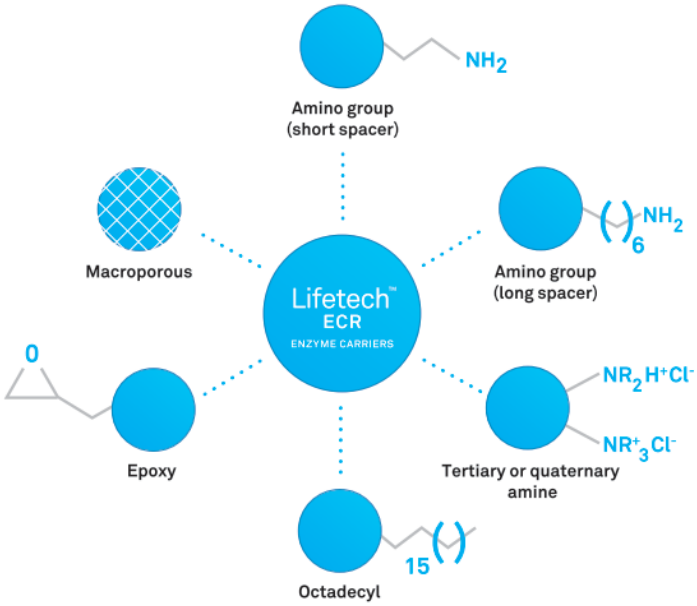

Figure 8 – Available chemistries of Life tech ECR resins for enzyme immobilisation. Source image: Purolite Lifetech™ ECR Enzyme Immobilisation Resins, Purolite product information (2015).

In this thesis, epoxy-activated resins are preferred for their ability to create covalent bonds between the enzyme and the resin. Epoxy methacrylate resins with epoxy groups form bonds with various protein groups, such as amino, thiol, and phenolic, under mild pH and temperature conditions (Figure 9). The carriers ECR8285 are available with a pore diameter of 400-600 Å, weak mechanical strength, weak hydrophilicity and average porosity. This resin has been reported to be suitable for the immobilisation of AcCO6[95] and lipase immobilisation.[129,149]

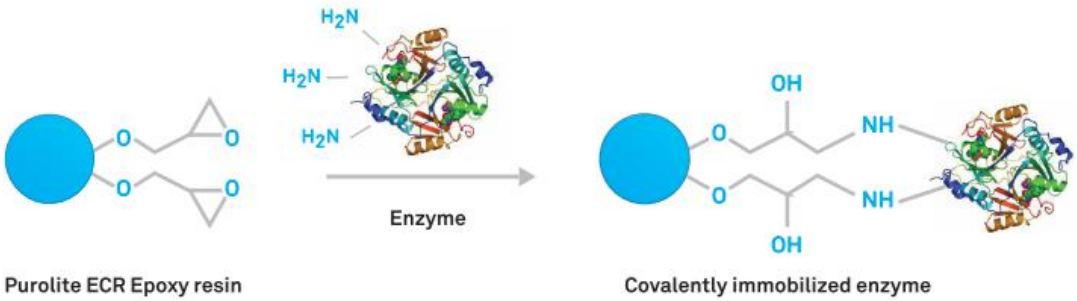

Figure 9 – Immobilisation of enzymes using epoxy carriers. Source image: Purolite Lifetech™ ECR Enzyme Immobilisation Resins, Purolite product information (2015).

In the upcoming chapters, His-tagged oxidases are discussed. To immobilize these oxidases, epoxy carrier ECR8285 is used, as it can create a strong covalent bond with amino groups. However, this resin is not selective towards only His-tag proteins and may form covalent bonds with multiple element carriers containing amino groups.

- **Purolite® amino C2 methacrylate resin**

Alternatively, amino-activated resins, such as Lifetech™ ECR8309F, are used for covalent immobilisation of enzymes. The resin is pre-activated with glutaraldehyde to afford an aldehyde linker and then imine covalent between activated resin and enzyme (Figure 10). The resin is non-selective towards His-tag proteins and forms a covalent link with multiple proteins with amino groups available.

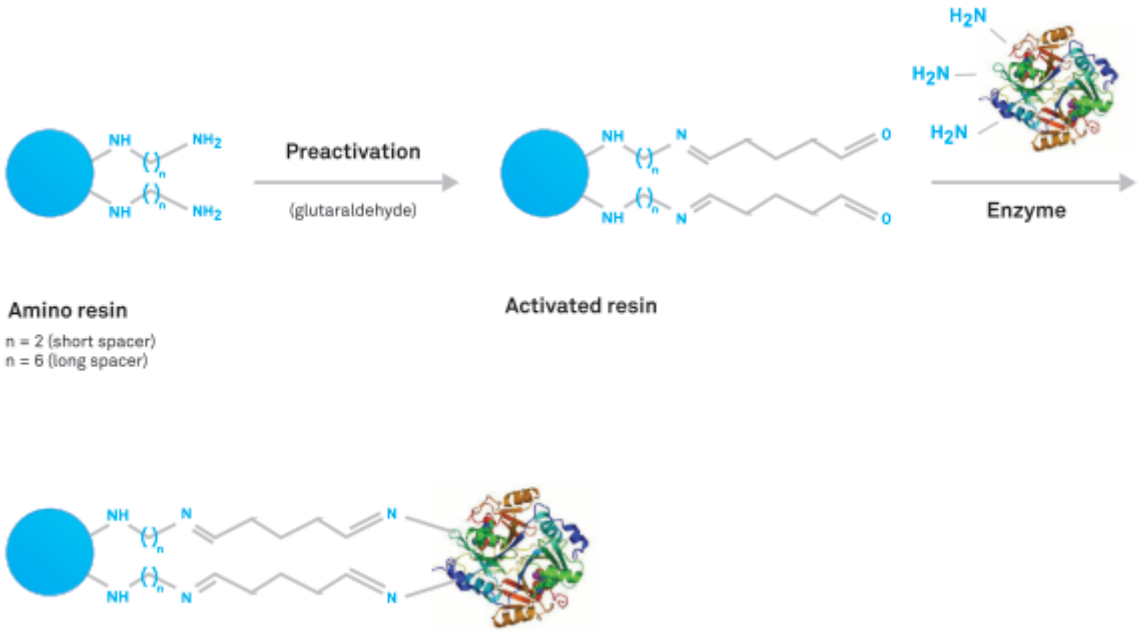

Figure 10 - Immobilisation of enzymes using amino carriers. Source image: Purolite Lifetech™ ECR Enzyme Immobilisation Resins, Purolite product information (2015).

- **EnginZyme EziG resin**

Contrary to Purolite® ECR resin, EziG resins from EnginZyme are made of controlled porosity glass (CPG) particles modified to bind protein affinity tags (Figure 11). These carriers contain chelated Fe(III) for His-tag binding. They are enzyme-selective. Three types of EziG have been commercialised as hydrophilic surface (EziG 1), from hybCPG with polyvinyl benzyl chloride has a hydrophobic surface (EziG 2) or from hybrid CGP (hybCPG) with a blended co-polymer for a somewhat hydrophilic surface (EziG 3 also named EziG Amber).

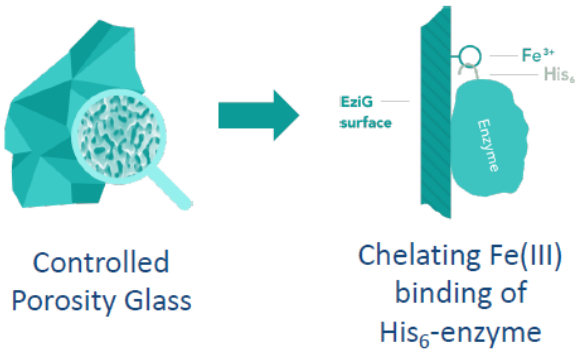

Figure 11 – Enzyme immobilisation from EnginZyme. Source: Enginzyme youtube chanel

1.2.4.3 Industrial reactor for biotransformation

Chemical reactions are often performed on an industrial scale, using large tanks that can hold up to a tonne of material. When producing APG, plants use a 21 Tonnes stirred tank reactor. However, scaling up from laboratory to industrial production can be challenging, particularly regarding the equipment and the biocatalyst used (CFE, pure or immobilised) in the reaction. One of the main concerns is the potential damage from stirring blades when using immobilised protein, which can decrease reaction reactivity and lower product yield. To address these concerns, the company SpinChem research new approaches for reactions and processes to reduce waste in reactions, for decontamination of liquids, and catalysing reactions. For this last purpose, rotating bed reactors (RBR) are designed with the double purposes of blade stirrer and enzyme container. As shown in Figure 12, a RBR is intended to prevent the disintegration of solid phase particles by retaining the particles inside a rotating cylinder during the reaction span.

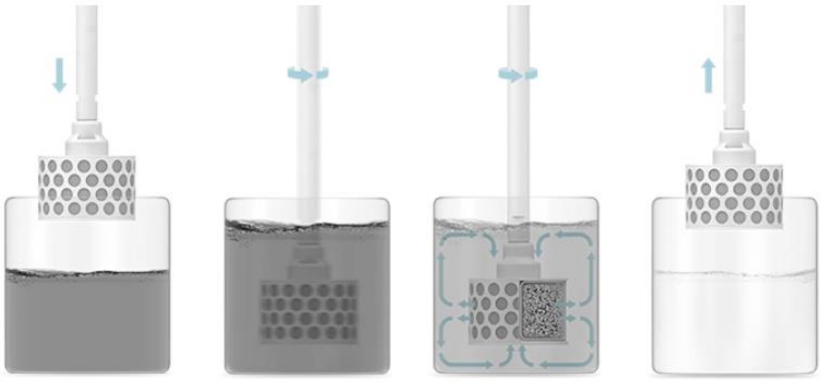

Figure 12 - Rotating bed reactor (RBR) applied in solution. Source: SpinChem

Here two examples for Ton scale reaction with SpinChem products are presented (Figure 13). For a used in-tank vessel for batch processing, ProRBR is a model of RBR that can be replaced a pre-existing stirred. An alternative is ProRBR plug-in with ProRBR reactor connected to the main reaction tank. This configuration can be used in both batch and flow modes.

Figure 13 - ProRBR direct install (left) and ProRBR plug-in (right). Source: SpinChem

1.3 Project outline

APG biosurfactants are nonionic surfactants produced from renewable resources and are popular ingredients worldwide. The APG market is growing extensively due to the rising demand for detergents, dyeing agents, personal care products and cosmetic products. The environmental impact of APG-based surfactants is negligible, with biodegradable properties and low toxicity. However, their industrial production relies on removing the excess fatty alcohol solvent required

for APG glycosylation. The sustainable removal of the alcohol solvent from APG surfactant remains an ongoing research area with many possibilities (technical and chemical). Therefore, one aim of this thesis is to establish a bioprocess for the purification of APGs biosurfactants under mild conditions. Chapter 2 focuses on the selection of two oxidases (choline oxidase AcCO6, long-chain alcohol oxidase HNX4)[70,150] to oxidise the excess of fatty alcohols used for APG production without modification of APG (Figure 14). In Chapter 3, one oxidase (AcCO6) with two supported resins (amino-based resin and aminooxy-based resin) is used for the development of the removal of the alcohol solvent necessary for APG production from analytical scale to gram-scale.

Chapter 4 extends the application of oxidase AcCO6 in a cascade reaction with a Wittig olefination by exploring the transformations of functionalised fatty alcohols (methylsulfanyls, halogens, silyls, azidos, aliphatics) in water followed by reaction with an ylide reagent (one stabilised ylide, one phosphonium salts).

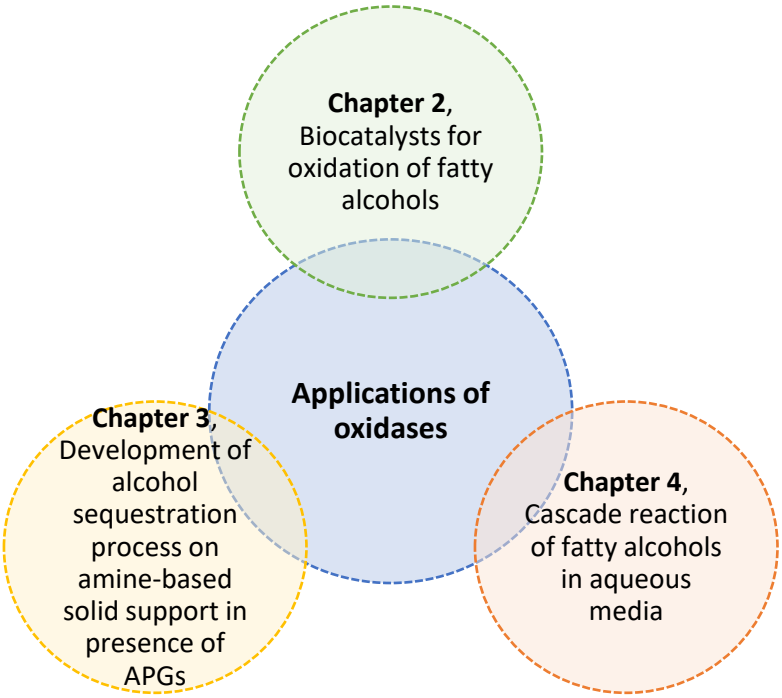

Figure 14 – Graphical overview of this thesis for the development of aliphatic chain compounds with oxidases in mild conditions

Chapter 2 - Biocatalysts for oxidation of fatty alcohols

2.1 Introduction

In this chapter, the potential of two oxidases, HNX4 and AcCO6, is studied for the oxidation of fatty alcohols **2** that are used to synthesise APGs **4**. These oxidases are selected from the literature.[70,150] They are expressed independently, characterised and purified in sections 2.2 and 2.4. Since aliphatic alcohols used in APG synthesis are already known compounds, their oxidation using biocatalyst (HXN4 section 2.3, AcCO6 section 2.5) is determined by ^{1}H NMR and GC-FID, as described in section 2.1.2.

The objective is to determine an oxidase that can selectively react with fatty alcohols **2** but remain inactive to APGs **4** surfactant (Scheme 13). To achieve this goal, the potential of HNX4 and AcCO6 for aliphatic alcohol is tested and their activities are explored on the biosurfactant alkyl monoglucosides **3** (AMGs), chemically synthesised in section 2.1.3.

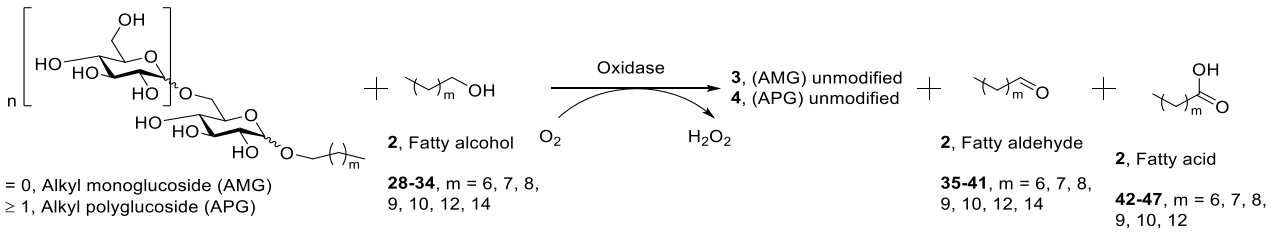

*Scheme 13 – Simplified scheme for the enzymatic oxidation of fatty alcohol **2** in the presence of biosurfactant (AMG **3** and APG **4**)*

2.1.1 Protein background

2.1.1.1 HNXH4

Rembezza *et al.* have discovered a novel long chain alcohol oxidase HNX4 (EC 1.1.3.20) from an uncultured marine euryarchaeota group II/III euryarchaeota KM3_72_H01 (*Eur*). This enzyme can oxidise 1-dodecanol.[150] Although HNX4 was previously annotated as L-gulonolactone oxidase (EC 1.1.3.8) in BRENDA,[151] it has been found to show activity with 1-dodecanol and does not share sequence similarity with other known long chain alcohol oxidases (LCAOs).

2.1.1.2 AcCO6

Heath *et al.* have published a study on the structure-guided evolution of choline oxidase to oxidation of primary alcohols, leading to the development of an engineered choline oxidase mutant named AcCO6 (EC 1.1.3.17).[70] AcCO6 is designed from the wild type (WT) FAD-containing choline oxidase from *Arthrobacter cholorphenolicus* (AcCO) and has been shown activity towards a panel of primary alcohols, including choline analogues and alkyl alcohols with 4-12 carbon length.[70,152] Furthermore, the WT can be expressed in *Escherichia coli* and has a high sequence similarity with choline oxidase from *Arthrobacter globiformis* (AgCO), whose crystal structure is known (PDB ID: 4MJW). [153]

2.1.2 Fatty alcohols with oxidase analysed by ^{1}H NMR and GC-FID

Fatty alcohols are composed of a saturated chain of carbons (C_n) terminated by an alcohol function. In this thesis, they are analysed by ^{1}H NMR and GC-FID. Fatty aldehydes and fatty acids have distinctive proton peaks, with aldehydes showing a singlet peak at δ_H 9.78 ppm and carboxylic acids a broad singlet at δ_H 11.45 ppm.[70,94,119,154–157] Due to these differences in chemical shifts, a crude mixture of alcohol, aldehyde and carboxylic acid can be identified. However, in some cases, the analysis of low-scale reactions by ^{1}H NMR (< 3 mL) may not be sufficient.

Instead, Gas chromatography GC-FID exploits the volatility and low boiling points of aliphatic alcohols with 2-16 carbon lengths (78–344 °C), even in low-scale reactions. [158] For example,

1-dodecanol **32** can undergo two oxidation levels (Scheme 14) to produce aldehyde **39** and carboxylic acid **46**. The oxidation level influences the physicochemical properties, including the boiling point (**32**: 259 °C, **39**: 257 °C; **46**: 298 °C). When a dilute mixture of **32/39/46** reaches the limits of ^{1}H NMR detection, the sample is analysed by Gas Chromatography. The sample solution containing **32/39/46** is injected into the instrument and eluted with a mobile phase (gas He) through the stationary phase (column) based on the volatility of each analyte.[158] A chromatogram is generated with three distinct peaks of separated analytes (Figure 15). This mixture ratio **32/39/46** is analysed as 0:61:38. Alcohol **32** is visible on the chromatogram, but its peak couldn't be integrated by the instrument, indicating the limits of GC-FID analysis in low-scale reaction. The peak intensity is the second indicator for GC analytical limits (<20 pA: uncertain results, >100 pA: confident results).

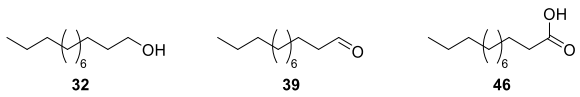

*Scheme 14 – Simplified oxidation levels of 1-dodecanol **32***

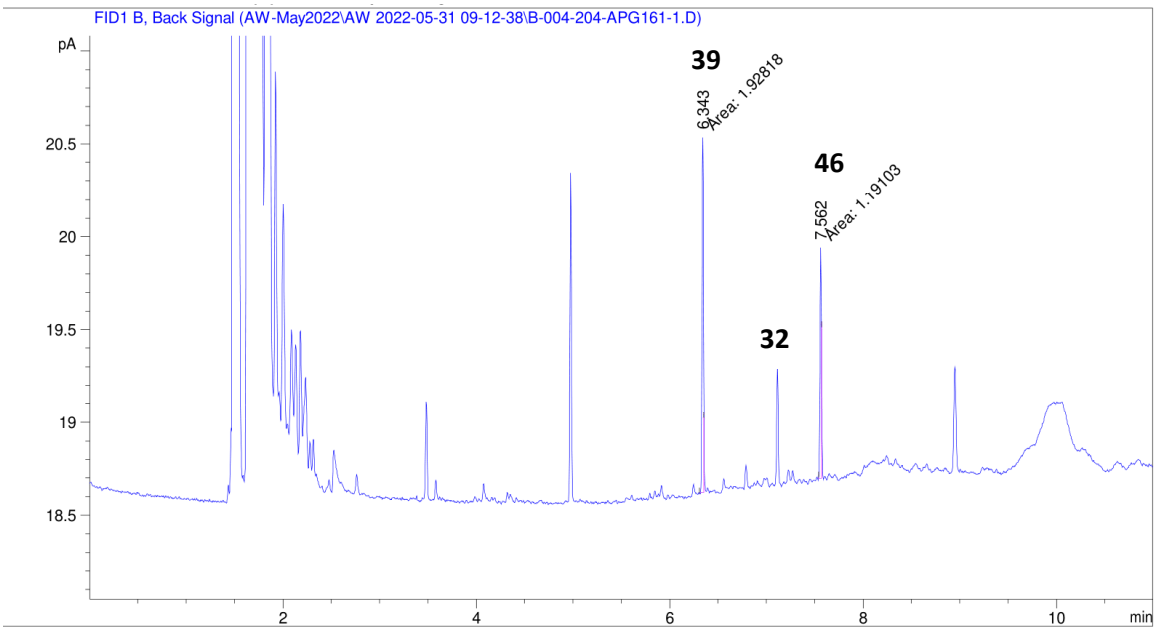

*Figure 15 – Chromatogram of 1-dodecanol biotransformation with HNX4 immobilised on epoxy resin ECR8285. Left to right: dodecanal **39**, dodecanol **32**, dodecanoic acid **46**.*

The aliphatic standards ranging from C_8 to C_{16} are purchased commercially (Sigma Aldrich, TCI and Alfa Aeser) and analysed by GC-FID using two different methods. The retention times observed are combined in the appendix. Noteworthy, alkyl alcohols have a higher retention time than their corresponding alkyl aldehydes but lower than their corresponding carboxylic acid: Rt(aldehyde) < Rt(alcohol) < Rt(carboxylic acid). This trend is similar to their boiling points: bp(aldehyde) < bp(alcohol) < bp(carboxylic acid).

2.1.3 Chemical synthesis of alkyl monoglucoside (AMG)

Alkyl monoglucosides (AMG) were synthesised chemically from the commercial monosaccharide **48**. As shown in Scheme 15, commercial β-D-glucopyranose pentaacetate **48** was firstly glycosylated with fatty alcohols (C_8, C_{10}, C_{12} and C_{14}) to obtain a series of protected alkyl glucopyranoside (octyl **49**, decyl **50**, dodecyl **51** and tetradecyl **52**.[159,160] Secondly, they were subjected to basic deprotection to provide the final AMG products: AMG-C_8 **53**, AMG-C_{10} **54**, AMG-C_{12} **55**, AMG-C_{14} **56**.

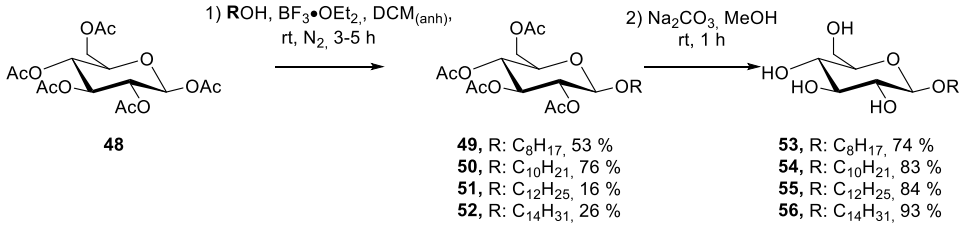

*Scheme 15 – Synthetic pathway of alkyl monoglucosides **49-53**. Reactions conditions: 1) glucopyranoside **48** (1.0 equiv.), alkyl alcohol (1.2-2.0 equiv.), $BF_3{\cdot}Et_2O$ (1.5–4.7 equiv.), $DCM_{(anh)}$, rt, 3-5 h. 2) protected alkyl monoglucoside **49-52** (1.0 equiv.), Na_2CO_3 (0.01 equiv.), MeOH, rt, 1 h.*

During the glycosylation step, commercial pentaacetate glucopyranose **48** was not completely consumed and eventually formed α-anomer after 3 h reaction. To prevent the formation of an anomeric mixture, each crude reaction mixture was stopped after 3 h reaction and purified on silica gel via flash column chromatography. This decision resulted in the formation of tetraacetate β-anomers **49-52** in sufficient yield (**49**: 53 %; **50**: 76 %; **51**: 16 %; **52**: 26 %). The yields were

calculated without considering the amount of starting material recovered. It was also observed that during the preparation of each glycosylation, alcohols with chain lengths longer than 10 carbons were dissolved in the reaction solvent at a slower rate than those with shorter chains. Therefore, the glycosylation rate depended on the length of the aliphatic alcohol aglycon. In the second step, complete deacetylation was carried out with sodium bicarbonate in methanol, which afforded AMGs in excellent yield (**53**: 74 %; **54**: 83 %; **55**: 84 %; **56**: 93 %). AMGs were synthesised with a good yield over two steps (AMG-C_8 **53**: 39 %; AMG-C_{10} **54**: 63 %; AMG-C_{12} **55**: 13 %; AMG-C_{14} **56**: 24 %).

2.2 Protein expression of biocatalyst HNX4

The pET21a vector containing the gene for HNX4 was obtained from Martin Engqvist through Addgene (A0A075HNX4).[150] HNX4 was transformed into *E. coli* BL21 (DE3). The protein was expressed by Studier LB auto-induction media (AIM)[161] by initially incubating with shaking at 30 °C for 5 h before being left at 20 °C overnight, harvested by centrifugation and confirmed by characterisation by SDS-PAGE gel (Figure 16). Following cell lysis by BugBuster™ from MilliporeSigma™, HNX4 was purified by Ni-NTA affinity column chromatography with buffer 20 mM HEPES at pH 7.5 and by PD-10 desalting column with buffer 20 mM HEPES. Expression of HNX4 was successful on the first trial. Since the initial expression, repeat expression in autoinduction media or through induction with isopropyl-β-D-thiogalactopyranoside (IPTG) was unsuccessful without explanations.

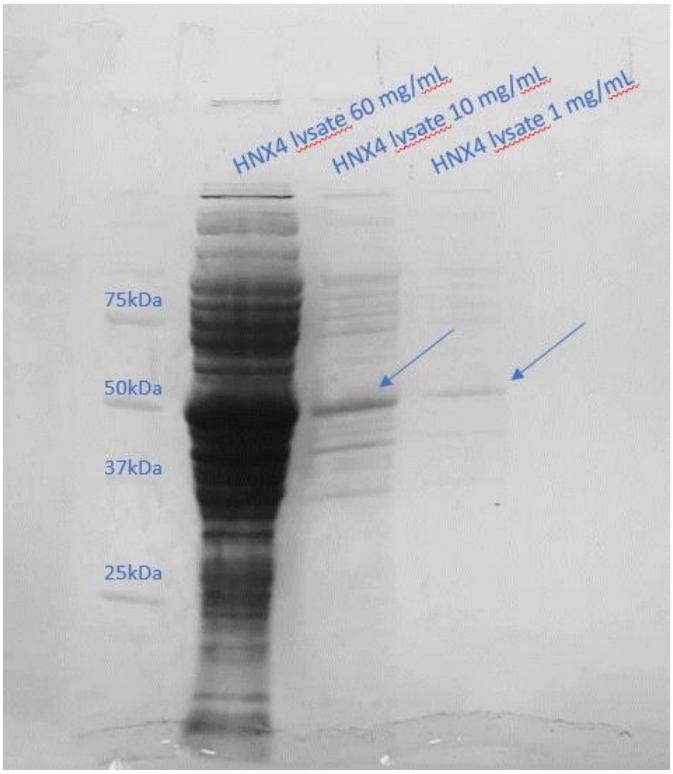

Figure 16 - SDS-PAGE gel of HNX4 lysate at different concentration (HNX4 protein: 56.2 kDa)

2.3 Biotransformation with HNX4

2.3.1 Enzymatic treatment of alkyl monoglucoside (AMG) with oxidase HNX4

The original scope of HNX4 included alkyl chain alcohols (C_{10}-C_{16}).[150] Among these alcohols, C_{12} fatty alcohol **32** was considered one of the best substrates for HNX4. Therefore, alcohol **32** was chosen as a positive control for the following oxidation reaction.

A colorimetric assay was conducted to demonstrate that HNX4 is inactive towards AMG and APG biosurfactant by treatment of AMGs **53-56** with HNX4 and horseradish peroxidase (HRP, Scheme 16). HNX4 oxidase used oxygen to oxidise a substrate and produced hydrogen peroxide as a side product, which rate was detected by HRP (from Sigma) and 2,4,6-tribromo-3-hydroxybenzoic acid/4-amino antipyrine dye (TBHBA/4-AAP, **61**/**62**, ε = 29400 $L.mol^{-1}.cm^{-1}$). Under the action of HRP, the nucleophilic substitution (SN) of 4-amino antipyrine **62** and 2,4,6-tribromo-3-

hydroxybenzoic acid **61** afforded the red/pink dye **63**, which was measured on a TECAN Infinite 200 Pro M Nano spectrophotometer. The absorbance data collected by the spectrophotometer was calculated using Beer-Lambert Law (Equation 1). The activity assays were performed in 100 mM KPi pH 7.0 buffer instead of 20 mM HEPES pH 7.4 buffer reported.[150] Unfortunately, this error could not be rectified with fresh protein HNX4 due to the repeated failure to express HNX4. No solutions were found explaining this recurrent protein expression issue. Therefore, different results from those reported in the literature were expected.

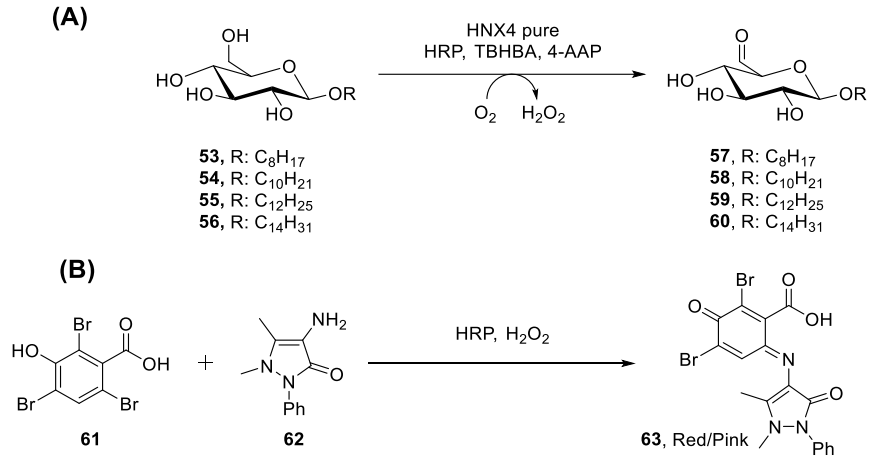

*Scheme 16 – (A) Biotransformation of 1 mM alkyl monoglucosides **53-56** in presence of 50 µg.mL^{-1} enzyme HNX4 pure, 0.03 mg.mL^{-1} HRP, 0.75 mM 4-aminoantipyrine **62**, 2.25 mM tribromo-3-hydrobenzoic **61**, 1 mM substrate in 150 mM KPi buffer pH 7.0 at 40 °C (B) Dye condensation during HRP assay when hydrogen peroxide was detected with TBHBA/4-AAP **61/62**.*

$$A = l \times c \times \varepsilon$$

Equation 1 - Beer-Lambert law. A: absorbance, l: pathlength (cm), c concentration (mol.L^{-1}), ε: molar extinction coefficient (L.mol^{-1}.cm^{-1})

As shown in Table 7, the HNX4 enzyme had a higher activity for alcohol **32** (entry 1, 1798 mU.mg^{-1}) than for AMG substrates **53-55** (entries 2-5, 13-274 mU.mg^{-1}). These low specific activities resulted in weak hydrogen peroxide production during the biotransformation of AMG.

This suggested that AMGs **53-55** were oxidised weakly by HNX4 and were considered non-substrates for this enzyme.

Table 7 – Specific activities of HNX4, where specific activity is the amount of product formed [µmol] per min per mg of enzyme (1 U is defined as 1 µmol.min^{-1}.mg^{-1})

Entry	Substrate	Specific activity (mU.mg^{-1}) ± SD
1	**32,** 1-dodecanol	1798.2 ± 159
2	**53,** AMG-C_8	142.7 ± 44
3	**54,** AMG-C_{10}	182.7 ± 14
4	**55,** AMG-C_{12}	274.2 ± 65
5	**56,** AMG-C_{14}	n.d.
Assay conditions: duplicate, 40 °C, 0.03 mg.mL^{-1} HRP, 0.75 mM 4-aminoantipyrine **62**, 2.25 mM tribromo-3-hydrobenzoic **61**, 1 mM substrate **53-55** prepared in DMSO, 50 µg.mL^{-1} HNX4 pure, λ 510 nm. n.d. : not detected.		

2.3.2 Enzymatic treatment of fatty alcohols by oxidase HNX4

Biotransformations using HNX4 oxidase were performed on fatty alcohols with carbon lengths ranging from 8 to 16 **28-34** (Scheme 17). They were followed by colorimetric assay, which encountered difficulties due to the buffer, as described in section 2.3.1. As previously, a colorimetric assay was conducted using the TBHBA/4-AAP dye (ε = 29400 L.mol^{-1}.cm^{-1}) and HRP. The reaction was measured on a TECAN Infinite 200 Pro M Nano spectrophotometer. The absorbance data collected by the spectrophotometer was calculated using Beer-Lambert Law (Equation 1).

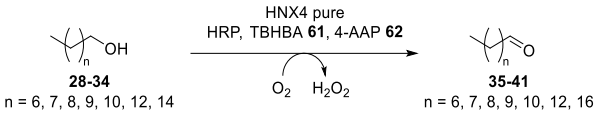

*Scheme 17 – Activity assay of HNX4 as biocatalyst for oxidation of 1 mM alkyl chain alcohols **28-34** prepared in DMSO or 1,4-dioxane with 50 µg.mL^{-1} enzyme HNX4 pure, 0.03 mg.mL^{-1} HRP, 0.75 mM 4-aminoantipyrine **62**, 2.25 mM tribromo-3-hydrobenzoic **61** at 40 °C.*

Alcohol stock solutions were prepared in DMSO for the assays. During the assay preparation, insolubility issues were noticed while preparing alcohol C_{14} **33** and C_{16} **34** stock solutions in DMSO. The solubility of C_{14} **33** and C_{16} **34** was improved when stock solutions were prepared in 1,4-dioxane. However, the alcohol stock solutions had to remain warm in non-polar solvent before being used in the absorbance assays. The difference in properties between DMSO and 1,4-dioxane didn't affect the assays. As shown in Table 8, specific activity was highest for C_{12} alcohol substrate **32** (entry 5, 105.6 mU.mg^{-1}). C_8 to C_{11} alcohols **28-31** exhibited moderate activity (entries 1-4, 30-50 mU.mg^{-1}). Similarly, C_{14} **33** and C_{16} **34** alcohols showed moderate activity (entries 6-7, 20-50 mU.mg^{-1}). These results suggested that fatty alcohols **28-34** were substrates of HNX4 but less reactive than alcohol C_{12} **32**, which had the highest specific activity, and confirmed the literature precedent.[150]

The colorimetric assays showed that alcohols **28-34** were detected as suitable substrates for HNX4 activity. However, HNX4 had low activity for carbohydrates **53-56**. Hence, HXN4 oxidase was considered a promising candidate for the treatment of fatty alcohols when combined with APG biosurfactant.

Table 8 – Specific activities of HNX4, where specific activity is the amount of product formed [µmol] per min per mg of enzyme (1 U is defined as 1 µmol.min^{-1}.mg^{-1}).

Entry	Substrate: alkyl chain C_n alcohol	Specific activity (mU.mg^{-1}) ± SD
1	**28**, C_8[a]	45.3 ± 6
2	**29**, C_9[a]	34.8 ± 1
3	**30**, C_{10}[a]	44.2 ± 6
4	**31**, C_{11}[a]	49.9 ± 3
5	**32**, C_{12}[a]	105.6 ± 25
6	**33**, C_{14}[b]	51.2 ± 10
7	**34**, C_{16}[b]	20.7 ± 6

a: stock solution was prepared in DMSO. b: stock solution was prepared in 1,4-dioxane.

Assay conditions: triplicate, 40 °C, 0.03 mg.mL^{-1} HRP, 0.75 mM 4-aminoantipyrine **62**, 2.25 mM tribromo-3-hydrobenzoic **61**, 1 mM substrate **28-34** prepared in DMSO or 1,4-dioxane, 50 µg.mL^{-1} HNX4 pure, λ = 510 nm.

2.4 Protein expression of choline oxidase AcCO6

The pET28b plasmid containing the gene for AcCO6 was provided by Heath *et al*.[70] AcCO6 was transformed into *E. coli* BL21 (DE3). The protein was expressed in Studier AIM161 by initially incubating with shaking at 30 °C for 4 h before being left at 20 °C overnight and harvested by centrifugation. Following cell lysis, AcCO6 was purified by Ni-NTA affinity column chromatography with buffer 50 mM HEPES at pH 7.5. Following the initial attempt, expressions of AcCO6 were unsuccessful by AIM and IPTG induction. Alternatively, AcCO6 CFE was purchased from Prozomix®, purified by Ni-NTA affinity column chromatography with buffer 50 mM HEPES at pH 7.5 and characterised by SDS-PAGE gel (Figure 17). Usually, Prozomix afforded protein CFE form because CFE form stabilised the protein during transport manipulation and contained 1 to 10 % of AcCO6 protein depending on the protein expression efficiency. To measure the kinetic activity of AcCO6,

AcCO6 CFE was purified by Ni-NTA affinity column chromatography with buffer 50 mM HEPES at pH 7.5. The amount of purified protein was measured by BCA assay and determined that 100 mg of CFE afforded by Prozomix contained 1.14 % of AcCO6 protein.

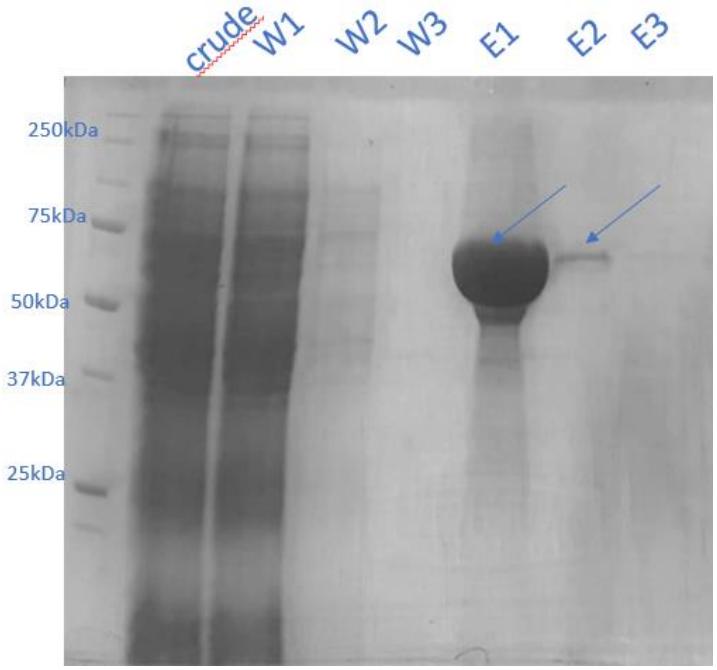

Figure 17 - SDS-PAGE gel of AcCO6 after Ni-NTA affinity chromatography column flow through (F1), wash (W1-W3) and elution fractions (E1-E3). (AcCO6 protein: 70 kDa)

2.5 Biotransformation with AcCO6

Previously, AcCO6 scope was tested on 50 primary alcohols, including aliphatic alcohols, aliphatic diols, unsaturated alcohols and aromatic alcohols.[70] The results showed that the oxidation activity of AcCO6 was generally higher than AgCO. In section 2.5.1, biocatalyst AcCO6 was used to treat alkyl monoglucosides (AMGs) **53-56** before testing aliphatic chain alcohols C_8-C_{14} **28-33** with AcCO6 (section 2.5.2).

2.5.1 Enzymatic treatment of alkyl monoglucoside (AMG) with oxidase AcCO6

The biotransformation of AMGs **53-56** was carried out using AcCO6 CFE in phosphate KPi buffer at 35 °C overnight, following the reaction conditions described in the literature (Scheme 18).[70] The

reaction results were analysed using ^{1}H NMR, and the C-6 primary alcohol oxidised to an aldehyde was easily identifiable due to the deshielding of the proton aldehyde (8.5-10 ppm).

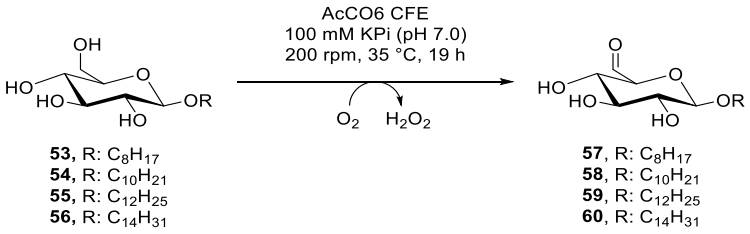

*Scheme 18 - Biotransformation of alkyl monoglucosides AMG **53-56** in presence of enzyme AcCO6. Reaction conditions: duplicate, 10 mg.mL^{-1} AcCO6 CFE, 20 mM substrate, 100 mM KPi buffer pH 7.0 at 35 °C for 19 h.*

According to the analysis conducted by ^{1}H NMR, when AMG-C8 **53** was treated with AcCO6, the C-6 position did not undergo oxidation. The protons H-6a (δ_{H6a} m, 3.91-3.84 ppm) and H-6b (δ_{H6a} m, 3.68-3.64 ppm) remained unchanged. Similar results were noticed for AMGs **54-56**. Since no aldehyde oxidation was observed, AMGs were considered not AcCO6 substrates.

2.5.2 Enzymatic treatment of functionalised fatty alcohols with oxidase AcCO6

2.5.2.1 Screening of aliphatic alcohols C_8-C_{14}

The original scope of oxidase AcCO6 toward covered saturated linear alcohols ranging from C_1 to C_{12}.[70] The colorimetric assay was reproduced as published on saturated linear alcohols with carbon length ranging from C_8 to C_{16} **28-34**. The samples were analysed on a TECAN Infinite 200 Pro M Nano spectrophotometer and evaluated using Beer-Lambert Law (Equation 1).[70]

Initially, dyeing agents TBHBA/4-AAP **61/62** were used. However, they were revealed to be incompatible with the evaluation of AcCO6 by interfering with the colorimetric reaction. Therefore, the dyeing agent was replaced by 2,2'-azino-bis(3-ethylbenzothiazoline-6-sulfonic acid) (ABTS) **64**, which is reduced by antioxidant hydrogen peroxide to a blue/green cation ABTS^{+2} **65** (Scheme

19).[70,162] 1-octanol **28** was considered as control substrate for comparison by ABTS assay as it is known to be a substrate of AcCO6.[70]

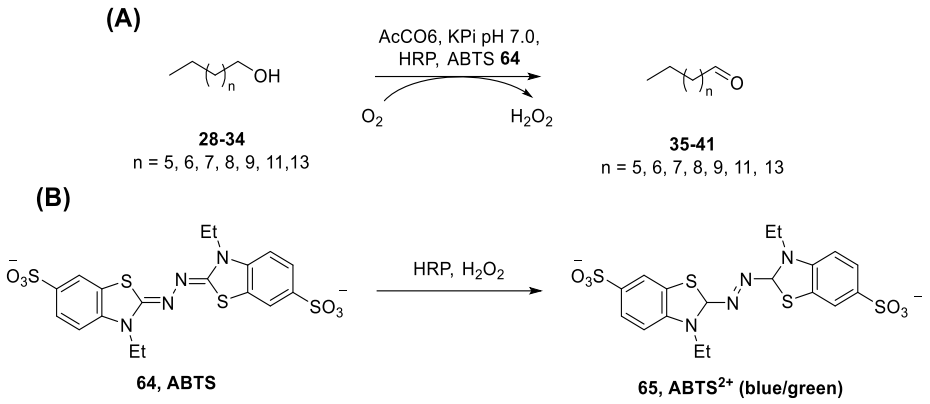

*Scheme 19 – (A) Activity assay of AcCO6 as biocatalyst for oxidation of 5 mM alkyl chain alcohols **28-34** in presence of 0.05 mg.mL^{-1} AcCO6 pure, 0.1 mg.mL^{-1} HRP, 0.7 mg.mL^{-1} ABTS at 30°C, λ = 420 nm. (B) Dye condensation during HRP assay when hydrogen peroxide was detected with ABTS **64**.*

As shown in Table 9, when the alkyl length chain alcohol was increased from C_8 to C_{12}, the enzyme activity decreased (entries 1-5). Alkyl alcohols with C14 **33** and C16 **34** had low activity and were confirmed as inadequate substrates of AcCO6 (entries 6-7). Among the alcohol series, octanol **28** was confirmed as the best substrate with a specific activity of 47 mU.mg^{-1}. This value was similar to the published value of 38 mU.mg^{-1},[70] although the differences in error calculation and laboratory practice could explained the disparities.

Table 9 - Specific activities of AcCO6, where specific activity was the amount of product formed [µmol] per min per mg of enzyme (1 U is defined as 1 µmol.min^{-1}.mg^{-1}).

Entry	Substrate: alkyl chain C_n alcohol	Specific activity (mU.mg^{-1}) ± SD
1	**28**, C_8[a]	47.8 ± 0.5
2	**29**, C_9[a]	20.5 ± 1.1
3	**30**, C_{10}[a]	13.1 ± 2.1
4	**31**, C_{11}[a]	5.9 ± 0.2
5	**32**, C_{12}[a]	6.7 ± 1.7
6	**33**, C_{14}[b]	n.d.
7	**34**, C_{16}[b]	n.d.

Assay conditions: triplicate, 30 °C, 0.5 mg.mL^{-1} HRP (stock solution: 2.0 mg.mL^{-1} HRP in 100 mM KPi pH 7.0), 0.7 mg.mL^{-1} ABTS **64** (stock solution: 2.8 mg.mL^{-1} ABTS in 100 mM KPi pH 7.0), 5 mM substrate **28-34** (stock solution: 50 mM substrate in 100 mM KPi pH 7.0 10% DMSO or in 100 mM KPi pH 7.0 10% 1,4-dioxane), 0.01 mg.mL^{-1} AcCO6 pure (stock solution: 0.05 mg.mL^{-1} AcCO6 pure in 100 mM KPi pH 7.0), λ = 420 nm. a: stock solution was prepared in DMSO. b: stock solution was prepared in 1,4-dioxane. n.d. : not detected.

The production process of alkyl polyglucosides (APG) involved using alkyl alcohols such as octanol/decanol **28**/**30** and nonanol/undecanol **29**/**31**. To investigate these alcohols further, the biotransformations of alkyl alcohols C_8 to C_{14} **28-33** and commercial mixtures of alcohols C_8/C_{10} **28/30** (44:56) and C_9/C_{11} **29/31** (35:65) were scaled up to 0.02 mmol of alcohol in the presence of catalase. Catalase was used to recycle hydrogen peroxide by-product to oxygen and analysed by GC-FID (Scheme 20).

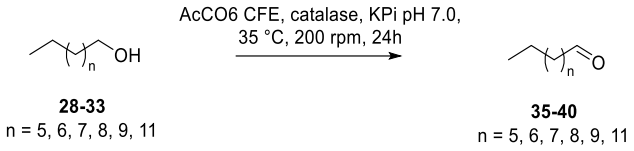

Scheme 20 – Conversion of fatty alcohols with AcCO6 CFE. Reaction conditions: triplicate, 40 mM alcohols, 10 mg.mL^{-1} AcCO6 CFE, 100 mM KPi (pH 7.0), 0.04 mg.mL^{-1} catalase, 35 °C, 200 rpm, 24 h, V_{tot} = 0.5 mL. Conversion measured by GC-FID.

As shown in Table 10, the oxidation to aldehyde from alcohol decreased as the number of carbons in the alkyl chain increased. Additionally, the bio-oxidations of individual alcohols **28-33** were also analysed by ^{1}H NMR (Figure 18), where the aldehyde proton was detected for **35-39** (δ_H 9.78 ppm, t, *J* = 1.9 Hz). An unknown impurity was detected at δ_H 9.38 ppm (s) by ^{1}H NMR. It was compared to samples of **28** alcohol and **35** aldehyde placed separately in buffer for 18 h. In an attempt to determine its origin, samples of **28** alcohol and **35** aldehyde were placed separately in buffer for 18 h and compared to the unknown impurity. However, the origin of the impurity could not be determined. Despite this impurity, biotransformations with AcCO6 were resumed without considering it. The acidic proton of carboxylic acid ($\delta_H \geq 10$ ppm) is exchangeable and serves as a marker to quantify over-oxidation pH dependent.

*Table 10 - Conversion of fatty alcohols **28-33** with AcCO6 CFE.*

Entry	Alkyl chain C_n	Alcohol (%) ± SD	Aldehyde (%) ± SD	Carboxylic acid (%) ± SD
1	**28**, C_8	2.1 ± 1.2	96.5 ± 0.9	1.3 ± 0.3
2	**29**, C_9	37.7 ± 3.6	60.6 ± 2.3	1.7 ± 1.6
3	**30**, C_{10}	33.4 ± 2.4	65.1 ± 2.2	1.5 ± 0.5
4	**31**, C_{11}	85.9 ± 1.2	13.9 ± 1.1	0.1 ± 0.1
5	**32**, C_{12}	96.7 ± 1.1	3.3 ± 1.1	0.0 ± 0.0
6	**33**, C_{14}	100 ± 0.0	0 ± 0.0	0.0 ± 0.0
7	**28**/**30**, C_8/C_{10}	67.5 (octanol: 6.8 ± 0.5; decanol: 60.7 ± 0.9)	32.2 (octanal: 24.2 ± 0.2; decanal: 8.0 ± 1.0)	0.3 (octanoic acid: 0.2 ± 0.0; decanoic acid: 0.1 ± 0.0)
8	**29**/**31**, C_9/C_{11}	71.9 (nonanol: 8.5 ± 1.2; undecanol: 63.5 ± 1.5)	28.1 (nonanal: 17.0 ± 0.4; undecanal: 11.1 ± 2.4)	0.0

Reaction conditions: triplicate, 40 mM alcohols 28-33, 10 $mg.mL^{-1}$ AcCO6 CFE, 100 mM KPi (pH 7.0), 0.04 $mg.mL^{-1}$ catalase, 35 °C, 200 rpm, 24 h, V_{tot} = 0.5 mL. Conversion measured by GC-FID.

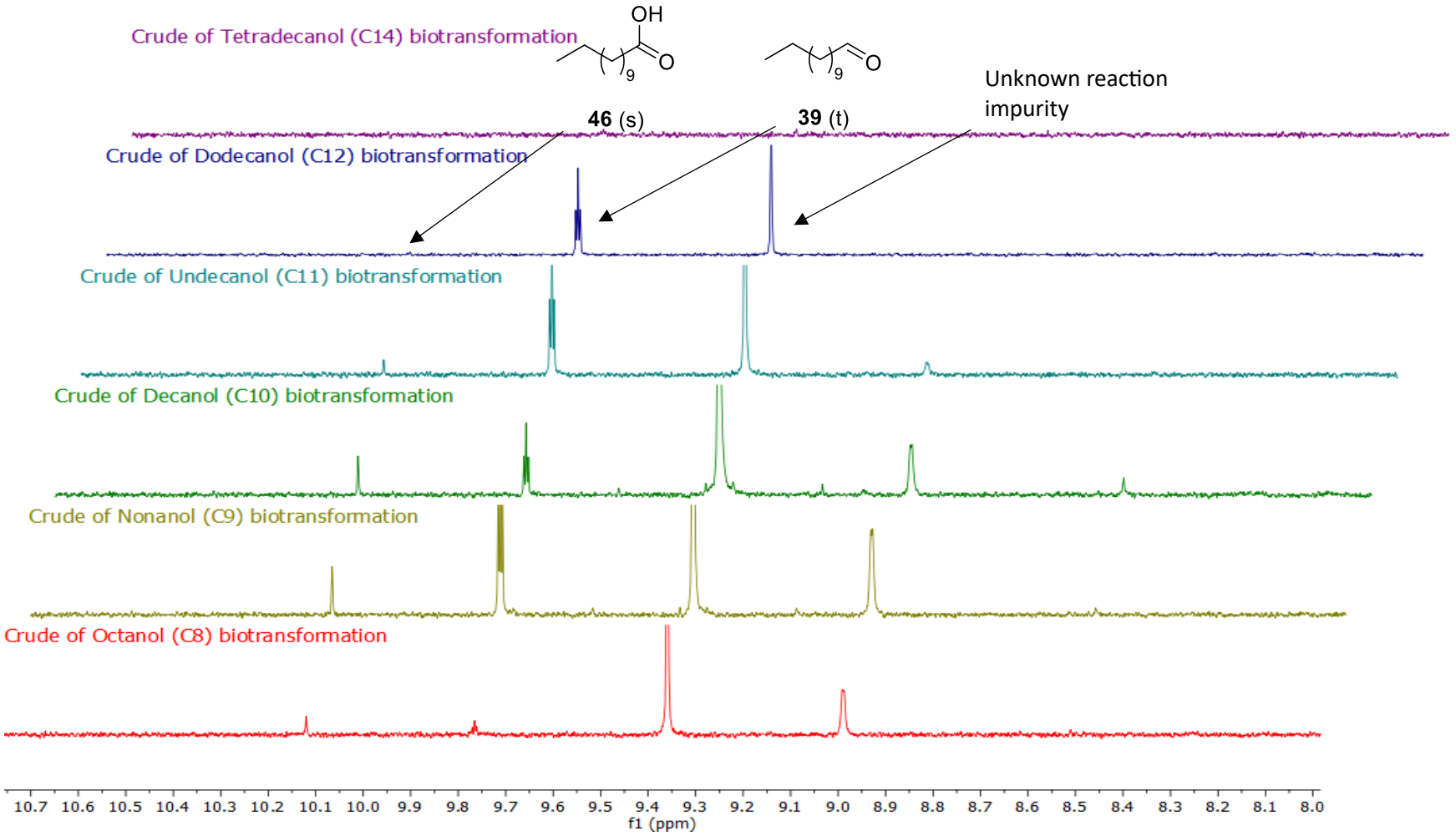

Figure 18 – ^{1}H NMR (400 MHz, $CDCl_3$) spectra of C_8-C_{14} fatty alcohols bio-oxidised with choline oxidase AcCO6: 10 ppm (s) carboxylic acid; 9.76 ppm (t) aldehyde; 9.35 ppm (s) unknown product.

The results of GC-FID and ^{1}H NMR confirmed that oxidation of the saturated alcohols **28-33** decreased as the carbon chain length increased from 8 to 14 carbons. The formation of aldehyde **35-39** and carboxylic acids conversion **42-45** (0 to 2 %, Table 10). Knowingly that FAD-AOx is able to oxidise alcohol to aldehyde, the presence of carboxylic acids confirmed the phenomenon of over-oxidation observed in the literature. [118,119]

After 24 h bio-oxidation reaction (entry 7, Table 10), the ratio mixture (**28**/**30**)/products changed to (6.8:60.7:32.5). When alcohols C_8 **28** and C_{10} **30** were treated separately, less alcohols remained (**28**/products 2.1:87.9; **30**/products 33.4:66.6). The biotransformation process of the mixture C_8/C_{10} (**28**/**30**) appeared to favour the oxidation of octanol **28** before the longer one, decanol **30**. As shown during the specific activity assay (Table 9) and 0.02 mmol scale up biotransformation (Table 10), AcCO6 first oxidised the shorter substrate, octanol **28**, indicating it is the preferred substrate of the alkyl alcohol **28-34**.

2.5.2.2 Kinetic parameters

As shown previously, promising results were obtained through the oxidation of two alcohols (**28** and **30**) using AcCO6 CFE as biocatalyst. Therefore, AcCO6 CFE was purified using a Ni-NTA column and concentrated by centrifugation. Subsequently, the pure batch of AcCO6 was measured by a Thermo Scientific Nanodrop 1000 to evaluate the kinetic parameters of AcCO6 with octanol **28** and decanol **30**. This evaluation enabled the study of enzyme-catalysed rates using the Michaelis-Menten equation and Lineweaver-Burk equation (Equation 2). Based on this analysis, the following parameters of AcCO6 were determined:

- K_M is the substrate concentration at which the reaction velocity is half of the maximum velocity. The lower the K_M, the higher the affinity of an enzyme for its substrate.
- V_{max} is the reaction rate when the substrate fully saturates the enzyme.
- k_{cat} is the turnover number, the number of times each enzyme site converts the substrate to product per unit time. The higher is k_{cat}, the faster an enzyme catalyses a reaction.

- Catalytic efficiency (k_{cat}/K_M) is the rate constant of the reaction when the enzyme is mostly free at a low concentration of the substrate. The higher the ratio, the higher rate of the reaction.

$$(A)\ \vartheta_0 = \frac{V_{max} \times [S]}{K_M + [S]} \qquad (B)\ \frac{1}{\vartheta} = \frac{[S]}{V_{max} \times [S]} + \frac{1}{V_{max}} \quad \rightarrow \quad V_{max} = k_{cat} \times [E_t]$$

Equation 2 – (A) Michalis-Menten equation (B) Lineweaver-Burk equation. v_0: initial reaction rate, K_M: Michaelis constant, V_{max}: maximum velocity, [S]: substrate concentration, k_{cat}: turnover number, $[E_t]$: total amount of enzyme.

The following results were repeated by other members of the Group to confirm the kinetic parameters of AcCO6 (Table 11). To provide clarity for the reader, their kinetics curves of AcCO6 activity on saturated alcohols C_8 to C_{11} **28-31** were included in Figure 19.

Table 11 – Kinetic parameters of choline oxidase variant AcCO6 with 1-octanol and 1-decanol.

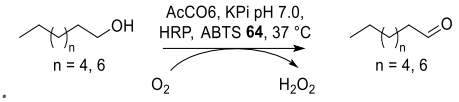

Substrate	**V_{max} ($\mu M.min^{-1}$)**	**K_M (mM)**	**k_{cat} (s^{-1})**	**k_{cat}/K_M ($s^{-1}.mM^{-1}$)**
28, Octanol	64.2 ± 12.8	34.6 ± 9.4	0.037	0.63
29, Decanol	26.2 ± 5.0	38.6 ± 9.9	0.015	0.02
Assay conditions: triplicate, 2.0 $mg.mL^{-1}$ AcCO6 pure, 0.1 $mg.mL^{-1}$ HRP (stock solution: 0.4 $mg.mL^{-1}$ HRP in 500 mM KPi pH 7.0), 0.7 $mg.mL^{-1}$ ABTS, (64-0.7 mM) substrate **28-29**, 37 °C, λ 420 nm.				

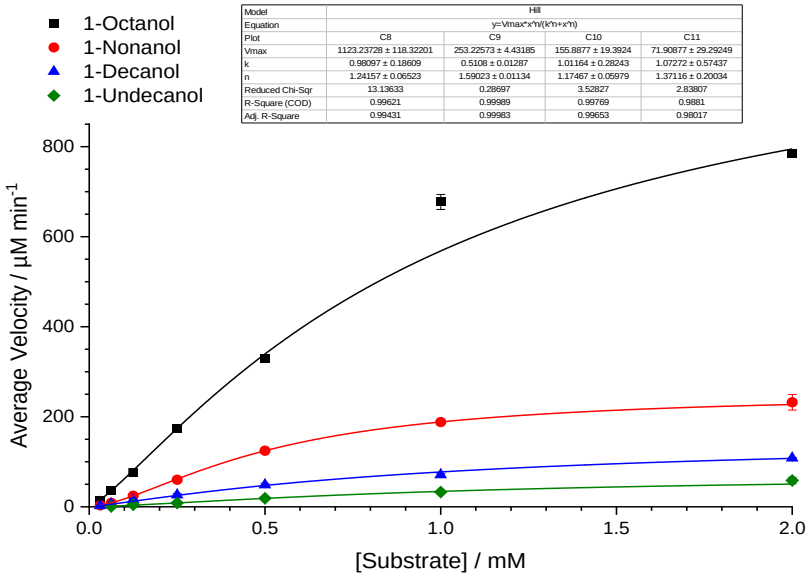

Model	Hill			
Equation	y=Vmax*x^n/(k^n+x^n)			
Plot	C8	C9	C10	C11
Vmax	1123.23728 ± 118.32201	253.22573 ± 4.43185	155.8877 ± 19.3924	71.90877 ± 29.29249
k	0.98097 ± 0.18609	0.5108 ± 0.01287	1.01164 ± 0.28243	1.07272 ± 0.57437
n	1.24157 ± 0.06523	1.59023 ± 0.01134	1.17467 ± 0.05979	1.37116 ± 0.20034
Reduced Chi-Sqr	13.13633	0.28697	3.52827	2.83807
R-Square (COD)	0.99621	0.99989	0.99769	0.9881
Adj. R-Square	0.99431	0.99983	0.99653	0.98017

*Figure 19 – Kinetic curves of choline oxidase variant AcCO6 with 1-octanol **28** (black) and 1-decanol **30** (blue)*

During the assays, inhibitory effects were observed when the substrate concentrations were above 32 mM (Table 11). The K_M values for octanol **28** and decanol **30** were comparable at 34.6 mM and 38.6 mM, respectively. However, the KM values determined that octanol **28** had a better affinity for the active site of AcCO6 than decanol **30**. The kcat value for octanol **28** (0.037 s^{-1}) was twice as high as decanol **30** (0.015 s^{-1}), indicating the turnover of octanol **28** was converted to an aldehyde product by AcCO6 faster than decanol **30**. Based on these observations, the catalytic efficiency (k_{cat}/K_M) of octanol **28** (0.63 $s^{-1}.mM^{-1}$) was six times higher than decanol **30** (0.02 $s^{-1}.mM^{-1}$). This suggested that AcCO6 was more efficient in converting octanol **28** than decanol **30**, which can explain the results observed for fatty alcohol oxidation in Table 10.

2.5.2.3 Biotransformation of octanol and decanol with AcCO6: analysis by ^{1}H NMR

The kinetic parameters of AcCO6 oxidase showed favourable affinities for octanol **28** and decanol **30,** respectively. Therefore, the reaction conditions for the bio-oxidation of octanol **28** and decanol **30** were explored and analysed using ^{1}H NMR. Their reaction conditions were optimised with 10 $mg.mL^{-1}$ AcCO6 CFE (Scheme 21). The AcCO6 CFE stock solution used in this thesis was not

centrifuged before being utilised. Centrifugation would have isolated non-water soluble elements and reduced the presence of lysate impurities in the reaction solution.

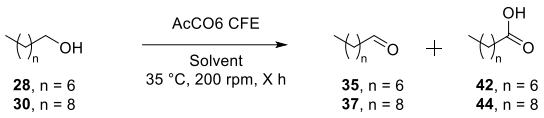

*Scheme 21 – Oxidation of octanol **28** and decanol **30** with AcCO6 CFE. Reaction conditions: triplicate, 10 mg.mL^{-1} AcCO6 CFE, alcohol (0.01-0.02 mmol), 100 mM KPi (pH 8.0), 35 °C, 200 rpm, V_{tot} = 0.5 mL*

The variation of alcohol concentrations was explored and approximated close to K_M values (20 mM, 40 mM) in phosphate buffer pH 8.0. Additionally, the influence of co-solvents (toluene, EtOAc, cyclohexane, hexane, %*v/v*: 20, 50) and acidity of phosphate buffer (pH 6.0, 7.0, 8.0) were also examined (Table 12).

Octanol **28** and decanol **30** were independently oxidised with AcCO6 for 24 h under the same reaction conditions. After the reaction, only a small amount of octanol remained (**28**: 20 mM, 26 %, entry 1), while half of decanol **30** remained (**30**: 20 mM, 49 %, entry 14). Octanol **28** was oxidised faster than decanol **30**, which was consistent with the kinetic parameters and alkyl-length chain substrate observed in the literature.[70] A substrate concentration of 20 mM alcohol was considered optimal for the screening by ^{1}H NMR due to the rapid consumption of substrate.

The following experiments were stopped and analysed after 4.5 h to decrease the screening time. The aim was to compare the presence of co-solvent (toluene, EtOAc, cyclohexane, hexane)[70] during biotransformation versus within phosphate buffer pH 8.0. The use of a co-solvent provided a two-layer system that could enhance the partition of the aldehyde product into the organic phase. However, after 4.5 h reaction time, a significant amount of starting material (25-50 %, **28**: entries 4-12, **30**: entries 16-23) remained regardless of the solvent used and its proportion (%*v*/*v*: 10, 20, 50). This was unexpected, as non-polar solvents, such as hexane and cyclohexane,

were expected to enhance the bio-oxidation of **28** or **30**, but instead left 50-70 % of the starting material. In contrast, reactions in KPi buffer left less starting material (**28**: 26 % entries 9-12, **30**: 49 % entries 20-23). These results contradicted the literature precedent, as 50 *%v/v* cyclohexane was shown to increase the oxidation of hexanol with AcCO6 by 20 % compared to reactions in KPi buffer.[70] The use of toluene and EtOAc (entries 4-8 and 16-19) resulted in more remaining alcohols than reaction without co-solvent (entries 3 and 15). In conclusion, none of the co-solvents improved alcohol oxidation and co-solvent systems were not considered further.

*Table 12 - ^{1}H NMR results of octanol **28** and decanol **30** remaining after bio-oxidation with AcCO6.*

Entry	Alcohol	Alcohol conc.	pH and Co-solvent	Reaction time	Alcohol remaining (%) ± SD
1	**28**	20 mM	pH 8.0	24 h	26 ± 0
2	**28**	40 mM	pH 8.0	24 h	44 ± 4
3	**28**	20 mM	pH 8.0	4.5 h	42 ± 11
4	**28**	20 mM	pH 8.0; toluene 20 %*v/v*	4.5 h	47 ± 2
5	**28**	20 mM	pH 8.0; toluene 50 %*v/v*	4.5 h	75 ± 36
6	**28**	20 mM	pH 8.0; EtOAc 10 %*v/v*	4.5 h	24 ± 34
7	**28**	20 mM	pH 8.0; EtOAc 20 %*v/v*	4.5 h	42 ± 11
8	**28**	20 mM	pH 8.0; EtOAc 50 %*v/v*	4.5 h	50 ± 0
9	**28**	20 mM	pH 8.0; cyclohexane 20 %*v/v*	4.5 h	46 ± 1
10	**28**	20 mM	pH 8.0; cyclohexane 50 %*v/v*	4.5 h	49 ± 0
11	**28**	20 mM	pH 8.0; hexane 20 %*v/v*	4.5 h	45 ± 1
12	**28**	20 mM	pH 8.0; hexane 50 %*v/v*	4.5 h	49 ± 1
13	**30**	20 mM	pH 8.0	24 h	49 ± 1
14	**30**	40 mM	pH 8.0	24 h	49 ± 1
15	**30**	20 mM	pH 8.0	4.5 h	49 ± 0
16	**30**	20 mM	pH 8.0; toluene 20 %*v/v*	4.5 h	50 ± 0
17	**30**	20 mM	pH 8.0; toluene 50 %*v/v*	4.5 h	50 ± 0
18	**30**	20 mM	pH 8.0; EtOAc 20 %*v/v*	4.5 h	50 ± 0
19	**30**	20 mM	pH 8.0; EtOAc 50 %*v/v*	4.5 h	83 ± 29
20	**30**	20 mM	pH 8.0; cyclohexane 20 %*v/v*	4.5 h	50 ± 0
21	**30**	20 mM	pH 8.0; cyclohexane 50 %*v/v*	4.5 h	50 ± 0
22	**30**	20 mM	pH 8.0; hexane 20 %*v/v*	4.5 h	50 ± 0
23	**30**	20 mM	pH 8.0; hexane 50 %*v/v*	4.5 h	50 ± 0

Reaction conditions: triplicate, 10 mg.mL^{-1} AcCO6 CFE, alcohol (0.01-0.02 mmol), 100 mM KPi (pH 8.0), 35 °C, 200 rpm, V_{tot} = 0.5 mL. Conversion measured by ^{1}H NMR.

The reactions presented in Table 12 were attempted using AcCO6 CFE, in contrast to the literature, which used purified AcCO6. Alternatively, the reactions should be redone with purified enzymes.

The screening by ^{1}H NMR analysis revealed that choline oxidase AcCO6 could efficiently oxidise alcohol at lower concentrations (20 mM) than K_M (**28**: 34.6 mM; **30**: 38.6 mM) in KPi buffer. However, the enzyme was less active in a co-solvent system. The presence of an organic solvent was observed to slow down the enzyme activity. The data collected by ^{1}H NMR and GC-FID were found to have an error level of 10-fold. GC-FID was primarily used for biotransformation analysis in this chapter due to the lack of adequate error analysis through ^{1}H NMR.

2.5.2.4 Biotransformation of octanol and decanol with AcCO6: analysis by GC-FID

As shown in Scheme 22, biotransformation of octanol **28** and decanol **30** using AcCO6 CFE in KPi buffer with pH variations was performed and analysed by GC-FID (Table 13).

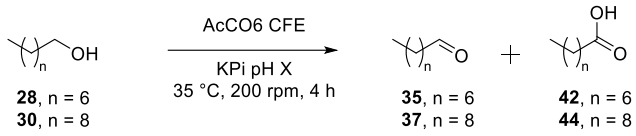

*Scheme 22 – Biotransformation of octanol **28** and decanol **30** with AcCO6 CFE. Reaction conditions: triplicate, 10 mg.mL^{-1} AcCO6 CFE, 20 mM alcohol (0.01 mmol), 100 mM KPi, 35 °C, 200 rpm, for 4 h, V_{tot} = 0.5 mL.*

After 4 h reaction period (Table 13), carboxylic acids **42** and **44** were not detected by GC-FID, indicating that over-oxidation did not occur. During the 4 h reaction (Table 13), decanol **30** was oxidised into decanal **37** using AcCO6. The conversion rate was better in 100 mM KPi buffer with a pH of 7.0 (entry 5, **37**: 31.7%) compared to 100 mM KPi buffer with a pH of 6.0 (entry 4, **37**: 19.3%) and pH 8.0 (entry 6, **37**: 19.1%). Under similar reaction conditions, octanol **28** was converted into aldehyde **35** identically in 100 mM KPi buffer pH 6.0 (**35**: 28.4 %, entry 1) and pH 7.0 (**35**: 27.9 %, entry 2) but decreased to **35** 18.2 % in pH 8.0. Octanol **28** and decanol **30** had different optimum reaction conditions (**28**: 100 mM KPi buffer pH 6.0; **30**: 100 mM KPi buffer pH 7.0). However, this project aimed to oxidise octanol **28** and decanol **30** as a commercial mixture **28/30** used for APG glycosylation. Therefore, reaction conditions were required to be identical for both substrates. The

optimum solvent for bio-oxidation of octanol **28** and decanol **30** was evaluated in 100 mM phosphate KPi buffer pH 6.0-7.0.

Table 13 – Effect of solvent variation on alcohol conversion using AcCO6 CFE.

Entry	Alcohol	Reaction solvent and co-solvent	Alcohol remaining (%) ± SD	Conversion to aldehyde (%) ± SD
1	**28**	100 mM KPi pH 6.0	71.6 ± 1.5	28.4 ± 1.5
2	**28**	100 mM KPi pH 7.0	72.1 ± 3.1	27.9 ± 3.1
3	**28**	100 mM KPi pH 8.0	81.8 ± 5.1	18.2 ± 5.1
4	**30**	100 mM KPi pH 6.0	80.7 ± 6.7	19.3 ± 6.7
5	**30**	100 mM KPi pH 7.0	68.6 ± 0.6	31.7 ± 0.6
6	**30**	100 mM KPi pH 8.0	80.9 ± 1.0	19.1 ± 1.0
Reaction conditions: triplicate, 10 mg.mL^{-1} AcCO6 CFE, 20 mM alcohol (0.01 mmol), 100 mM KPi, 35 °C, 200 rpm, for 4 h, V_{tot} = 0.5 mL. Conversion measured by GC-FID.				

The biotransformations of octanol **28** and decanol **30** were carried out at 35 °C in 100 mM KPi buffer pH 6.0-7.0. During the bio-oxidation process, oxygen was converted into hydrogen peroxide, which was then recycled back into oxygen using catalase in order to minimise oxygen usage (Scheme 23).[70,119,163] To achieve maximum alcohol conversion, the reaction time was increased from 4.5 h to 24 h and alcohol concentrations were varied close to KM values (20 mM, 40 mM).

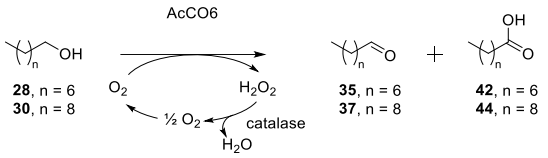

*Scheme 23 - In vitro recycling of oxygen-mediated reduction of fatty alcohols **28,30** to aldehydes **35,37.** Reaction conditions: triplicate, 10 mg.mL^{-1} AcCO6 CFE, 20 mM alcohol (0.01-0.03 mmol), 100 mM KPi, 35 °C, 200 rpm, for 24 h, V_{tot} = 0.5 mL.*

After 24 h reaction (Table 14), the biotransformation process of 20 mM octanol **28** using AcCO6 was completed with catalase in KPi pH 6.0 and 7.0 (entries 1-4). A control reaction was conducted without catalase, resulting in complete octanol oxidation. Similarly, biotransformation of decanol **30** was carried out using catalase alongside a control reaction without catalase. After analysis, catalase had increased the conversion of 20 mM decanol **30** to 30 % in 100 mM KPi pH 6.0 (entries 9-10) and remained unchanged in pH 7.0 (entries 11-12). When catalase was added for biotransformation of 20 mM alcohols, over-oxidation to octanoic acid **42** and decanoic acid **44** increased to 10-20 % (entries 2, 10 and 12). The phenomenon of overoxidation proved that bio-oxidation was excessively rapid and led to the formation of undesired acids **42** and **44**. Therefore, the alcohol concentration was increased to saturate the enzyme more on substrate (40 mM), which is a closer value to K_M with AcCO6.

Table 14 - Biocatalysis results after 24 h and variation of alcohol concentration in presence and absence of catalase with AcCO6 CFE.

Entry	Alcohol	Alcohol conc.	100 mM KPi	Catalase (mg.mL^{-1})	Alcohol remaining (%) ± SD	Conversion Aldehyde (%) ± SD	Conversion C. acid (%) ± SD
1	**28**	20 mM	pH 6.0	-	0.6 ± 0.6	97.9 ± 0.4	1.4 ± 0.5
2	**28**	20 mM	pH 6.0	0.04	0 ± 0.0	67.9 ± 1.9	32.1 ± 1.9
3	**28**	20 mM	pH 7.0	-	0 ± 0.0	98.6 ± 0.2	1.4 ± 0.2
4	**28**	20 mM	pH 7.0	0.04	0 ± 0.0	96.9 ± 0.4	3.1 ± 0.4
5	**28**	40 mM	pH 6.0	-	12.6 ± 10.9	86.7 ± 10.7	0.7 ± 0.2
6	**28**	40 mM	pH 6.0	0.04	4.1 ± 1.5	82.5 ± 0.3	14.4 ± 1.3
7	**28**	40 mM	pH 7.0	-	15.2 ± 17.0	84.2 ± 16.7	0.6 ± 0.4
8	**28**	**40 mM**	**pH 7.0**	**0.04**	**2.2 ± 1.2**	**96.5 ± 0.9**	**1.3 ± 0.3**
9	**30**	20 mM	pH 6.0	-	44.2 ± 17.4	52.7 ± 16.8	3.1 ± 0.6
10	**30**	20 mM	pH 6.0	0.04	14.7 ± 20.0	61.4 ± 12.7	23.9 ± 7.4
11	**30**	20 mM	pH 7.0	-	22.8 ± 9.4	70.3 ± 6.6	6.9 ± 2.9
12	**30**	20 mM	pH 7.0	0.04	23.8 ± 16.7	49.4 ± 6.2	26.9 ± 14.6
13	**30**	40 mM	pH 6.0	-	58.0 ± 4.5	41.1 ± 3.9	0.9 ± 0.6
14	**30**	40 mM	pH 6.0	0.04	21.8 ± 2.2	70.4 ± 1.8	7.8 ± 0.6
15	**30**	40 mM	pH 7.0	-	31.2 ± 4.5	65.1 ± 4.1	3.7 ± 0.5
16	**30**	**40 mM**	**pH 7.0**	**0.04**	**33.4 ± 2.4**	**65.1 ± 2.2**	**1.5 ± 0.5**

Reaction conditions: triplicate, 10 mg.mL^{-1} AcCO6 CFE, 20 mM alcohol (0.01-0.03 mmol), 100 mM KPi, 35 °C, 200 rpm, for 24 h, V_{tot} = 0.5 mL.. Conversion measured by GC-FID.

Octanol **28** and decanol **30** were oxidised with biocatalyst AcCO6 at a substrate concentration of 40 mM in 100 mM KPi buffer (pH 7.0) and catalase (0.04 mg.mL^{-1}). GC analysis showed that under these conditions, there was minimal over-oxidation to carboxylic acid (≈1 % octanoic acid **42**, ≈1.5 % decanoic acid **44**) and maximum conversion to aldehyde (≈96 % octanal **35**, ≈65 % decanal **37**). Therefore, the optimal reaction conditions for the bio-oxidation of **28** and **30** were established as follows: 10 mg.mL^{-1} AcCO6 CFE, 100 mM KPi (pH 7.0), 0.04 mg.mL^{-1} catalase, 35 °C, 200 rpm, 24 h.

2.6 Protein immobilisation of oxidases

The thesis aims to transition to sustainable production of APG surfactant by pursuing enzyme recycling through protein immobilisation. The process involves the immobilisation of oxidases HNX4 and AcCO6 in an attempt to recycle biocatalysts. Protein immobilisation is a method to stabilise and reuse a protein multiple cycles before becoming inactive.

2.6.1 Protein immobilisation of HNX4 on Purolite® ECR8285 carrier

Oxidase HNX4 from an uncultured marine euryarchaeota was discovered in 2022 by Rembeza *et al*.[150] As there were no previous reports on the immobilisation protocol of HNX4, immobilisation of HNX4 was attempted on epoxy butyl methylacrylate ECR8285, a non-enzyme selective carrier, using HNX4 CFE. This process was performed using 100 mM sodium phosphate buffer pH 8.0 with 300 mM NaCl in a ratio of 250 mg HNX4 CFE for 1.80 g resin. The success of the immobilisation was confirmed by performing an SDS-PAGE gel (Figure 20).

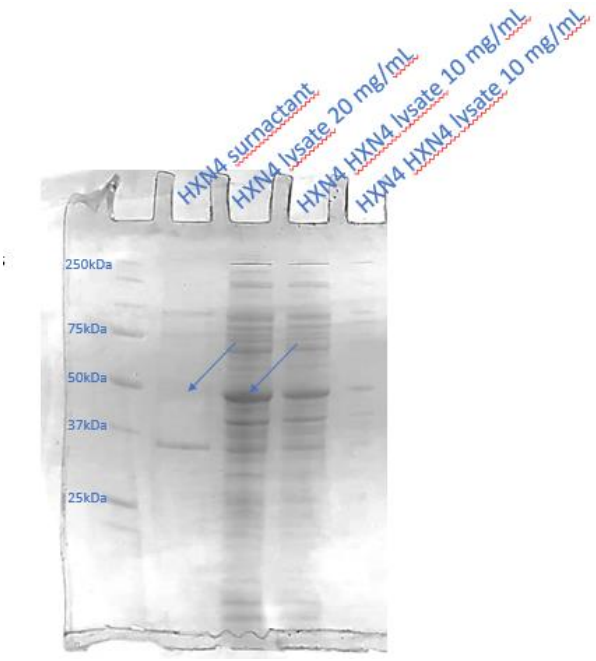

Figure 20 – SDS-PAGE gel of HNX4 after immobilisation on epoxy butyl methylacrylate ECR8285.

(HNX4 protein: 56.2 kDa)

Based on the supplier's information, epoxy butyl methylacrylate ECR8285 can immobilised until 10 % protein of its mass. The SDS-PAGE gel (Figure 20) did not show the presence of an HXN4 protein band, which led to the assumption that 1.80 g of ECR resin can immobilise a maximum of 180 mg of HXN4. After immobilisation, immobilised HNX4 was used as a biocatalyst to oxidise dodecanol **32** in HEPES buffer pH 8.0 at 37 °C (Scheme 24). The temperature was decreased to 37 °C compared to the previous section (40 °C), based on the literature precedent.[150]

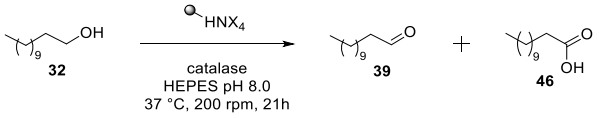

*Scheme 24 – Oxidation of dodecanol **32** with immobilised HNX4 on epoxy resin ECR8285. Reaction conditions: triplicate, 20 g.L^{-1} immobilised HNX4 (100 mg support), 40 mM dodecanol **32** (0.04 mmol), 80 mM HEPES (pH 8.0), 0.1 mg.mL^{-1} catalase, 37 °C, 200 rpm, 21 h, V_{tot} = 0.5 mL.*

The analysis by GC-FID showed the absence of C_{12} alcohol **32** and the presence of C_{12} aldehyde **39** (59 %) and C_{12} carboxylic acid **46** (41 %), confirming that the immobilisation of HXN4 on ECR8285 was partially successful. However, the chromatogram (Figure 21) indicated that all the peaks of C_{12} alkyl species (**32**, **39** and **46**) had low intensity (≤ 25 pA), indicating low confidence in data accuracy. Due to the detection limit of the GC equipment, the results would need to be confirmed by scaling up the oxidation reaction to a minimum of 0.1 mmol alcohol. Scaling up the reaction would afford products with higher yield, higher peak intensity by GC analysis and more reliable GC analysis.

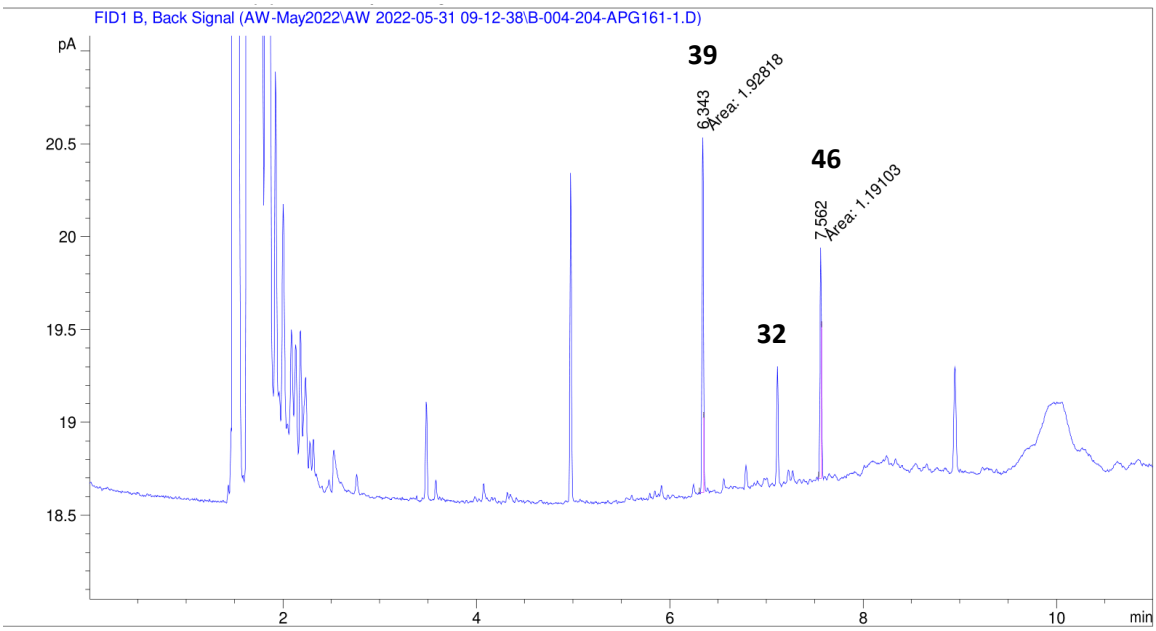

*Figure 21 – Chromatogram of 1-dodecanol **32** biotransformation with HNX4 immobilised on epoxy resin ECR8285. (**39**) dodecanal (**32**) 1-dodecanol (**46**) dodecanoic acid*

The protein HXN4 was challenging to express in AIM, but enough amount was produced to identify its enzymatic activity toward C_8-C_{16} alkyl chain alcohols **28-34** and AMG alcohols **53-56**. The enzyme was then immobilised in a non-selective protein carrier ECR8285 and used as a biocatalyst to perform the biotransformation of dodecanol **32**, which was analysed by GC. Unfortunately, the difficulties in expressing and obtaining HXN4 oxidase were not overcome. Therefore, HXN4 was not investigated further in this thesis for the treatment of APGs surfactant.

2.6.2 Protein immobilisation of AcCO6: carriers ECR8285, EziG Amber and ECR8309F

According to the literature, the engineered oxidase AcCO6 was successfully immobilised on Purolite epoxybutyl methacrylate beads (ECR8285).[164] Immobilised AcCO6 was reported to achieve good conversions (>78 %) of aliphatic primary alcohols (fatty alcohols, phenolic compounds). However, no immobilisation of AcCO6 on EziG carriers, known to immobilise His-tagged enzymes, was reported.

First, the immobilisation of AcCO6 on epoxy resin ECR8285 was achieved with AcCO6 CFE in an equilibration buffer (100 mM sodium buffer pH 8.0, 300 mM NaCl) for 2 days (ratio 250 mg lysate AcCO6 for 1.80 g of resin) according to the supplier guidelines.[165] Secondly, immobilisation on EziG Amber (semi-hydrophilic surface) was proceeded over 30 min, with a ratio of protein/resin recommended by the supplier (ratio: 100 mg lysate AcCO6 for 90 mg of resin).[166]

- **Simultaneous biotransformation of octanol with AcCO6 immobilised on carrier epoxy methacrylate ECR8285 and carrier EziG Amber**

After the enzyme immobilisation, a biotransformation process was carried out on 40 mM octanol **28** (0.02 mmol). The octanol oxidation was simultaneously performed using AcCO6 immobilised on ECR8285 and AcCO6 immobilised on EziG Amber (Scheme 25). The resulting samples were evaluated by GC and compared to the previous results with AcCO6 CFE (Table 15). The immobilised proteins were easier to separate from the reaction products by simply pipetting the reaction solution to a new vial before extraction. In contrast, CFE protein biotransformation had to be quenched before extraction, risking pipet protein pellet impurities. The immobilised protein beads were subsequently washed, dried and ready for reuse.

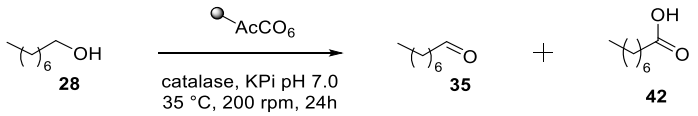

*Scheme 25 – Oxidation of octanol with immobilised AcCO6 (ECR8285 or EziG). Reaction conditions: 100 mg AcCO6 immobilised, 40 mM octanol **28** (0.02 mmol), 100 mM KPi (pH 7.0), 0.1 mg.mL^{-1} catalase, 35 °C, 200 rpm, 24 h, V_{tot} = 0.5 mL.*

After 24 h reaction (Table 15), oxidation of octanol **28** with AcCO6 ECR8285 showed 74 % alcohol conversion, whereas AcCO6 CFE had a higher conversion of 90 % (entries 1 and 2, Table 15). However, when AcCO6 EziG was used, only a 5 % conversion of alcohol **28** (entry 3, Table 15). In the presence of catalyst AcCO6 ECR8285, the amount of carboxylic acid **42** (2–6 %) was higher than AcCO6 used in CFE form (entry 1-3, Table 15). The biotransformations with immobilised AcCO6

occurred slower than the ones with AcCO6 CFE, which explains the lower alcohol conversion. Therefore, over-oxidation would also occurred slowly with an immobilised catalyst. In summary, the oxidation of octanol **28** with AcCO6 CFE had the highest conversion rate compared to both immobilised catalysts. Due to the weak activity of AcCO6 EziG, the EziG Amber carrier was not considered further.

*Table 15 – Results of oxidation of octanol **28** with immobilisation of AcCO6 on solid-support (ECR8285 or EziG) compared to AcCO6 CFE.*

Entry	Biocatalyst	Alcohol 28 (%) ± SD	Aldehyde 36 (%) ± SD	Acid carboxylic 42 (%) ± SD
1	AcCO6 CFE	2.2 ± 1.2	96.5 ± 0.9	1.3 ± 0.3
2	AcCO6 immobilised on epoxy resin ECR8285	25.7 ± 1.0	67.1 ± 0.0	7.1 ± 1.0
3	AcCO6 immobilised on EziG Amber	94.7 ± 0.7	4.3 ± 0.5	1.0 ± 0.4
4	AcCO6 CFE at 50 °C **(individual replicates shown)**	1) 7.1 2) 28 3) 39	1) 92.9 2) 71.8 3) 60.8	1) 0 2) 0 3) 0
5	AcCO6 immobilised on epoxy resin ECR8285 at 50 °C	49.9 ± 0.0	40.6 ± 0.0	0 ± 0.0

Reaction conditions: triplicate, 100 mg AcCO6 immobilised or 10 $mg.mL^{-1}$ AcCO6 CFE, 40 mM octanol (0.02 mmol), 100 mM KPi (pH 7.0), 0.1 $mg.mL^{-1}$ catalase, 35 °C, 200 rpm, 24 h, triplicate, V_{tot} = 0.5 mL. Conversion measured by GC-FID.

Oxidase AcCO6 was reported to be denatured at temperatures ≥ 42 °C.[84] Meanwhile, immobilised proteins were reported to remain stable at higher temperatures compared to their CFE

form.[70,123,130,164] To verify this theory about AcCO6 catalyst, a test reaction at 50 °C was carried in triplicate with AcCO6 ECR8285 and compared to AcCO6 CFE. After 24 h reaction, oxidation at 50 °C with CFE AcCO6 (entry 4, Table 15) did not provide repeatable triplicate, which delivered irregular activity between the replicates. Meanwhile, oxidation at 50 °C with AcCO6 on solid-support ECR8285 remained stable (entry 5, Table 15).

- **Relative activity of AcCO6 immobilised on ER8285**

After each biotransformation of octanol **28** was performed with catalyst AcCO6 ECR8285, the relative activities of AcCO6 immobilised on epoxy resin ECR8285 were determined and calculated with Equation 3.

$$Activity\ yield\ (\%) = \frac{specific\ activity\ (immobilised\ enzyme)}{specific\ activity\ (free\ enzyme)} \times 100\ \%$$

$$= \frac{sum\ of\ products\ (aldehyde, acid) with\ AcCO6\ immobilised}{sum\ of\ products\ (aldehyde, acid)\ with\ AcCO6\ CFE\ lyophilised} \times 100\ \%$$

*Equation 3 – Equation of relative activity yield of octanol **28** oxidation with AcCO6 immobilised on ECR8285*

The experiment involved using epoxy resin ECR8285 as a carrier for AcCO6 to convert octanol **28** during the first cycle (Figure 22). The results were encouraging with more than 70 % conversion achieved. The same batch of AcCO6 was then reused for eight cycles under the same conditions. However, its activity levels decreased gradually, with the conversion rate dropping to 50-34 % in the first five cycles before reaching a maximum of 32 %. This decline in activity was attributed to the enzyme unbinding from the support surface (known as the "leaching effect"), which diminished the enzyme's active lifetime and limited its reusability. Despite this decline in activity, epoxy resin ECR8285 was deemed a suitable carrier of AcCO6 in terms of relative activity, and further research was recommended to investigate its potential as a biocatalyst for removing alcohol solvent from APGs surfactant. Future studies could explore other immobilisation procedures, carriers, activity yields, loading yields and thermostability tests.

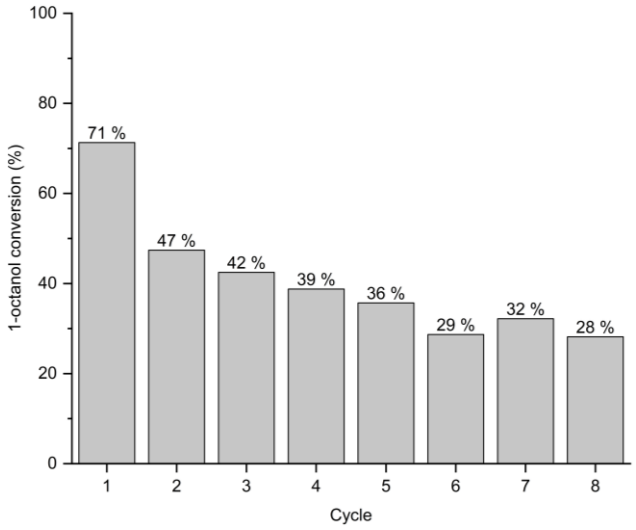

*Figure 22 – Relative activity yield of octanol **28** oxidised with AcCO6 immobilised by epoxy resin ECR8285 after 24 h. Conversion analysed by GC-FID.*

- **AcCO6 immobilised ECR8309F**

After pre-activating amino resin ECR8309F with 2 % glutaraldehyde solution, AcCO6 CFE was immobilised on resin ECR8309F (ratio 0.50 g AcCO6 CFE for 4.5 g of resin) as described in the supporting information. The immobilisation was tested with a colorimetric ABTS/HRP that involved the biotransformation of 40 mM octanol **28** (0.02 mmol) with 100 mg AcCO6 ECR8309F placed in 1.5 mL vial with 1.0 $mg.mL^{-1}$ HRP and 1.3 $mg.mL^{-1}$ ABTS, shaken at 200 rpm at 37 °C for 1 h. The reaction tube appeared visually unchanged, indicating no hydrogen peroxide production was observed. Therefore, no biotransformation occurred with the batch of AcCO6 ECR8309F used. Nevertheless, a supplementary reaction on octanol **28** with AcCO6 ECR8309F was performed for 3 h and 4 days and analysed by GC-FID.

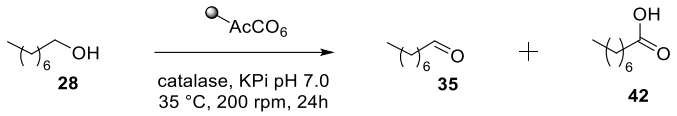

*Scheme 26 – Oxidation of octanol **28** with AcCO6 immobilised on ECR8309F. Reaction conditions: triplicate, 100 mg AcCO6 immobilised, 30 mM octanol **28** (0.015 mmol), 100 mM KPi (pH 7.0), 0.04 mg.mL^{-1} catalase, 35 °C, 200 rpm, 3 h – 4 days, V_{tot} = 0.5 mL.*

After 3 h reaction, octanol **28** conversion (11.3 %, entry 1 Table 16) occurred slowly and increased to full consumption after 4 days (entry 2). The colorimetric test of AcCO6 immobilisation on ECR8309F was contradicted by GC analysis of octanol **28** biotransformation. However, the resin was not investigated further in the context of this thesis.

*Table 16 – Oxidation of octanol **28** with AcCO6 immobilised on ECR8309F*

Entry	Reaction time	Alcohol 28 (%) ± SD	Aldehyde 36 (%) ± SD	Acid carboxylic 42 (%) ± SD
1	3 h	88.6 ± 1.7	9.6 ± 1.2	1.7 ± 0.4
2	4 days	0.0 ± 0.0	68.1 ± 7.6	31.8 ± 7.6
Reaction conditions: triplicate, 100 mg AcCO6 immobilised, 30 mM octanol **28** (0.015 mmol), 100 mM KPi (pH 7.0), 0.04 mg.mL^{-1} catalase, 35 °C, 200 rpm, 3 h – 4 days, V_{tot} = 0.5 mL. Conversion measured by GC-FID.				

2.7 Conclusion and future work

In this chapter, enzyme-mediated oxidation focused on two oxidases, HNX4 and AcCO6, as biocatalysts to oxidise alkyl alcohols of APG surfactants. The objective was to selectively oxidize alkyl alcohols without oxidizing the mimics of APG biosurfactants (AMG **48-52**).

After its protein expression, the activity of HNX4 was evaluated positively by absorbance assay toward long-chain alcohols. Dodecanol **32** was confirmed as a suitable substrate of HNX4. Unfortunately, only a couple of investigations with HNX4 were possible since the repetition of

HNX4 protein expression failed. The protein expression of AcCO6 was also unsuccessfully repeated on the first trial without explanation. Hence, HXN4 was abandoned and AcCO6 CFE was purchased from Prozomix® for further investigation. Alternatively, the transformation of oxidases could be performed using a different *E. coli* vector (HMS174(DE3),[167] BL21(DE3)pLySs[168]).

No oxidation of the primary alcohol of AMG **17-20** was detected by ^{1}H NMR when oxidase AcCO6 was used as a biocatalyst. Similarly, colorimetric assays noticed no specific activity during the oxidation of AMG **17-20** with HNX4. Therefore, both oxidases have the potential to transform fatty alcohol solvents that are used for manufacturing APG biosurfactants without consequences on the APG material. In Chapter 3, oxidase AcCO6 could be used to oxidise mixtures of alkyl alcohols in the presence of APG.

The immobilisation of the AcCO6 enzyme was successful on three different carriers: the His-tag specific carrier (EziG amber) and two unspecific carriers (ECR8285 and ECR8309F). The immobilised AcCO6 was tested as a biocatalyst for the biotransformation of octanol **28**. Only the carrier ECR8285 showed octanol **28** conversion ≥ 70 % and was reusable for five cycles with octanol **28** conversion ≤ 45 %. AcCO6 immobilised on carrier ECR809F was able to oxidise octanol **28** and could be investigated further to determine its performance and reusability. Therefore, additional carriers for oxidase immobilisation could be screened with covalent ligation, such as aminooxy resins, amin-based resins, and resins with tertiary amine links, as they are less susceptible to protein leakage.

Chapter 3 - Development of aliphatic alcohol sequestration process on amine-based solid support in the presence of alkylpolyglucosides

Chapter 3 will discuss the potential of two amine-functionalised solid-supported resins to sequester alkyl aldehydes. Firstly, the procedure will be optimised for the treatment of commercial alkyl alcohol (section 3.1). Secondly, it will applied to remove selectively aldehydes, which were produced biocatalytically (sections 3.2and 3.3). The procedure will be applied to commercial biosurfactant samples to remove the excess alcohol solvent, which will have been oxidised to aldehyde with the engineered choline oxidase AcCO6 (Figure 23, section 3.4).

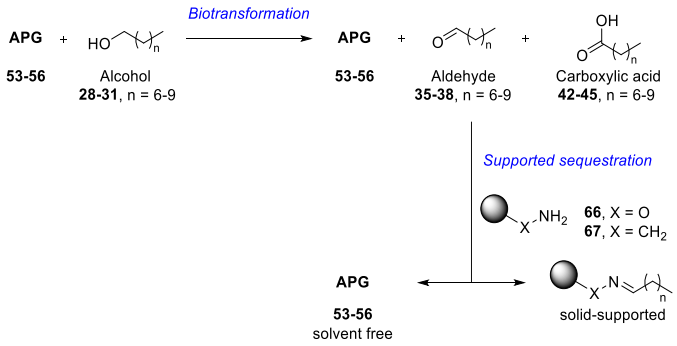

*Figure 23 – Process development of aliphatic alcohol biotransformation followed by immediate sequestration on solid supports **66** or **67** in presence of alkylpolyglucosides **53-56***

To describe these findings, supported ligations will be analysed by IR spectroscopy. Meanwhile, alcohol conversion will be analysed by GC-FID and calculated as described in Chapter 7. When preparative scale reactions are attempted, purity samples will be determined by NMR spectroscopy.

3.1 Introduction of amine-based resin

In this manuscript, two solid-supported resins functionalised with a nitrogen atom were investigated (Figure 24). These resins were the commercially available hydroxylamine Wang resin Novabiochem® **66** and aminomethyl polystyrene resin **67**. These cross-linked polystyrenes (PS) were insoluble in all common solvents, both aqueous and organic. The manufacturers recommended their use for Fmoc solid-phase peptide synthesis (SPPS) and suggested preactivating them by swelling in the aprotic solvent DMF before use.[169,170]

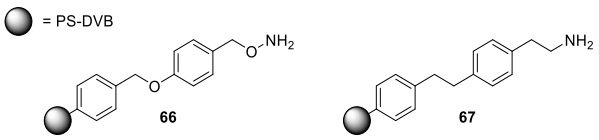

*Figure 24 - Amine-functionalised resins with a core of polystyrene-divinylbenzene (PS-DVB), hydroxylamine Wang resin **66** and aminomethyl polystyrene resin **67***

Usually, SPPS has been a popular technique for synthesising peptide therapeutics[171] and preparing biological nitrogen-containing compounds[172] on a solid-phase support. Here, the highly reactive nitrogen atoms in resins **66** and **67** were used to form Schiff bases with carbonyl in aldehydes.[173] Schiff bases are imines bearing a hydrocarbyl group on the nitrogen atom $R_1C{=}NCR_2$, named after Hugo Schiff (Scheme 27).[174–176] Precedents about the formation of Schiff base on solid-phase between alkyl aldehydes and amine-based resin were limited.[177] However, imine stability toward hydrolysis was reported to be lower than oxime bonds.[178–180] Oxime functionality, like hydroxylamine resin **66**, has a double bond C=N more stable toward hydrolysis than imine groups. The resonance forms of oximes benefit from the adjacent heteroatom to the sp^2 nitrogen (Scheme 27). For supported sequestration, the chemistries of hydroxylamine-based resin **66** and amine-based resin **67** with alkyl aldehyde will permit oxime and imine ligations, respectively, on solid support resin.

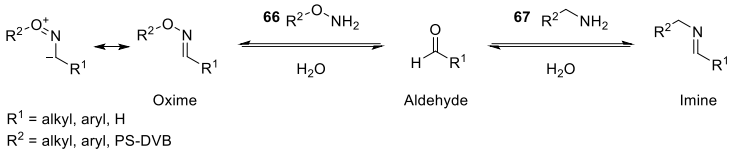

*Scheme 27 – Schiff reaction with aldehyde for oxime ligation **66** and imine ligation **67**.*

3.1.1 Sequestration of alkyl aldehydes on aminomethyl resin

To conduct analytical scale reactions with a volume of 0.5 mL, aminomethyl resin **67** (40 mg, 0.08 mmol, 4.0 equiv.) was swelled in DMF for at least 4 h, rinsed with DCM and added to a 40 mM solution of octanal **35** (2.6 mg, 0.02 mmol, 1.0 equiv.) (Scheme 28). The formation of imine was monitored by analysing the resin by FTIR spectroscopy every two hours (Table 17). Simultaneously, a control reaction was carried out by preparing a 40 mM solution of octanal **35** in water. The reaction solution was extracted with EtOAc and analysed using GC-FID Method A (see experimental for details) to monitor the process.

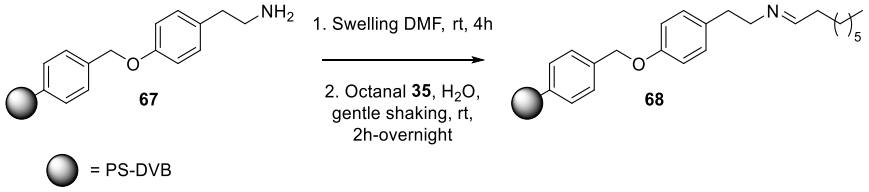

*Scheme 28 – Sequestration of octanal **35** to aminomethyl resin **67.** Reaction conditions: duplicate, 1) resin **67** (0.08 mmol, 4.0 equiv.) was swelled in DMF for 4 h. 2) addition to solution of 40 mM octanal **35** (0.02 mmol, 1.0 equiv.), gentle shaking, rt, from 2 h to overnight, V_{tot} = 0.5 mL.*

The diagnostic frequency analysis confirmed the presence of a medium stretch C=N band at ≈1673 cm^{-1}, which suggested the formation of imine **68** (Figure 25).[181] It was accompanied by the absence of octanal **35** carbonyl band at 1728 cm^{-1}. A standard reaction time of a minimum of 2 h was chosen for the sequestration of octanal **35** (Table 17). After the reaction, the reaction solution was analysed by GC-FID and showed traces of aldehyde **35**. However, the positive control solution still contained octanal **35**. FTIR analysis confirmed the formation of imine function on resin **68** and GC analysis indicated only traces of aldehyde **35** after reaction. The sequestration of

octanal **35** traces could be enhanced by increasing the amount of resin (**67**: 0.20 mmol, 10.0 equiv.) in the reaction solution.

*Table 17 – Treatment of octanal **35** in aqueous solution with aminomethyl resin **67,** pre-swelled in DMF, variation of reaction time.*

Entry	Reaction time	FTIR results (cm^{-1})	GC-FID results of sequestration (%)	GC-FID of octanal 35 solution in water (%)
1	2 h	1674	Traces of octanal **35**	100
2	4 h	1674	Traces of octanal **35**	100
3	6 h	1674	Traces of octanal **35**	100
4	Overnight	1674	Traces of octanal **35**	100

Reaction conditions: duplicate, 1) resin **67** (0.08 mmol, 4.0 equiv.) was swelled in DMF, rt, 4 h. 2) addition to solution of 40 mM octanal **35** (0.02 mmol, 1.0 equiv.), gentle shaking, rt, from 2 h to overnight, V_{tot} = 0.5 mL.

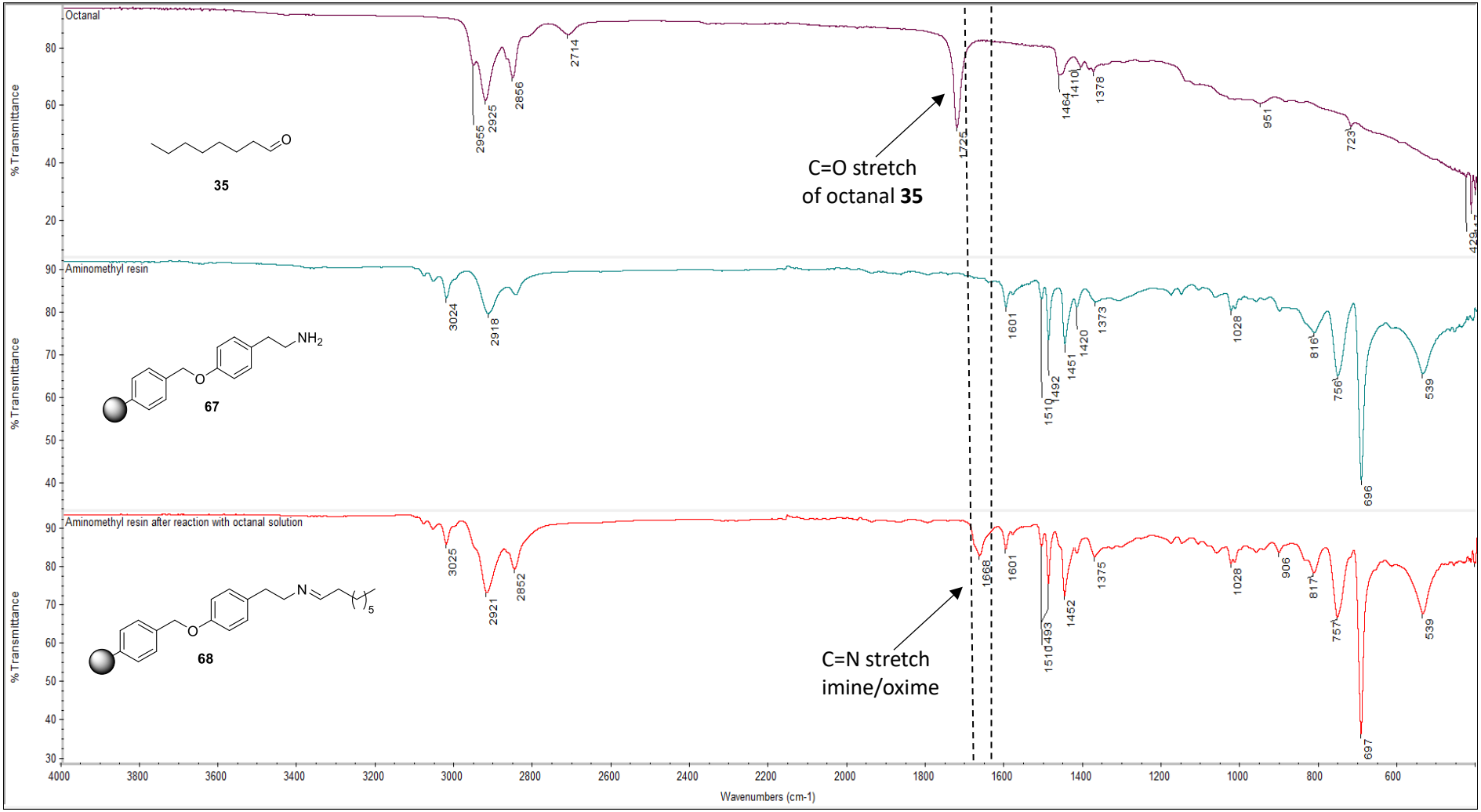

*Figure 25- IR spectra of sequestration of octanal **35** on aminomethyl resin **67** (bottom), aminomethyl resin **67** before sequestration (middle) and octanal **35** (top)*

The scope of this protocol was expanded to include alkyl aldehydes from 8 to 14 carbons **35-40** on resin **67** (Scheme 29, Table 18). FTIR analysis indicated a medium stretch C=N band at ≈1674 cm^{-1} for all aldehydes C_8-C_{14} **35-40** bounded with resin **67**. The reaction aqueous phases were extracted, analysed by GC-FID and showed only traces of aldehyde. These results confirmed the successful sequestration of aldehydes on resin **67** with the ligation of an imine function.

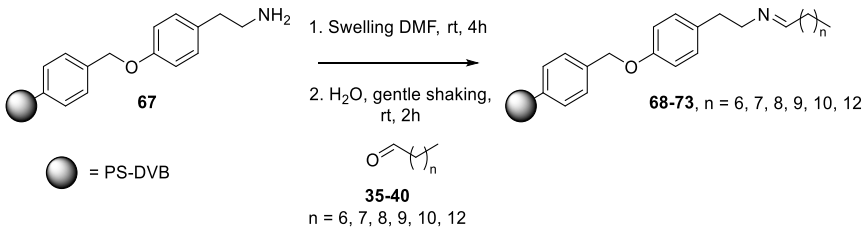

*Scheme 29 – Sequestration of aldehyde **35-40** to aminomethyl resin **67.** Reaction conditions: duplicate, 1) resin **67** (0.08 mmol, 4.0 equiv.) was swelled in DMF for 4 h. 2) addition to solution of 40 mM aldehyde **35-40** (0.02 mmol, 1.0 equiv.), gentle shaking, rt, 2 h, V_{tot} = 0.5 mL.*

*Table 18 - Treatment of alkyl aldehyde **35-40** in aqueous solution with aminomethyl resin **67**, pre-swelled in DMF.*

Entry	Alkyl aldehyde C_n	FTIR results (cm^{-1})	GC-FID results (%)
1	**35**, C_8	1667	Traces of aldehyde
2	**36**, C_9	1674	Traces of aldehyde
3	**37**, C_{10}	1674	Traces of aldehyde
4	**38**, C_{11}	1673	Traces of aldehyde
5	**39**, C_{12}	1674	Traces of aldehyde
6	**40**, C_{14}	1674	Traces of aldehyde
Reaction conditions: duplicate, 1) resin **67** (0.08 mmol, 4.0 equiv.) was swelled in DMF for 4 h. 2) addition to solution of 40 mM aldehyde **35-40** (0.02 mmol, 1.0 equiv.), gentle shaking, rt, 2 h, V_{tot} = 0.5 mL.			

3.1.2 Sequestration of alkyl aldehydes on hydroxylamine Wang resin

To conduct small-scale reactions (0.5 mL), 40 mg (0.08 mmol, 4.0 equiv.) of hydroxylamine Wang resin **67** was swelled in DMF for at least 3 h and then rinsed with DCM. The resin was then added to a 40 mM solution of octanal **35** (2.6 mg, 0.02 mmol, 1.0 equiv.) (Scheme 30). The oxime ligation was monitored by analysing the resin by FTIR spectroscopy every two hours (Table 19).

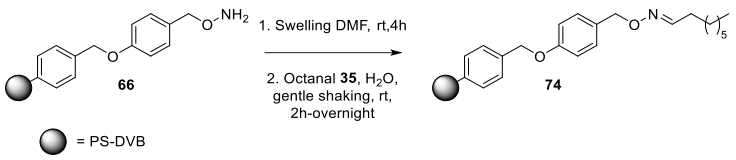

*Scheme 30 – Sequestration of octanal **35** to hydroxylamine Wang resin **67**. Reaction conditions: duplicate, 1) resin **67** (0.08 mmol, 4.0 equiv.) was swelled in DMF for 4 h. 2) addition to solution of 40 mM octanal **35** (0.02 mmol, 1.0 equiv.), gentle shaking, rt, from 2 h to overnight, V_{tot} = 0.5 mL.*

The diagnostic frequency observed a medium stretch bond C=N at ~1674 cm^{-1}. This bond was indicative of the formation of oxime **74.** Additionally, the octanal **35** carbonyl band at 1728 cm^{-1} was absent (Figure 26).[181] A minimum 2 h reaction was chosen as the standard reaction time for sequestering octanal **35**. After the solid-phase reaction, the reaction solution was analysed using GC-FID. The reaction solution contained traces of aldehyde **35** at the end of the solid-phase reaction, while the control solution contained 100 % octanal **35**. The formation of oxime function on resin **74** was confirmed by FTIR analysis and GC analysis indicated traces of aldehyde **35** after the reaction. To enhance the sequestration of octanal **35** traces, the amount of resin (**66**: 0.20 mmol, 10.0 equiv.) in the reaction solution could be increased.

*Table 19 – Treatment of octanal **35** in aqueous solution with hydroxylamine Wang resin **66** pre-swelled in DMF over-time.*

Entry	Reaction time	FTIR results (cm^{-1})	GC-FID results of sequestration (%)	GC-FID of octanal 35 solution in water (%)
1	2 h	1674	Traces of octanal **35**	100
2	4 h	1675	Traces of octanal **35**	100
3	Overnight	1675	Traces of octanal **35**	100

Reaction conditions: duplicate, 1) resin **66** (0.08 mmol, 4.0 equiv.) was swelled in DMF for 4 h. 2) addition to solution of 40 mM octanal **35** (0.02 mmol, 1.0 equiv.), gentle shaking, rt, from 2 h to overnight, V_{tot} = 0.5 mL.

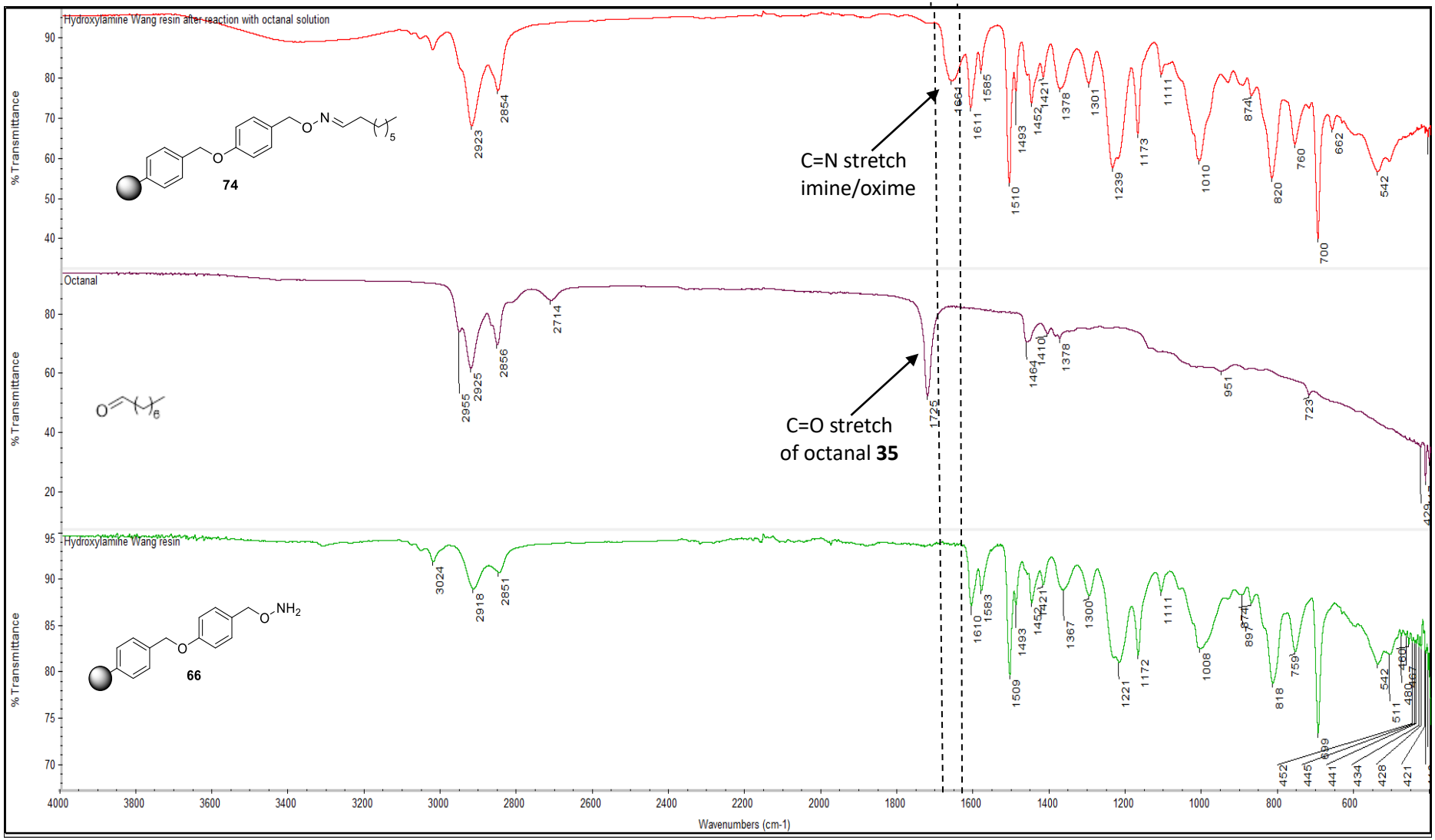

*Figure 26 - IR spectra of sequestration of octanal **35** with hydroxylamine Wang resin **66** (top), octanal **35** (middle) and hydroxylamine Wang resin **66** before sequestration (bottom)*

This protocol was extended to scavenge alkyl aldehydes from 8 to 14 carbons **35-40** on resin **66** (Scheme 31, Table 20). FTIR analysis showed a medium stretch C=N at 1670-1650 cm^{-1} band for all aldehyde C_8-C_{14} **35-40** treated with resin **66**. The aqueous phase of the reaction was extracted with EtOAc, analysed by GC-FID and showed traces of aldehyde **35-40**. These results confirmed that the aldehydes were sequestered on resin **66** through an oxime linker.

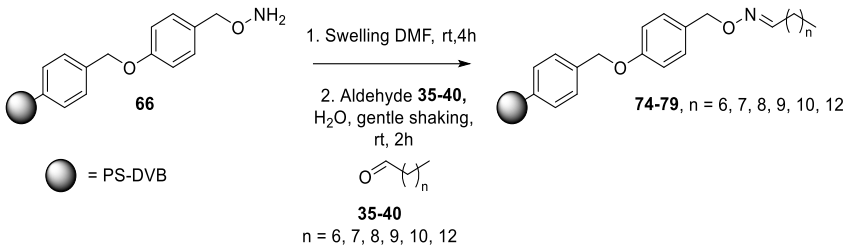

*Scheme 31 – Sequestration of aldehyde **35-40** to hydroxylamine Wang resin **66.** Reaction conditions: duplicate, 1) resin **66** (0.08 mmol, 4.0 equiv.) was swelled in DMF for 4 h. 2) addition to solution of 40 mM aldehyde **35-40** (0.02 mmol, 1.0 equiv.), gentle shaking, rt, 2 h, V_{tot} = 0.5 mL.*

*Table 20 - Treatment of alkyl aldehyde **35-40** in aqueous solution with hydroxylamine Wang resin **66** pre-swelled in DMF.*

Entry	Alkyl aldehyde Cn	FTIR results (cm^{-1})	GC-FID results (%)
1	**35**, C_8	1664	Traces of aldehyde
2	**36**, C_9	1656	Traces of aldehyde
3	**37**, C_{10}	1665	Traces of aldehyde
4	**38**, C_{11}	1659	Traces of aldehyde
5	**39**, C_{12}	1656	Traces of aldehyde
6	**40**, C_{14}	1656	Traces of aldehyde
Reaction conditions: duplicate, 1) resin **66** (0.08 mmol, 40 equiv.) was swelled in DMF for 4 h. 2) addition to solution of 40 mM aldehyde **35-40** (0.02 mmol, 1.0 equiv.), gentle shaking, rt, 2 h.			

3.2 Selective alcohol bio-oxidation followed by imination on aminomethyl resin support

This chapter aimed to create a bioprocess that captured fatty alcohols on a solid support using a Schiff base. Previous research has established a process that involves the oxidation of primary alcohols followed by condensation with amines,[182–187] but this process has yet to be used on solid supports.

Before the successful sequestration of fatty aldehydes **35-40** on aminomethyl resin **67** (section 3.1), fatty alcohols were oxidised by biotransformation with choline oxidase AcCO6 (Chapter 2), then aldehyde sequestration was performed using amine-functionalised PS resin **67**. To use resin **67**, it had to be pre-activated in DMF. However, the toxicity of DMF solvent could affect enzyme activity. Therefore, aminomethyl resin **67** was first swollen in DMF for at least 4 h and rinsed thoroughly with deionised water. After rinsing, resin **67** was used in the presence of oxidase AcCO6 to capture octanol **28** (section 3.2.1) and more fatty alcohols (section 3.2.2).

3.2.1 Octanol as a substrate for bioprocess

Small-scale experiments (0.5 mL) were conducted using 40 mM octanol **28** (2.6-5.2 mg, 0.02-0.04 mmol, 1.0 equiv.) as a substrate. They involved the tandem reactions of bio-oxidation-sequestration with AcCO6 biocatalyst and aminomethyl resin **67** (40-50 mg, 0.08-0.10 mmol, 4.0–5.0 equiv.) (Scheme 32).

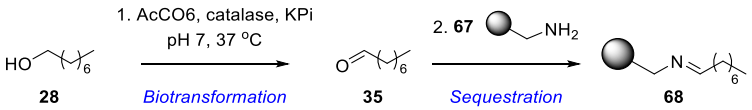

*Scheme 32 – Octanol **28** bio-oxidation followed by imination of octanal **35** on amine-based resin **67**. Reagents and conditions: 1) 40 mM octanol **28** (1.0 equiv.), AcCO6 (CFE or immobilised), 0.04 mg.mL^{-1} catalase (CFE), 100 mM KPi buffer (pH 7.0), 35 °C, 200 rpm, V_{tot} = 0.5 mL. 2) Amine-based resin **67** (4.0-5.0 equiv.), orbital rotation at 18 rpm, V_{tot} = 0.5 mL.*

The reaction was performed in a one-pot process with AcCO6 and resin **67**. In this process, octanol **28** was oxidised with the biocatalyst AcCO6 CFE to afford octanal **35**, which was directly sequestered on resin **67**. In addition to the one-pot process, a positive control of the biotransformation was performed to confirm the octanol **28** biotransformation. After 3 h reaction, the aqueous phase was separated from the resin and transferred to a new vial. The aqueous phase containing the biocatalyst was quenched with a 5.0 M NaOH solution (C_f = 0.1 M). Resin **67** was rinsed with methanol before further analysis. After the reaction, it was extracted with EtOAc and analysed by GC-FID. Meanwhile, resin **68** was rinsed successively with deionised water and methanol. Resin **68** was air-dried and analysed by IR.

In Table 21, GC-FID analysis of the aqueous phase showed the presence of octanol **28** and the absence of octanal **35** (entry 3, **28**/**35** 1:0), while resin **68** had a medium peak at 1648 cm^{-1} by IR analysis. Similar results were observed after 20 h reaction (entry 4, **28**/**35** 1:0). Since IR confirmed imine sequestration, octanal **35** was afforded during the reaction but not observed in aqueous solution by GC-FID. Nevertheless, octanol **28** bio-oxidation with AcCO6 CFE was incomplete after 20 h reaction, while a complete conversion of octanol **28** was observed without resin **67** (entry 2). It is possible that covalent binding interactions between CFE and the aminomethyl resin **67** occurred and affected alcohol bio-oxidation and aldehyde sequestration, leading to protein immobilisation on amino-activated resin.[61,123,188] Future research could explain these results by studying resin swelling in the presence of CFE precipitate or computational docking between the AcCO6 crystal structure and CFE content.

*Table 21 – One-pot process oxidation of octanol **28** and sequestration with resin **67**.*

Entry	Reaction time	GC-FID (%): Proportion of Octanol/Octanal (28/35)	FTIR (cm^{-1}) of 68
1, (no resin 67)	3 h	54:46	n.c.
2, (no resin 67)	20 h	4:96	n.c.
3	3 h	1:0	1648
4	20 h	1:0	1667

Reagents and conditions: duplicate, 40 mM alcohol **28** (0.02 mmol, 1.0 equiv.), 20 $mg.mL^{-1}$ AcCO6 (CFE), 0.04 $mg.mL^{-1}$ catalase (CFE), 100 mM KPi buffer (pH 7.0), aminoethyl resin **67** (0.08 mmol, 4.0 equiv.), 35 °C, 200 rpm.

n.c.: not concerned

After the mixed results of the one-pot bioprocess, a two-step reaction was attempted with an intermediate filtration between the biotransformation and solid-supported sequestration (Scheme 33). The AcCO6 CFE stock solution was not centrifuged before being used, leading to insoluble elements in the solution. Nevertheless, the biotransformation of octanol **28** with AcCO6 CFE was stopped after 5 h reaction, quenched with 5.0 M NaOH solution (C_f = 0.05 M) and filtered through 5-13 µm filter paper to remove excess of AcCO6 CFE not soluble in buffer. The resulting filtrate was added to pre-swollen resin **67** and left to stand for 45 min.

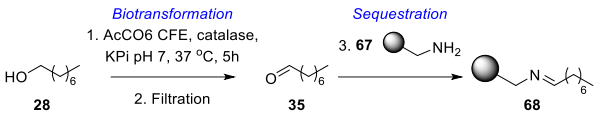

*Scheme 33 – Octanol **28** bio-oxidation followed by imination of octanal **35** on amine-based resin **67**. Reagents and conditions: 1) 40 mM octanol **28** (0.02 mmol, 1.0 equiv.), 20 mg.mL^{-1}AcCO6 (CFE), 0.04 mg.mL^{-1} catalase (CFE), 100 mM KPi buffer (pH 7.0), 35 °C, 5 h, 200 rpm, V_{tot} = 0.5 mL. 2) filtration through filter paper (95 × 110 mm, Fisherbrand®). 3) Amine-based resin **67** (0.1 mmol, 5.0 equiv.) stand for 45 min, V_{tot} = 0.5 mL.*

The resulting analysis revealed that the aqueous phase contained octanol **28** and octanal **35** (**28**/**35** 8:2) by GC-FID and C=N (1667 cm^{-1}) formation by IR (entry 1, Table 22). This additional filtration made the biotransformation of octanol **28** and the sequestration of newly formed aldehyde **35** possible. The final ratio of **28**/**35** (8:2) indicated 20 % of aldehyde **35** remained after sequestration. The biotransformation was incomplete due to the short reaction time, but aldehyde sequestration was achieved successfully.

*Table 22 – Oxidation of octanol **28**, followed by filtration through filter paper and sequestration with resin **67**.*

Entry	Reaction time of biotransformation	GC-FID (%): Proportion of Octanol/Octanal (28/35)	FTIR (cm^{-1}) of 68
1	5 h	8:2	1667
Reagents and conditions: singlate, 1) 40 mM octanol **28** (0.02 mmol, 1.0 equiv.), 20 mg.mL^{-1} AcCO6 (CFE), 0.04 mg.mL^{-1} catalase (CFE), 100 mM KPi buffer (pH 7.0), 35 °C, 200 rpm, for 5 h. 2) filtration through 5-13 µm filter paper. 3) filtrate was added to aminoethyl resin **67** (0.1 mmol, 5.0 equiv.), rt, stand for 45min, V_{tot} = 0.5 mL.			

To determine the time required to sequester the intermediate aldehyde **35** to resin **67** in the presence of AcCO6 CFE, a sequential approach was investigated (Scheme 34, Table 23). After 16 h

reaction, the reaction solution was filtered through 5-13 µm filter paper. The filtrate containing aldehyde **35** was mixed with resin **67** with a slow agitation (orbital rotation 18 rpm) at rt (Table 23). The agitation time was varied from 1 h to 5 days. As the sequestration time increased, the ratio **35**/**28** changed from 89:11 (1 h, entry 1) to 99:1 (3 h, entry 3). Therefore, biotransformation was successful and the amount of aldehyde **35** in solution decreased as the aldehyde sequestration time increased.

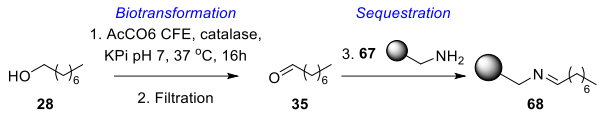

*Scheme 34 – Sequential oxidation of octanol **28** and sequestration with resin **67**. Reagents and conditions: singlate, 1) 40 mM octanol **28** (0.02 mmol, 1.0 equiv.), 20 mg.mL^{-1} AcCO6 (CFE), 0.04 mg.mL^{-1} catalase (CFE), 100 mM KPi buffer (pH 7.0), 35 °C, 200 rpm, for 5 h. 2) filtration through 5-13 µm filter paper. 3) filtrate was added to resin **67** (0.1 mmol, 5.0 equiv.), rt, orbital rotation 18 rpm.*

*Table 23 - Sequential oxidation of octanol **28** and sequestration with resin **67**.*

Entry	Agitation time with resin 67	GC-FID (%): proportion of Octanol/Octanal (28/35)	FTIR (cm^{-1}) of 68
1	1 h	89:11	1674
2	2 h	95:5	1674
3	3 h	99:1	1674
Reagents and conditions: singlate, 1) 40 mM octanol **28** (0.02 mmol, 1.0 equiv.), 20 mg.mL^{-1} AcCO6 (CFE), 0.04 mg.mL^{-1} catalase (CFE), 100 mM KPi buffer (pH 7.0), 35 °C, 200 rpm, for 5 h. 2) filtration through 5-13 µm filter paper. 3) filtrate was added to resin **67** (0.1 mmol, 5.0 equiv.), rt, orbital rotation 18 rpm.			

An additional analytical scale reaction (0.5 mL) for bioremediation of octanol **28** was performed with immobilised AcCO6 on ECR8285 epoxymethacrylate and amin-resin **67**. The reaction was carried out as a one-pot reaction for 24 h at 37 °C (Scheme 35). The GC-FID analysis revealed weak conversion of octanol **28** (**28**/**35** 97:3), while IR analysis showed the presence of a weak C=N band (1659 cm^{-1}) on resin **68**. Due to the methacrylate beads being ground during sample preparation for IR spectroscopy, the analysis of the mixture of AcCO6 methacrylate beads and amine-based resins was challenging, and their signals were overlapping and not distinguishable. Therefore, an analytical scale reaction that combined immobilised AcCO6 and amine-functionalised resin **67** was not investigated further. However, the bioprocess with immobilised protein was proven possible.

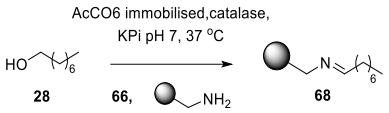

*Scheme 35 – One-pot reaction of octanol **28** bio-oxidation and imination on solid support **67**. Reagents and conditions: triplicate, 40 mM octanol **28** (0.02 mmol, 1.0 equiv.),0.2 mg.mL^{-1} AcCO6 ECR8285, 0.04 mg.mL^{-1}catalase (CFE), amine-based resin **67** (0.1 mmol, 5.0 equiv.), 100 mM KPi buffer (pH 7.0), 35 °C, 200 rpm, 24 h.*

3.2.2 Scope for selective alcohol bio-oxidation followed by aldehyde sequestration on aminomethyl resin

The sequestration of octanal **35** on resin **67** introduced in section 3.2.1 was successful. Therefore, the research scope was expanded to include other substrates of biocatalyst AcCO6, specifically the alkyl alcohols **28-31**, which are necessary to manufacture APG (Scheme 36). These alkyl alcohols were first treated independently and second as a commercial mixture of two alcohols: octanol/decanol **28**/**30** (43:57) and nonanol/undecanol **29/31** (35:65).

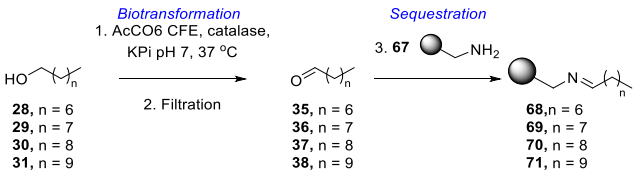

*Scheme 36 – Biotransformation of alkyl alcohols **28-31**, followed by filtration and aldehyde sequestration on aminomethyl resin **67**. Reagents and conditions: singlate. 1) 40 mM alcohol **28-31** (0.02 mmol, 1.0 equiv.), 20 mg.mL^{-1} AcCO6 (CFE), 0.04 mg.mL^{-1} catalase (CFE), 100 mM KPi buffer (pH 7.0), 35 °C, 200 rpm, 15 h, V_{tot} = 0.5 mL. 2) Filtration through 5-13 µm filter paper. 3) aldehyde **35-38** sequestration on aminomethyl resin **67** (0.1 mmol, 5.0 equiv.), orbital rotation at 18 rpm, 3 h.*

As part of bioprocess optimisation, a control reaction without aminomethyl resin **67** was conducted to confirm enzyme activity in the biotransformation process (Table 24). After 15 h reaction, the biotransformation control reaction was incomplete. The incomplete oxidation could be due to the batch of AcCO6 CFE being less concentrated on choline oxidase. However, despite the incomplete biotransformation, the control reaction was considered a valid control for the biotransformation (Table 24).

*Table 24 – Results of alkyl alcohols biotransformation, followed by filtration then aldehyde sequestration aminomethyl resin **67**.*

Entry	Substrate	Positive control of biotransformation (GC-FID): proportion of Alcohol/Aldehyde/Carboxylic acid (%)	GC-FID results (%)	FTIR (cm^{-1})
1	**28**, C_8	85:14:0	Traces of alcohol	1674
2	**29,** C_9	87:8:3	Traces of alcohol	1673
3	**30**, C_{10}	82:14:1	Traces of alcohol	1673
4	**31**, C_{11}	86:12:1	Traces of alcohol	1673
5	**28/30** C_8/C_{10} alcohol mixture	73:25:2	Alcohol/Car. Acid 26:74 (traces)	1673
6	**29/31** C_9/C_{11} alcohol mixture	12:51:36	Traces of carboxylic acid	1674
Reagents and conditions: singlate. 1) 40 mM alcohol **28-31** (0.02 mmol, 1.0 equiv.), 20 $mg.mL^{-1}$ AcCO6 (CFE), 0.04 $mg.mL^{-1}$ catalase (CFE), 100 mM KPi buffer (pH 7.0), 35 °C, 200 rpm, 15 h, V_{tot} = 0.5 mL. 2) Filtration through 5-13 µm filter paper. 3) aldehyde sequestration on aminomethyl resin **67** (0.1 mmol, 5.0 equiv.), orbital rotation at 18 rpm, 3 h.				

The three step bioprocess of individual alcohols **28-31** (entries 1-4, Table 24) began on the overnight bio-oxidation with AcCO6, followed by quenching with 5.0 M NaOH solution (C_f = 0.05 M). Secondly, the filtration of the reaction mixture was conducted through 5-13 µm filter paper, and finally, the sequestration on solid support **67** was performed. After 3 h sequestration, the reaction solution was transferred to a clean vial, extracted with EtOAc and analysed by GC-FID. Analysis of the chromatogram indicated traces of alcohols, and IR spectroscopy showed the presence of a C=N band (~1673 cm^{-1}), indicative of aldehyde sequestration.

The commercial mixture of alcohols (entry 5-6, Table 24) were also oxidised to a mixture of aldehydes and sequestered successfully on solid support **67** with C=N band (~1673 cm^{-1}). As demonstrated in Chapter 2, the shortest alkyl alcohol (octanol **28**) was converted more easily than the longer alcohol (undecanol **31**) when oxidised with biocatalyst AcCO6. Therefore, when the three-step reaction was performed on the mixture of C_8/C_{10} **28**/**30** alcohols with AcCO6 and resin **67**, octanol **28** was oxidised to octanal **35** and then directly sequestered on resin **67** faster than decanol **30**. For future work, the bioprocess rate and the size of resin **67** during the bioprocess could be studied to better understand the sequestration rate in the presence of the enzyme.

3.3 Selective alcohol bio-oxidation followed by imination on hydroxylamine Wang resin support

The bioprocess combining alcohol bio-oxidation with AcCO6 and aldehyde sequestration on amine-functionalised resin **67** was successful (section 3.2). It will be expanded by combining AcCO6 with hydroxylamine Wang resin **66** and optimised with similar investigations (section 3.3).

3.3.1 Octanol as substrate for bioprocess

Investigations were conducted on analytical scale (0.5 mL) using 40 mM octanol **28** (2.6 – 5.2 mg, 0.02 – 0.04 mmol, 1.0 equiv.) as substrate. Hydroxylamine Wang resin **66** (40 – 50 mg, 0.08 – 0.1 mmol, 4.0 – 5.0 equiv.) was used for the sequestration of intermediate **35** (Scheme 37).

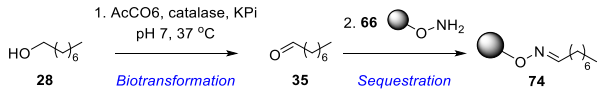

*Scheme 37 – Octanol **28** bio-oxidation followed by imination of octanal **35** on aminooxy-based resin **66**. Reagents and conditions: 1) 40 mM alcohol **28** (0.02 mmol, 1.0 equiv.), AcCO6 (CFE or immobilised), 0.04 mg.mL^{-1} catalase (CFE), 100 mM KPi buffer (pH 7.0), 35 °C, 200 rpm, 17 h. 2) hydroxylamine resin **66** (0.1 mmol, 5.0 equiv.), orbital rotation at 18 rpm, 4h.*

The reaction was performed as a one-pot process with AcCO6 and aminooxy-functionalised resin **66**. Octanol **28** was oxidised with AcCO6 CFE to afford octanal **35** (entry 2**,** Table 25). The resulting octanal **35** was directly sequestered on resin **66**. A positive control of octanol **28** biotransformation was also performed for comparison (entry 1, Table 25). After 20 h, the one-pot reaction was stopped by transferring the reaction solution to a new vial, where the biocatalyst was quenched with a 5.0 M NaOH solution (C_f = 0.1 M). Resin **66** was rinsed with methanol before further analysis. After sequestration, reaction solution was extracted with EtOAc and analysed by GC-FID. Resin **74** was rinsed successively with deionised water and methanol before being air-dried and analysed by IR.

In Table 25, GC-FID analysis revealed the presence of octanol **28** and a small amount of octanal **35** (**28**/**35** 91:9, entry 2). Resin **74** presented by IR a weak peak at 1670 cm^{-1} associated with a C=N stretch band. The weak band detected suggested that the oxime bond formation might have been slowed down by an element present in the enzymatic solution, as previously described.

Alternatively, sequential addition was attempted by performing bio-oxidation of octanol **28** for 74 h at 37 °C followed by the addition of resin **66** to the reaction solution and agitation at 37 °C for 4 h (entry 3, Table 25). GC results showed the same amount of aldehyde **35** as the positive control (87-89 %) and no detection of C=N band by IR. The sequential addition of resin **66** did not lead to the sequestration of newly formed aldehyde **35** (entry 3, Table 25). As previously described, the interaction of aminooxy resin **66** with the enzyme residue might have created a bond sabotaging the creation of a covalent bond between aldehyde **35** and amine-residue supported **66**.[61,123,188]

To solve this issue (entry 4, Table 25), the initial bio-oxidation of octanol **28** was performed to completion. Next, the reaction solution was filtered through a 5-13 µm filter paper to remove the excess of AcCO6 CFE insoluble in the buffer. Finally, the resulting filtrate was added to resin **66**. After reaction, the reaction solution still contained an excess of aldehyde **35** (82 %) and a weak peak at 1668 cm^{-1}. However, it was proven that aldehyde sequestration was possible.

*Table 25 – Octanol **28** bio-oxidation followed by imination of octanal **35** on amine-based resin **66**.*

Entry	Method	GC-FID (%) : Proportion of Octanol/Octanal 28/35	FTIR (cm^{-1}) of 74
1 (no resin 66)	Positive control	13:87	-
2	One-pot	91:9	1670 weak
3	Sequential addition	11:89	n.d.
4	Three steps	18:82	1668
Reagents and conditions: 1) 40 mM octanol **28** (0.02 mmol, 1.0 equiv.), 20 $mg.mL^{-1}$ AcCO6 (CFE), 0.04 $mg.mL^{-1}$ catalase (CFE), 100 mM KPi buffer (pH 7.0), 35 °C, 200 rpm, 17 h. 2) Amine-functionalised resin **66** (0.1 mmol, 5.0 equiv.), orbital rotation at 18 rpm, 4 h.			

3.3.2 Scope for selective alcohol bio-oxidation followed by aldehyde sequestration on hydroxylamine Wang resin

The successful sequestration of octanal **35** in section 3.2.1 led to an expansion of the bioprocess with hydroxylamine Wang resin **66** to substrates of biocatalyst AcCO6. The substrates in question were the alkyl alcohols **28-31**, which are required to manufacture APG (Scheme 38). Each alcohol was first treated individually and secondly as a commercial mixture of two alcohols: octanol/decanol **28**/**30** (43:57), nonanol/undecanol C9/C11 **29**/**31** (35:65).

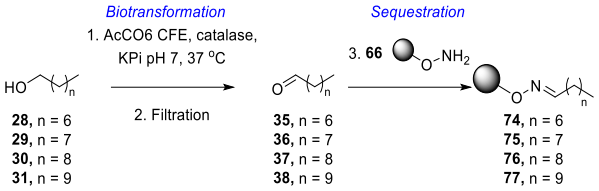

*Scheme 38 – Biotransformation of alkyl alcohols, followed by filtration and aldehyde sequestration hydroxylamine resin **66**. Reagents and conditions: 1) 40 mM alcohol **28-31** (0.02 mmol, 1.0 equiv.), 20 mg.mL^{-1}AcCO6 (CFE), 0.04 mg.mL^{-1}catalase (CFE), 100 mM KPi buffer (pH 7.0), 35 °C, 200 rpm, overnight. 2) Filtration through 5-13 µm filter paper. 3) aldehyde sequestration on hydroxylamine resin **66** (0.1 mmol, 5.0 equiv.), orbital rotation at 18 rpm, 3 h.*

The bioprocess for converting alkyl alcohols **28**-**31** involved three steps. Firstly, bio-oxidation was carried out using AcCO6 and quenched with a 5.0 M NaOH solution (C_f = 0.05 M). Next, the mixture was filtered through 5-13 µm filter paper and finally sequestered on resin **66**. The solid support **66** was analysed using IR, while the reaction solution was analysed using GC-FID (Table 26). Resins **66** used for reactions with alkyl alcohol from 8 to 11 carbons **28-31** indicated the formation of a C=N bond (1668 cm^{-1}) on resins **74-77** and confirmed the sequestration of aldehyde. The reaction solution was examined and the enzymatic oxidation of primary alcohols was confirmed for alcohols **28-31**. The analysis also indicated the presence of aldehydes **35-38** as major products.

*Table 26 – Results of alkyl alcohols **28-31** biotransformation, followed by filtration and aldehyde sequestration hydroxylamine resin **66**.*

Entry	Substrate	GC-FID (%): Proportion of Alcohol/Aldehyde/Acid	FTIR (cm^{-1})
1	**28**, C_8 octanol	28:71:0	1668
2	**29**, C_9 nonanol	15:85:0	1669
3	**30**, C_{10} decanol	27:30:43	1669
4	**31**, C_{11} undecanol	61:31:6	1668
5	**28/30,** C_8/C_{10} alcohol mixture	66:27:7	1668
6	**29/31,** C_9/C_{11} alcohol mixture	76:10:14	1668
Reagents and conditions: 1) 40 mM alcohol **28-31** (0.02 mmol, 1.0 equiv.), 20 $mg.mL^{-1}$AcCO6 (CFE), 0.04 $mg.mL^{-1}$catalase (CFE), 100 mM KPi buffer (pH 7.0), 35 °C, 200 rpm, overnight. 2) Filtration through 5-13 µm filter paper. 3) aldehyde sequestration on hydroxylamine resin **66** (0.1 mmol, 5.0 equiv.), orbital rotation at 18 rpm, 3 h.			

3.4 Application of bioprocess on APG biosurfactant

Aminooxy-based resin **67** and amine-based resin **66** were able to sequester alkyl aldehydes produced by biotransformation (sections 3.2 and 3.3). Hence, the purification of APG biosurfactant with the previous would be tested with oxidase AcCO6 and aminomethyl resin **67**. Firstly, the bioprocess would be performed on a mixture of AMG-C_8/octanol **53**/**28** (9:1 %*w*/*w*) prepared in the laboratory. Secondly, the process would be evaluated on authentic APG-C_8/C_{10} **53/54** samples from the manufacturing process. Both pre- and post-distillation APG samples were selected for this purpose.

3.4.1 Simple mixture of alkyl monoglucoside and alcohol (AMG-C_8/C_8OH)

A 50 mg mixture (**53**/**28** 9:1 %*w/w*) of alkyl monoglucoside with an alkyl chain of 8 carbons (AMG-C_8 **53**) and octanol **28** was treated with aminomethyl resin **67** and oxidase AcCO6 CFE (Scheme 39). As the process scale was increased to a preparative scale, the concentration of biocatalyst AcCO6 was also increased (110 mg.mL^{-1}, CFE) to ensure maximum alcohol oxidation.

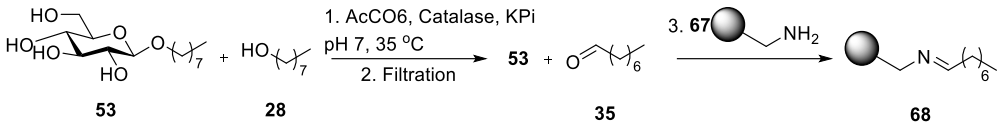

*Scheme 39 – Bioprocess for removal of octanol **28** from on AMG-C_8/octanol **53/28** mixture. Reactions conditions: singlate, 1) **53/28** (9:1 %w/w, **53:** 45 mg, **28:** 5 mg (0.04 mmol, 1.0 equiv.)), 110 mg.mL^{-1}AcCO6 (CFE), 0.04 mg.mL^{-1}catalase (CFE), 100 mM KPi (pH 7.0), 37 °C, 20 rpm, 3 days, V_{tot} = 1.9 mL. 2) Filtration through protein concentrator. 3) aldehyde **35** sequestration on aminomethyl resin **67** (1.0 g, 2.0 mmol, 50.0 equiv.), orbital rotation 18 rpm, 4 h, rt.*

After 3 days reaction, the reaction was quenched with 5.0 M NaOH (C_f = 1.0 M). To analyse the reaction products, 200 µL of the solution was extracted with ethyl acetate and subjected to GC-FID, where 65 % of octanol **28** was converted. Although the biocatalyst AcCO6 was active, the alcohol transformation was incomplete, possibly due to a low level of active AcCO6 in the protein batch expression.

In the second step of the bioprocess, biocatalyst AcCO6 was filtered using a commercial centrifugal filter (Figure 27). Ultrafiltration was commonly used for protein purification, protein concentration and purification of biodiesel and surfactants.[189–191] Here, the membrane of the centrifugal filter retained protein residues while 5-13 µm filter paper retained only insoluble excess. The resulting permeate, containing AMG-C_8 **53**, alcohol **28** and aldehyde **35**, had a minimal amount of CFE residues during aldehyde sequestration on solid support **67**. The necessity to wash the centrifugal

filter before being used with deionised was rapidly discovered to avoid contamination due to the commercial filter. The reaction solution was filtered through a protein concentrator and centrifuged at 3024 × *g* for 20 min. The filtered solution and the retained solution were freeze-dried overnight and analysed by ^{1}H NMR. AMG-C_8 **53** was detected in both solutions, but newly produced octanal **35** was not detected by ^{1}H NMR. The literature indicated that aldehydes, like octanal **35**, were partially volatile in raw freeze-dried food.[192–194] Therefore, to confirm this statement with the available equipment, a 30 mM octanal **35** solution (2 mg, 0.01 mmol) was freeze-dried and analysed by ^{1}H NMR with quantitative recovery. For these reasons, octanal **35** in the filtered solution and the retained solution had reached the detection limits of apparatus NMR. The retained solution was spun further to gather the remaining AMG-C_8 **53** into the filtered solution.

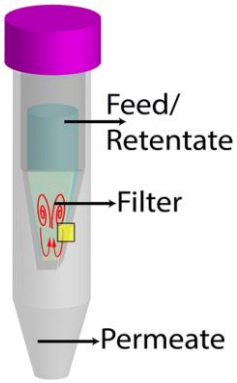

*Figure 27 - Commercial centrifugal filter. Image taken and unmodified from reference H. Feroz, H. Kwon, J. Peng, H. Oh, B. Ferlez, C. S. Baker, J. H. Golbeck, G. C. Bazan, A. L. Zydney and M. Kumar, Analyst, 2018, **143**, 1378–1386 with permission of RSC publishing.*

Octanal sequestration occurred with an excess of aminomethyl resin **67** and was shaken for 4 h at room temperature. After the reaction, resin **68** was rinsed with deionised water and methanol and air-dried overnight. After analysis by IR, no C=N band was detected on amine support **68**. However, if an excess of resin **67** was used, the sequestration of aldehyde could be complete, but the detection of imine function by IR could be limited. The final crude was analysed by NMR (D_2O, ^{1}H,

^{13}C, ^{31}P). The ^{1}H NMR spectrum was compared with commercial octanol **28** and standard AMG-C_8 **53** (Figure 28). The major product detected was AMG-C_8 **53**, while octanal **35** was not detected. Impurities were also detected by NMR (^{1}H, ^{31}P): impurity **80** was detected and one impurity was identified as KPi buffer (δ_P 1.61 ppm).

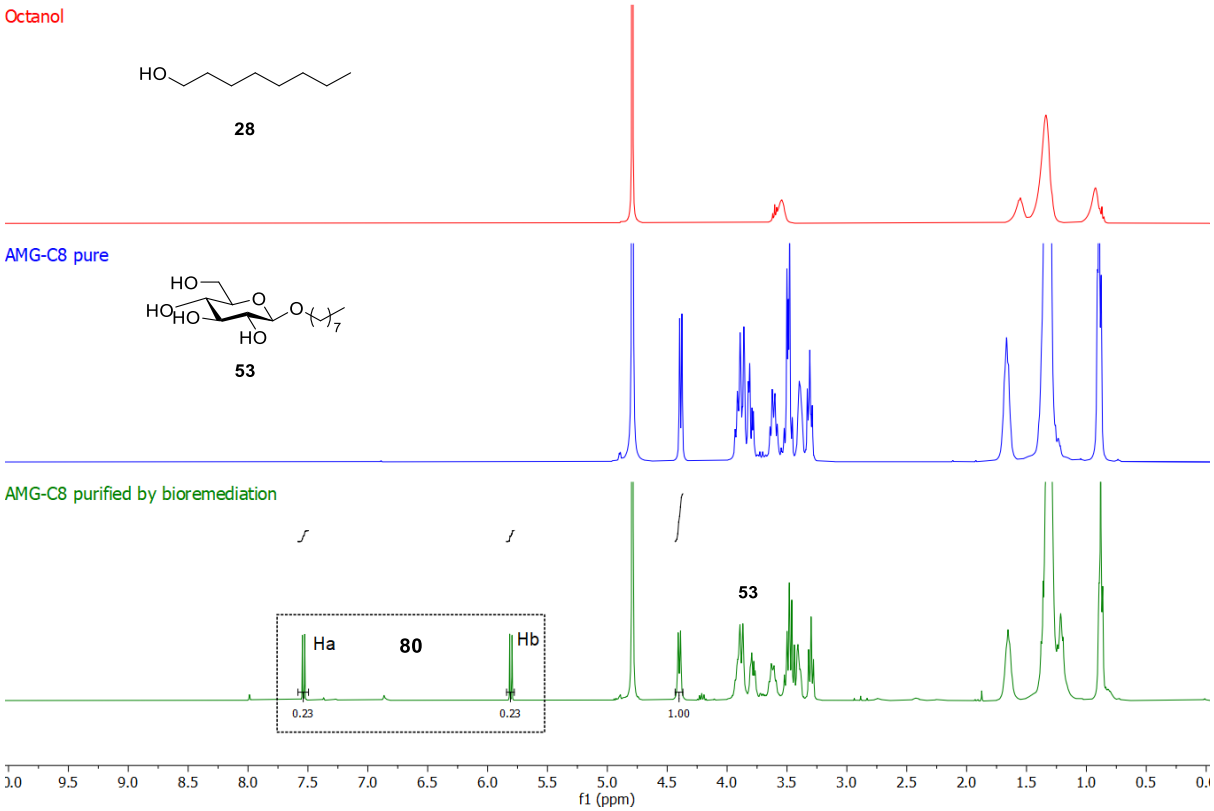

*Figure 28 - Stacked spectra of mixture of AMG-C_8/1-octanol **53/28** (9:1 %w/w) treated with bioremediation with AcCO6 CFE and amine-based resin **67** and final purification via column chromatography (bottom), pure AMG-C_8 **53** (middle) and commercial octanol **28** (top) in ^{1}H NMR (400 MHz, D_2O)*

Impurity **80**, highlighted in Figure 28, was recorded with the following data: ^{1}H NMR (D_2O, 400 MHz) δ 7.53 (dd, *J* = 7.7 Hz, *J* = 0.9 Hz, 1H, Ha), 5.80 (dd, *J* = 7.7 Hz, *J* = 0.9 Hz, 1H, Hb); ^{13}C NMR (100 MHz, D_2O) δ 143.5 (Ca), 101.2 (Cb). Purification via flash chromatography did not succeed to isolate and identify the impurity **80**. Further ^{1}H NMR comparison confirmed that impurity **80** did not come from the commercial centrifugal filter or from AcCO6 CFE. No further investigations on

AcCO6 CFE were performed to determine the origin of impurity **80**. Eventually, impurity **80** came from the coating or leaching effect from amine-based resin **67**. No precedent was found to attest to this theory. In summarise, the initial mixture of AMG-C_8 **53** (45 mg) and octanol **28** (5 mg) was treated with the three-step reaction (bio-oxidation with AcCO6 followed by filtration and final aldehyde sequestration with aminomethyl resin **67**) to afford AMG-C_8 **53** with a purity of 80 % and yield of 62 %.

3.4.2 Bioprocess of commercial APGs biosurfactant: analytical scale

Authentic industrial samples of surfactant APG-C_8/C_{10} before distillation **81** and post-distillation **82** were treated with AcCO6 CFE and commercial resin **66** and **67** on analytical scale (Scheme 40, Table 27). All samples were analysed by GC-FID with Method B (see experimental for details).

Sample **81** of APG-C_8/C_{10} **53/54** was obtained from Fischer glycosylation between D-glucose and a mixture of C_8/C_{10} **28/30** alcohols without purification. As a result, sample **81** contained 50 %*w/w* of APG- C_8/C_{10} **53/54** and 50 %*w/w* alcohols (mixture of alcohols C_8/C_{10} **28/30** 44:56). Sample **82** was a surfactant APG-C_8/C_{10} **53/54** post-distillation, consisting of 99 %*w/w* of APG-C_8/C_{10} **53/54** and 1 %*w/w* of alcohols mixture (mixture of alcohols C_8/C_{10} **28/30** 6:94). To afford sample **82**, distillation under vacuum was used to remove first the alcohol with lower boiling point, such as octanol **28** (bp 195 °C), followed by decanol **30** (bp 230 °C).[195]

Alcohol concentrations were estimated based on octanol **28**. For example, 10 g of sample **81** contained 5 g of alcohol, consisting of 2.2 g of octanol **28** and 2.8 g of decanol **30**. When diluted in 650 mL of deionised water, the resulting alcohol concentrations were ≈26 mM octanol **28** and ≈27 mM decanol **30**. To simplify the calculation, the concentrations were calculated based on the molecular weight of octanol **28** (130.23 $g.mol^{-1}$). Therefore, the dilution of 10 g sample **81** in 650 mL deionised water gave an alcohol concentration of ≈60 mM.

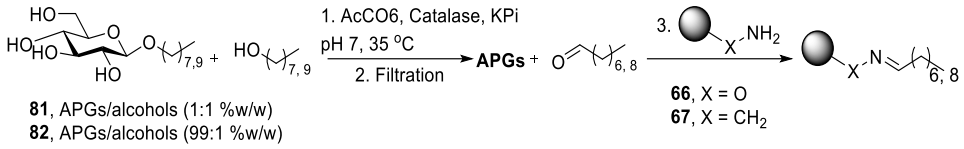

*Scheme 40 - Biotransformation of commercial APG-C_8/C_{10} **53/54** samples **81** and **82**, followed by filtration then aldehyde sequestration on solid supported resin **66** or **67**.*

Analytical scale reaction were first performed and analysed in Table 27. In samples **81** and **82**, alcohols were oxidised with AcCO6 CFE to aldehydes and carboxylic acids and detected by GC analysis. Noteworthy, traces of aldehydes were detected in mixture **81**, which the excess of alcohols present can explain, while no aldehydes were detected in mixture **82**. Enzymatically produced aldehydes were confirmed to be sequestered on resins **66** and **67** by IR analysis, which showed C=N stretches at 1675 cm^{-1} and 1669 cm^{-1} respectively (Table 27).

*Table 27 – Results of commercial APG-C_8/C_{10} **53/54** samples **81** and **82** biotransformation, followed by filtration then aldehyde sequestration on functionalised resin **66** or **67**.*

Entry	Substrate	Resin	GC-FID (%) : Proportion of Alcohol/Aldehyde/Acid	FTIR (cm^{-1})
1	**81**, APGs/alcohols (1:1 %*w/w*)	**66**, 4.0 equiv.	13:35:52	1674
2	**82**, APGs/alcohols (99:1 %*w/w*)	**66**, 200.0 equiv.	12:44:42	1675
3	**81**, APGs/alcohols (1:1 %*w/w*)	**67**, 5.0 equiv.	0:32:67	1669
4	**82**, APGs/alcohols (99:1 %*w/w*)	**67**, 250.0 equiv.	0:0:55	1669

Reagents and conditions: analytical scale, singlate, 1) alcohol (**81**: 0.02 mmol, 20 mM, 1.0 equiv.; **82**: 0.4 µmol, 0.4 mM, 1.0 equiv.), 20 $mg.mL^{-1}$ AcCO6 (CFE), 0.04 $mg.mL^{-1}$ catalase (CFE), 100 mM KPi buffer (pH 7.0), 35 °C, 200 rpm, overnight, V_{tot} = 1.0 mL. 2) Filtration through 5-13 µm filter paper. 3) aldehyde sequestration on **66** (0.08 mmol) or **67** (0.1 mmol), orbital rotation at 18 rpm, 4 h.

3.4.3 Bioprocess of commercial APGs biosurfactant: preparative scale

Biosurfactants were produced industrially on a Tonne scale, including a distillation step.[196] The bioprocess introduced earlier can reduce the costs due to biosurfactant distillation and reduce possible side reactions occurring during distillation. To bridge the gap between analytical and large-scale synthesis, preparative scales of 2–10 g of samples **81** and **82** were chosen with commercial glassware scale mimicking tonne scale processes. The bead sizes of immobilised protein and size resins of **66** (75-150 µm) and **67** (35-75 µm) were essential to ensure compatibility with a Rotating Bed Reactor (RBR) required for the scale-up reaction. The RBR container can isolate solid beads from the reaction solution and act as a tank reactor's stirring blade.[197] It was compatible with immobilisation resins from Purolite but was not tested for aminooxy-based resin **66** and amine-based resin **67**. Only one size of solid-supported resin was attempted in this section: aminomethyl resin **67**.

3.4.3.1 Bioprocess scale up: catalase, oxygen and filtration

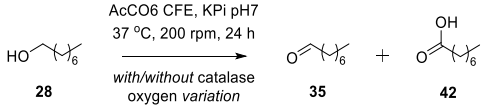

*Scheme 41 – Biotransformation of octanol **28** with variations of oxygen level and catalase. Reagents and conditions: singlate, 30 mM octanol **28** (100 mg, 0.8 mmol, 1.0 equiv.), 50 mg.mL^{-1}AcCO6 (CFE), catalase, 100 mM KPi buffer (pH 7.0), 37 °C, 200 rpm, 24 h, V_{tot} = 25 mL.*

The bioprocess was initially tested on octanol **28** (100 mg, 0.8 mmol, 1.0 equiv.) with AcCO6. The experiment was conducted in a baffled flask and both open and closed systems were tested to observe the effect of catalase and oxygen (Scheme 41). In previous biotransformations with AcCO6, oxygen gas was used in a closed system. However, it was uncertain whether uncontrolled oxygen levels due to an open baffle flask would have an impact. Changes in oxygen concentration could either increase alcohol oxidation to carboxylic acid level or inhibit enzyme activity.

*Table 28 – Biotransformation of octanol **28** with variations of oxygen level and catalase.*

Entry	Catalase	Oxygen level (open/closed lid)	Physical observation	GC-FID (%): Alcohol/Aldehyde/Acid 28/35/42
1	0.04 $mg.mL^{-1}$	Unlimited (open)	Solution volume normal	2:11:87
2	0.04 $mg.mL^{-1}$	Limited (closed)	Dry (no liquid)	1:9:91
3	No	Unlimited (open)	Solution volume normal	20:1:79
4	No	Limited (closed)	Solution volume decreased by half	11:0:89
Reagents and conditions: singlate, 30 mM octanol **28** (100 mg, 0.8 mmol, 1.0 equiv.), 50 $mg.mL^{-1}$AcCO6 (CFE), catalase, 100 mM KPi buffer (pH 7.0) in deionised water (25 mL), 37 °C, 200 rpm, 24 h then quenched with 8.0 M HCl (C_f = 0.3 M).				

After 24 h, the reaction volume decreased (entries 2 and 4, Table 28) when the flask was closed and exposed to a temperature of 37 °C for an extended period. Deionised water was added to return the reaction mixture to a 25 mL total volume. The solutions were quenched with 8.0 M HCl (C_f = 0.3 M), concentrated to dryness and extracted with EtOAc before GC analysis. Octanol **28** (100 mg, 0.8 mmol, 1.0 equiv.) was fully converted in the presence of catalase after 24 h reaction at 37 °C (entries 1 and 2). However, all entries showed significant over-oxidation to octanoic acid **42** (≥75 %), which was not noticed in analytical scale (Chapter 2) and in the literature with such intensity (≤5 %).[94] The oxygen level was supposedly unlimited when the reaction flask was open. Consequently, oxygen concentration could have subjected octanal **35** to react beyond

its given properties and to over-oxidise by propensity.[119,198] This behaviour depended on the groups (EWG, EDG) of the molecule with aldehyde function and its molecular state.

Industries used flange flasks and stirrer blades to mimic tanks and impeller blades, allowing constant temperature and flow throughout the reaction. To replicate this industrial process, a 1 L flange flask with a stirrer blade and a 1 L conical flask shaken in an incubator were chosen with a minimum reaction volume of ≈450 mL. The bio-oxidation of colourless octanol **28** (500 mg, 3.8 mmol, 1.0 equiv.) was performed in a 550 mL reaction solution in a conical flask at 37 °C for 24 h (Scheme 42). The solution was then filtered using 5-13 µm filter paper, separated into two equal volumes, and quenched differently.

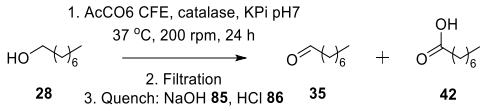

*Scheme 42 – Biotransformation of octanol **28** with variations of quenching method. Reagents and conditions: singlate 1) 1 mM octanol **28** (500 mg, 3.8 mmol, 1.0 equiv.), 50 mg.mL^{-1} AcCO6 (CFE), 0.04 mg.mL^{-1} catalase (CFE), 100 mM KPi buffer (pH 7.0), 37 °C, 200 rpm, 24 h, V_{tot} = 550 mL. 2) separation in two batches of equal volumes followed by filtration through 5-13 µm filter paper. 3) quenching with 5.0 M NaOH **83** or 5.0 M HCl **84**.*

After 24 h, the reaction solution remained opaque and colourful with foaming occurring during the reaction (Image 1). One batch **84** was quenched with strong acid 5.0 M HCl (C_f = 0.2 M, pH_f = 6), while batch **83** was quenched with strong base 5.0 M NaOH (C_f = 0.2 M, pH_f = 11). Both batches were filtered through Büchner filtration using WHATMAN grade 1 filter paper (11 µm) to remove the excess of CFE. Unfortunately, the filter was clogged and retained the filtrate. Batches **83** and **84** were centrifuged independently at 3024 × *g* for 4 min. The supernatants were collected (Image 1).

*Image 1 – Biotransformation of octanol **28** (500 mg) with AcCO6 CFE after 24 h reaction (left), which solution was separated in equal volume and quenched with 5.0 M NaOH **83** (middle) or quenched with 5.0 M HCl **84** (right)*

As shown in Table 29 and Image 1, the quench method impacted the pH of the filtrates and their appearance. Batch **83** had a basic pH (pH 11) and opaque solution, whereas batch **84** had a pH closer to neutral (pH 6) and transparent solution. However, the ratios of octanol **28** conversion were similar, which refuted the participation of the quench method in the over-oxidation phenomenon. Antifoaming was added to the reaction solutions to facilitate future experiments, and an HCl solution was chosen to quench the reaction with AcCO6 CFE.

*Table 29 – Biotransformation of octanol **28** (500 mg, 3.8 mmol, 1.0 equiv.) with variations of quenching method.*

Entry	Batch	Quench method	pH reaction solution after quenched	Appearance after quench and filtration	GC-FID (%): Alcohol/Aldehyde/Acid 28/35/42
1	**83**	Strong base	11	Brown opaque	7:13:80
2	**84**	Strong acid	6	Orange transparent	10:14:76

Reagents and conditions: singlate 1) 1 mM octanol **28** (500 mg, 3.8 mmol, 1.0 equiv.), 50 $mg.mL^{-1}$ AcCO6 (CFE), 0.04 $mg.mL^{-1}$ catalase (CFE), 100 mM KPi buffer (pH 7.0), 37 °C, 200 rpm, 24 h, V_{tot} = 550 mL. 2) separation in two batches of equal volumes followed by filtration through 5-13 µm filter paper. 3) quenching with 5.0 M NaOH **83** or 5.0 M HCl **84**.

3.4.3.2 Bioprocess scale up: rotating bed reactor (RBR) in industry

Before the filtration difficulties due to bio-oxidation of octanol **28** (100 mg, 0.8 mmol, 1.0 equiv.) with AcCO6 CFE, the process was improved by switching to an immobilised enzyme. The use of immobilised biocatalyst resolved the filtration issues and eliminated the need for a vacuum filtration step. AcCO6 was immobilised on the carrier epoxymetacrylate ECR8285 and used for the following bio-oxidation. However, it was observed that epoxy butylmethacrylate ECR8285 beads were prone to grinding easily (section 3.2). To maximise the biocatalysis, a rotating bed reactor (RBR) was used, where the biocatalyst beads were placed (Figure 29). Hence, bioprocess with immobilised AcCO6 was attempted under various conditions, including with and without the RBR.

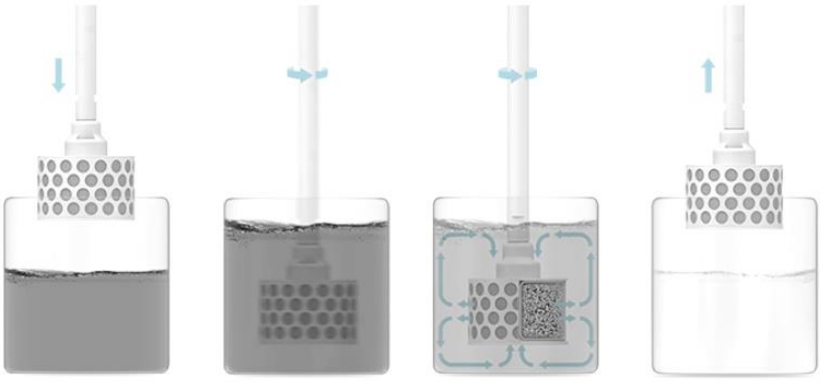

Figure 29 - Rotating bed reactor (RBR) applied in solution. Source: SpinChem

3.4.3.2.1 Comparison of octanol biotransformation with equipment variation (flasks, temperature distribution, RBR)

As shown in Scheme 43, the oxidation of octanol **28** (100 mg, 0.8 mmol, 1.0 equiv.) using AcCO6 was carried out using AcCO6 and different types of equipment. The equipment mimicked a tonne scale tank. For comparison purposes, an additional experiment was conducted using a flange flask and jacketed reactor with a blade stirrer or RBR. The resulting colour reaction was also reported as the industry aimed to produce colourless biosurfactants.

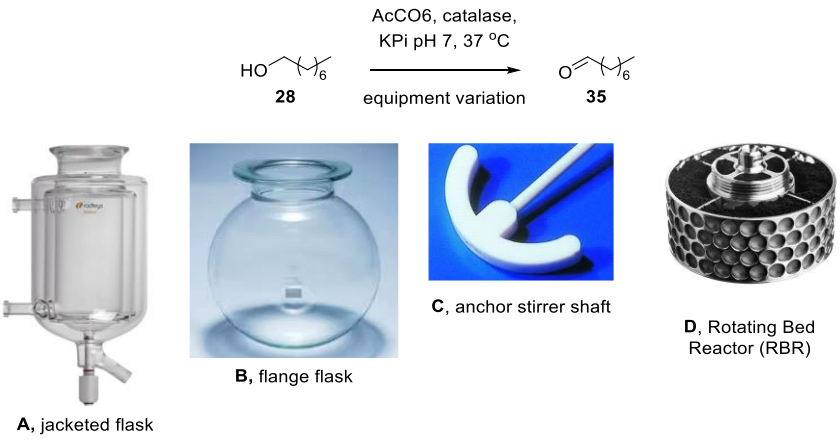

*Scheme 43 - Bioprocess of octanol **28** (100 mg, 0.8 mmol, 1.0 equiv.) with equipment variation, AcCO6 form and aminomethyl resin **66.** Reagents and conditions: singlate, 1.7 mM octanol **28** (100 mg, 0.8 mmol, 1.0 equiv.), AcCO6 (immobilised or CFE), 0.04 mg.mL^{-1} catalase (CFE), aminomethyl resin **67**, 100 mM KPi buffer (pH 7.0), 37 °C, 200 rpm, overnight. Source image: Radleys®, Sigma-Aldrich®, Spinchem®.*

According to Table 30, immobilised AcCO6 had a similar octanol **28** conversion (89 %, entry 2) to AcCO6 CFE (entry 1) but with a slightly opaque solution. The immobilised AcCO6 beads were damaged during the reaction that was carried out in a baffled flask, making them more difficult to recover than immobilised beads placed in RBR (entry 3). The flange flask reactions were heated with a hotplate, which resulted in non-homogenous diffusion temperature in the reaction solution within the flask. An alternative reaction using a jacketed reactor was attempted and showed a similar octanol **28** conversion to the reaction carried out with a flange flask (entries 3 and 4).

A difference in colour reaction was observed between the experiments (Table 30). When AcCO6 CFE was used, the reaction solution was orange (entry 1). However, when immobilised AcCO6 was used, the solution turned white or transparent (entries 2, 3 and 4). The use of immobilised AcCO6 resulted in a more transparent reaction solution than AcCO6 CFE. Additionally, when immobilised AcCO6 was placed in RBR, it allowed the recovery of undamaged protein beads instead of free beads in the solution (entry 2).

*Table 30 – Bioprocess of octanol **28** (100 mg, 0.8 mmol, 1.0 equiv.) with variations of equipment, AcCO6 form and aminomethyl resin **67**.*

Entry	AcCO6	RBR	Aminomethyl resin 67	Equipment	GC-FID (%): Alcohol/Aldehyde/Acid 28/35/42	Comments
1	CFE, 0.06 mg.mL^{-1}	No	n.a.	Baffled flask	11:8:81	Solution slightly opaque
2	Immobilised, 0.03 mg.mL^{-1}	No	n.a.	Baffled flask	11:66:69	Solution white opaque
3	Immobilised, 0.03 mg.mL^{-1}	Yes	n.a.	Flange flask	5:9:86	Solution transparent
4	Immobilised, 0.03 mg.mL^{-1}	Yes	n.a.	Jacketed reactor	3:7:90	Solution transparent
5	Immobilised, 0.03 mg.mL^{-1}	Yes	**67** Free in solution, 200 mg, 0.4 mmol, 0.5 equiv.	Flange flask	8:5:88	IR: medium 1644 cm^{-1}, resin **67** not recovered
6	Immobilised, 0.03 mg.mL^{-1}	Yes	**67** placed in RBR, 200 mg, 0.4 mmol, 0.5 equiv.	Flange flask	86:0:14	IR: weak 1644 cm^{-1}, all beads were mixed

Reagents and conditions: singlate, 1.7 mM octanol **28** (100 mg, 0.8 mmol, 1.0 equiv.), AcCO6, 0.04 mg.mL^{-1} catalase (CFE), aminomethyl resin **67**, 100 mM KPi buffer (pH 7.0), 37 °C, 200 rpm, overnight, V_{tot} = 450 mL. n.a.: not applicable.

The RBR has been shown to be advantageous for the enzymatic oxidation of octanol **28**. However, the over-oxidation to acid octanoic **42** kept occurring. To solve this, a one-pot process was attempted by adding amine-based resin **67** (Scheme 44). The one-pot process relied on the oxidation of octanol **28** with immobilised AcCO6 in RBR to octanal **35**, sequestered *in situ* on resin **67** and reducing the formation of octanoic acid **42**. Two experiments were conducted: one with immobilised AcCO6 in RBR and resin beads **67** placed free in solution (entry 5, Table 30), and the other with both beads (immobilised AcCO6 and resin **67**) placed in separate chambers of the RBR (entry 6). However, GC results confirmed the presence of octanoic acid **42** in both cases and IR analysis did not confirm the sequestration of aldehyde. Additionally, resin **67** was not recovered when free in solution, even after careful filtration. When placed in RBR, resin **67** leaked through the RBR filter and was either free in solution or mixed with immobilised enzyme in a different chamber.

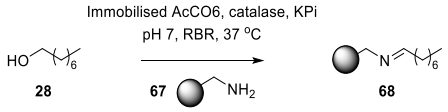

*Scheme 44 – Bioprocess of octanol **28** (100 mg, 0.8 mmol, 1.0 equiv.) with immobilised AcCO6 and aminomethyl resin **67** using RBR reactor**.** Reagents and conditions: singlate, 1.7 mM octanol **28** (100 mg, 0.8 mmol, 1.0 equiv.), 0.03 mg.mL^{-1} immobilised AcCO6, 0.04 mg.mL^{-1} catalase (CFE), aminomethyl resin **67** (200 mg, 0.4 mmol, 0.5 equiv.), 100 mM KPi buffer (pH 7.0), 37 °C, 200 rpm, overnight.*

To understand the leakage of resin **67,** the size of resin **67** beads and ECR8285 epoxymethacrylate beads and RBR pore size were studied. The particle size of resin **67** was 200-400 mesh, which correspond to 35-75 microns (µm).[169,170] ECR8285 epoxymethacrylate had a particle size of 2500-1000 µm.[199]

Discussions with Spinchem® highlighted the limitation of the RBR filter (Figure 30). The RBR filter pore size of 104 µm was smaller than the particle size of ECR8285 binding AcCO6 (which ranged

from 250-1000 µm) but was bigger than aminomethyl resin **67** (with a particle size of 35-75 µm). As a result, the flow generated during the reaction pushed resin **67** out of the RBR reactor while retaining the immobilised protein in the reactor. To overcome this issue, SpinChem® recommended the use of cartridges with a pore size of 40 µm, which would retain small beads like resin **67**. The immobilised enzyme and amine resin **67** were loaded into separate cartridges and kept separate during stirring (Figure 30C).

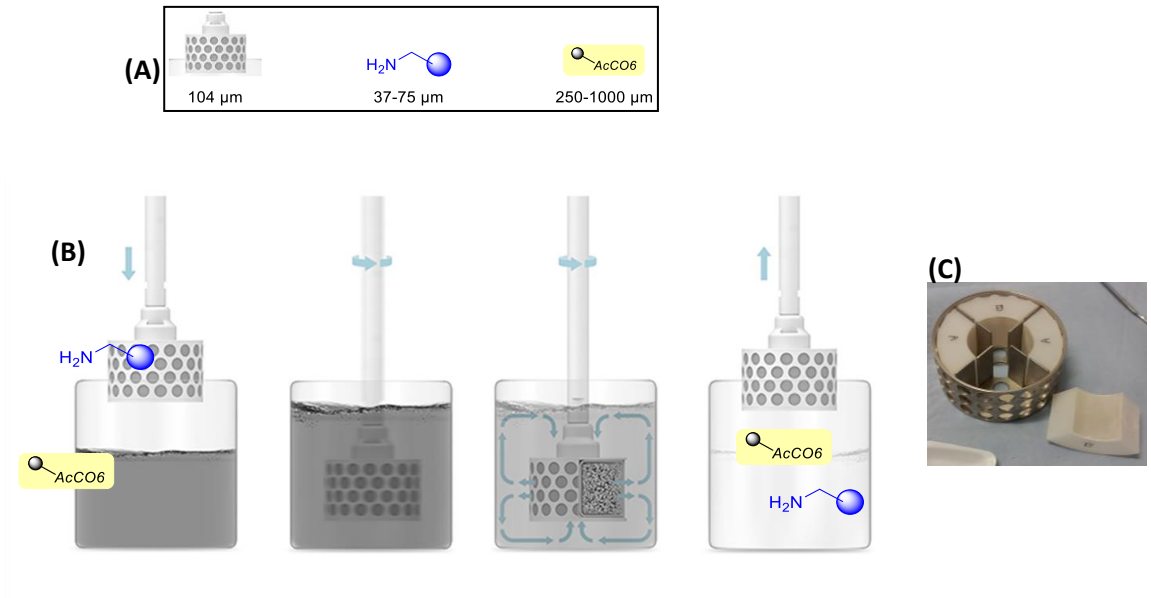

*Figure 30 - Size compatibility of RBR, aminomethyl resin **67** and immobilised AcCO6. (A) size of RBR filter and beads. (B) flow reaction allowed leakage of **67** and retained immobilised AcCO6. (C) SpinChem® cartridges.*

3.4.3.2.2 Applications to APG surfactant samples

3.4.3.2.2.1 Applications to APG surfactant sample pre-distillation

During the experiment, bioprocess was used on sample **81** instead of APG distillation (Scheme 45). The aim was to explore the limits of alcohol oxidation in the presence of APGs without resin **67**, time variation and scale variation. The recovered APG was expected to be the same amount as the initial APG. Both the aqueous and organic phases contained carbohydrates due to the amphiphilic properties of AMG-C_8 **53** and AMG-C_{10} **54**. The volume reaction was varied to achieve an alcohol concentration close to the K_M value of AcCO6 with octanol **28** (34.6 mM). After 16 h, the reactions

were quenched, evaporated and extracted with EtOAc. All reactions were expected to contain only APGs and KPi salt buffer before extraction. For instance, when processing 2.50 g of sample **81**, the crude mass expected was 12.55 g, consisting of 1.25 g of APGs and 11.3 g of KPi salt buffer.

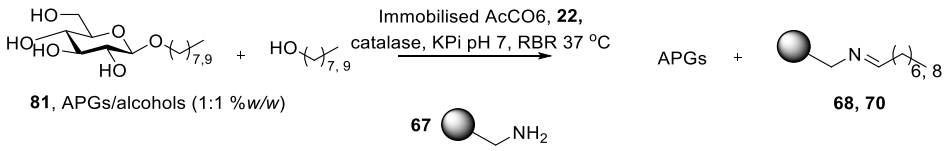

*Scheme 45 - Bioprocess of commercial APG-C_8/C_{10} **53/54** sample **81**. Reagents and conditions: singlate, sample **81**, immobilised AcCO6 placed in RBR, aminomethyl resin **67** placed in RBR, 0.04 mg.mL^{-1} catalase (CFE), 100 mM KPi buffer (pH 7.0), 37 °C, 200 rpm.*

As indicated in Table 31, the oxidation using immobilised AcCO6 was limited to 25 % conversion when the alcohol concentration was ≥K_M (entry 1). However, when sample **81** was diluted to reach a concentration of around 15 mM alcohol (entry 4), the conversion rate increased to a maximum of 50 %. The oxidation process was found to be independent of reaction time, and the maximum conversion rate was reached regardless of whether the reaction lasted for a short or long time (entries 2 and 3). Instead of stopping after 4 h reactions, the experiments proceeded overnight and colorimetric analysis indicated a decolouration over time. The colour of the reaction solution decreased during oxidation from 0.5 G after 5 h experiment to 0.0 G after 15 h experiments (entries 2 and 3). The dilution of **81** and the production of hydrogen peroxide were responsible for the initial low Gardner (G) colour (entries 2 and 3).

In Table 31 (entries 5-9), sample **81** was treated with immobilised AcCO6 and aminomethyl resin **67**, which were loaded in RBR cartridges. The solid support **67** was added as a one-pot with AcCO6 and **67** (entries 7, 8 and 9) or after 16 h reaction (entry 6). The colour of these reactions was increased from 0.8 G to 1.3–3.7 G. However, no technical or chemical reason could explain this colour change. Perhaps the Gardner colour increased in the presence of alcohol.

During the experiments with resin **67**, the alcohol proportion remained as important as for experiments performed without resin **67** (20-30 % alcohol conversion, entries 5 and 9). Calibration curves on GC-FID were attempted to estimate the recovered masses of APGs and alcohols in every phase collected. Unfortunately, only the ratio between alcohol, aldehyde and acid was determined, but not their masses (in grams). More understanding of analytical gas chromatography was required, which couldn't be covered in the context of this thesis. IR instruments were insufficient to detect C=N band, which was necessary to confirm successful aldehyde sequestration. NMR analysis did not permit to determine the ratio of AMGs/KPi. Accordingly, only qualitative answers were obtained about the alcohol biotransformation, the aldehyde sequestration, the product colour and the product purity due to these analysis limits.

After the reaction, an additional purification step was performed to recover APG (entry 9, Table 31). The crude sample obtained was dry-loaded onto silica or a celite plug and purified by column chromatography silica gel to attempt the removal of the excess of KPi buffer salts. However, instead of full recovery, APG surfactant was obtained in an 11 % yield with a purity of 100 %. The low recovery could be attributed to the partition of APG during extraction water-EtOAc and the inadequate solvent system used during column chromatography.

*Table 31 – Bioprocess of commercial APG-C_8/C_{10} **53/54** sample **81**.*

Entry	Amount of AMG-C_8/C_{10} in sample 81 (g)	Amount of C_8/C_{10} 28/30 alcohols in 81 (g)	AcCO6 immobilised ($mg.mL^{-1}$)	Resin 67	Time reaction	Gardner colorimetry after reaction (no work up)	GC-FID (%): after reaction Alcohol/Aldehyde/Acid	Reaction method	IR (cm^{-1})
1	5	5 (≈60 mM)	0.03	n.a.	16 h	0.4	96:0:4	n.a.	n.a.
2	2.5	2.5 (≈30 mM)	0.03	n.a.	5 h	0.8	76:0:24	n.a.	n.a.
3	2.5	2.5 (≈30 mM)	0.03	n.a.	16 h	0.0	76:0:24	n.a.	n.a.
4	1.25	1.25 (≈15 mM)	0.03	n.a.	15 h	0.4	48:0:51	n.a.	n.a.
5	1.25	1.25 (≈15 mM)	0.03	200 mg, 0.4 mmol, 0.04 equiv.	15 h	3.7	81:1:18	n.a.	n.d.
6	1.25	1.25 (≈15 mM)	0.03	200 mg, 0.4 mmol, 0.04 equiv.	16h+5h	2.8	87:2:11	Addition of **67** after 16 h	n.d.
7	1.25	1.25 (≈15 mM)	0.31	200 mg, 0.4 mmol, 0.04 equiv.	4 h	2.4	77:0:23	One-pot	n.d.
8	1.25	1.25 (≈15 mM)	0.03	200 mg, 0.4 mmol, 0.04 equiv.	20 h	2.2	73:1:26	One-pot	n.d.
9	1.25	1.25 (≈15 mM)	0.31	200 mg, 0.4 mmol, 0.04 equiv.	15 h	1.3	74:0:26	One-pot; Purification by column chromatography	n.d.

Reagents and conditions: singlate, sample **80**, immobilised AcCO6 placed in RBR, aminomethyl resin **67** placed in RBR, 0.04 $mg.mL^{-1}$ catalase (CFE), 100 mM KPi buffer (pH 7.0), 37 °C, 200 rpm, V_{tot} = 650 mL. n.a.: not applicaple. n.d.: not detected.

3.4.3.2.2.2 Applications to APG surfactant sample post-distillation

After distilling sample **81**, sample **82** was obtained, which contained 99 *%w/w* of APGs biosurfactant and 1 *%w/w* of alcohol. Sample **82** underwent treatment with immobilised AcCO6 and aminomethyl resin **67** in RBR cartridges (Scheme 46).

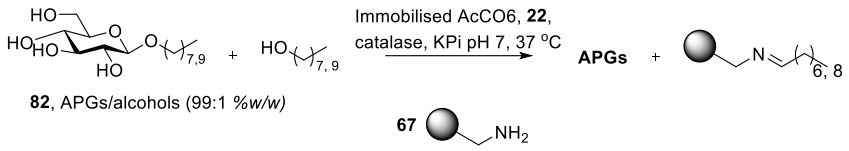

*Scheme 46 - Bioprocess of commercial APG-C_8/C_{10} **53/54** sample **82**. Reagents and conditions: singlate, sample **82**, immobilised AcCO6 placed in RBR, aminomethyl resin **67** placed in RBR, 0.04 mg.mL^{-1} catalase (CFE), 100 mM KPi buffer (pH 7.0), 37 °C, 200 rpm.*

Sample **82** was diluted to reach ≈2.9 mM alcohol concentration and treated with immobilised AcCO6 in the presence or absence of resin **67** (Table 32). Without resin **67**, alcohol conversion reached 87 % after 24 h reaction with Gardner 0.0 G (entry 1). In the presence of resin **67**, aldehyde sequestration was confirmed by IR with a weak band C=N (1652 cm^{-1}, entry 2) with minimal presence of overoxidation (14 % octanoic acid). The bioprocess was successful regardless of the mass of APG present.

The alcohol concentration of sample **82** was increased to ≈7.0 mM. The colour of each reaction solution became orange with 3.1–4.5 G independently of the presence or absence of resin **67** and the time-reaction (entries 3, 4, 5 and 6, Table 32). Sample **82** was treated by bioprocess 4 h and 24 h. The oxidation continued to reach 50 %, then 64 % alcohol conversion (entries 3 and 4), which showed immobilised AcCO6 remained active after 16 h reaction. The rate of alcohol conversion was influenced by the amount of immobilised enzyme, as shown by the equal conversion (50 %, entries 3 and 5Table 32). Addition of amin resin **67** with immobilised AcCO6 (0.03 mg.mL^{-1}) permitted the sequestration of aldehydes in total, as no aldehydes were detected by GC-FID. Even

after the reaction, alcohols were still detected as the major species while over-oxidation occurred (ratio alcohols/aldehyde/acid 86:0:14).

The bioprocess has been found effective in oxidising alcohols diluted to 1.7 mM, including fatty alcohol mixtures, with or without APG biosurfactant. The proportion of alcohol/carbohydrate in sample **81** (APG/alcohol 1:1 *%w/w*) and sample **82** (APG/alcohol 99:1 *%w/w*) did not hinder the bioprocess. However, further optimisation would be required.

*Table 32 – Bioprocess of commercial APG-C_8/C_{10} **53/54** sample **82**.*

Entry	Amount of AMG-C_8/C_{10} in sample 82 (g)	Amount of C_8/C_{10} 28/30 alcohols 82 (g)	AcCO6 immobilised (mg.mL^{-1})	Resin 67	Time reaction	Gardner colorimetry after reaction (no work up)	GC-FID (%): After reaction Alcohol/Aldehyde/Acid	IR (cm^{-1})
1	1.85	0.25 (≈2.9 mM)	0.03	-	24 h	0.0	12:1:87	-
2	1.85	0.25 (≈2.9 mM)	0.03	200 mg, 0.4 mmol, 0.2 equiv.	24 h	0.7	86:0:14	Weak 1652
3	4.41	0.59 (≈7.0 mM)	0.03	-	4 h	4.1	50:0:50	-
4	4.41	0.59 (≈7.0 mM)	0.03	-	24 h	3.1	36:30:34	-
5	4.41	0.59 (≈7.0 mM)	0.015	-	24 h	4.5	48:1:51	-
6	4.41	0.59 (≈7.0 mM)	0.03	200 mg, 0.4 mmol, 0.1 equiv.	24 h	4.2	86:0:14	Weak 1652
Reagents and conditions: singlate, sample **82**, immobilised AcCO6 placed in RBR, aminomethyl resin **67** placed in RBR, 0.04 mg.mL^{-1} catalase (CFE), 100 mM KPi buffer (pH 7.0), 37 °C, 200 rpm, V_{tot} = 650 mL.								

3.5 Conclusion and future work

In this chapter, various methods were discussed to enhance bio-oxidation and resin chemistry in accordance with green chemistry principles.[4,200] The chapter extended the knowledge on the aminooxy-based resin **66** and amine-based resin **67** to the sequestration of fatty aldehydes **35-40** at room temperature. Furthermore, a bioremediation combining enzymatic oxidation of fatty alcohols **28-31** and Schiff base chemistry on solid supports **66** and **67** was examined for purifying APG biosurfactant (Figure 31).

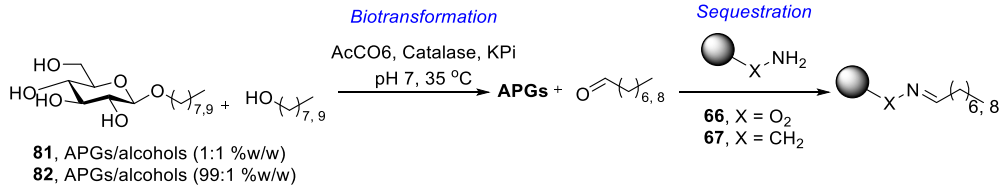

Figure 31 - Bioprocess of biocatalytic oxidation followed by sequestration on solid support

DMF as a swelling solvent should be replaced for resins **66** and **67** due to its toxic effects on enzymes. Instead, greener alternatives such as DCM and 1,4-dioxane could be used.[201–204] There were various solvent combinations that could be attempted for[171,205–207] including DMSO/EtOAc (1:9),[208] cyrene/diethyl carbonate (3:7),[206,209] DMSO/dioxolane (3:7) and biodegradable PolarClean solvent.[210] The impact of these solvents on AcCO6 would be studied too.

Bio-oxidation with AcCO6 and aldehyde sequestration were attempted by adding an intermediate filtration of protein CFE. The process was scaled up to oxidise octanol **28** from 2 mg to 100 g and to treat commercial mixtures of alcohols such as octanol/decanol **28/30** and nonanol/undecanol **29/31**. The biocatalytic process was carried out to remove alcohol solvent from manufacture samples (**81** and **82**) of APG biosurfactant. The alcohol removal was possible when the alcohol concentration was lower than the KM value of AcCO6 (AcCO6: K_M = 32 mM for octanol **35**). To ensure reliable results, analytical methods such as NMR, IR, and GC were used. GC was found to be the most reliable analytical tool for biosurfactant analysis. Its utilisation for APG

monitoring could be enhanced by using calibration curves, internal standards and carbohydrate derivatisation.[211–213]

The bioprocess was facilitated by immobilising AcCO6 on epoxymethacrylate beads and physically separating it from amine-based resin **67**. The physical restriction of the two types of beads led to the consideration of replacing the blade stirrer with a rotating bed reactor (RBR). The cartridges in the RBR contained the beads without causing any leakage. In the future, carriers for protein immobilisation (His-tagged specific and amino-specific) with long-term recycling would be screened.

Extensive dilution of APG sample **82** was required, which went against the principles of green chemistry that encouraged minimal use of solvents. However, several settings could be optimised to improve the process, such as dilution factors, oxygen concentration, concentration of KPi buffer, extraction methods, analysis methods, swelling solvent, alcohol concentration, resin quantity, scale-up effect and rotation speed of the RBR. To explore the appropriate conditions, the turnover of immobilised AcCO6 would be determined for scale-up reactions with different volumes (0.65 L, 1.00 L, 10 L). The oxygen concentration would be varied using an oxygenated buffer, an oxygen probe for monitoring, and a controlled flow of oxygen in the reaction solution within a closed system.

Chapter 4 - Cascade reaction of fatty alcohols in aqueous media

The American Chemical Society (ACS) Green Chemistry Institute (GCI) Pharmaceutical Roundtable (PR) has been promoting the use of green chemistry and green engineering in the pharmaceutical industry since 2005.[214–216] One of the promoted chemical reactions is carbon-carbon double bond formation through catalytic Wittig olefination, which can be done base-free or in continuous flow.[214–217]

This chapter will discuss the contribution to a greener Wittig olefination in mild reaction conditions. Firstly, fatty alcohols will be evaluated as substrates of choline oxidase AcCO6. Alongside the exploration of AcCO6 substrate scope, the potential for Wittig olefination in aqueous media will be explored and optimised. Finally, a cascade approach for alkene formation will be designed utilising bio-oxidation of fatty alcohols with AcCO6 followed by Wittig olefination in aqueous media.[5]

4.1 Identification of novel substrates of oxidase AcCO6

4.1.1 Screening of functionalised aliphatic alcohols

The substrate scope of choline oxidase AcCO6 was reported by Heath *et al.*[70] on saturated fatty alcohols from 2 to 16 carbon lengths, saturated alkyl alcohols and benzyl alcohols. Here, insights into AcCO6 potential were explored with different types of fatty alcohol with functional groups, such as halogens, silyl group, thiomethyl and azido. Most of these functionalised alcohols were obtained commercially from Sigma-Aldrich, TCI and Alfa Aeser. However, the two azido alcohols, namely 4-azido-1-ol **87** and 5-azido-pentan-1-ol **88**, were synthesised chemically by nucleophilic substitution (SN) of 4-bromo-butan-1-ol **85** and 5-bromopentan-1-ol **86**, respectively, with sodium azide NaN_3 (Scheme 47) in good yield, (**87**: 44 %; **88**:75 %).[218]

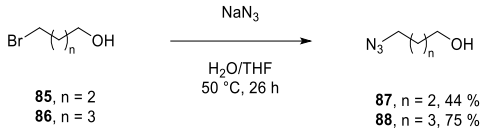

*Scheme 47 – Synthesis of azido alcohols **87** and **88** with NaN_3. Reactions conditions: 4-bromobutanol **85** (13.1 mmol, 1.0 equiv.) or 5-bromopentanol **86** (13.1 mmol, 1.0 equiv.), NaN_3 (18.3 mmol, 1.4 equiv.) in H_2O/THF (1:1 %v/v) at 50 °C for 26 h.*

Hence, specific activity of AcCO6 was expanded to fatty alcohols **85-95** with ABTS assay (Scheme 47) performed on a TECAN Infinite 200 Pro M Nano spectrophotometer and evaluated with Beer-Lambert Law (Equation 4) similar to Heath *et al*.[70] For this assay, octanol **28** was considered as a control substrate for ABTS assay with AcCO6.[70] The functional groups of **87-92** were acting as electron withdrawing groups (EWG) and thiomethyl **93-95** acted as electron donating group (EDG).

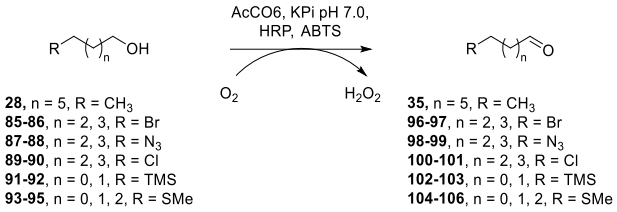

*Scheme 48 – Activity assay of AcCO6 as biocatalyst for oxidation of 5 mM fatty alcohols **85-95** in presence of 0.01 mg.mL^{-1} AcCO6 pure, 0.5 mg.mL^{-1} HRP, 0.7 mg.mL^{-1} ABTS at 30 °C, λ = 420 nm.*

$$A = l \times c \times \varepsilon$$

Equation 4 - Beer-Lambert law. A: absorbance, l: pathlength (cm), c: concentration (mol.L^{-1}), ε: molar extinction coefficient (L.mol^{-1}.cm^{-1})

As shown in Table 33, the specific activity of octanol **28** with AcCO6 was detected at 48.9 mU.mg^{-1} (entry 1), while it was initially reported at 38 mU.mg^{-1}.[70] This difference was due to the experimenter's execution but did not affect the assay interpretation. The absorbances of trimethylsilyl alcohols **91-92** (entries 8 and 9) and 2-thiomethylethanol **93** (entry 10) were 1.1-2.4 higher than octanol **28.** Thiomethyl alcohols with C3 **94** and C4 **95,** chloro alcohols **89-90**, bromo

alcohols **85-86** and azido alcohols **87-88** showed a fold 7.3–11.4 times higher than specific activity of octanol **28** with AcCO6, indicating that AcCO6 had an impressive production of hydrogen peroxide. The differences in the specific activities of these substrates **85-95** (entries 4-12) were induced by the carbon chain length ranging from 2 to 5 carbons and the steric hindrance of the substrate terminal functional group.

The chemistry of halogens, which are atoms rich in electrons, and their ability to bind protein-ligand for non-covalent interaction could explain the high folds of specific activity observed in alkyl halides **86-86** and **89-90**.[219–222] About the butyl alkyl halides **85** and **89**, the absorbance was higher for chloro substrate **89**, which had a smaller halogen atom (356 $mU.mg^{-1}$, entry 2) than substrate with bromine atom **85** (437.0 $mU.mg^{-1}$, entry 6). The difference in atom size between halogens could explain the reactivity of **85** and **89** with AcCO6. However, this observation was not witnessed on pentyl alkyl halides **86** and **90**; bromo alkyl **86** (553.9 $mU.mg^{-1}$, entry 3) had a specific activity higher than chloro alkyl **90** (544.9 $mU.mg^{-1}$, entry 7). The nature, chain length and hindrance of the alkyl substrate were accountable for AcCO6 reactivity.

The biocatalyst AcCO6 demonstrated impressive specific activity, making all alcohols **85**-**95** potential substrates for scale-up reaction and analysis by ^{1}H NMR.

Table 33 - Specific activities of AcCO6, where specific activity was the amount of product formed [µmol] per min per mg of enzyme (1 U is defined as 1 µmol.min^{-1}.mg^{-1}).

Entry	Substrate	Specific activity (mU.mg^{-1}) ± SD	Fold increase[a]
1	 **28**	48.9 ± 0.8	n.a.
2	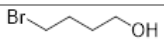 **85**	356.0 ± 6.0	7.3
3	 **86**	553.9 ± 11.2	11.4
4	 **87**	387.4 ± 7.5	8.0
5	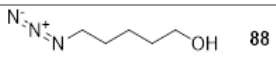 **88**	544.2 ± 12.8	11.2
6	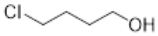 **89**	437.0 ± 2.7	9.0
7	 **90**	544.9 ± 9.1	11.2
8	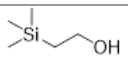 **91**	118.8 ± 1.1	2.4
9	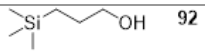 **92**	55.5 ± 0.9	1.1
10	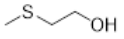 **93**	108.1 ± 3.4	2.2
11	 **94**	514.0 ± 6.4	10.6
12	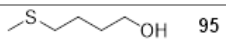 **95**	484.8 ± 4.4	10.0

Assay conditions: triplicate, 30 °C, 0.5 mg.mL^{-1} HRP (stock solution: 2.0 mg.mL^{-1} HRP in 100 mM KPi pH 7.0), 0.7 mg.mL^{-1} ABTS (stock solution: 2.8 mg.mL^{-1} ABTS in 100 mM KPi pH 7.0), 5 mM substrate **28,85-95** (stock solution: 50 mM substrate in 100 mM KPi pH 7.0 10% DMSO), 0.01 mg.mL^{-1} AcCO6 pure (stock solution: 0.05 mg.mL^{-1} AcCO6 pure in 100 mM KPi pH 7.0), λ = 420 nm.

[a]Fold increase in specific activity with **28** octanol as standard.

n.a.: not applicable

4.1.2 Bio-oxidation of 4-azidobutanol with AcCO6

In section 4.1.1, eleven substrates were introduced. Among these, substrate 4-azidobutanol **87** (1.00-2.00 mg, 0.01-0.02 mmol, V_{tot} = 0.5-1.0 mL) was oxidised with AcCO6 and analysed by ^{1}H NMR to confirm the formation of azido aldehyde **98** (Scheme 49). The oxidation of alcohol **87** was performed with AcCO6 CFE because AcCO6 CFE was easily available. After the reaction, the mixture was quenched with 5.0 M NaOH (C_f = 0.05 M), extracted with EtOAc and analysed by ^{1}H NMR.

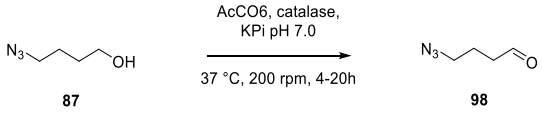

*Scheme 49 – Oxidation of azido alcohol **87** with AcCO6. Reaction conditions: 20 mM alcohol **87** (0.01-0.02 mmol), 75 mg.mL^{-1}AcCO6 (CFE), 0.04 mg.mL^{-1} catalase (CFE), 100 mM KPi (pH 7.0) in incubator 200 rpm, 37 °C, 4–20 h, V_{tot} = 0.5-1.0 mL.*

As shown in Table 34, bio-oxidation of 4-azidobutanol **87** after 4 h reaction was confirmed by ^{1}H NMR with a (bs) signal at 9.80 ppm instead of a triplet signal expected (entry 1).[223] Attempts were made to increase the aldehyde **98** signal and improve the biotransformation by performing biphasic reactions in toluene or hexane (20 %*v/v* organic solvent, entries 2-3). The biphasic reacting system contained two immiscible phases and product yield depended on their physicochemical properties. The purpose of this method was to transfer the newly formed aldehyde **98** into the organic layer, thus increasing its yield and decreasing its concentration in the aqueous layer. As a result, the proton aldehyde signal of 4-azidobutanal **98** was detected as a singlet with 20 %*v/v* toluene, but was absent with 20 %*v/v* hexane (entries 2-3). The presence of 20 %*v/v* organic solvent did not improve the formation of alkyl **98** in 0.01 mmol scale.

*Table 34 – Oxidation of azido alcohol **87** with AcCO6 with volume variation, solvent variation and time variation.*

Entry	Total volume	Solvent variations	Reaction time	Aldehyde product 98 (^{1}H NMR in $CDCl_3$)
1	500 µL (**87**: 0.01 mmol)	n.a.	4h	9.80 ppm, bs
2	500 µL (**87**: 0.01 mmol)	20 %*v/v* toluene	4 h	9.80 ppm, s
3	500 µL (**87**: 0.01 mmol)	20 %*v/v* hexane	4 h	n.d.
4	1 mL (**87**: 0.02 mmol)	n.a.	4 h	9.81 ppm, s
5	1 mL (**87**: 0.02 mmol)	n.a.	20 h	n.d.

Reaction conditions: singlate, 20 mM alcohol **87** (0.01-0.02 mmol), 75 $mg.mL^{-1}$ AcCO6 (CFE), 0.04 $mg.mL^{-1}$ catalase (CFE), 100 mM KPi (pH 7.0) in incubator 200 rpm, 37 °C, 4–20h, V_{tot} = 0.5-1.0 mL.

n.a. : not applicable. n.d. : not detected

The experiment involving the biotransformation of azido alcohol **87** was repeated with an increased reaction scale of 0.2 mmol (entries 4-5, Table 34). After 4 h reaction, azido aldehyde **98** peaks were detected at 9.80 ppm as a singlet. The experiment was further replicated for 20 hours, after which the peak of aldehyde **98** was no longer detected. This suggests that 4-azidobutanal **98** is a time-sensitive and reaction-sensitive compound at 37°C, and it may decompose over time.

Alcohols **85-95** had a specific activity with AcCO6 five times higher than octanol **28**, like azido alcohol **87** (section 4.1.1). Knowingly that azido aldehyde **98** might decompose after 4 h bio-oxidation at 37 °C, aldehydes **96-106** might also be unstable after 4 h oxidation. For these reasons, the following reactions from Chapter 4 were conducted for a maximum time of 4 h, unless otherwise specified. In order to explore a different analytical method than ^{1}H NMR, GC-FID apparatus was utilised in section 4.1.3.

4.1.3 Preparation of azido alkyl standards for GC-FID analysis

NMR data of azido alcohols **87-88** and fatty aldehydes **98-99** were available in the literature.[223] However, their analysis using GC methods and retention times hadn't been reported yet. To establish reliable GC-FID methods for azido alcohols **87-88** and azido aldehydes **98-99**, product standards were first synthesised. Alcohol standards **87-88** were chemically synthesised as previously described (Scheme 47). Aldehyde standards **98-99** were also synthesised chemically using Dess-Martin oxidation from alcohols **87-88** (Scheme 50).

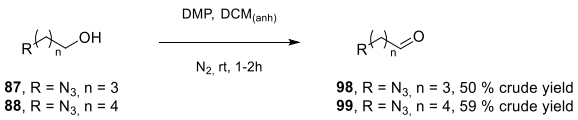

*Scheme 50 – Oxidation of azido alcohols **87-88** by Dess-Martin oxidation. Reaction conditions: 4-azidobutanol **87** (0.9 mmol, 1.0 equiv.) or 5-azidopentanol **88** (0.77 mmol, 1.0 equiv.), DMP (1.3 equiv.), $DCM_{(anh)}$ under N_2 atmosphere at rt for 1-2 h.*

The azido aldehydes **98** and **99** were synthesised from azido alcohols **87** and **88** with a crude yield 50 % and 59 %, respectively. These yields were lower than what was expected based on the literature (83-95 %).[224,225] They were used as GC-FID standards without further purification. Consequently, chromatograms of standards **87-88** and **98-99** were generated with the major peak associated to the desired standard analyte (Table 35). In the future, complementary analysis by GC-MS could confirm this explanation.

GC analysis methods had to be optimised to obtain separate peaks and different retention times between alcohol and aldehyde. To this purpose, a mixture of standard analytes, such as the sample of mixture **88**/**99** (1:4), was prepared and analysed by GC-FID. As shown in Figure 32, standard 5-azidopentanol **88** was identified at 4.6 min retention time with a high intensity peak without an overlapping peak (>400 pA).

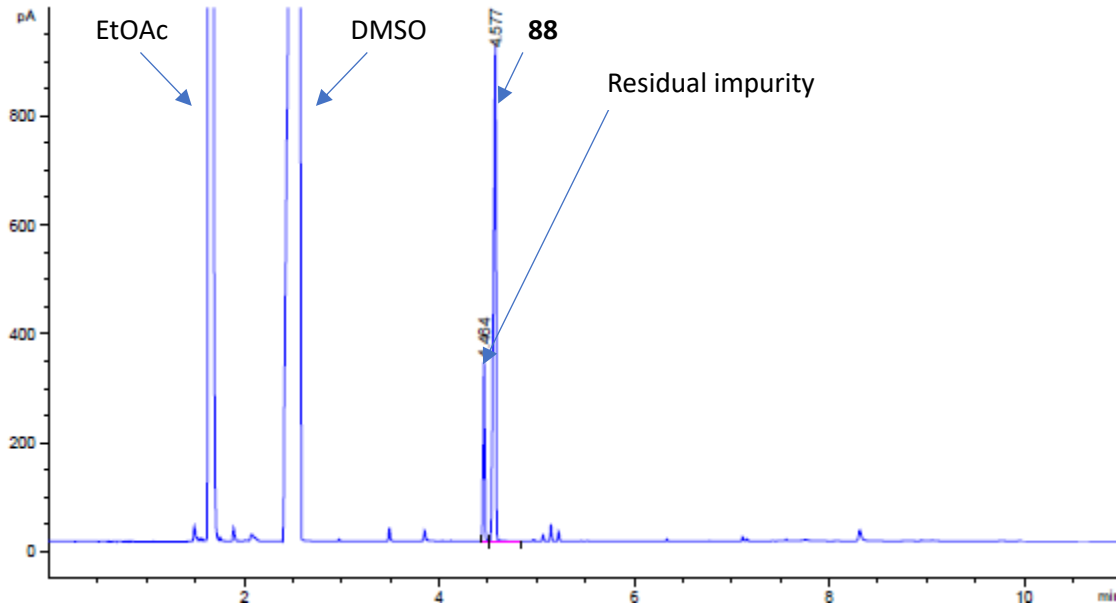

*Figure 32 – Chromatogram from analysis of standard 5-azidopentanol **88** on GC-FID with method A.*

GC-FID analysis of **87**-**88** and **98**-**99** using method A (see experimental information for details) afforded distinct peaks for 5-azidopentanol **88** (4.6 min) and 5-azidopentanal **99** (4.2 min). However, 4-azidobutanol **87** and 4-azidobutanal **98** had overlapping peaks at 3.7 min (Table 35). The temperature ramp of the oven was modified from 20 °C.min^{-1} (method A) to 10 °C.min^{-1} (method C) and 5 °C.min^{-1} (method D). For every method tested, 4-azidobutanol **87** and 4-azidobutanal **98** (entry 1) had similar retention times, which suggested that **87** and **98** had similar boiling points (**87** bp 76-78 °C (10 Torr); **98** bp unknown).[226] Oppositely, 5-azidopentanol **88** and 5-azidopentanal **99** had different boiling points (**88** bp 127-129 °C

(28 Torr); **99** bp 60 °C (2 Torr))[227] and were separable for every method (entry 2). The method with the longest time elapsing between two analytes was privileged, such as method C for **88** and **99**.

*Table 35 – GC-FID Methods and retention times for standard of azido alcohols **87-88** and azido aldehydes **98-99**. (Rt: retention time).*

Entry	Alcohol substrate	Method	Rt alcohol (min)	Rt aldehyde (min)
1	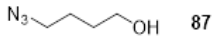 **87**	A	**87**, 3.8	**98**, 3.7
		C	**87**, 4.6	**98**, 4.5
		D	**87**, 5.4	**98**, 5.3
2	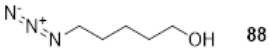 **88**	A	**88**, 4.6	**99**, 4.2
		C	**88**, 5.9	**99**, 5.2
		D	**88**, 7.6	**99**, 6.4
The methods used were carried out with a GC-7820A apparatus (Agilent Technologies) equipped with a flame ionization detector (FID) and a HP5 column (Agilent) with dimensions 30 m × 0.320 mm × 0.25 µm with a flow of 2 mL.min^{-1} He, oven at 70 °C with a ramp to 20 °C.min^{-1} to 200 °C hold for 5 min detector temperature 300 °C and injector temperature 250 °C (method A), ramp to 10 °C.min^{-1} (method C), ramp to 5 °C.min^{-1} (method D). Samples were prepare with the following ration alcohol/aldehyde (1:4, 0.02/0.08 mmol).				

To optimise the GC-FID analysis conditions for analytes **85-106**, it may be beneficial to modify the following settings: column choice, column dimensions, mobile phase flow, oven temperature and ramp temperature, detector temperature, injector temperature, and analyte concentration.

4.1.4 Comparison of oxidation of 5-chloropentanol *via* Dess-Martin oxidation and *via* biotransformation with AcCO6

To investigate the biotransformation of 5-chloropentanol **90**, the reaction crudes were quenched with 5.0 M HCl (C_f = 0.23 M), extracted with EtOAc and analysed by ^{1}H NMR. The ^{1}H NMR spectra between chemical and enzymatic oxidation of 5-chloropentanol **90** showed a significant difference in purity. To confirm this observation, the biotransformation of **90** with AcCO6 was scaled up to a preparative scale (0.06 mmol, V_{tot} = 3.0 mL) and compared to Dess-Martin oxidation of **90** (1.00 mmol, Scheme 51).[228]

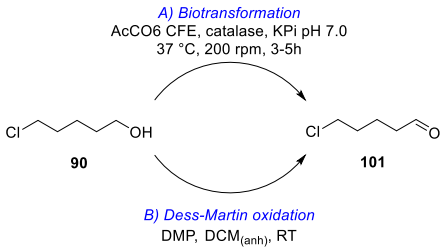

*Scheme 51 – Two methods of oxidation for 5-chloropentanol **90**. Reactions conditions: A) 20 mM 5-chloropentanol **90** (0.06 mmol, 1.0 equiv.), 40 mg.mL^{-1} AcCO6 (CFE), 0.04 mg.mL^{-1} catalase (CFE), 100 mM KPi (pH 7.0), 200 rpm, 37 °C, 5 h, V_{tot} = 3.0 mL. B) 5-chloropentanol **90** (1.0 mmol, 1.0 equiv.), DMP (1.3 mmol, 1.3 equiv.), $DCM_{(anh)}$ under N_2 atmosphere at rt for 1 h.*

After the reactions were quenched with 5.0 M HCl (C_f = 0.23 M) for bio-oxidation and with saturated $NaHCO_3$ for Dess-Martin oxidation, reaction solutions were extracted with EtOAc. The reaction crudes were analysed and compared by ^{1}H NMR analysis (Figure 33). Both methods afforded 5-chlorobutanal **101** with a triplet signal indicating the presence of an aldehyde (δ_H: 9.79 ppm, t, *J* = 1.5 Hz, 1H). As shown on the ^{1}H NMR spectrum, the biotransformation crude contained impurities (6.5-3.5 ppm) but no subsequent aromatic impurities were detected. The crude of Dess-Martin oxidation showed impurities in the aromatic protons region, characteristics of Dess-Martin periodinane and the by-product 1-acetoxy-1,2-benziodoxol-3-one (δ_H: 8.30-7.68 ppm, m).

Enzymatic oxidation produced crude chloroaldehyde **101** with fewer impurities than chemical oxidation.

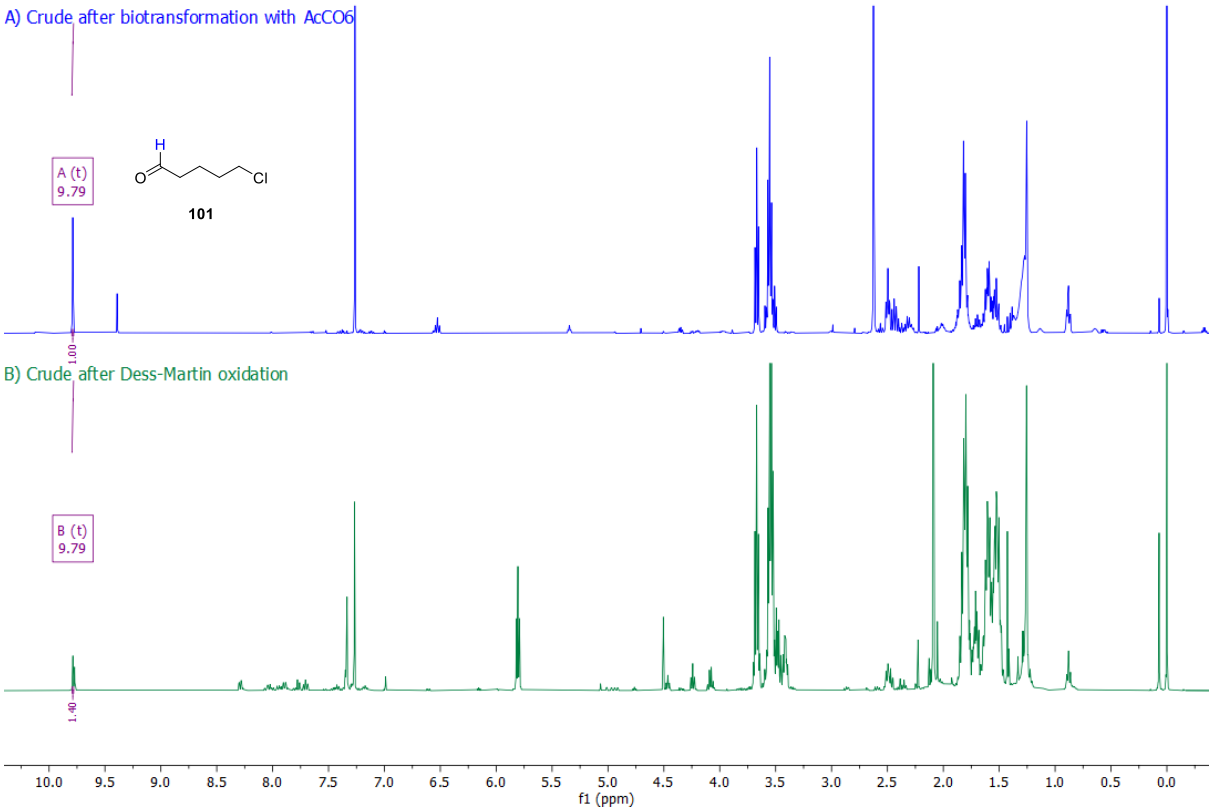

*Figure 33 – Stacked ^{1}H NMR (400 MHz, $CDCl_3$) spectra of 5-chloroentanol **90** oxidation by biotransformation with AcCO6 CFE (A, top) and by Dess-Martin oxidation (B, bottom)*

Extended purification methods were not used. However, the crude **101** obtained from biotransformation can be further purified by using liquid-liquid extraction (water-EtOAc). This process can help to increase the concentration of **101** in the organic layer. Oppositely, crude **101** obtained from Dess-Martin oxidation required a more tedious purification by using silica gel column chromatography.[228]

4.2 Wittig reaction performed in water with alkyl aldehydes

4.2.1 Mechanism of Wittig olefination

In 1954, Wittig reaction was reported by G. Wittig (Nobel Prize in Chemistry in 1979).[229,230] As shown in Figure 34, this reaction converts a carbonyl **110** (aldehyde or ketone) with a triphenyl phosphonium ylide **107** into alkenes **114**. To generate the ylide **108**, a phosphonium salt **107** is deprotonated with a strong base, such as LHMDS, LiOH, NaOH, $NaHCO_3$.[231–237] The resulting ylide **108** is defined as a species with positive and negative charges on adjacent atoms in equilibrium with phosphorane **109**.[238] When the ylide **108** and carbonyl **110** are in proximity, a (2+2) cycloaddition occurs to form a four-membered ring intermediate, oxaphosphetane **111-112**. The reactivity of the ylide **108** depends on the geometry of oxaphosphetane intermediate **111-112**. A stabilised ylide **108** (R' = EWG) is more reactive than a semi-stabilised ylide, which is more reactive than a phosphonium salt **109**. The four membered-ring intermediate **112** is slowly formed from the stabilised ylide **108**. **114**-(*E*)-alkene is predominantly afforded with a stable phosphine oxide **113** by opening oxaphosphetane ring **112**. Non-stabilised ylides **108** are more reactive ylides, which leads to a rapid cycloaddition with carbonyl **110** followed by a rapid ring opening of oxaphosphetane **111** to afford **114'**-(*Z*)-alkene.

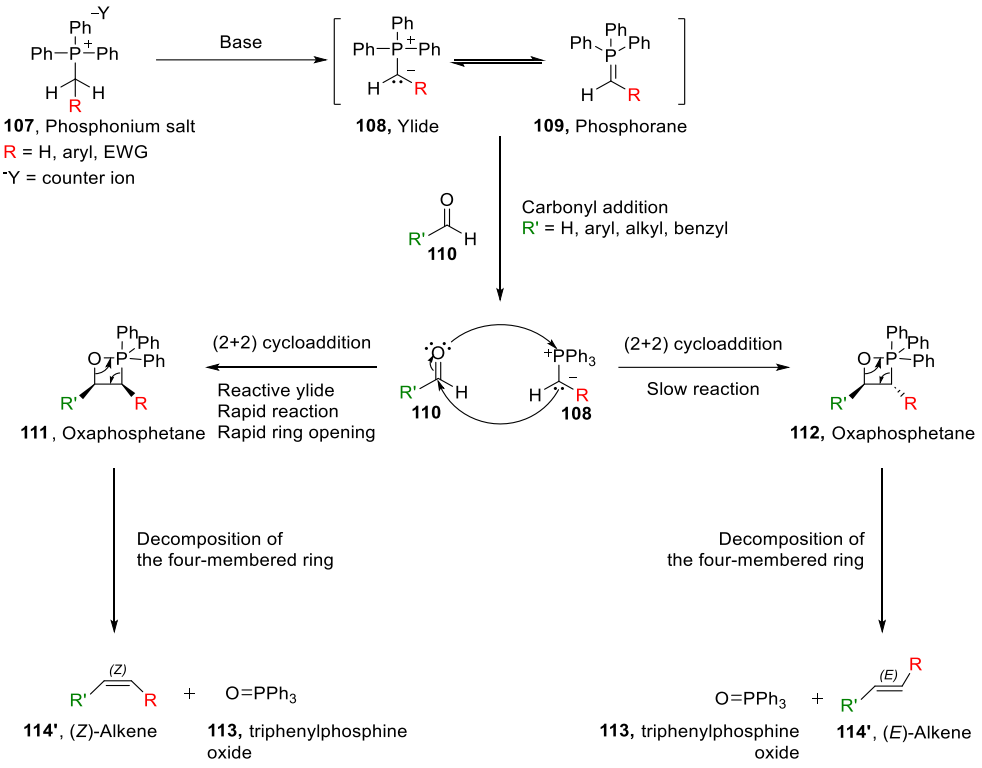

*Figure 34 – Mechanism of the Wittig reaction with aldehyde **110**. Mechanism inspired from J. Clayden, N. Greeves, S. Warren.* Organic chemistry. *Oxford University Press, USA, 2012 and others.*[229–240]

Studies on the Wittig reaction have led to modifications aimed at improving stereochemistry. These include steric approaches with stabilised phosphorus ylides (resulting in (E)-selectivity through the Horner-Wadsworth-Emmons reaction)[241] multistep synthesis with phenylsulfonyl carbanion ((*E*)-selectivity, Julia Olefination)[242] and addition of additive lithium salt ((*E*)-selectivity, Schlosser Modification).[243–245] Additionally, methods for the synthesis of carbon-carbon double bond (*Z*)-selectivity have been investigated through the use of *N*-sulfonyl imine for (*Z*)-stillbenes.[246,247]

4.2.2 Literature of Wittig reaction performed in aqueous media

Wittig reaction is a type of chemical reaction that produced alkenes with good chemical yield and good isomer selectivity in both organic solvents[248–251] and aqueous media.[5] For instance (Scheme 52), when the same aldehyde **115** and ylide **116** were used in a Wittig reaction, enoate **117** was produced. The reaction was also performed in the presence of water as a solvent, which improved the reaction rate. The yield of enoate **117** was increased from 70 % in 4 weeks when using DCM[252] or 95 % yield in 18 h in refluxing acetonitrile[253] to 67 % in just 2 h with refluxing water.[5]

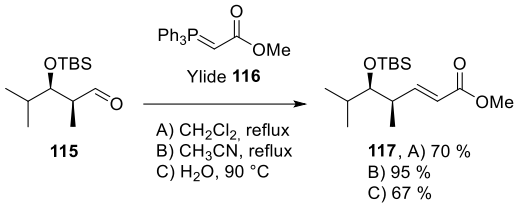

*Scheme 52 - Wittig olefination of silyl pentanal **115** with ylide **116** with solvent variations. Reactions conditions: A) aldehyde **115** (0.08 mmol, 1.0 equiv.), ylide **116** (0.08 mmol, 1.0 equiv.), DCM, stirring, reflux, 4 weeks, V_{tot} = 5.0 mL. B) aldehyde **115** (20.0 mmol, 1.0 equiv.), ylide **116** (31.9 mmol, 1.6 equiv.), dry acetonitrile, stirring, reflux, 18 h, V_{tot} = 80.0 mL. C) aldehyde **115** (1.0 mmol, 1.0 equiv.), ylide **116** (1.2-1.5 mmol, 1.2-1.5 equiv.), water, stirring, 90 °C, 2 h, V_{tot} = 5.0 mL.*

Before the goal of green chemistry, Wittig olefinations could be performed with water as solvent,[254–256] or in biphasic media by hydrophobic interactions between reactants and solvents[231–233,256–262] or solventless.[263–265] However, the use of aqueous solvent for Wittig olefination hadn't been widely accepted as a green chemistry practice. Despite this, researchers have continued investigating alternative reaction conditions that would allow for Wittig olefination in aqueous media by increasing the solubility of phosphonium salt in water.[254–256,266] As a result, water-soluble semi-stabilised ylides with aldehydes[267] in the presence of sodium hydroxide[268] had mitigated results. Despite plenty of research and the recognition that water has a hydrophobic effect with

reactants,[269] the influence of water molecules on the mechanism of Wittig olefination hadn't been clearly understood.[5,270]

4.2.3 Difference observed between *E/Z* alkenes by NMR spectroscopy

Fatty alkenes of this chapter were analysed by ^{1}H NMR in $CDCl_3$. Both (*E*)-alkenes and (*Z*)-alkenes displayed common signals and chemical shifts for methine alkene protons. This observation was illustrated for methyl chloro vinyl ester **118** in Figure 35.

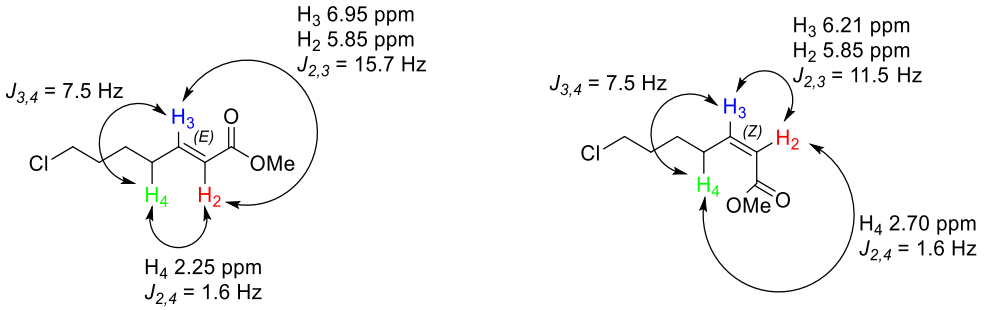

*Figure 35 – Comparison of ^{1}H NMR (400 MHz, $CDCl_3$) data for methyl (E/Z)-7-chlorohept-2-enoate **118***

For both E/Z-isomers, methine group H_2 was coupled to methylene group H_4 ($^4J_{2,4}$ = 1.6 Hz) and methine group H_3 was coupled to methylene group H_4 ($^3J_{3,4}$ = 7.5 Hz). Hydrogen H_2 of (*E*)-isomers was coupled with hydrogen H_3 with $^3J_{2,3}$ = 15.7 Hz, while Hydrogen H_2 of (*Z*)-isomers had a lower coupling constant with hydrogen H_3 ($^3J_{2,3}$ = 11.5 Hz). These observations were noticed with similar signals of doublet of triplet (*dt*) at different chemical shifts. For example (Figure 36), methine group H_3 of (*E*)-alkene **118** was more deshielded than methine group H_3 of (*Z*)-alkene **118'** (**118**: δ_{H3} 6.95 ppm; **118'**; δ_{H3}: 6.22 ppm).

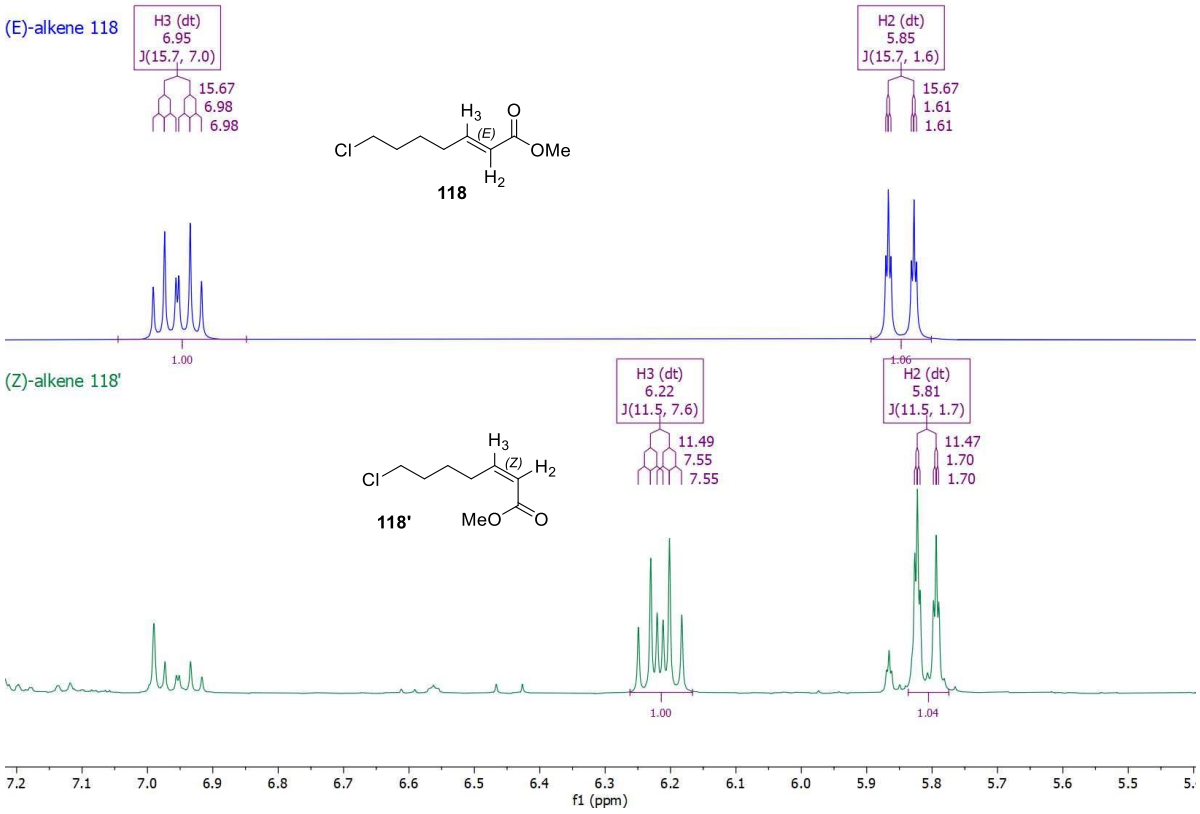

*Figure 36 – Stacked ^{1}H NMR (400 MHz, $CDCl_3$) spectra of methyl 7-chlorohept-2-enoate with (E)-alkene (top) **118** and (Z)-alkene **118'** (bottom).*

4.2.4 Confirmation of Wittig olefination with alkyl aldehydes

The application of the Wittig reaction in this chapter was inspired by Bergdahl's group findings about the advantage of using stabilised ylides with aldehydes in water[5] and in aqueous sodium bicarbonate solution[271,272] for the promotion of chemistry using less organic solvent and to limit the impact on the environment. To confirm this procedure, stabilised ylide methyl (triphenylphosphoranylidene)acetate **116** was screened with fatty aldehydes **35-40** in water to afford vinyl esters **119-124**, (*E*)-isomer as major alkene (Scheme 53). [5]

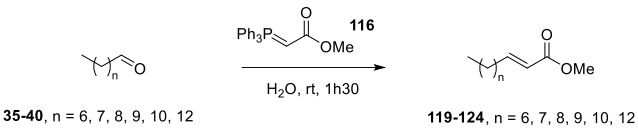

*Scheme 53 – Wittig olefination in water of fatty aldehydes **35-40** with methyl (triphenylphosphoranylidene)acetate **116**. Reaction conditions: 200 mM aldehyde **35-40** (1.0 mmol, 1.0 equiv.), methyl (triphenylphosphoranylidene)acetate **116** (1.5 mmol, 1.5 equiv.) in deionised water (5.0 mL) at rt, 1.5 h.*

The reactions were monitored by TLC (Hexane/EtOAc, 4:1) and stopped after 1.5 h reaction. The resulting crudes were analysed by ^{1}H NMR and GC-FID to determine the ratio of alkenes. However, only esters **119** and **121** were reported by GC-FID with different settings.[273,274] Crudes **119-124** were first analysed by ^{1}H NMR and soon after their NMR samples were analysed by GC. The crudes were purified by column chromatography and the isolated yields were collected in Table 36. The resulting pure alkenes **119-124** were used as standard samples for GC analysis. The chromatograms of crude **119-124** and pure **119-124** were overlapped and permitted to deduce the retention times of the missing alkenes **120,122-124**.

*Table 36 –Wittig reaction in deionised water of fatty aldehydes **35-40** with (triphenylphosphoranylidene)acetate **116** and retention times of resulting vinyl alkene **119-124.***

Entry	Alkyl aldehyde	Alkene ester	Crude *E/Z* (^{1}H NMR)	Crude *E/Z* (GC-FID)	[a]Final E/Z (^{1}H NMR)	Isolated yield (%)	Rt *E*-alkene (min)	Rt *Z*-alkene (min)
1	 **35**	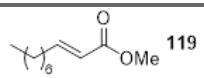 **119**	86:14	87:13	88:12	73	**119**, 6.2	**119'**, 5.8
2	 **36**	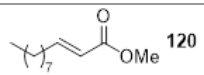 **120**	82:18	85:15	9:1	41	**120**, 6.8	**120'**, 6.5
3	 **37**	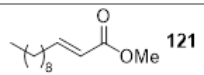 **121**	87:13	88:12	86:14	79	**121**, 6.8	**121'**, 6.5
4	 **38**	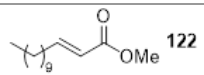 **122**	82:18	85:15	93:7	69	**122**, 8.1	**122'**, 7.7
5	 **39**	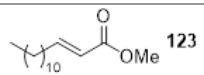 **123**	9:1	85:15	92:8	61	**123**, 8.1	**123'**, 7.7
6	 **40**	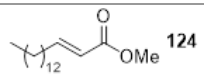 **124**	9:1	8:2	9:1	40	**124**, 11.0	**124'**, 10.2

Reaction conditions: 200 mM aldehyde **35-40** (1.0 mmol, 1.0 equiv.), methyl (triphenylphosphoranylidene)acetate **116** (1.5 mmol, 1.5 equiv.) in deionised water (5.0 mL), stirring, rt, 1h30. Alkenes ratio was determined on the crude by GC-FID and ^{1}H NMR. GC-FID analysis were performed with method A (see supporting information). Rt: retention time. [a]analysis was run after purification by column chromatography

Alkene ester **119** was reported with 80-86% yield (*E/Z* ratio 4:1 by ^{1}H NMR),[5,271] which was in agreement with isolated yield (73 %, entry 1, Table 36) and isomers ratio (final *E/Z* ratio 88:12 by ^{1}H NMR).

Alkene esters **119**-**124** were synthesised in good yield of 40-79 % after being purified through silica gel chromatography. The final isomers ratio determined by ^{1}H NMR was similar to the crude ratio determined by ^{1}H NMR and GC-FID (Table 36). However, it was observed that there were significant differences between crude *E/Z* 9:1 **124** analysed by ^{1}H NMR and crude *E/Z* 8:2 **124** analysed by GC-FID.

4.3 Cascade reaction: biotransformation followed by Wittig olefination in aqueous media

In section 4.2, the potential of alkyl aldehydes **35**-**40** to participate in Wittig olefination was demonstrated. Subsequently, olefination was used for a chemoenzymatic cascade reaction using AcCO6 and an ylide (Scheme 54). During the cascade reaction, alkyl alcohol was first oxidised to the corresponding aldehyde. The aldehyde was then able to undergo a Wittig reaction with both a stabilised ylide **116** and an unstabilised ylide **125** (Scheme 54A).

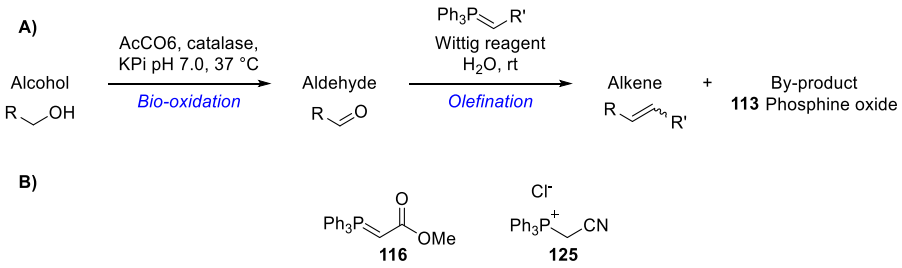

Scheme 54 – A) chemoenzymatic cascade reaction using AcCO6 and Wittig reagent B) Wittig reagents tested for chemoenzymatic Wittig olefination

4.3.1 Stabilised ylide **116** as Wittig reagent

4.3.1.1 Procedure optimisation : methods

The process of creating alkene through chemoenzymatic means was optimised by first oxidising 5-chloropentanol **90** (0.001 mmol, 1.0 equiv., 20 mM) with AcCO6, followed by olefination with an excess of ylide **116** (100 equiv.). The biocatalyst AcCO6 was used with CFE form. To reduce the environmental impact of the process, a two-step reaction was not considered as it would have required an extraction with an organic solvent to extract the intermediate aldehyde **101**. Instead, sequential addition of ylide **116** and one-pot reaction were considered (Scheme 55). The reactions were stopped arbitrarily after 4 h reaction.

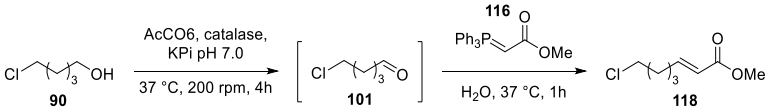

*Scheme 55 – Bio-oxidation of 5-chloropentanol **90** followed by olefination of resulting aldehyde **103** with methyl (triphenylphosphoranylidene)acetate **116.** Reaction conditions: duplicate, 20 mM 5-chloropentanol **90** (0.001 mmol, 1.0 equiv.), 40 mg.mL^{-1} AcCO6 (CFE), 0.04 mg.mL^{-1} catalase (CFE), 100 mM KPi pH 7.0, ylide **116** (0.1 mmol, 100 equiv.) in deionised water (3.0 mL) at 37 °C, 4 h.*

The bio-oxidation of **90** with AcCO6 CFE proceeded for 4 h before the addition of Wittig reagent **116** in excess (100 equiv.). The resulting reaction mixture was shaken for 1 h supplementary at 37 °C. The reaction was quenched with 5.0 M HCl (C_f = 0.03 M) to reach the final pH 6.0. Analysis by ^{1}H NMR revealed that 60 % of alcohol **90** was converted to alkenes **118** without traces of aldehyde **101.** Additionally, 40 % of unreacted alcohol **90** was still present (entry 1, Table 37).

The alliance of the biocatalyst and ylide **116** in a 4 h one-pot reaction increased the conversion of 5-chloropentanol **90** to 80 % and improved (*E*)-selectivity to 92 % (entry 2, Table 37). The difference of the *E/Z* ratio was also noticed in the literature that the faster the Wittig reaction proceeded, the

lower the *E/Z* ratio.[271] In this case, the sequential addition leading to Wittig reaction was carried out for 1 h. This may favoured the formation of planar oxaphosphetane **111** for *(Z)*-alkene. However, in a one-pot reaction, a 4 h Wittig reaction was allowed to proceed, which may have formed puckered oxaphosphetane **112** for (*E*)-alkene. During one-pot cascade, an equilibrium between oxaphosphetanes **111** and **112** may exist in favour of (*E*)-selectivity.

In Table 37, two methods were used to produce aldehyde **101**: the sequential approach (entry 1) and the one-pot approach (entry 2). Aldehyde **101** was not detected for either method. However, the desired product **118** was detected. Hence, intermediate aldehyde **101** was produced via biotransformation and quickly consumed for the olefination with Wittig reagent **116**. Ultimately, the biotransformation of **118** occurred simultaneously with the Wittig reaction.

*Table 37 – Oxidation of 5-chloropentanol **92** followed by aqueous olefination to afford alkene **118**.*

Entry	Method	Reagent 116	Alcohol 90 remaining (%)	Conversion to alkene 118 (%)	Crude *E/Z*
1	Sequential addition of **116** after 4h reaction and shaken for 1h more	100 equiv.	40	60	86:14
2	One-pot for 4h	100 equiv.	20	80	92:8

Reaction conditions: duplicate, 20 mM 5-chloropentanol **90** (0.001 mmol, 1.0 equiv.), 40 mg.mL^{-1} AcCO6 (CFE), 0.04 mg.mL^{-1} catalase (CFE), 100 mM KPi pH 7.0, ylide **116** (0.1 mmol, 100 equiv.) in deionised water (3.0 mL) at 37 °C, 4 h. Conversion and alkenes ratio were determined on the crude by ^{1}H NMR.

4.3.1.2 Procedure optimisation : Wittig reagent 116

One-pot reaction (V_{tot} = 20 mL) of 5-chloropentanol **90** was scale-up (**90**: 0.4 mmol, 20 mM) in a falcon tube (50 mL) to afford alkene ester **118**. The amount of Wittig reagent **116** was optimised (Scheme 56, Table 38). After 5 h, the one-pot reaction was quenched with 5.0 M HCl (C_f = 0.03 M). The aqueous medium was extracted twice with polar organic solvent EtOAc and centrifuged at 3024 × *g* for 10 min to compact the proteinic pellet between aqueous and organic phases. During centrifugation, the excess of solid reagent **116** migrated to the bottom of the tube.

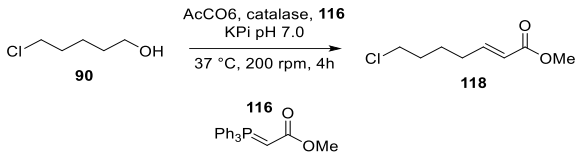

*Scheme 56 – One-pot cascade of biotransformation of 5-chloropentanol **90** and olefination with methyl (triphenylphosphoranylidene)acetate **116** to vinyl alkene **118.** Reaction conditions: 20 mM 5-chloropentanol **90** (0.4 mmol, 1.0 equiv.), 40 mg.mL^{-1} AcCO6 (CFE), 0.04 mg.mL^{-1} catalase (CFE), 100 mM KPi pH 7.0, methyl (triphenylphosphoranylidene)acetate **116** in deionised water (20 mL), 37 °C, 5 h.*

After 4 h reaction on alcohol **90**, two phosphine species were detected in the organic phase, with a ratio of phosphine oxide/reagent **113/116** (3:1) determined by ^{31}P NMR (**113**: δ_P 18.3 ppm, s; **116**: δ_P 29.5 ppm, m).[275,276] Even when an excess of **116** migrated at the bottom of the tube, both phosphine oxide **113** and Wittig reagent **116** were partially soluble in the organic phase.[277] As shown in Table 38, when Wittig reagent **116** was added in a minimum excess of 2.0 equiv, 5-choropentanol **90** was completely converted to alkene ester **118**. The (*E*)-selectivity remained major, with an *E*/*Z* ratio of (9:1)[5,271] and was not influenced by the amount of ylide **116.** After purification on silica gel chromatography, chloroalkene ester **118** was isolated in excellent yield (95-97 %, entries 1 and 2, Table 38).

*Table 38 – Oxidation of 5-chloropentanol **90** followed by aqueous olefination.*

Entry	Phosphine 116	Alcohol remaining (%)	Conversion to alkene 118 (%)	Isolated yield (%)	Final *E/Z*
1	4 equiv.	0	Quant.	95	99:1
2	3 equiv.	0	Quant.	97	86:14
3	2 equiv.	10	90	50	89:11
4	1 equiv.	26	74	70	91:9

Reaction conditions: 20 mM 5-chloropentanol **90** (0.4 mmol, 1.0 equiv.), 40 $mg.mL^{-1}$ AcCO6 (CFE), 0.04 $mg.mL^{-1}$ catalase (CFE), 100 mM KPi pH 7.0, methyl (triphenylphosphoranylidene)acetate **116** in deionised water (20 mL) at 37 °C, 5 h. Conversion was determined on the crude by ^{1}H NMR. Alkenes ratio were determined after purification by column chromatography by ^{1}H NMR.

According to the literature, the synthesis of (*E*)-chloroalkene ester **118** was achieved by cross-metathesis of 6-chloro-1-hexene, *p*-cresol and methyl acrylate in toluene at 120 °C in 80 % isolated yield.[278] However, these chemicals are toxic, flammable, and can cause reproductive toxicity, skin irritation, eye damage, oral toxicity and harm aquatic life.[279–282] Alternatively, the one-pot cascade involving AcCO6 and ylide **116** can afford ester **118** with excellent yield in mild conditions with an environmentally friendly solvent and Wittig reagent without toxicity reported.[283] This novel approach applied to 5-chloropentanol **90** seemed more sustainable than Grubbs chemistry reported in producing ester **118**.[278]

4.3.1.3 Scope of cascade reaction of olefination from primary alcohol

The one-pot process was performed on linear alcohol substrates of oxidase AcCO6 (Scheme 57), which included alkyl alcohols **28-30** and functionalised primary alcohols **85-95**. Reactions with alkyl alcohols **28-30** were performed overnight due to their specific activity with AcCO6 (octanol

28: 48.9 mU.mg^{-1}, Table 33) being lower than most functionalised primary alcohols **85-95** (for instance, 4-bromoalcohol **85**: 356 mU.mg^{-1}Table 33).

Reactions on substrates **85**-**95** were carried out at 37 °C, stopped after 6 h or 22 h, quenched with 5.0 M HCl (C_f = 0.23 M), extracted with EtOAc and centrifuged. Crudes were analysed by ^{1}H NMR. No mass spectrometry data was obtained during the investigation for any fatty alkenes introduced in this chapter to confirm these findings. The fragments of every product were too weak to be attributed accurately and confidently by HRMS.

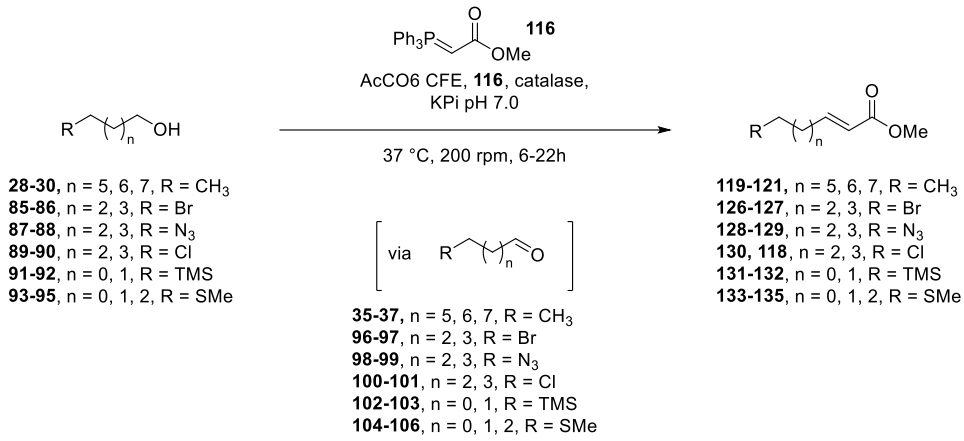

*Scheme 57 – One-pot cascade of biotransformation of linear alcohols **28-30,85-95** and olefination with methyl (triphenylphosphoranylidene)acetate **116** to afford alkene esters **118-121,126-135**. Reaction conditions: 20 mM alcohol **28-30, 85-95** (0.4 mmol, 1.0 equiv.), ylide **116** (0.8 mmol, 2.0 equiv.), 40 mg.mL^{-1} AcCO6 (CFE), 0.04 mg.mL^{-1} catalase (CFE), 100 mM KPi pH 7.0, V_{tot} = 20.0 mL, 37 °C, 200 rpm.*

As shown in Table 39, the desired alkenes **118-121,126-135** had a crude isomers ratio in favour of (*E*)-alkene (*E*/*Z* from 3:1 to 9:2). Weak conversions to aldehyde intermediate were observed in all reactions (alcohol+alkene/aldehyde 99-96:1-4). Therefore, the one-pot cascade successfully afforded vinyl esters **118-121,126-135.** Most alkenes were obtained from their corresponding alcohols with good conversion (conversion to alkene: 50-100 %). The isolated yields were obtained

after purification by silica gel chromatography and the final *E/Z* ratios were determined by ^{1}H NMR.

Alkyl esters **119**-**121** were usually synthesised with a minimum yield of 60 % from palladium hydrogenation,[284] β-elimination with Sm metal,[285] from the corresponding aldehyde with a strong base (pyridine,[286–288] sodium hydride [289,290]), from the corresponding aldehyde **35-37** with metallic reagent (TiCl4,[288] ZnCl2,[288] Rh catalyst[287]) or other reagents (triphenylarsine,[291] stabilised ylide **116** in benzene solvent [292]). The one-pot cascade was attempted overnight on alkyl alcohols **28**-**30** to rival with literature precedents. Therefore, after 22 h one-pot reaction, the isolated yield of linear alkyl acetates **119-121** (entries 1-3) decreased as the length chain increased. For instance, the yield for dec-2-enoate **119** was 88 %, while undec-2-enoate **120** had 52 % yield, and dodeca-2-enoate **121** had 35 % yield. The same trend was observed for the conversion to alkenes **119**-**121**, with **119** conversion to 97 %, **120** conversion to 89 % and **121** conversion to 64 %. This slower formation of alkenes with an increase in the alkyl chain length was also observed during the specific activity of AcCO6 towards alcohols **28**-**30**, where octanol **28** (kcat = 0.037 s^{-1}) was converted faster than decanol **30** (kcat = 0.015 s^{-1}). Therefore, bio-oxidation with AcCO6 of octanol **28** followed by olefination of intermediate aldehyde **35** could compete with conventional chemistry.

4-halogen-1-butanols (4-bromo **85,** 4-chloro **89**) were converted into bromo alkenes **126** and chloro alkenes **130,** respectively**,** with a ratio of alcohol/alkenes (1:1) after 6 h one-pot reaction. Eventually, substrates **85** and **89** had similar interactions with AcCO6 active site despite the Van der Waals radius of bromide (195 pm) being more significant than chloride (180 pm).[293] In the literature, 6-halogenhexoates (bromo **126** and chloro **130**) were synthesised from corresponding aldehydes, 4-bromo-1-butanal **96** and 4-chloro-1-butanal **100**, respectively, via Wittig olefination performed in benzene (yield ~50 %),[294,295] with sodium hydride in THF (yield 85 %)[296,297] or via Grubbs metathesis (80 %)[298] and palladium catalysed alkoxycarbonylation (62 %).[299] Here, when

4-chloro-1-butanol **89** and 5-chloro-1-pentanol **90** were treated with one-pot cascade (Table 39), chloro esters **118** and **130** were afforded with good yield (6-chlorohexoate **130**: 73 %, entry 8; 7-chloroheptanoate **118**: 97 %, entry 9) and excellent (*E*)-selectivity (*E/Z* 99:1). Eventually, the cascade could be completed by adding a toxic solvent[294–297] for a biphasic system olefination. Bromo esters **126-127** weren't afforded after purification on silica gel chromatography and likely decomposed because of the lability of C-Br bond with silica gel.[295,296] Similarly, 5-halogen-1-pentanols (5-bromo **86,** 5-chloro **90**) were converted into bromo alkenes **127** and chloro alkenes **118** with good ratio (alcohol/alkenes 1:99, entries 5 and 9) after 6 h reaction. Both alkenes were isolated in excellent yield (**127**: 85 %; **118**: 97 %). Halogen alcohols with a 5 carbon length chain (5-bromo **86,** 5-chloro **90**) seemed better substrate for the one-pot cascade reaction than halogen alcohols with 4 carbon length chain (4-bromo **85,** 4-chloro **89**).

As per the available literature, azido aldehydes **98-99** were afforded by Dess-Martin[224] or Swern[225] oxidations. In 1987, azido esters **128-129** were synthesised by Wittig olefination with *E/Z* 95:5, but further details about the procedures and yield still needed to be provided.[300] In this thesis, the one-pot process AcCO6-mediated bio-oxidation and subsequent aqueous Wittig reaction from azido alcohols **87-88** did not enhance the conversion to azido alkenes **128-129** as compared to the literature. The yield for hexanoate **128** was correct with 52 % (entry 6), while the yield for azido heptanoate **129** was very low with 13 % (entry 7).

*Table 39 – One-pot cascade reaction of alcohols **28-30, 85-95** with bio-oxidation using AcCO6 and Wittig olefination with methyl (triphenylphosphoranylidene)acetate **116.***

Entry	Alcohol	Product	Time reaction	Conversion to aldehyde (%)	Conversion to alkene (%)	Crude *E/Z*	Final *E/Z*	Isolated yield (%)
1	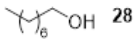 **28**	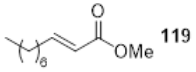 **119**	22 h	1	97	87:13	94:6	88
2	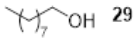 **29**	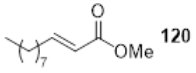 **120**	22 h	3	89	85:15	88:12	52
3	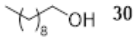 **30**	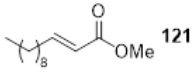 **121**	22 h	3	64	84:16	86:14	35
4	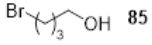 **85**	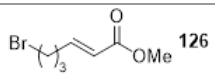 **126**	6 h	0	47	75:25	n.a.	n.a
5	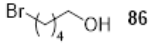 **86**	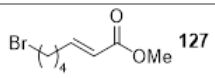 **127**	6 h	1	98	86:14	99:1	85
6	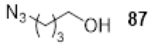 **87**	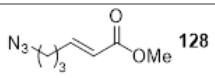 **128**	6 h	4	61	8:2	97:3	52
7	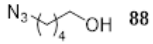 **88**	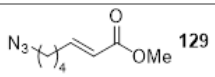 **129**	6 h	3	51	8:2	99:1	13

8	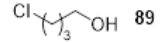 89	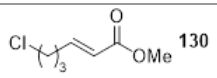 130	6 h	1	50	87:13	99:1	73
9	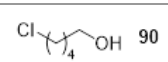 90	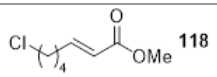 118	6 h	0	Quant.	89:11	99:1	97
10	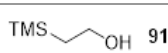 91	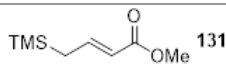 131	6 h	0	28	89:11	n.a.	n.a.
11	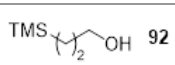 92	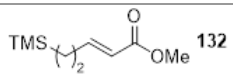 132	6 h	1	88	85:15	n.a.	n.a.
12	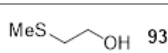 93	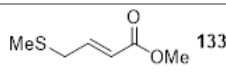 133	7 h	0	94	8:2	n.a.	n.a.
13	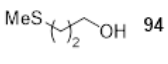 94	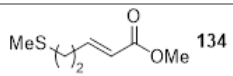 134	7 h	2	92	87:13	87:13	92
14	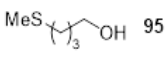 95	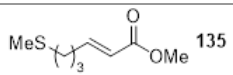 135	7 h	2	70	87:13	87:13	71

Reaction conditions: 20 mM alcohol **28-30, 85-95** (0.4 mmol, 1.0 equiv.), methyl (triphenylphosphoranylidene)acetate **116** (0.8 mmol, 2.0 equiv.), 40 $mg.mL^{-1}$ AcCO6 (CFE), 0.04 $mg.mL^{-1}$ catalase (CFE), 100 mM KPi pH 7.0, V_{tot} = 20.0 mL, 37 °C, 200 rpm. Conversions and ratio were measured on the crude by ^{1}H NMR. n.a.: not available

Silylated alcohol **91** with 2 carbon length was weakly converted to alkene **131** (conversion to alkene: 28 %, entry 10, Table 39). In contrast, silylated alcohol **92** with 3 carbons length was converted to alkene **132** in 88 % (entry 11). However, after 6 hours of reaction, the reaction crudes of esters **131**-**132** showed rapid signs of decomposition on ^{1}H NMR spectra. The reaction temperature was not believed to cause the decomposition, as alkene **131** was reportedly synthesised at a higher temperature of 80 °C in THF.[301] Attempts to purify the crudes **131**-**132** on silica gel and alumina columns did not isolate the final products **131-132**. The stabilities of compounds **131**-**132** toward silica gel were first believed to be the cause of lost compounds, even when compound **131** (entry 10) was reported to be purified by silica gel column chromatography in 70 % yield.[301] Therefore, purifications on alumina column were also attempted with similar results. There was no precedent for compound **132** to explain the results. Retrospectively, the aqueous medium reaction and interactions with the enzyme may have caused the compounds decomposition by reacting with the $SiMe_3$ leaving group.

Previously, the synthesis of methylsulfanyl-buteanoate **133** and -penteanoate **134** were reported through Wittig olefination of corresponding bromo acetate nucleophilic substitution (100 % yield) and used without further purification.[302,303] However, no literature was reported for the synthesis of 6-methylsulfanylhex-2-enaote **135**. The one-pot reaction with AcCO6 of thiomethyl alcohols **93-95** (entries 12, 13 and 14, Table 39) afforded thiomethyl alkenes **133-135** in good conversion (ratio alcohol/aldehyde/alkene 28:2:70 to 6:0:94). The (*E*)-olefin was the major isomer in all cases, with *E/Z* ratios ranging from 8:2 to 87:13. Methylsulfanyl with 8 and 9 atom chain lengths were isolated with yields of 92 % for **134** and 71 % for **135**, respectively. However, **133** was not isolated after column chromatography, raising questions about its stability over time and purification conditions.

All reactions were subjected to acid quenching to neutralise the enzyme. This quenching method did not affect the stability of bromo ester **126,** silylated esters **131-132** and sulfanyl ester **133**, as they were successfully identifiable by ^{1}H NMR. The column chromatography conditions were also disregarded to

explain the absence of isolated yield for **131**, **132** and **133** (Table 39). Retrospectively, extraction methods could be modified. After the enzyme quenching, the aqueous media could be extracted with polar organic solvent (such as EtOAc), followed by a thorough washing of the organic layers with deionised water to transfer the excess phosphine oxide in the aqueous phase. Eventually, purification by column chromatography might be avoided. Although, organic extractions with diethyl ether solvent or DCM were attempted, the partition of reactants between organic and aqueous layers was less efficient than with EtOAc.

To summarise, the novel cascade reaction bio-oxidation-olefination in aqueous media afforded ten olefins (**118-121**, **127-130,** and **134-135**), including the novel compound **135**.

4.3.2 Phosphonium salt 125 as Wittig reagent

4.3.2.1 Phosphonium salt 125 as Wittig reagent for olefination of octanal

An attempt was made to perform Wittig olefination on commercial octanal **35** to produce nitrile ester **136** using ((cyanomethyl)triphenylphosphonium chloride **125**) as a phosphonium salt (Scheme 58). The phosphonium salt required activation with a base (NaOH) to form a stabilised ylide (P=C bond) and the reaction was carried out for 17 h.[271]

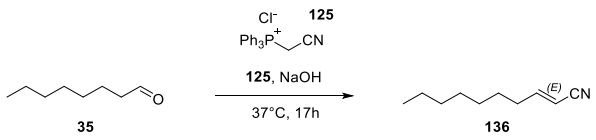

*Scheme 58 - Olefination of octanal **35** with phosphonium salt **125** in water. Reaction conditions: 20 mM octanal **35** (0.4 mmol, 1.0 equiv.), phosphonium salt **125** (0.4 mmol, 1.0 equiv.), 0-20 mM NaOH, 37 °C, 200 rpm, 17 h, V_{tot} = 20.0 mL.*

As presented in Table 40, the conversion to alkene **136** increased significantly in the presence of 20 mM NaOH (entry 2, aldehyde/nitrile **35**/**136** 21:79) than without base (entry 1, **35**/**136** 68:32). The pH of the solution also affected the isomers ratio; at neutral pH, (*E*)-olefin was the major product

(*E/Z* 68:32), while under basic pH, the ratio of olefins was almost equal (*E/Z* 59:41). These results were consistent with the literature,[271] which suggested that the use of non-stabilised ylide, such as phosphonium salt **125**, in aqueous media predominantly resulted in the formation of (*Z*)-isomer.

*Table 40 – Olefination of octanal **35** with phosphonium salt **125** in water.*

Entry	Base	Conversion to alkene 136 (%)	Crude *E/Z*
1	No base	32	68:32
2	NaOH 20 mM	79	59:41

Reaction conditions: 20 mM octanal **35** (0.4 mmol, 1.0 equiv.), phosphonium salt **125** (0.4 mmol, 1.0 equiv.), deionised water (20 mL), 37 °C, 200 rpm, 17 h, V_{tot} = 20.0 mL. Conversion and alkenes ratio were measured by ^{1}H NMR.

4.3.2.2 Phosphonium salt 125 as Wittig reagent for olefination of 4-methylthiobutanal

The concentration of NaOH required for Wittig olefination with salt **125** was measured on 4-methylthiobutanal **106**, which was produced by bio-oxidation with AcCO6 (Scheme 59). During the olefination step with salt **125**, the solution pH was modified from neutral to basic due to the presence of NaOH. Prior to performing the reaction with salt **125**, it would have been beneficial to optimize the reaction conditions using a commercial aldehyde with high purity to prevent any potential side reactions caused by the presence of AcCO6 CFE.

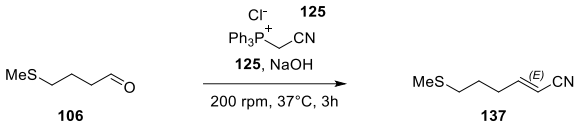

*Scheme 59 - Olefination of 4-methylthiobutanal **106** with phosphonium salt **125** in water with influence of NaOH concentration. Reaction conditions: 20 mM 4-methylthiobutanal **106** (0.08 mmol, 1.0 equiv.), phosphonium salt **125** (0.08 mmol, 1.0 equiv.), 0-400 mM NaOH, 100 mM KPi pH 7.0, deionised water (20 mL), 37 °C, 200 rpm, 3 h.*

As shown in Table 41, less than 100 mM NaOH didn't afford the desired product **137** (entries 1 and 2). However, increasing the amount of base provided full activation of phosphonium salt **125** and complete olefination of aldehyde **106** to nitrile alkene **137** (entries 3-5). However, higher NaOH concentration resulted in low alkene selectivity (E/Z 1:1), as commented in the literature.[304] Alternatively, other bases such as LiOH with LiCl and $NaHCO_3$ could be explored to activate the phosphonium salt **125** to its ylide form.[245,272] Unfortunately, pH changes were not monitored during the screening of NaOH concentration.

*Table 41 - Olefination of 4-methylthiobutanal **106** with phosphonium salt **125** in water influence of NaOH concentration.*

Entry	Base	Conversion to alkene 137 (%)	Crude *E/Z*
1	No base	0	n.a.
2	NaOH, 20 mM, 0.12 mmol, 1.5 equiv.	0	n.a.
3	NaOH, 100 mM, 0.6 mmol, 7.5 equiv.	84	56:44
4	NaOH, 200 mM, 1.2 mmol, 15 equiv.	96	44:56
5	NaOH, 400 mM, 2.4 mmol, 30 equiv.	97	49:51

Reaction conditions: 20 mM 4-methylthiobutanal **106** (0.08 mmol, 1.0 equiv.), phosphonium salt **125** (0.08 mmol, 1.0 equiv.), 0-400 mM NaOH, 100 mM KPi pH 7.0, deionised water (20 mL), 37 °C, 200 rpm, 3 h. Conversion and alkenes ratio were measured on the crude by ^{1}H NMR.

n.a.: not applicable

4.3.2.3 Cascade reaction of 4-methylthiobutanol with AcCO6 and nitrile phosphonium salt 125

The cascade reaction of bio-oxidation and aqueous olefination was investigated on 4-methylthiobutanol **95** as alcohol substrate (Scheme 60). The importance of activating reagent **125** was highlighted in section 4.3.2.3. Both a one-pot reaction and sequential addition of phosphonium salt **125** and NaOH were considered (Table 42).

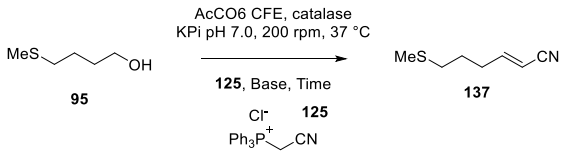

*Scheme 60 – Oxidation of 4-methylthio-butanol **95** followed by aqueous olefination. Reaction conditions: 20 mM 4-methylthiobutanol **95** (0.4 mmol, 1.0 equiv.), 40 mg.mL^{-1} AcCO6 (CFE), 0.04 mg.mL^{-1} catalase (CFE), 100 mM KPi pH 7.0, phosphonium salt **125**, base (2.0-5.0 equiv.), deionised water (20 mL), 200 rpm, 37 °C, 5-24 h.*

As presented in Table 42, most reaction conditions modified the *E*/*Z* ratio (1:1). The formation of Alkene **137** occurred even without base, resulting in a 46 % conversion (entry 1). However, conversion to alkene **137** decreased significantly to 3 % with 300 mM NaOH in a one-pot reaction (entry 4). Because of these results, NaOH was added to the reaction at 5 h (entries 5-12). Several variations were attempted to observe the completion of alkene **137**: base (entries 2-4), one-pot reaction (entries 1-4), sequential addition (entries 5-12) and reaction time.[235,264] Despite these attempts, alkene **137** was not observed to completion. Maximum conversion to **137** (91 %, entry 12) was observed when salt **125** was added in excess (5.0 equiv.) without pre-activation.

*Table 42 – Oxidation of 4-methylthio-butanol **95** followed by aqueous olefination with phosphonium salt **125**. The sequential addition of salt **125** and 5.0 M NaOH (C_f = 0.30 M) occurred after 5 h reaction.*

Entry	Phosphine 125 (equiv.)	Method	Reaction Time	Conversion to alkene 137 (%)	Crude *E/Z*
1	2.0	One-pot (no base)	5 h	46	6:4
2	2.0	One-pot (40 mM NaOH)	5 h	40	57:43
3	2.0	One-pot (saturated $NaHCO_3$)	5 h	47	6:4
4	2.0	One-pot (300 mM NaOH)	8 h	3	37:63
5	2.0	Sequential addition	8 h	38	48:52
6	2.0	Sequential addition	8 h	34	51:49
7	3.0	Sequential addition	8 h	58	52:48
8	1.0	Sequential addition	22.5 h	39	54:46
9	2.0	Sequential addition	22.5 h	54	51:49
10	3.0	Sequential addition	22.5 h	59	50:50
11	4.0	Sequential addition	19 h	87	46:54
12	5.0	Sequential addition	19 h	91	48:52

Reaction conditions: 20 mM 4-methylthiobutanol **95** (0.4 mmol, 1.0 equiv.), 40 $mg.mL^{-1}$ AcCO6 (CFE), 0.04 $mg.mL^{-1}$ catalase (CFE), 100 mM KPi pH 7.0, phosphonium salt **125**, 5.0 M NaOH (C_f = 0.30 M), deionised water (20 mL), 200 rpm, 37 °C, 5h-24h. The sequential addition of salt **125** and 5.0 M NaOH (C_f = 0.30 M) occurred after 5 h reaction

As an alternative, literature suggested that an aqueous base might be responsible for the decomposition of phosphorus ylide,[305,306] which would explain incomplete olefination unless an excess ylide amount is used. Regarding the novel process investigated, no sign of ylide **125** decomposition was observed by the action of the basic solution. The process could be attempted with additional lithium chloride to bias the base effect, increase the hydrophobic effect and accelerate Wittig olefination.[307] The solubility property of substrate **95** and the addition of phosphine **125** were the keys to understanding this novel cascade bio-oxidation-Wittig olefination from a primary alcohol.

4.3.2.4 Scope of Wittig reaction with Phosphine 125

Historically, olefin nitriles **136-149** were conventionally synthesised in organic solvent[300,308–314] from the corresponding aldehydes **35-37,96-106** via Horner-Wadsworth-Emmons (HWE) reaction ((*Z*)-selectivity, yield 99 %),[308] Wittig-Horner (WH) reaction (yield 35-78 %)[315–318] and cross metathesis reaction.[319–323] Although incomplete optimisation was done in section 4.3.2.3, the cascade reaction in aqueous media was extended to alcohol substrates to alcohol substrates **28-30,85-95** (Scheme 61). Firstly, the oxidation with AcCO6 was carried out for 5 h at 37 °C, then phosphonium salt **125** and NaOH solution were added to the reaction mixture. The resulting mixture was shaken for a minimum of 16 h at 37 °C to provide olefin nitriles **136**-**149**.

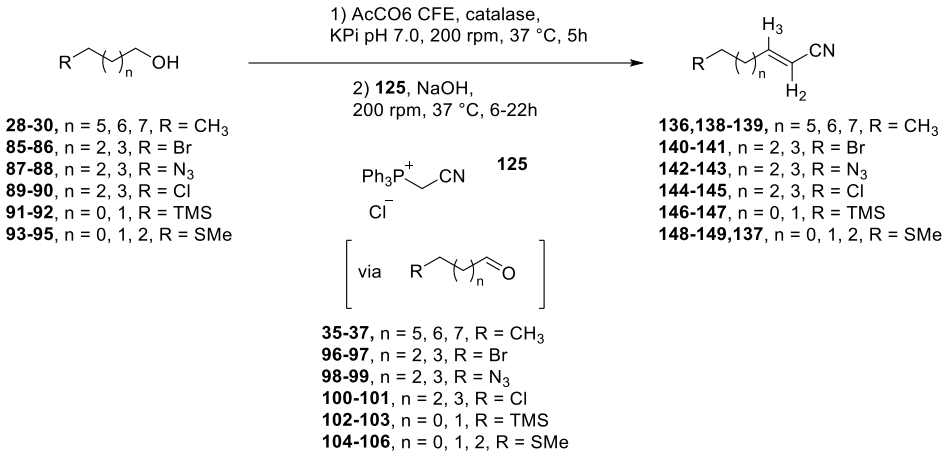

*Scheme 61 – One-pot oxidation and olefination of alcohols **28-30, 85-9** with cyanophosphonium salt **125**. Reactions conditions: 1) 20 mM alcohol **28-30,85-95** (0.4 mmol, 1.0 equiv.), 40 mg.mL^{-1} AcCO6 (CFE), 0.04 mg.mL^{-1} catalase (CFE), 100 mM KPi pH 7.0, 37 °C, 200 rpm, 5 h, in deionised water (20 mL), 200 rpm, 37 °C for 22-52 h. 2) cyanophosphonium salt **125** (1.2 mmol, 3.0 equiv.) and 23 mM NaOH after 5 h reaction*

After the reactions, the crude materials were quenched with 5.0 M HCl (C_f = 0.24 M), extracted with EtOAc and analysed by ^{1}H NMR (Table 43). Determining the conversions to desired alkenes was challenging as the signals of alcohols and alkenes signals appeared weak on ^{1}H NMR spectra. Despite the weak signals, after 22 h to 52 h reaction, most desired nitrile alkenes were detected with (*E*)-olefin protons (H_3: δ_H 6.72 ppm, dt, $^3J_{H3\text{-}H2}$ = 16.3 Hz, $^3J_{H3\text{-}H4}$ = 7.0 Hz; H_2: 5.38 ppm, dt, $^3J_{H2\text{-}H3}$ = 16.3 Hz, $^4J_{H2\text{-}H4}$ = 1.7 HzTable 43). Finally, the crude materials were purified by column chromatography.

As shown in Table 43, alkyl olefins **136, 138-139** (entries 1-3) were detected as (*E*)-selective like chloro nitrile **144** (entry 6), bromo nitriles **140-141** (entries 8-9) and silyl nitrile **146** (entry 10). Alkene nitriles with crude isomer ratio *E*/*Z* 1:1 were observed for chloro nitrile **145** (entry 7)**,** silyl nitrile **147** (entry 11) and sulfanyl nitrile **149** and **137** (entries 13 and 14). Only methylsulfanyl alkene **137** was purified by column chromatography with an isolated yield of 40 % (*E*/*Z*, 51:49, entry 14).

After conducting a literature review, no explanations were found to highlight the difference in isomers ratio and the reactivity of the starting alcohols with the cascade reaction. The HRMS of the crude materials (compounds **136**, **138**, **139**, **144**, **145**, **149** and **137**) did not confirm the formation of the nitrile alkenes, even when data from commercial phosphonium salt **129** were subtracted from HRMS analysis. Similarly, pure alkene nitrile **137** wasn't successfully detected by HRMS.

The cascade reaction with non-stabilised ylide **125** hadn't been confirmed as appropriate for the cascade synthesis. Only weak signals from ^{1}H NMR confirmed the synthesis of nitriles **136-141, 143-149**. The results were questioned as final products **136-139**, **142-143** and **147-149** were not isolated or confirmed by mass spectrometry. Optimising reaction conditions and scaling up reactions to 1.0 mmol fatty alcohols **28-30** and **85-95** would afford new insights upon the cascade reaction.

*Table 43 – One-pot oxidation and olefination of alcohols **28-30,85-95** with cyanophosphonium salt **125**.*

Entry	Alcohol	Alkene product	Time reaction	Conversion to alkene (%)	*E/Z* (crude)	Isolated yield (%)
1	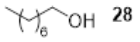 **28**	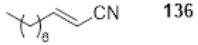 **136**	52 h	50	1:0	n.d.
2	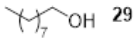 **29**	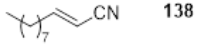 **138**	52 h	15	1:0	n.d.
3	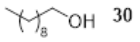 **30**	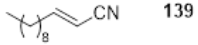 **139**	52 h	15	1:0	n.d.
4	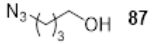 **87**	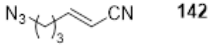 **142**	22 h	n.d.	n.d.	n.d.
5	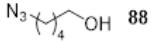 **88**	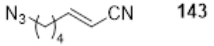 **143**	22 h	75	36:64	n.d.
6	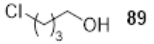 **89**	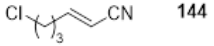 **144**	22 h	94	1:0	n.c.
7	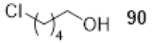 **90**	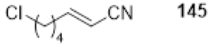 **145**	22 h	98	53:47	n.c.
8	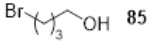 **85**	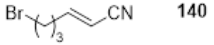 **140**	22 h	90	1:0	n.c.
9	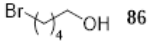 **86**	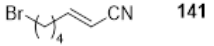 **141**	22 h	86	1:0	n.c.
10	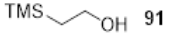 **91**	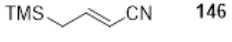 **146**	22 h	53	1:0	n.c.

11	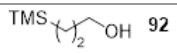 **92**	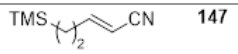 **147**	22 h	36	53:47	n.d.
12	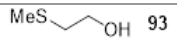 **93**	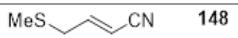 **148**	22 h	94	75:25	n.d.
13	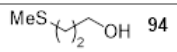 **94**	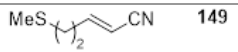 **149**	22 h	25	53:47	n.d.
14	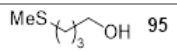 **95**	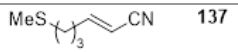 **137**	22 h	30	45:55	40 (*E/Z*, 51:49)

Reaction conditions: 1) 20 mM alcohol **28-30,85-95** (0.4 mmol, 1.0 equiv.), 40 mg.mL^{-1} AcCO6 (CFE), 0.04 mg.mL^{-1} catalase (CFE), 100 mM KPi pH 7.0, 37 °C, 200 rpm, 5 h, in deionised water (20 mL), 200 rpm, 37 °C for 22-52 h. 2) cyanophosphonium salt **125** (1.2 mmol, 3.0 equiv.) and 5.0 M NaOH (C_f = 300 mM) after 5 h reaction. Conversion and alkenes ratio were measured by ^{1}H NMR of the crude.

n.d.: not detected

n.c.: not concerned, no further purification performed

4.4 Conclusion and future work

Combinations of oxidase and chemical reactions have been proven possible under mild conditions, with respect for green chemistry principles (non-damaging solvent, less chemical used, utilisation of biocatalyst).[88,324]

4.4.1 Specific activity of AcCO6

In this chapter, choline oxidase AcCO6 demonstrated successful specific activities for alcohol substrates **85-95** when tested via colorimetry assay.[70] Bio-oxidation of 4-azidobutanol **87** was performed again on 0.01 mmol scale, analysed level by ^{1}H NMR and confirmed the oxidation of its primary alcohol to aldehyde **98**.

In the future, the kinetic parameters of the enzyme AcCO6 will be performed toward functionalised alcohols **85-95**. Substrates **85-95** could be compared individually and in interaction with the enzyme's active site using computational investigations. The limitations of the produced aldehyde and the oxidation-olefination cascade reaction could be predicted by interpreting the kinetic parameters and the enzyme-substrate relationship.

4.4.2 Cascade reaction with stabilised ylide

Chemical reactions are often performed in organic solvents, which can be harmful to the environment. A chemoenzymatic reaction was developed in water, a solvent not detrimental to the environment to address this issue. This reaction involved the combination of two chemical reactions on cascade: alcohol oxidation and olefination (Scheme 62). It was explored for the oxidation of alkyl alcohols **28-31** and functionalised alcohols **85-95** with biocatalyst AcCO6, followed by Wittig olefination of the aldehydes (**35-38** and **96-106**) formed *in situ*. A novel methylsulfanyl ester **135** was characterised and a novel chemoenzymatic approach was presented to afford thirteen known olefins (**118** and **126-134**). To enhance the activity of AcCO6, investigations of its crystals and alcohol ligands will be performed by molecular docking. Comparison of ligands by molecular docking will improve the comprehension of ligand

conformations, weak/strong interactions between ligand and active site, electronic effect and enzyme turnover.

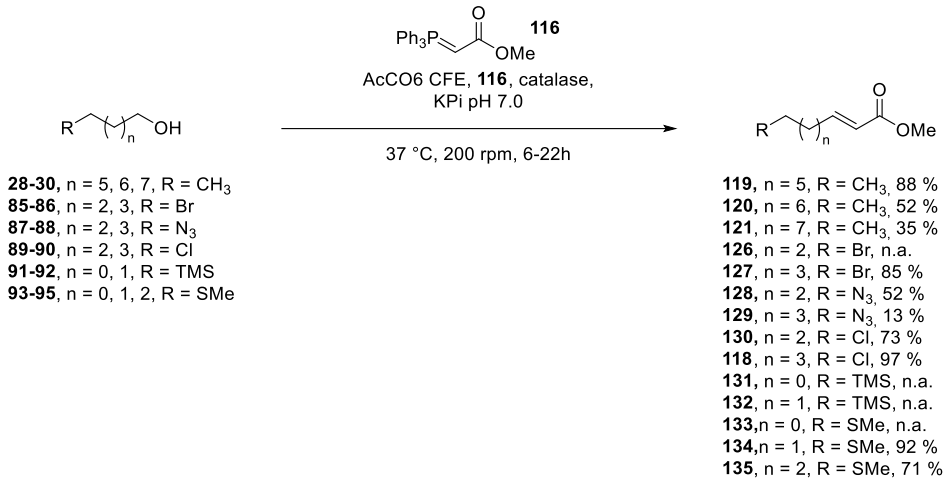

*Scheme 62 – Cascade reaction of enzymatic oxidation followed by Wittig olefination with stabilised ylide **116***

In order to purify sensitive compounds such as **126**, **129** and **131-133**, the work-up and complete analysis of the reaction crude will be optimised further. This will involve improving liquid-liquid extraction by using more washes with brine and water, and extracting with polar organic solvents like EtOAC and Et_2O. Additionally, excess phosphine will be removed, and purification will be carried out by column chromatography using alumina gel instead of silica gel or HPLC. The compounds will be characterised using mass spectrometry, GC-MS, and melting point analysis.

More thorough optimisations of the cascade reaction with Wittig reagent **116** and AcCO6 oxidase could be possible by extending it to a biphasic system (EtOAc, heptane, cyclohexane) in the presence of AcCO6 (CFE, pure, immobilised) or modifying time-reaction and temperature (two step approach at 90 °C).[5,271] Eventually, the process could be screened to alcohols oxidised to become Michael acceptor (benzyl alcohol, unsaturated alcohol),[70] to stabilised Wittig reagents **I-VI** (Scheme 63A) would open a broad scope to Wittig reaction from primary alcohol. The cascade reaction was successful in affording (*E*)-chloro alkene **118**, which could be used as an alternative step for the

cross metathesis in the synthesis of the alkaloid intermediate (-)-allosedridine **150** (Scheme 63B).[325]

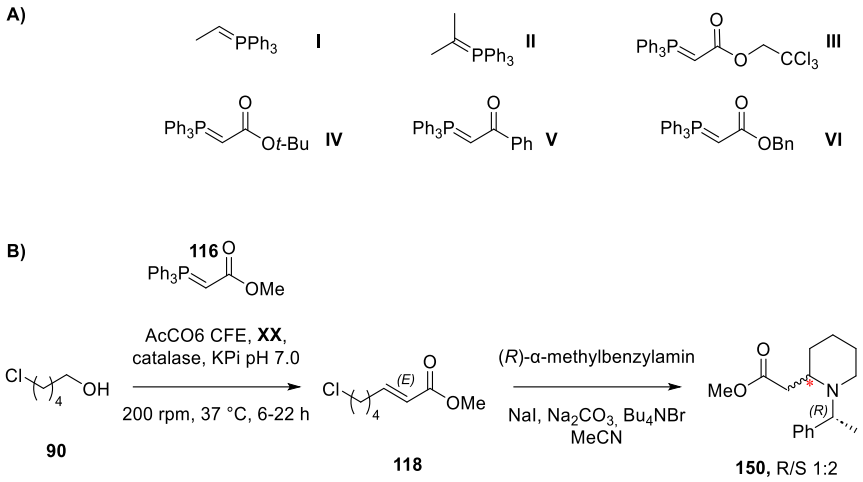

*Scheme 63 – A) Stabilised ylides reagent for Wittig olefination. B) Suggested pathway to afford **110**, necessary for amine ring **150**.*

4.4.3 Cascade reaction with non-stabilised ylide

The chemoenzymatic approach was used to process alcohols **85-95** with a phosphonium salt **125** and NaOH solution (Scheme 64A). Methylsulfanyl nitrile **137** was successfully isolated, but thirteen other nitriles **140-149** were not isolated. The non-stabilised ylide **125** must be activated with a strong base without inhibiting the enzyme AcCO6. A sequential addition method was found to be effective in achieving this purpose.

Alternatively, strong bases to activate phosphonium salts **125** will be explored further (LiCl, LiOH, NaOH conc., $NaHCO_3$, AcCOH). Similarly, ylide pre-activation could be prepared in a separate container and the resulting ylide will be added to the biotransformation. To optimise the process, the following setting could be adjusted: keep pH basic, add an additive, use of an organic solvent (10-50 *%v/v*, EtOAc, DMSO, acetonitrile). Once the activation of reagent **125** is fully optimised, more non-stabilised ylides will also be screened (Scheme 64B).

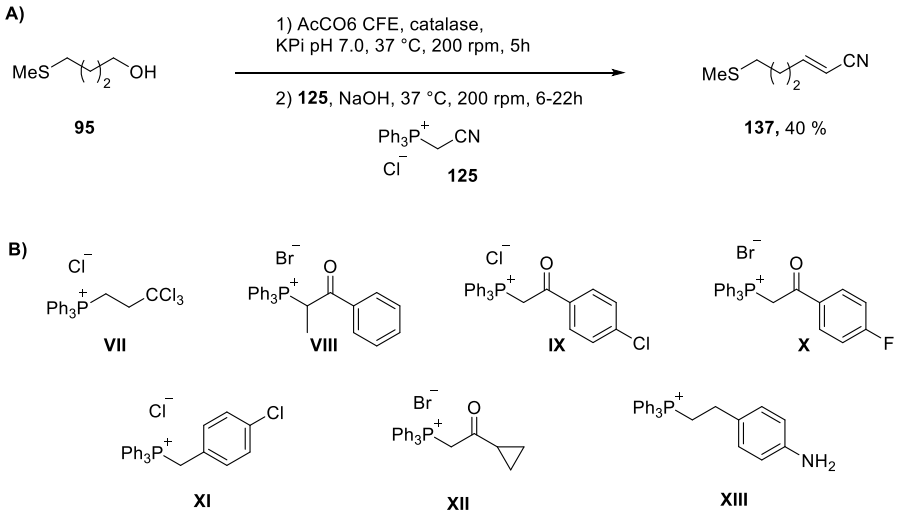

*Scheme 64 – A) Cascade reaction of enzymatic oxidation followed by Wittig olefination with non-stabilised ylide **125**. B) Non-stabilised ylides for Wittig olefination.*

Chapter 5 - Biochemical Experimental

5.1 General methods and equipments

Sterilisation of media and equipment was carried out in a Prestige Medical bench top autoclave at 126 °C for 15 min. The bench was cleaned with 70 % EtOH solution to maintain an aseptic environment. Bacterial cultures were incubated in a SciQuip INCU-shake MIDI or SciQuip Floor Standing INCU-shake TL6-5R. LB-agar plates, 96-well assay plates and enzymatic reactions were incubated in a Grant-Bio Orbital shaker incubator ES-20 IKA KS4000i control incubator or Wolf Laboratory Galaxy R CO_2 static incubator.

Centrifugation was performed using either a Sorvall RC5C Plus, SciQuip Sigma 2-16P, Eppendorf 5810 or Beckman Coulter™ Microfuge20. Spectrophotometric readings were performed using a Thermo Scientific Nanodrop 1000. SDS-PAGE was carried out using Bio-Rad mini protean 3 apparatus using Bio-Rad mini-PROTEAN TGX precast gels. Proteins were concentrated either using 10 KDa MWCO Thermo Scientific™ Pierce™ protein concentrator PES or Amicon® Ultra-15 Centrrifugal protein concentrators. Analytical grade reagents were supplied by commercial suppliers and used without further purification. Bacterial plasmid DNA extraction & purification were performed using Thermo Scientific GeneJET Plasmid Miniprep kit. Plate based assays were performed using TECAN Infinite 200 Pro M Nano. UV-Vis Spectroscopy was performed on a Varian Cary® 50 UV-Vis Spectrophotometer with OMNIC™ Specta software.

5.2 Media and Buffers

Buffers and media were made in-house unless otherwise stated using analytical grade reagents supplied by commercial suppliers. All common buffers and media were prepared with 18.2 MΩ water to the required volume. The pH of the solutions was adjusted using 5 M NaOH or H_3PO_4 followed by filtration using Thermo Scientific™ Nalgene™ Membrane and Prefilter Disks, material Nylon, pore size 0.2 µm. Media was sterilised by autoclave at 126 °C for 15 min.

5.2.1 Growth media

Millers lysogeny broth (LB) medium: 1.0 *%w/v* Tryptone, 0.5 *%w/v* Yeast Extract, 1.0 *%w/v* NaCl.

Millers lysogeny broth (LB) agar: 1.0 *%w/v* Tryptone, 0.5 *%w/v* Yeast Extract, 1.0 *%w/v* NaCl, 1.5 *%w/v* Agar.

2TY medium: 1.6 *%w/v* Tryptone, 1.0 *%w/v* Yeast Extract, 0.5 *%w/v* NaCl.

Super Optimal Culture (SOC): 2.0 *%w/v* Tryptone, 0.5 *%w/v* Yeast Extract, 10 mM NaCl, 2.5 mM KCl, 10 mM $MgCl_2$, 10 mM $MgSO_4$. Solution autoclaved at 120 °C for 20 min before addition of 20 $mL.L^{-1}$ of 1 M glucose.

Auto induction medium: 2.0 *%w/v* Tryptone, 0.5 *%w/v* Yeast Extract, 0.5 *%w/v* NaCl, 50 mM K_2HPO_4. Solution autoclaved at 126 °C for 15 min before addition of 1 $mL.L^{-1}$ 50 *%w/v* glucose, 10 $mL.L^{-1}$ 20 *%w/v* lactose and 10 $mL.L^{-1}$ 50 *%v/v* glycerol.

5.2.2 General Buffers for working with Proteins

5.2.2.1 Buffers for enzymatic reaction

Phosphate reaction buffer: 500 mM K_2HPO_4, to pH 7.0.

HEPES reaction buffer: 500 mM HEPES, pH 8.0.

5.2.2.2 His-Tagged Protein Buffers

Lysis buffer: 50 mM HEPES, 200 mM NaCl, pH 7.5.

Ni-NTA equilibration buffer: 10 mM Imidazole, made up with lysis buffer.

Ni-NTA Wash buffer: 25 mM Imidazole, made up with lysis buffer.

Ni-NTA Elution buffer: 500 mM Imidazole, made up with lysis buffer.

5.2.2.3 SDS-PAGE Buffers

SDS-PAGE running buffer: 25 mM Tris-base, 192 mM Glycine, 0.1 *%w/v* SDS.

SDS-PAGE loading buffer: 5 mM DTT, 0.5 *%w/v* Glycerol, 2.5 mM Tris-HCl, 0.1 *%w/v* SDS, 0.005 *%w/v* bromophenol blue dye pH 6.8.

Coomassie stain: Coomassie G-250 0.625 *%w/v*, 40 *%v/v* methanol, 10 *%v/v* acetic acid.

Coomassie destain: 40 *%v/v* methanol, 10 *%v/v* acetic acid.

Bio-Rad™ QC Colloidal Coomassie stain : Coomassie G-250 (proportion unspecified), ethanol 10-20 *%v/v*, phosphoric acid 1.0-2.5 *%v/v*.

5.2.2.4 PD-10 desalting chromatography

PD-10 equilibration buffer: 20 mM HEPES, 300 mM NaCl, 10 mM $MgCl_2$, pH 7.4

5.2.2.5 Immobilisation buffers

Epoxy/butyl methacrylate ECR8285 Immobilisation buffer: 100 mM KPi, 300 mM NaCl, pH 7.0.

Amino C2 methacrylate ECR8309F Immobilisation buffer: 50 mM KPi, pH 7.0.

Amino C2 methacrylate ECR8309F washing buffer: 50 mM KPi, 50 mM NaCl, pH 7.0.

EziG Amber immobilisation buffer: 20 mM potassium phosphate, 300 mM NaCl, pH 7.5.

EziG Amber immobilisation buffer with imidazole: 20 mM potassium phosphate, 300 mM NaCl, 50 mM imidazole, pH 7.5.

Glutaraldehyde buffer: 5 *%v/v* glutaraldehyde made up with amino C2 methacrylate ECR309F Immobilisation buffer

5.2.3 General buffers for working with DNA

Resuspension buffer (Thermo Scientific): 50 mM Tris, 10 mM EDTA, 0.01 *%w/v* RNase A, pH 8.0

Lysis buffer (Thermo Scientific): 200 mM NaOH, 1 *%w/v* SDS

Neutralisation buffer (Thermo Scientific): 4.2 M Guanidine HCl, 0.9 M potassium acetate, pH 4.8

DNA wash buffer (Thermo Scientific): 10 mM Tris, 80 *%v/v* ethanol, pH 7.5

5.3 Standard protocols

5.3.1 Cell Growth and protein overexpression

5.3.1.1 Transformation of chemically competent E. coli cells.

50 µL of *E. coli* BL21 competent cells and 1-2 µL of plasmid were mixed together in a sterile Eppendorf tube on ice. The cells were incubated for 10 min to allow diffusion of the plasmid, followed by a heat shock for 45 seconds at 42 °C and another incubation on ice for 10 min to allow plasmid uptake. SOC media (950 µL) was added to the cells and they were incubated at 37 °C with shaking (200 rpm) for 1 hour. A 100 µL or 20 µL and concentrated cell aliquots were used to inoculate sterilised agar plates containing either ampicillin (100 $\mu g.mL^{-1}$) or kanamycin (50 $\mu g.mL^{-1}$). Concentrated cell aliquots were taken from the remaining cell culture which was centrifuged (13,000 × *g*, 30 seconds). 800 µL of supernatant was removed and the pelleted cells resuspended in the remaining media, a 20 µL aliquot of this concentrate was used inoculate a sterilised agar selection plate. The plates were incubated at 37 °C overnight and removed in the morning to stop growth. Plates were stored at 4 °C until use, maximum of 1 week.

5.3.1.2 Preparation of Mini-culture

A single colony from the transformed *E. coli* cells grown on the sterilised agar plates overnight or glycerol stock stab was picked and incubated with shaking (200 rpm) in 5 mL of LB media containing the necessary antibiotic (ampicillin (100 $\mu g.mL^{-1}$) or kanamycin (50 $\mu g.mL^{-1}$)) at 37 °C overnight. This mini-culture was used to inoculate 1 L of overexpression media and/or glycerol stocks were made using a 1:1 mixture of the cells and 80% sterilised glycerol (in deionised water). Glycerol stocks were left at room temperature for 15 min then stored at −80 °C for future use.

5.3.1.3 Overexpression in LB media

1 L of sterilised LB media containing the desired antibiotic (ampicillin (100 $\mu g.mL^{-1}$) or kanamycin (50 $\mu g.mL^{-1}$)) in a 2 L flask was inoculated with 1 mL of cells from the overnight culture. The culture was incubated at 37 °C with shaking (200 rpm) for 3-4 h and overexpression by the addition of IPTG (0.5 mM) when OD_{600}~0.6. The cells were incubated overnight at 20 °C before being collected

by centrifugation (6,000 × *g*, 10 min, 4 °C). Cells were either used immediately or stored at −80 °C for future lysis and purification.

5.3.1.4 Overexpression in Auto-induction media

1 L of sterilised auto-induction media containing the desired antibiotic (ampicillin (100 µg.mL^{-1}) or kanamycin (50 µg.mL^{-1})) in a 2 L flask was inoculated with 1 mL of cells from the overnight culture. The culture was incubated at 30 °C with shaking (200 rpm) for 4 h then the incubator temperature was reduced to 20 °C. The cells were incubated overnight before being collected by centrifugation (6,000 × *g*, 10 min, 4 °C). Cells were either used immediately or stored at -80 °C for future lysis and purification.

5.3.2 Protein purification

5.3.2.1 Lysis of *E. coli* containing soluble proteins

E. coli cells were resuspended in the lysis buffer at 4 °C and treated with DNase. The cell mixture was lysed by sonication on ice using a US Solid Ultrasonic processor sonicator (output 40 %, 50 % time pulses, 3 × 30 sec on and 3 × 30 sec off). The cell debris was pelleted by centrifugation (10,000 × *g*, 45 min, 4 °C) and the cell lysate was decanted off. Purification of the clarified lysate was performed by Ni-NTA affinity chromatography.

5.3.2.2 Purification of His_6-tagged protein using Ni-NTA chromatography

HisPur Ni-NTA Spin column was equilibrated with 5 column volumes of equilibration buffer. The solution containing the His-tagged protein was loaded twice to the column. The resin was washed with 5 column volumes of Ni-NTA wash buffer. The protein was eluted in 10 mL fractions using 5 column volumes of Ni-NTA elution buffer. Fractions were monitored using Bradford reagent. The protein size, expression level and purity were assessed by SDS-PAGE.

5.3.2.3 Concentration of protein samples

Protein containing fractions from Ni-NTA column were combined and concentrated to an appropriate volume either using a 10 KDa MWCO Thermo Scientific™ Pierece™ protein

concentrator PES or Amicon® Ultra-15 centrifugal filter device, centrifuging at 4000 × *g* for as long as required. A 200 µL pipette was used to resuspend the protein every 15 minutes, if required, as the protein collects on the centrifugal filter (for 1.0 g AcCO6 CFE, yield: 21.5 mg, 2 %).

5.3.2.4 PD-10 desalting chromatography

PD-10 column was equilibrated with PD-10 equilibration buffer (total volume 25 mL). Concentrated protein samples following affinity column purification were concentrated to between 500 µL and 2.5 mL. A maximum of 2.5 mL of sample was added to the column. When sample volumes were less than 2.5 mL, equilibration buffer was added to adjust the volume up to 2.5 mL after the sample had entered the packed bed. The flow through was discarded, and the buffer exchanged protein collected in a clean tube, eluting with 3.5 mL of buffer.

5.3.2.5 Regeneration of Ni-NTA column

After being used for protein purification, the Ni-NTA agarose resin was regenerated for future use. Firstly, the resin was washed with 18.2 MΩ water (5 column volumes). The Ni^{2+} was removed by chelation with 100 mM ethylenediaminetetraacetic acid (EDTA, 5 column volumes), the resin was washed with 0.5 M NaOH (5 column volumes) and deionised water (10 column volumes) and regenerated with 100 mM $NiSO_4$ (2 column volumes). A final wash with deionised water was done to remove any excess Ni^{2+} and the column was flushed and stored in 20 % EtOH.

5.3.3 Protein Analysis

5.3.3.1 SDS Polyacrylamide Gel Electrophoresis

Mass based separation of protein was performed by SDS polyacrylamide gel electrophoresis. 20 µL of the protein samples were added to 5 µL of 5 × SDS-PAGE loading buffer. Mini-PROTEAN® TGX AnyKD SDS-PAGE gel transferred to a Bio-Rad electrophoresis tank. The inside of the tank, where the gel was fixed, was filled with SDS-PAGE running buffer to ensure no leaks and finally the surrounding section was half filled with running buffer. 10 µL aliquots of each sample were

loaded into the sample wells and gel electrophoresis was run at 180 V in SDS loading buffer for 30 min, or until the bromophenol blue bands can be seen to have reached the bottom of the gel.

5.3.3.2 Gel imaging with stain Coomassie stain

Once electrophoresis had finished, the gels were removed from the casts and stained with Coomassie Blue G-250. Gels were stained for 12 h on a rocker at room temperature. The stain was decanted and replaced with Coomassie de-stain and incubated for a further 3 h with rocking, then washed with water.

5.3.3.3 Gel imaging with Bio-Rad™ QC Colloidal Coomassie stain

As indicated by the supplier, once electrophoresis had finished, the gels were removed from the casts, rinsed in a shallow staining tray with deionised water and the rinsing solution was discarded. The gels were fixed with Coomassie de-stain for 15 min with gentle agitation. The fixing solution was discarded. The gel was rinsed with deionised water and the rinsing solution was discarded. The gel was stained with Bio-Rad™ QC Colloidal Coomassie stain. Gels stained were stained for 1-24 h on a rocker at room temperature. The stain was decanted. The gels were de-stained with deionised water for 1-3 h with gentle agitation on a rocker, then washed with deionised water.

5.3.3.4 BCA assay

Protein concentrations were determined using the ThermoScientific Pierce bicinchoninic acid (BCA) Protein Assay Kit according to the manufacturer's instructions, with bovine serum albumin (BSA) as standard in 96-well microplate polystyrene flate bottom (Grenier 655101) with TECAN Infinite M200 spectrophotometer.

A protein assay was determined by using BSA and 4 % cupric sulphate solution at a ratio of 20:1. The solution was prepared using a 20:1 volume ratio of BSA and 4 % cupric sulphate. A 0.05 mL of immobilised/free enzyme solution was added to the solution. The mixture was incubated for 30 min at 37 °C. After incubation, the resultant colour change in the mixture was measured at

562 nm with a TECAN Infinite M200 spectrophotometer. A calibration curve was plotted for references.

5.3.3.5 Specific activity measurements of choline oxidase AcCO6

Specific activity measurements were carried out in triplicates with a 1:1 ratio assumed in the oxidation of substrate to production of hydrogen peroxide. The rate of production of hydrogen peroxide was detected by HRP (Type I, Sigma) and (Alfa-Aesar) (ε = 36000 $L.mol^{-1}.cm^{-1}$). Substrates were dissolved in DMSO to 1 M then 20× stocks of each solution (50 mM) were prepared in 100 mM KPi (pH 7.0) containing 10 % DMSO. HRP was dissolved in 100 mM KPi (pH 7.0) at 2.0 $mg.mL^{-1}$ (4× stock), ABTS was dissolved in 100 mM KPi (pH 7.0) at 2.8 $mg.mL^{-1}$ (4× stock). 20 µL substrate (5 mM final), 50 µL ABTS (0.7 $mg.mL^{-1}$ final) and 50 µL HRP (0.5 $mg.mL^{-1}$ final) and 40 µL 100 mM KPi (pH 7.0) were added to a 96 well plate (path length 0.56 cm). The assay was started by adding 40 µL purified enzyme (C_f = 0.01 $mg.mL^{-1}$). The absorbance at 420 nm was followed over time on a TECAN Infinite M200 spectrophotometer at 30 °C.

5.3.3.6 Specific activity measurements of long-chain alcohol oxidase HNX4

Specific activity measurements were carried out in triplicates with a 1:1 ratio assumed in the oxidation of substrate to production of hydrogen peroxide. The rate of production of hydrogen peroxide was detected by HRP (Type I, Sigma) and 4-amino antipyrine/2,4,6-tribromo-3-hydroxybenzoic acid dye (ε = 29400 $L.mol^{-1}.cm^{-1}$). Substrates were dissolved in DMSO to 1 M then 200× stocks of each solution (5 mM) were prepared in 100 mM KPi (pH 7.0) containing 10 % DMSO. The dye was prepared by adding 100 µL 4-amino antipyrine (100 $mg.mL^{-1}$) and 30 µL (20 $mg.mL^{-1}$) 2,4,6-tribromo-3-hydroxybenzoic acid to 100 mM KPi (pH 8.0) to afford 7× stock. HRP was dissolved in 100 mM KPi (pH 7.0) at 0.2 $mg.mL^{-1}$ (7× stock). 20 µL substrate (C_f = 1 mM), 15 µL dye and 15 µL HRP (C_f = 0.03 $mg.mL^{-1}$) were added to a 96 well plate (path length 0.28 cm). The assay was started by adding 50 µL purified enzyme (C_f =0.05 $mg.mL^{-1}$). The absorbance at 510 nm was followed over time on a TECAN Infinite M200 spectrophotometer at 40 °C.

5.3.3.7 Data processing for specific activity measurements

Specific activity was calculated using the following equation:

Equation 5 – Specific activity measurements (mU.mg^{-1})

$$\frac{\left(\frac{\left(\frac{A}{l\varepsilon}\times V\right)}{T}\right)}{[E]}\times 10^3$$

Where A was final absorbance, l was pathlength in cm, ε was the molar extinction coefficient of ABTS (36000 L.mol^{-1}.cm^{-1}), V was the volume of the reaction in µL, T is the time of reaction completion in minutes and $[E]$ was the final enzyme concentration in mg.mL^{-1}. Values were multiplied by 10^3 to give specific activity in mU.mg^{-1}.

5.3.4 Kinetic Assay

5.3.4.1 Kinetic protocol for choline oxidase AcCO6

A 1:1 ratio was assumed in the oxidation of substrate to production of hydrogen peroxide. The rate of production of hydrogen peroxide was detected by HRP (Type I, Sigma) and ABTS (Alfa-Aesar) (ε = 36000 L.mol^{-1}.cm^{-1}). Substrates were dissolved in DMSO to 1 M then 10× stocks of each solution were prepared in 100 mM KPi (pH 7.0) containing 10 % DMSO. Multiple substrate concentrations were prepared by 2-fold serial dilution from 20 mM down to 0.313 mM (10× stocks). Stock solution of HRP was prepared by dissolving HRP in 100 mM KPi (pH 7.0) at 2.0 mg.mL^{-1} (4× stock). Stock solution of ABTS was prepared by dissolving ABTS was dissolved in 100 mM KPi (pH 7.0) at 2.8 mg.mL^{-1} (4× stock). Stocked solution of purified enzyme was prepared by dilution in 100 mM KPi (pH 7.0) at 0.05 mg.mL^{-1} (5x stocks). 20 µL substrate, 50 µL ABTS (C_f = 0.7 mg.mL^{-1}) and 50 µL HRP (C_f = 0.5 mg.mL^{-1}) and 40 µL 100 mM KPi (pH 7.0) were added to a 96 well plate (path length 0.56 cm). The assay was started by adding 40 µL purified enzyme (C_f = 0.5 mg.mL^{-1}). The absorbance at 420 nm was followed over time on a TECAN Infinite M200 spectrophotometer at 30 °C and used to calculate initial rates. The rate was plotted against the

substrate concentration and *Vmax* and K_M values were extracted using OriginPro 9.6 non-linear curve fit analysis using the Hill model (section 5.3.4.2.2). The errors on the K_{cat} and K_M values represent the 95 % confidence interval based on the standard error of the regression.

5.3.4.2 Data processing

5.3.4.2.1 Standard error

All samples were analysed in triplicate. The error of each sample was calculated as standard error (*Equation 6*) where n equals the samples size, x was the observed initial rate value for each sample and $\tilde{x}$ was the mean rate value for each sample.

Equation 6 - Standard error in initial rate obtained for each sample

$$standard\ error = \frac{\sqrt{\frac{\sum(x-\bar{x})^2}{(n-1)}}}{\sqrt{n}}$$

5.3.4.2.2 Hill model

Equation 7 - Hill model

$$V = \frac{V_{max} \times [S]^n}{(K_{0.5})^n + [S]^n}$$

Where V is the reaction velocity (mol.min^{-1}), V_{max} is the maximum velocity of the reaction (mol.min^{-1}), $[S]$ is the substrate concentration (mol.L^{-1}), $K_{0.5}$ is the half-maximal concentration constant (mol.L^{-1}) and n is the Hill coefficient.

5.3.5 Enzyme immobilisation

5.3.5.1 Purolite Lifetech™ ECR enzyme immobilisation resins

Resin	Functional group	Immobilisation	Porosity (Å)
ECR8285 Epoxy/butyl methacrylate	Epoxy	Covalent	400 – 600
ECR8309F amino C2 methacrylate	NH_2	Covalent (hydrophilic) or ionic	600 – 1200

5.3.5.2 Lifetech™ ECR8285 epoxy/butyl methacrylate resin

As described by the manufacturer instructions, resin (7.0 g) was equilibrated by washing the resin with immobilisation buffer (35 *%w/v*) 2 to 4 times and remove the excess liquid by pipetting. The AcCO6 enzyme (1.0 g of CFE) was dissolved in immobilisation buffer (5 *%w/v*) and was transferred in the vessel of ECR epoxy resin. The slurry was mixed gently for 18 h and was left without mixing for another 20 h at rt. The resin was washed with 18.2 MΩ water 2 to 4 times under gentle mixing and the excess of liquid was removed by pipetting.

5.3.5.3 Lifetech™ ECR8309F amino C2 methacrylate resin

As described by the manufacturer instructions, resin (3.6 g) was equilibrated by washing the resin with immobilisation buffer (18 *%w/v*) 2 to 4 times and remove the excess liquid by pipetting. The resin was pre-activated by addition of a glutaraldehyde buffer (18 *%w/v*). The resulting slurry was mixed gently for 1 h at rt. The excess liquid was pipetted out. The resin was washed 2 to 4 times with immobilisation buffer (18 *%w/v*) followed by pipetting out the excess liquid. The AcCO6 enzyme (0.5 g of CFE) was dissolved in immobilisation buffer (2.5 *%w/v*) and was transferred in the vessel of ECR amino resin. The slurry was mixed gently for 18 h at rt. The liquid phase was pipetted out. The resin was washed with immobilisation buffer once and 18.2 MΩ water.

5.3.5.4 EziG™ Amber

As described by the manufacturer instructions, enzyme solution of AcCO6 cell free extracts (100 mg) was prepared in immobilisation buffer (0.5 *%w/v*). EziG™ Amber resin (90 mg) was added to the enzyme solution. The slurry was mixed gently for 30 min at rt. The liquid phase was pipetted out. The resin was washed with 18.2 MΩ water (1 *%w/v*).

5.3.6 DNA manipulation, purification and analysis

5.3.6.1 Small scale DNA isolation (mini-prep)

DH5α *E. coli* cells, harbouring the desired plasmid, were collected under sterile conditions from a glycerol stock or LB-agar plate, and added to a falcon tube with 5 mL of LB media which had been inoculated with the appropriate antibiotic (ampicillin (100 $\mu g.mL^{-1}$) or kanamycin (50 $\mu g.mL^{-1}$)). The culture was incubated at 37 °C with shaking (200 rpm) for 18 h. The bacterial cell pellet was isolated from the mini cultures by centrifugation (4500 × *g*, 15 min) at room temperature and the DNA was extracted using a GeneJET Plasmid Mini Prep Kit following the manufacturers recommended protocol. All centrifugation steps were carried out at 17,000 *× g* in a microfuge at rt.

As described by the manufacturer instructions, the cell pellet was resuspended in buffer P1 (250 µL) and mixed thoroughly with buffer P2 (250 µL). Buffer N3 (350 µL) was added and the Eppendorf tube inverted until the solution turned colourless. Insoluble debris was pelleted by centrifugation for 10 min. The supernatant was applied to a QIAprep Spin column and centrifuged for 1 min to bind the DNA to the column. The flow through was discarded and column washed with buffer PE (750 µL) and centrifuged for 2 × 1 min. The flow through was discarded and spin filter transferred to a sterile Eppendorf tube. The DNA sample was eluted with 18.2 MΩ water (50 µL) and centrifuged for 1 min.

5.3.6.2 DNA quantification

DNA concentrations were measured using a Thermo Scientific NanoDrop 1000 spectrophotometer. The instrument was blanked with deionised water and absorbance at 260 nm of a 2 µL sample was measured. Concentration was estimated using *Equation 8*.

Equation 8 – DNA concentration calculation

$$Concentration\ (\mu g.mL^{-1}) = A_{260} \times 50\ \mu g.mL^{-1}$$

Chapter 6 - Chemistry Experimental

6.1 General

Chemicals and materials were purchased from Acros UK, Aldrich UK, Alfa Aesar, Fisher UK, Sigma Aldrich, TCI, Purolite and Novabiochem and used as receivedCommercial hydroxylamine Wang resin Novabiochem® **66** (CAS 65307-53-1) was provided from Sigma Aldrich. . Aminomethyl polystyrene resin **67** (cross-linked with 1 % DVB 200-400mesh, 2.0-3.0 mmol.g^{-1}) was provided from TCI (product number: A2047). All solvents and reagents were purified and dried where necessary. Where appropriate and if not stated otherwise, all non-aqueous reactions were performed under an inert atmosphere of nitrogen, using a vacuum manifold with nitrogen passed through drierite molecular sieves. Brine refers to a saturated aqueous solution of sodium chloride. Hexane refers to the fraction from petroleum ether boiling between 40-60 °C.

Infra-red spectra were recorded neat on a Thermo Scientific Nicolet iS10 spectrometer; selected absorption frequencies (vmax) are reported in cm^{-1}. Infra-red spectra were analysed on OMNIC™ Spectra Software.

Gardner colorimetry was recorded on PFX-i Series Spectrocolorimeter Lavibond with cuvette 1 cm 10.00.

Mass spectrometry data was collected by the EPSRC UK National Mass Spectrometry Facility in Swansea and Keele University Accurate Mass Service on LQT Orbitrap XL1, Xevo G2-S ASAP, nanoESI and Agilent 6530 Q-TOF LC/MS instruments in positive/negative ionisation modes as appropriate.

Analytical thin layer chromatography (TLC) was carried out on pre-coated 0.25 mm Merck KGaA 60 F_{254} silica gel plates. Visualisation was by adsorption of UV light (254 nm), or thermal development after dipping in a H_2SO_4 in MeOH (5 % *v/v*) or a $KMnO_4$ stain.

Column chromatography was carried out on silica gel (VWR International 40-63 µm) under a positive pressure of compressed air. *Automatic flash column chromatography* was carried out on silica gel (Reveleris® X2 system) under a positive pressure of compressed air.

pH solution was measured on Fisherbrand™ accumet™ AE150 Benchtop pH Meter.

Centrifugation was performed using a Beckman Coulter™ Microfuge20 for analytical scale reaction and VWR® Mega Star600 for preparative scale reaction.

Gas chromatography data was collected with a GC-7820A apparatus (Agilent Technologies) equipped with a flame ionization detector (FID) and an HP-5 GC column (30 m × 0.320 mm × 0.25 µm). Nitrogen (200 kPa) was used as carrier gas. Alternatively, gas chromatography data was collected with a GC-2010Plus apparatus (Shimadzu Technologies) equipped with (FID) and an DB-1 column (60 m x 0.320 mm x 5.00 µm). Hydrogen (65 psi) was used as carrier gas.

^{1}H NMR spectra were recorded on a Bruker Avance 400 (400 MHz) instrument using deuterated indicated solvent as reference. The chemical shift data for each signal were given as δ in units of parts per million (ppm) relative to tetramethylsilane (TMS) where δ = 0.00 ppm. The multiplicity of each signal was indicated by: s (singlet), bs (broad singlet), d (doublet), dd (doublet of doublets), dt (doublet of triplets), dq (double of quartets), t (triplet), app. t (apparent triplet), qd (quartet of doublets), m (multiplet). The number of protons (n) for a given resonance was indicated by nH. Coupling constants (*J*) are quoted in Hz and recorded to the nearest 0.1 Hz.

^{13}C NMR spectra were recorded on a Bruker Avance 400 (100 MHz) instrument. The chemical shift data for each signal are given as δ in units of parts per million (ppm) relative to the deuterated solvent peak.

^{31}P NMR spectra were recorded on a Bruker Avance 400 (161 MHz) instrument. The chemical shift data for each signal are given as δ in units of parts per million (ppm).

Assignment of ^{1}H and ^{13}C atoms of carbohydrate, alcohol and alkene in NMR analysis follows the generic numbering system shown below:

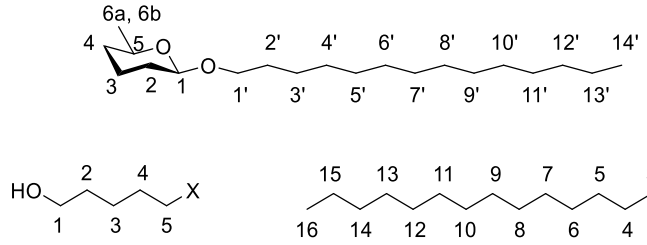

6.2 Synthesis of alkyl monoglucoside (AMG)

6.2.1 Procedure A: Glycosylation of acetylated glucose using alkyl alcohol

To a stirred solution of 1,2,3,4,6-penta-*O*-acetyl-β-D-glucopyranoside **48** (1.0 equiv.) in anhydrous DCM (25 mL) at rt, were added successively, alcohol (1.2–2.0 equiv.) and $BF_3{\cdot}Et_2O$ (1.5–4.7 equiv.). The yellow-orange solution formed was stirred at rt for 3–5 h and monitored by TLC analysis (Pet. Ether/EtOAc). The reaction was quenched slowly by the addition of saturated $NaHCO_3$ (20 mL). The organic layer was washed with saturated $NaHCO_3$ (2 × 40 mL) and the combined aqueous layers were extracted with DCM (35 mL). The organic layers were combined and dried over $MgSO_4$, filtered and concentrated under reduced pressure. The crude material was purified by column chromatography to afford protected alkyl monoglucoside.

6.2.2 Procedure B: Deacetylation of protected AMG

To a stirred solution of protected glucopyranose (1.0 equiv.) in MeOH (25 mL), Na_2CO_3 (0.01 equiv.) was added at rt. The mixture was stirred for 1–3 h, then neutralised with ion exchange Amberlite 120 (H^+) resin, filtered, and concentrated under reduced pressure. The crude material was purified by column chromatography to afford deprotected alkyl monoglucoside.

6.2.3 Octyl (2,3,4,6-tetra-*O*-acetyl)-β-D-glucopyranoside **49**

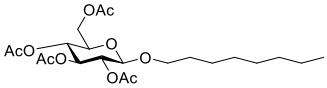

49

Prepared as per Procedure A using commercial **48** (3.90 g, 10.0 mmol, 1.0 equiv.), 1-octanol **27** (3.03 mL, 19.2 mmol, 1.9 equiv.) and $BF_3{\cdot}Et_2O$ (6.00 mL, 47.0 mmol, 4.7 equiv.) in DCM (25mL). Reaction time: 3 h. Purification by column chromatography (Pet. Ether/EtOAc, 9:1 to 7:3) to afford the product octyl **49** as a white solid (2.47 g, 5.4 mmol, 53 %).

R_f = 0.85 (Pet. Ether/EtOAc, 6:4); **^{1}H NMR (400 MHz, $CDCl_3$)**: δ 5.20 (t, $^3J_{H3\text{-}H2/H4}$ = 9.5 Hz, 1H, H-3), 5.08 (t, $^3J_{H4\text{-}H3/H5}$ = 9.5 Hz, 1H, H-4), 4.97 (dd, $^3J_{H2\text{-}H3}$ = 9.4 Hz, $^3J_{H2\text{-}H1}$ = 8.1 Hz, 1H, H-2), 4.50 (d, $^3J_{H1\text{-}H2}$ = 8.0 Hz, 1H, H-1), 4.27 (dd, $^2J_{H6a\text{-}H6b}$ = 12.2 Hz, $^3J_{H6a\text{-}H5}$ = 4.6 Hz, 1H, H-6a), 4.13 (dd, $^2J_{H6b\text{-}H6a}$ = 12.2 Hz, $^3J_{H6b\text{-}H5}$ = 2.1 Hz, 1H, H-6b), 3.89-3.84 (m, 1H, H-1a'), 3.72-3.68 (m, 1H, H-5), 3.50-3.45 (m, 1H, H-1b'), 2.08 (s, 3H, OCOC*H*$_3$), 2.03 (s, 3H, OCOC*H*$_3$), 2.02 (s, 3H, OCOC*H*$_3$), 2.00 (s, 3H, OCOC*H*$_3$), 1.58-1.55 (m, 2H, $CH_{2(2')}$), 1.37-1.23 (m, 10H, CH_2), 0.89-0.86 (m, 3H, C*H*$_{3(8')}$); **^{13}C NMR (101 MHz, $CDCl_3$):** δ 170.5 (C=O), 170.1 (C=O), 169.2 (C=O), 169.0 (C=O), 100.6 (C-1), 72.7 (C-3), 71.5 (C-5), 71.2 (C-2), 70.3 (C-1'), 68.3 (C-4), 61.8 (C-6), 31.6 (C-1'), 29.2 (C-2'), 29.0 (C-4', C-5'), 25.6 (C-6'), 22.4 (C-7'), 20.5 (CH_3), 20.4 (CH_3), 20.4 (CH_3), 20.4 (CH_3), 13.8 (C-8'); **HRMS** *m/z* (ESI$^+$) found $(M+NH_4)^+$ 478.2651, $C_{26}H_{44}O_{10}NH_4$ required 478.2647. These data were in agreement with published literature values.[326]

6.2.4 Decyl 2,3,4,6-tetra-*O*-acetyl)-β-D-glucopyranoside **50**

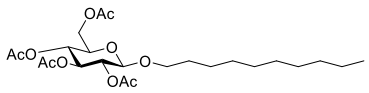

50

Prepared as per Procedure A using commercial **48** (3.87 g, 9.9 mmol, 1.0 equiv.), 1-decanol (3.76 mL, 19.7 mmol, 2.0 equiv.) and $BF_3{\cdot}Et_2O$ (6.00 mL, 47.0 mmol, 4.7 equiv.) in DCM (25 mL). Reaction time: 3.5 h. Purification by column chromatography (Pet. Ether/EtOAc, 9:1 to 7:3) to afford the product **50** as a colourless oil (2.11 g, 4.3 mmol, 76 %).

R_f = 0.66 Pet. Ether/EtOAc (6:4); **^{1}H NMR (400 MHz, $CDCl_3$):** δ 5.20 (t, $^3J_{H3\text{-}H2/4}$ = 9.5 Hz, 1H, H-3), 5.08 (t, $^3J_{H4\text{-}H3/5}$ = 9.5 Hz, 1H, H-4), 4.98 (dd, $^3J_{H2\text{-}H3}$ = 9.5 Hz, $^3J_{H2\text{-}H1}$ = 8.0 Hz, 1H, H-2), 4.89 (d, 1H, $^3J_{H1\text{-}H2}$ = 8.0 Hz, 1H, H-1), 4.26 (dd, $^2J_{H6a\text{-}H6b}$ = 12.2 Hz, $^3J_{H6a\text{-}H5}$ = 4.7 Hz, 1H, H-6a), 4.13 (dd, $^2J_{H6b\text{-}H6a}$ = 12.2 Hz, $^3J_{H6b\text{-}H5}$ = 2.3 Hz, 1H, H-6b) 3.89-3.84 (m, 1H, H-1a'), 3.70-3.66 (m, 1H, H-5), 3.49-3.43 (m, 1H, H-1b'), 2.08 (s, 3H, OCOC*H*$_3$), 2.03 (s, 3H, OCOC*H*$_3$), 2.02 (s, 3H, OCOC*H*$_3$), 2.00 (s, 3H, OCOC*H*$_3$), 1.57-1.51 (m, 4H, $CH_{2(2')}$, CH_2), 1.230-1.28 (m, 12 H, CH_2), 0.94-0.87 (m, 3H, C*H*$_{3(10')}$); **^{13}C NMR (101 MHz, $CDCl_3$):** δ 170.7 (C=O), 170.3 (C=O), 169.4 (C=O), 169.2 (C=O), 100.8 (C-1), 72.8 (C-3), 71.7 (C-5), 71.3 (C-2), 70.2 (C-1'), 68.4 (C-4), 62.0 (C-6), 40.8 (C-2'), 31.8 (CH_2), 29.5 (CH_2), 29.5 (CH_2), 29.3 (CH_2), 29.2 (CH_2), 25.7

(CH_2), 22.6 (CH_2), 14.0 (C-10'); **HRMS** *m/z* (ESI^+) found $(M+NH_4)^+$ 506.2965, $C_{26}H_{44}O_{10}NH_4$ required 506.2960. NMR data was in agreement with published literature values.[327]

6.2.5 Dodecyl (2,3,4,6-tetra-*O*-acetyl)-β-D-glucopyranoside **51**

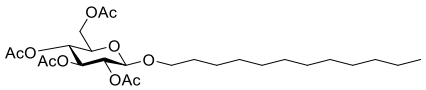

51

Prepared as per Procedure A using commercial **48** (2.00 g, 5.1 mmol, 1.0 equiv.) $BF_3{\cdot}Et_2O$ (3.64 mL, 25.6 mmol, 5.0 equiv.) and dodecanol (1.38 mL, 6.1 mmol, 1.2 equiv.) in DCM (10 mL). Purification by column chromatography (Pet. Ether/EtOAc, 95:5 to 7:3) to afford the product **51** as a white solid (0.13 g, 0.4 mmol 5 %).

R_f = 0.34 Pet. Ether/EtOAc (4:1); **^{1}H NMR (400 MHz, $CDCl_3$):** δ 5.21 (t, $^3J_{H3\text{-}H2/H4}$ = 9.5 Hz, 1H, H-3), 5.09 (t, $^3J_{H4\text{-}H3/H5}$ = 9.7 Hz, 1H, H-4), 4.98 (dd, $^3J_{H2\text{-}H3}$ = 9.6 Hz, $^3J_{H2\text{-}H1}$ = 8.0 Hz, 1H, H-2), 4.49 (d, $^3J_{H1\text{-}H2}$ = 8.0 Hz, 1H, H-1), 4.27 (dd, $^2J_{H6a\text{-}H6b}$ = 12.3 Hz, $^3J_{H6a\text{-}H5}$ = 4.7 Hz, 1H, H-6a), 4.14 (dd, $^2J_{H6b\text{-}H6a}$ = 12.3 Hz, $^3J_{H6b\text{-}H5}$ = 2.5 Hz, 1H, H-6b), 3.90 – 3.83 (m, 1H, H-1a'), 3.69 (ddd, $^3J_{H5\text{-}H4}$ = 9.7 Hz, $^3J_{H5\text{-}H6a}$ = 4.7 Hz, $^3J_{H5\text{-}H6b}$ = 2.5 Hz, 1H, H-5), 3.51 – 3.43 (m, 1H, H-1b'), 2.09 (s, 3H, OCOC*H*$_3$), 2.04 (s, 3H, OCOC*H*$_3$), 2.02 (s, 3H, OCOC*H*$_3$), 2.01 (s, 3H, OCOC*H*$_3$), 1.63-1.56 (m, 2H, $CH_{2(2')}$), 1.30-1.26 (m, 18H, CH_2), 0.88 (t, $^3J_{CH3(12')\text{-}CH2(11')}$ = 6.8 Hz, 3H, C*H*$_{3(12')}$); **^{13}C NMR (101 MHz, $CDCl_3$):** δ 170.6 (C=O), 170.3 (C=O), 169.3 (C=O), 169.2 (C=O), 100.8 (C-1), 72.9 (C-3), 71.7 (C-5), 71.3 (C-2), 70.2 (C-1'), 68.5 (C-4), 62.0 (C-6), 31.8 (CH_2), 29.6 (CH_2), 29.6 (CH_2), 29.5 (CH_2, C-2'), 29.3 (CH_2), 29.3 (CH_2), 29.3 (CH_2), 25.7 (CH_2), 22.6 (CH_2), 20.6 (CH_3), 20.6 (CH_3), 20.6 (CH_3), 20.5 (CH_3), 14.0 (C-12'). **HRMS** *m/z* (ESI^+) found $(M+NH_4)^+$ 534.3269, $C_{26}H_{44}O_{10}NH_4$ required 534.3273. NMR data were in agreement with published literature values.[328,329]

6.2.6 Tetradecyl 2,3,4,6-tetra-*O*-acetyl)-β-D-glucopyranoside **52**

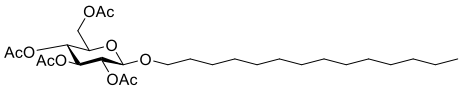

52

Prepared as per Procedure A using commercial **48** (1.00 g, 2.6 mmol, 1.0 equiv.), $BF_3{\cdot}Et_2O$ (0.47 mL, 3.8 mmol, 1.5 equiv.), tetradecanol (0.66 g, 3.1 mmol, 1.2 equiv.) in DCM (5 mL). Reaction time: 5 h. Purification by column chromatography (Pet. Ether/EtOAc, 1:0 to 7:3) to afford the product **52** as a white solid (0.36 g, 0.7 mmol, 26 %).

R_f = 0.66 Pet. Ether/EtOAc (7:3); **^{1}H NMR (400 MHz, $CDCl_3$):** δ 5.20 (t, $^3J_{H3\text{-}H2/H4}$ = 9.5 Hz, 1H, H-3), 5.09 (t, $^3J_{H4\text{-}H3/H5}$ = 9.7 Hz, 1H, H-4), 4.98 (dd, $^3J_{H2\text{-}H3}$ = 9.6 Hz, $^3J_{H2\text{-}H1}$ = 8.0 Hz, 1H, H-2), 4.49 (d, $^3J_{H1\text{-}H2}$ = 8.0 Hz, 1H, H-1), 4.27 (dd, $^2J_{H6a\text{-}H6b}$ = 12.3 Hz, $^3J_{H6a\text{-}H5}$ = 4.7 Hz, 1H, H-6a), 4.14 (dd, $^2J_{H6b\text{-}H6a}$ = 12.3 Hz, $^3J_{H6b\text{-}H5}$ = 2.4 Hz, 1H, H-6b), 3.87 (dd, $^2J_{H1a'\text{-}H1b'}$ = 9.6 Hz, $^3J_{H1a'\text{-}CH2(2')}$ = 6.4 Hz, 1H, H-1a'), 3.69 (ddd, $^3J_{H5\text{-}H4}$ = 9.9 Hz, $^3J_{H5\text{-}H6a}$ = 4.7 Hz, $^3J_{H5\text{-}H6b}$ = 2.5 Hz, 1H, H-5), 3.47 (dd, $^2J_{H1b'\text{-}H1a'}$ = 9.6 Hz, $^3J_{H1b'\text{-}CH2(2')}$ = 6.8 Hz, 1H, H-1b'), 2.09 (s, 3H, OCOCH_3), 2.04 (s, 3H, OCOCH_3), 2.02 (s, 3H, OCOCH_3), 2.01 (s, 3H, OCOCH_3), 1.58-1.55 (m, 2H, $CH_{2(2')}$), 1.29-1.25 (m, 22H, CH_2), 0.87 (t, $^3J_{CH3(14')\text{-}CH2(13')}$ = 6.9 Hz, 3H, C$H_{3(14')}$); **^{13}C NMR (101 MHz, $CDCl_3$):** δ 170.6 (C=O), 170.3 (C=O), 169.3 (C=O), 169.2 (C=O), 100.8 (C-1), 72.8 (C-3), 71.7 (C-5), 71.3 (C-2), 70.2 (C-1'), 68.4 (C-4), 61.9 (C-6), 31.9 (CH_2), 29.6 (CH_2), 29.6 (CH_2), 29.6 (CH_2), 29.5 (CH_2), 29.3 (CH_2), 29.3 (CH_2), 29.3 (C-2'), 25.7 (CH_2), 22.6 (CH_2), 20.7 (CH_3), 20.6 (CH_3), 20.6 (CH_3), 20.5 (CH_3), 14.0 (C-14'). **HRMS** *m/z* (ESI$^+$) found $(M+NH_4)^+$ 562.3594, $C_{28}H_{48}O_{10}NH_4$ required 562.3586. NMR data were in agreement with published literature values.[330]

6.2.7 Octyl-β-D-glucopyranoside **53**

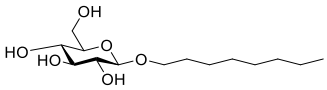

53

Prepared as per Procedure B using glucopyranoside **13** (2.47 g, 5.36 mmol, 1.0 equiv.) in MeOH (25 mL) and Na_2CO_3 (6.00 mg, 0.06 mmol, 0.01 equiv.). Reaction time: 1 h. Purification by column chromatography (Pet. Ether/EtOAc, 1:9 to 0:1) to afford the product **53** a white foam (1.16 g, 4.0 mmol, 74 %).

R_f = 0.52 ($CHCl_3$/MeOH/H_2O, 7:3:1); **^{1}H NMR (400 MHz, MeOD)**: δ 4.25 (d, $^3J_{H1\text{-}H2}$ = 7.8 Hz, 1H, H-1), 3.91-3.84 (m, 2H, H-1a', H-6a), 3.67 (dd, $^2J_{H6b\text{-}H6a}$ = 11.9 Hz, $^3J_{H6b\text{-}H5}$ = 5.3 Hz, 1H, H-6b), 3.56-3.50 (m, 1H, H-1b'), 3.37-3.35 (m, 1H, H-3), 3.28-3.25 (m, 2H, H-4, H-5), 3.17 (dd, $^3J_{H2\text{-}H3}$ = 8.9 Hz, $^3J_{H2\text{-}H1}$ = 7.8 Hz, 1H, H-2), 1.64-1.58 (m, 2H, CH_2), 1.39-1.30 (m, 9H, CH_2), 0.94-0.87 (m, 3H, $CH_{3(8')}$); **^{13}C NMR (101 MHz, MeOD)**: δ 104.3 (C-1), 78.0 (C-3), 77.8 (C-4), 75.0 (C-2), 71.6 (C-5), 70.8 (C-1'), 62.7 (C-6), 32.9 (C-2'), 30.7 (C-3'), 30.5 (C-4'), 30.3 (C-5'), 27.0 (C-6'), 23.6 (C-7'), 14.4 (C-8'); **HRMS** *m/z* (ESI^-) found $(M\text{-}H)^-$ 291.1812, $C_{14}H_{27}O_6$ required 291.1813. These data were in agreement with published literature values.[331]

6.2.8 Decyl β-D-glucopyranoside **54**

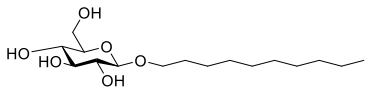

54

Prepared as per Procedure B using glucopyranoside **14** (1.00 g, 2.0 mmol, 1.0 equiv.) in MeOH (10 mL), Na_2CO_3 (0.80 mg, 7 µmol, 0.005 equiv.). Reaction: 2h. Purification by column chromatography (Hexane/EtOAc, 1:9) to afford product **54** as a white powder (0.18 g, 0.1 mmol, 49 %).

R_f = 0.54 $CHCl_3$/MeOH/H_2O (7:3:1); **^{1}H NMR (400 MHz, MeOD):** δ 4.25 (d, $^3J_{H1\text{-}H2}$ = 7.8 Hz, 1H, H-1), 3.92 – 3.84 (m, 2H, H-1a', H-6a), 3.67 (dd, $^2J_{H6b\text{-}H6a}$ = 11.9 Hz, $^3J_{H6b\text{-}H5}$ = 5.1 Hz, 1H, H-6b), 3.53 (m, 1H, H-1b'), 3.37 – 3.23 (m, 3H, H-3, H-4, H-5), 3.17 (t, $^3J_{H2\text{-}H1/H3}$ = 8.3 Hz, 1H, H-2), 1.65-1.58 (m, 2H, $CH_{2(2')}$),

1.37-1.29 (m, 14H, CH_2), 0.93-0.87 (m, 3H, $CH_{3(10')}$); **^{13}C NMR (101 MHz, MeOD):** δ 104.2 (C-1), 78.0 (C-3), 77.8 (C-4), 75.0 (C-2), 71.6 (C-5), 70.8 (C-1'), 62.7 (C-6), 33.0 (CH_2), 30.7 (CH_2), 30.7 (CH_2), 30.6 (CH_2), 30.5 (CH_2), 30.4 (CH_2), 27.0 (CH_2), 23.6 (CH_2), 14.4 (C-10'). **HRMS** *m/z* (ESI^-) found $(M-H)^-$ 319.2126, $C_{16}H_{31}O_6$ required $(M-H)^-$ 319.2125. NMR data were in agreement with published literature values.[327]

6.2.9 Dodecyl β-D-glucopyranoside **55**

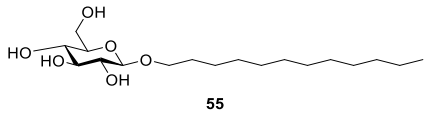

55

Prepared as per Procedure B using glucopyranoside **15** (66.00 mg, 0.1 mmol, 1.0 equiv.) in MeOH (1 mL), Na_2CO_3 (3.00 mg, 0.1 mmol, 0.2 equiv.). Reaction time: 2.5 h. Purification by column chromatography (EtOAc, 100 %) to afford the product **55** as a white crystal (38.00 mg, 0.1 mmol, 84 %).

R_f = 0.28 EtOAc (100 %); **^{1}H NMR (400 MHz, MeOD):** δ 4.26 (d, $^3J_{H1\text{-}H2}$ = 7.8 Hz, 1H, H-1), 3.94 – 3.84 (m, 2H, H-1a', H-6a), 3.68 (dd, $^2J_{H6b\text{-}H6a}$ = 11.9 Hz, $^3J_{H6b\text{-}H5}$ = 5.3 Hz, 1H, H-6b), 3.54 (dt, $^2J_{H1b'\text{-}H1a'}$ = 9.5 Hz, $^3J_{H1b'\text{-}CH2(2')}$ = 6.8 Hz, 1H, H-1b'), 3.36 (t, $^3J_{H3\text{-}H2/H4}$ = 8.9 Hz, 1H, H-3), 3.33 – 3.25 (m, 2H, H-4, H-5), 3.18 (dd, $^3J_{H2\text{-}H3}$ = 8.9 Hz, $^3J_{H2\text{-}H1}$ = 8.0 Hz, 1H, H-2), 1.68 – 1.58 (m, 2H, $CH_{2(2')}$), 1.41 – 1.26 (m, 18H, CH_2), 0.91 (t, $^3J_{CH3(12')\text{-}CH2(11')}$ = 6.9 Hz, 3H, $CH_{3(12')}$); **^{13}C NMR (101 MHz, MeOD):** δ 104.3 (C-1), 78.1 (C-3), 77.8 (C-4 or C-5), 75.1 (C-2), 71.6 (C-4 or C-5), 70.9 (C-1'), 62.7 (C-6), 33.0 (CH_2), 30.7 (CH_2), 30.7 (CH_2), 30.6 (CH_2), 30.4 (CH_2), 27.1 (CH_2), 23.7 (CH_2), 14.4 (CH_3). **HRMS** *m/z* (ESI^-) found $(M-H)^-$ 347.2437, $C_{18}H_{35}O_6$ required 347.2439. NMR data were in agreement with published literature values.[329]

6.2.10 Tetradecyl-β-D-glucopyranoside **56**

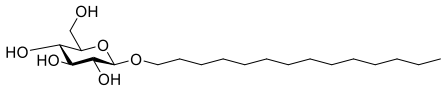

56

Prepared as per Procedure B using glucopyranoside **16** (0.32 g, 0.6 mmol, 1.0 equiv.), Na_2CO_3 (5.00 mg, 0.1 mmol, 0.08 equiv.) in MeOH (4.5 mL). Reaction time: 2 h. The crude was crystallised in a small amount of hot MeOH to afford the product **56** as a white solid (0.21 g, 0.6 mmol, 93 %).

R_f = 0.33 EtOAc (100 %); **^{1}H NMR (400 MHz, MeOD):** δ 4.26 (d, $^3J_{H1\text{-}H2}$ = 7.8 Hz, 1H, H-1), 3.94 – 3.84 (m, 2H, H-6a, H-1a'), 3.68 (dd, $^2J_{H6b\text{-}H6a}$ = 11.9 Hz, $^3J_{H6b\text{-}H5}$ = 5.3 Hz, 1H, H-6b), 3.54 (dt, $^2J_{H1b'\text{-}H1a'}$ = 9.4 Hz, $^3J_{H1b'\text{-}CH2(2')}$ = 6.7 Hz, 1H, H-1b'), 3.32-3.31 (m, 1H, H-3), 3.30 – 3.26 (m, 2H, H-4, H-5), 3.18 (t, $^3J_{H2\text{-}H1/H3}$ = 8.4 Hz, 1H, H-2), 1.68 – 1.58 (m, 2H, $CH_{2(2')}$), 1.41 – 1.25 (m, 22H, CH_2), 0.91 (t, $^3J_{CH3(14')\text{-}CH2(13')}$ = 6.8 Hz, 3H, $CH_{3(14')}$); **^{13}C NMR (101 MHz, MeOD):** δ 104.3 (C-1), 78.1 (C-3), 77.9 (C-4 or C-5), 75.1 (C-2), 71.6 (C-4 or C-5), 70.9 (C-1'), 62.7 (C-6), 33.0 (CH_2), 30.7 (CH_2), 30.7 (CH_2), 30.7 (CH_2), 30.7 (CH_2), 30.6 (CH_2), 30.4 (CH_2), 27.1 (CH_2), 23.7 (CH_2), 14.4 (C-14'). **HRMS** *m/z* (ESI^-) found $(M\text{-}H)^-$ 375.2749, $C_{20}H_{39}O_6$ required 375.2752 NMR data were in agreement with published literature.[332]

6.3 Synthesis of azido alcohols

6.3.1 4-azido-butan-1-ol **87**

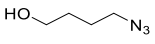

87

NaN_3 (1.19 g, 18.3 mmol, 1.4 equiv.) was added to a solution of 4-bromobutanol **85** (2.00 g, 13.1 mmol, 1.0 equiv.) in H_2O/THF (1:1 *v*/*v*, 10 mL). The resulting mixture was stirred for 26 h at 50 °C. The reaction was then cooled to rt and extracted with Et_2O (3 × 10 mL). The combined organic layers were dried over $MgSO_4$ and concentrated under reduced pressure to afford azide **87** as a colourless oil (0.67 g, 5.8 mmol, 44%). The crude material was used without further purification.

R_f = 0.11 Pet. Ether/EtOAc (7:3); **^{1}H NMR (400 MHz, $CDCl_3$):** δ 3.69 (t, $^3J_{H4\text{-}H3}$ = 6.1 Hz, 2H, H-4), 3.33 (t, $^3J_{H1\text{-}H2}$ = 6.4 Hz, 2H, H-1), 1.79 – 1.59 (m, 4H, H-2, H-3); **^{13}C NMR (101 MHz, $CDCl_3$):** δ 62.2 (C-4), 51.3 (C-1), 29.8 (C-2), 25.4 (C-3). These data were in agreement with published literature.[333]

6.3.2 5-azido-pentan-1-ol **88**

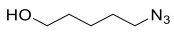

88

NaN_3 (1.19 g, 18.3 mmol, 1.4 equiv.) was added to a solution of 5-bromopentanol **86** (2.18 g, 13.1 mmol, 1.0 equiv.) in H_2O/THF (1:1 *v*/*v*, 10 mL). The resulting mixture was stirred for 26 h at 50 °C. The reaction was then cooled to rt and extracted with Et_2O (3 × 10 mL). The combined organic layers were dried over $MgSO_4$ and concentrated under reduced pressure to afford azide **88** as a colourless oil (1.27 g, 9.8 mmol, 75 %). The crude material was used without further purification.

R_f = 0.16 Pet.Ether/EtOAc (3:2); **^{1}H NMR (400 MHz, $CDCl_3$):** δ 3.81 – 3.71 (t, $^3J_{H5\text{-}H4}$ = 6.7 Hz, 2H, H-5), 3.66 (t, $^3J_{H1\text{-}H2}$ = 6.4 Hz, 2H, H-1), 1.71 – 1.56 (m, 4H, H-2, H-4), 1.51 – 1.38 (m, 2H, H-3); **^{13}C NMR (101 MHz, $CDCl_3$):** δ 62.6 (C-5), 51.3 (C-1), 32.1 (C-2), 28.6 (C-4), 22.9 (C-3). These data were in agreement with published literature.[334]

6.4 Synthesis of azido aldehyde

6.4.1 4-azido-butan-1-al **98**

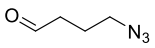

98

The solution of azido alcohol **87** (100.00 mg, 0.9 mmol, 1.0 equiv.) and Dess-Martin periodinane (0.48 g, 1.1 mmol, 1.3 equiv.) in $DCM_{(anh)}$ (2 mL) was stirred at rt and followed by TLC until completion (2 h). The reaction mixture was diluted with EtOAc (15 mL), followed by saturated $NaHCO_3$ (5 mL), and quenched by saturated solution of $Na_2S_2O_3$ (5 mL). The solution was stirred for 10 min. The aqueous phase was extracted with EtOAc (3 × 15 mL). The combined organic phases were washed with saturated solution $NaHCO_3$ (3 × 15 mL), saturated solution $Na_2S_2O_3$ (2 × 15 mL) and brine (20 mL) and

dried over $MgSO_4$. After filtration, the filtrate was concentrated under reduced pressure to afford product **98** (0.05 g, 0.4 mmol, 54 %). The crude material was used without further purification.

R_f = 0.12 Pet. Ether/Et_2O (1:1); **^{1}H NMR (400 MHz, $CDCl_3$):** δ 9.80 (t, $^3J_{H1\text{-}H2}$ = 1.2 Hz, 1H, H-1), 3.33 (t, $^3J_{H4\text{-}H3}$ = 6.5 Hz, 2H, H-4), 2.58 (td, $^3J_{H2\text{-}H3}$ = 7.1 Hz, $^3J_{H2\text{-}H1}$ = 1.2 Hz, 2H, H-2), 1.97 – 1.87 (m, 2H, H-3); **^{13}C NMR (101 MHz, $CDCl_3$):** δ 202.2 (C=O), 50.6 (C-4), 40.9 (C-2), 22.7 (C-3). These data were in agreement with published literature.[223]

6.4.2 5-azido-pentan-1-al **99**

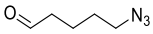

99

The solution of azido alcohol **88** (100.00 mg, 0.8 mmol, 1.0 equiv.) and Dess-Martin periodinane (0.43 g, 1.0 mmol, 1.3 equiv.) in $DCM_{(anh)}$ (2 mL) was stirred at rt and followed by TLC until completion (1 h). The reaction mixture was diluted with EtOAc (10 mL), followed by saturated $NaHCO_3$ (5 mL), and quenched by saturated solution of $Na_2S_2O_3$ (5 mL). The solution was stirred for 10 min. The aqueous phase was extracted with EtOAc (3 × 15 mL). The combined organic phases were washed with saturated solution $NaHCO_3$ (3 × 15 mL), saturated solution $Na_2S_2O_3$ (2 × 15 mL) and brine (20 mL) and dried over $MgSO_4$. After filtration, the filtrate was concentrated under reduced pressure to afford product **99** (58.00 mg, 0.4 mmol, 57 %). The crude material was used without further purification.

R_f = 0.28 Pet. Ether/EtOAc (5:1); **^{1}H NMR (400 MHz, $CDCl_3$):** δ 9.79 (t, $^3J_{H1\text{-}H2}$ = 1.5 Hz, 1H, H-1), 3.36 – 3.24 (m, 2H, H-5), 2.54 – 2.46 (m, 2H, H-2), 1.83 – 1.55 (m, 4H, H-3, H-4); **^{13}C NMR (101 MHz, $CDCl_3$):** δ 201.7 (C=O), 50.9 (C-5), 43.2 (C-2), 29.6 (C-3 or C-4), 19.2 (C-3 or C-4). These data were in agreement with published literature.[223]

6.5 Procedure for biotransformation of alkyl alcohols

6.5.1 Procedure for biotransformation of primary alcohols – in solution

AcCO6 CFE was diluted to 50 mg.mL^{-1} with deionised water. Biotransformations were carried out with 500 µL enzyme reaction in a 1.5 mL centrifuge tube containing KPi pH 7.0 (100 mM) and catalase (0.04 mg.mL^{-1}). Alcohol substrates **28-34,85-95** were added either from a 1.0 M solution made up in DMSO (Sigma). Typically, reactions were incubated at 37 °C, 200 rpm for 24 h. Biotransformations were extracted with EtOAc (2 × 500 µL) and vortexed. Samples were centrifuged at 17968 *g* for 10 min to separate the phases and the organic phase was analysed by GC-FID.

6.5.2 Procedure for biotransformation of alkyl alcohols – solid supported

6.5.2.1 Biotransformation with AcCO6 immobilised on Purolite Lifetech™ (ECR8285, ECR8309F)

The solid supported AcCO6 on ECR8285 (100 mg) or ECR8309F (40 mg) was suspended in a reaction buffer (500 µL) containing KPi pH 7.0 (100 mM), 1-octanol **28** (40 mM) and catalase (0.1 mg.mL^{-1}, CFE) in a 1.5 mL centrifuge tube. The reaction was incubated at 37 °C, 200 rpm for 24 h. Reactions were quenched by pipetting out the reaction solution in a 1.5 mL centrifuge tube while solid supported AcCO6 remained in the 1.5 mL centrifuge tube. The liquid phase was extracted with EtOAc (2 × 500 µL). The combined organic layers were analysed by GC-FID. For comparison of activity, reactions containing equal quantities of soluble enzyme and substrate were performed according procedure 6.5.1, analysed simultaneously and compared to the immobilisates.

6.5.2.2 Biotransformation with AcCO6 immobilised on EziG™ Amber

The solid supported AcCO6 on EziG™ Amber (20 mg) was suspended in a reaction buffer (500 µL) containing KPi pH 7.0 (100 mM), 1-octanol **28** (40 mM) and catalase (0.1 mg.mL^{-1}, CFE) in a 1.5 mL centrifuge tube. The reaction was incubated at 37 °C, 200 rpm for 24 h. Reactions were quenched by pipetting the reaction solution in a 1.5 mL centrifuge tube while solid supported AcCO6 remained in the 1.5 mL centrifuge tube. The liquid phase was extracted with EtOAc (2 × 500 µL). The combined

organic layers were analysed by GC-FID. For comparison of activity, reactions containing equal quantities of soluble enzyme and substrate were performed according procedure 6.5.1, analysed simultaneously and compared to the immobilisates.

6.6 Procedure for solid support synthesis

6.6.1 Preparation of amine-based resin

On analytical scale (0.5–1.0 mL), a 1.5 mL centrifuge tube, resins **66** (40 mg, 0.06 mmol, 60 mM) and **67** (40 mg, 0.08 mmol, 80 mM) were each placed in a clean vial (1.5 mL) and swollen in DMF (1.0 mL) without shaking at rt for a minimum of 3 h each. DMF was pipetted out. Resin beads were rinsed by pipetting with DCM (2 × 1.0 mL) to remove the excess of DMF.

6.6.2 Sequestration alkyl aldehydes with resin 66 or 67

On analytical scale (0.5–1.0 mL), aldehyde **35-41** (40.0 µmol, 1.0 equiv., 40 mM) or bio-oxidised alcohol according to procedure 6.5 **28-31** (40.0 µmol, 1.0 equiv., 40 mM) was added to a 1.5 mL centrifuge tube containing swollen resin **66** (40 mg, 60.0 µmol, 1.5 equiv., 120 mM) or **67** (40 mg, 80.0 µmol, 2.0 equiv., 160 mM). Deionised water was added for a total volume of 500 µL. The mixture was shaken from rt to 37 °C in an incubator 200 rpm or on carrousel 30 rpm from 1 h to 4 days. Once complete, the aqueous solution was transferred by pipetting to a clean 1.5 mL centrifuge tube and extracted with EtOAc (2 × 500 µL). The combined organic phases were analysed by GC-FID. The resin was rinsed with deionised water and methanol, dried under vacuum and analysed by IR spectroscopy.

6.6.3 Procedure for biotransformation of alkyl alcohols with AcCO6 CFE on amine-solid supported in presence of alkyl monoglucoside 53

In a 15 mL centrifuge tube, a mixture AMG-C_8/C_8OH **53**/**28** (50 mg, 9:1 %*w*/*w*, C_8OH: 5 mg, 0.04 mmol, 20 mM) was incubated with AcCO6 (110 mg.mL^{-1}, CFE), KPi pH 7.0 (100 mM) and catalase (0.04 mg.mL^{-1}, CFE) for a total reaction volume of 2.0 mL. The reaction was incubated 200 rpm at 37 °C for 3 days. The oxidation of alcohol to aldehyde was followed by analysing 100 µL of the reaction

solution by GC-FID. The reaction was neutralised with 5.0 M NaOH (C_f = 0.24 M), followed by filtration trough a filter paper (95 × 110 mm, Fisherbrand®) and ultrafiltration using 10k MWCO Amicon Ultra-15.

In a 15 mL centrifuge tube, aminomethyl polystyrene resin **67** (0.50 g, 1.0 mmol, 26.0 equiv., 100 mM) was swelled in DMF (10 mL) overnight. DMF was removed by pipetting and the resin was washed by pipetting with DCM (3 × 10 mL). The filtrate from ultrafiltration was added to the resin and the mixture incubated on a rotating carrousel 30 rpm for 4.5 h. The resin beads were filtered, rinsed with deionised water then methanol, dried under vacuum and analysed by IR. The resulting filtrate was purified by column chromatography (Pet. Ether/EtOAc 1:1, 1:9, then EtOAc/MeOH, 1:0, 9:1). The product was concentrated under reduced pressure, diluted with deionised water and freeze dried overnight before being analysed by NMR. The desired product was afforded as a white solid (28 mg, **53** recovered 50 %) in presence of unassigned impurity **80** (**53**/**82** 4:1).

Impurity **80**: **^{1}H NMR (D_2O, 400 MHz):** δ 7.53 (dd, *J* = 7.7 Hz, *J* = 0.9 Hz, 1H, Ha), 5.80 (dd, *J* = 7.7 Hz, *J* = 0.9 Hz, 1H, Hb); **^{13}C NMR (100 MHz, D_2O):** δ 143.5 (Ca), 101.2 (Cb).

6.6.4 Procedure for biotransformation of alkyl alcohols with immobilised AcCO6 on amine-solid supported

On analytical scale (0.5–1.0 mL), the solid supported AcCO6 was suspended in a reaction buffer (500 µL) containing KPi pH 7.0 (100 mM), 1-octanol **28** (40.0 µmol, 1.0 equiv., 40 mM) and catalase (0.1 mg.mL^{-1}, CFE) in a 1.5 mL centrifuge tube. The reaction was incubated at 37 °C, 200 rpm for 24 h. Reaction was extracted with EtOAc (2 × 500 µL) centrifuged 14900 × *g* for 5 min. The combined organics was analysed and conversion to the corresponding aldehyde was determined by GC-FID. For comparison of activity, reactions containing equal quantities of soluble enzyme and substrate were performed as described in procedure 6.5.1, worked up and analysed simultaneously and compared to the immobilisates.

6.6.5 Procedure for biotransformation of alkyl alcohols with immobilised AcCO6 on amine-solid supported with Rotating Bed Reactor (RBR)

On 650 mL scale reaction, aminomethyl resin **67** (7.00 g, 14.0 mmol, 1.5 equiv., 0.47 M) was swollen in DMF 30 mL for 3 h at rt. Resin **67** was filtered through filter paper and rinsed with DCM (2 × 15 mL).

Mixture **81** (APG/alcohols 1:1 %*w/w*, 2.50 g mixture containing 1.25 g of alcohols (9.6 mmol, 1.0 equiv., ≈30 mM)) or mixture **82** (APG/alcohols 99:1 %*w/w*, 5.00 g mixture containing 0.59 g of alcohols (4.5 mmol, 1.0 equiv., ≈7 mM)) was added in 1 L flange flask. Buffer 100 mM KPi (pH 7.0) and deionised water were added for a final volume 650 mL. The solid supported AcCO6 on ECR8285 (5.0 g) was loaded in two RBR cartridges in equal amount. Similarly, 20 mM aminomethyl resin **67** (7.00 g, 14.0 mmol, 1.5 equiv.) was loaded in two RBR cartridges in equal amount. Cartridges were placed in RBR reactor alternating cartridge of immobilised protein and cartridge of aminomethyl resin **67**. The RBR was placed in the mixture solution where the top of the flange flask was covered of aluminium foil. The reaction was stirred at 37 °C, 200 rpm for 16 h. RBR was removed from the mixture. The solution was concentrated under reduced pressure to afford a crude syrup. 100 µL of EtOAc was added to the crude for a small extraction and was pipetted out to be analysed by GC-FID. The crude was freeze dried and analysed by NMR (MeOD, ^{1}H, ^{31}P). Aminomethyl resin **67** was rinsed with deionised water and MeOH. Resin **67** was air dried and analysed by IR.

To remove excess of phosphate salt, crude **81** was extracted with EtOAc (50 mL × 10). Organic phases were gathered, dried over $MgSO_4$ filtered and concentrated under reduced pressure to afford final APGs **81.** The final product **81** was analysed by NMR (MeOD, ^{1}H, ^{31}P). For further purification, APGs **81** was purified by column chromatography (Hexane/EtOAc, 1:0, 1:1, 1:3, then EtOAc/MeOH 9:1, and DCM/MeOH, 8:2) afforded pure APGs product **81** (138 mg, recovery: 11 %).

6.7 Gas Chromatography

6.7.1 GC-FID methods

Method A: The method used was carried out with a GC-7820A apparatus (Agilent Technologies) equipped with a flame ionization detector (FID) and a HP5 column (Agilent) with dimensions 30 m × 0.320 mm × 0.25 µm with a flow of 2 $mL.min^{-1}$ He, oven at 70 °C with a ramp to 20 $°C.min^{-1}$ to 200 °C hold for 5 min detector temperature 300 °C and injector temperature 250 °C.

Method B: The method used was carried out with a GC-2010Plus apparatus (Shimadzu Technologies) equipped with (FID) on a DB-1 column (Agilent) with dimensions 60 m × 0.320 mm × 5.00 µm with a flow of 1.41 $mL.min^{-1}$ H_2, oven at 50 °C with a ramp to 20 $°C.min^{-1}$ to 300 °C hold for 5 min detector temperature 325 °C and injector temperature 200 °C.

Method C: The method used was carried out with a GC-7820A apparatus (Agilent Technologies) equipped with a flame ionization detector (FID) and a HP5 column (Agilent) with dimensions 30 m × 0.320 mm × 0.25 µm with a flow of 2 $mL.min^{-1}$ He, oven at 70 °C with a ramp to 10 $°C.min^{-1}$ to 200 °C hold for 5 min detector temperature 300 °C and injector temperature 250 °C.

Method D: The method used was carried out with a GC-7820A apparatus (Agilent Technologies) equipped with a flame ionization detector (FID) and a HP5 column (Agilent) with dimensions 30 m × 0.320 mm × 0.25 µm with a flow of 2 $mL.min^{-1}$ He, oven at 70 °C with a ramp to 5 $°C.min^{-1}$ to 200 °C hold for 5 min detector temperature 300 °C and injector temperature 250 °C.

6.7.2 Data processing

6.7.2.1 Standard error

All samples were analysed in triplicate. The error of each sample was calculated as standard error (*Equation 6*) where n equals the samples size, x was the observed initial rate value for each sample and $\tilde{x}$ was the mean rate value for each sample.

Equation 9 - Standard error in initial rate obtained for each sample

$$standard\ error = \sqrt{\frac{\sum(x - \bar{x})^2}{(n-1)}}$$

6.7.2.2 Data processing for analyte measurements

Equation 10- Determination of alcohol conversion measured by GC-FID

$$Alcohol\ conversion\ (\%) = 100\% \times \frac{peak\ area\ of\ products\ detected\ (pA * s)}{total\ area\ of\ analytes\ integrated\ (pA * s)}$$

$$= 100\% \times \frac{peak\ area\ of\ (aldehyde + carboxylic\ acid)\ detected\ (pA * s)}{total\ peak\ area\ of\ starting\ material\ and\ products\ detected\ (pA * s)}$$

Where peak area is measured by picoamperes per second (pA*s). When peak height is measured <20 pA on the chromatogram, the analyte is considered to be a trace amount in the sample.

6.8 Synthesis of aliphatic alkenes

6.8.1 Procedure C: Wittig reaction to alkene ester from aldehyde

As described in the literature,[5] aldehyde (1.0 equiv.) and methyl (triphenylphosphoranylidene)acetate (1.2–1.5 equiv.) were placed in 10 mL round bottom flask. Deionised water (5.0 mL) was added. The reaction mixture was stirred at rt for 1.5-2 h and followed by TLC until completion. The aqueous phase was extracted with DCM (3 × 10 mL). The combined organic layers were dried over $MgSO_4$ and concentrated under reduced pressure. The crude was purified *via* automated flash chromatography (Hexane/EtOAc 1:0, 9:1, 0:1).

6.8.2 Procedure D: Wittig reaction to alkene ester from aliphatic alcohol

In a 50 mL Falcon™ tube, the alcohol substrate (1.0 equiv.) was placed followed by addition of methyl (triphenylphosphoranylidene)acetate **116** (1.5–3.0 equiv.), 40 $mg.mL^{-1}$ AcCO6 (CFE), 0.04 $mg.mL^{-1}$ catalase (CFE), 100 mM KPi (pH 7.0) and deionised water to reach a total volume reaction of 20 mL. The tube was capped, and the content was shaken in an incubator 200 rpm at 37 °C from 5 to 24 h. The reaction solution was quenched with 5.0 M HCl (C_f = 0.23 M). The aqueous phase was extracted

with EtOAc (3 × 20 mL) and centrifuge 3024 × *g* for 10 min. After removal of the solvent *in vacuo*, the crude material was dried under reduced pressure and the ratio of isomers *E/Z* was determined by ^{1}H NMR spectroscopy on the crude material. The crude product was subsequently purified by column chromatography.

6.8.3 Procedure E: Wittig reaction to alkene nitrile from alcohol

In a 50 mL Falcon™ tube, the alcohol substrate (1.0 equiv.) was placed followed by addition of 40 mg.mL^{-1} AcCO6 (CFE), 0.04 mg.mL^{-1} catalase (CFE), 100 mM KPi (pH 7.0) and deionised water to reach 20 mL. The tube was capped, and the content was shaken in incubator 200 rpm at 37 °C. After 5 h, (cyanomethyl)triphenylphosphonium chloride **125** (3.0-7.0 equiv.) was added with a solution of 1.0 M NaOH (15 equiv.). The reaction mixture was shaken in incubator 200 rpm at 37 °C overnight. The reaction mixture was quenched with 5.0 M HCl (C_f = 0.23 M). The aqueous phase was extracted with EtOAc (3 × 20 mL) and centrifuge 3024 × *g* for 10 min. After removal of the solvent *in vacuo*, the crude material was dried under reduced pressure and the ratio of isomers *E/Z* was determined by ^{1}H NMR spectroscopy on the crude material. The crude product was subsequently purified by column chromatography.

6.8.4 Methyl (*E*)-7-chlorohept-2-enoate 118

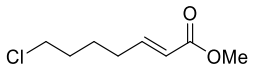

118, *E/Z* 99:1

Prepared as per Procedure D using 5-chloropentanol **90** (50.00 mg, 0.4 mmol, 1.0 equiv.) with methyl (triphenylphosphoranylidene)acetate **116** (0.40 g, 1.2 mmol, 3.0 equiv.). Reaction time: 5.5 h. Final ratio *E/Z* 99:1. Purification by column chromatography (Pet. Ether/Et_2O, 1:0, 9:1) afforded the product **118** as a yellow oil (68.00 mg, 0.4 mmol, 97 %).

R_f = 0.60 Pet. Ether/ Et_2O (1:1); **(*E*)-isomer: ^{1}H NMR (400 MHz, $CDCl_3$):** δ 6.94 (ddt, $^{3}J_{H3\text{-}H2}$ = 15.7 Hz, $^{3}J_{H3\text{-}H4}$ = 6.9 Hz 1H, H-3), 5.84 (dt, $^{3}J_{H2\text{-}H3}$ = 15.6 Hz, $^{4}J_{H2\text{-}H4}$ = 1.6 Hz, 1H, H-2), 3.73 (s, 3H, OCH_3), 3.54 (t, $^{3}J_{H7\text{-}H6}$ = 6.5 Hz, 2H, H-7), 2.24 (ddd, $^{3}J_{H4\text{-}H3/H5}$ = 7.2 Hz, $^{3}J_{H4\text{-}H2}$ = 1.8 Hz, 2H, H-4), 1.84 – 1.76 (m, 2H,

H-6), 1.68 – 1.58 (m, 2H, H-5); **^{13}C NMR (101 MHz, $CDCl_3$):** δ 186.7 (C=O), 125.5 (C-3), 121.4 (C-2), 51.4 (OCH_3), 44.5 (C-7), 31.8 (C-4), 31.3 (C-6), 25.2 (C-5). These data were in agreement with published literature.[298] **HMRS** *m/z* (ESI$^+$) found $(M+H)^+$ 177.0677, $C_8H_{13}ClO_2H$ required 177.6077. **(*Z*)-isomer: ^{1}H NMR (400 MHz, $CDCl_3$):** δ 6.22 (dt, $^3J_{H3\text{-}H2}$ = 11.5 Hz, $^3J_{H3\text{-}H4}$ = 7.5 Hz, 1H), 5.89 – 5.77 (m, 1H, H-2), 3.71 (s, 3H, OCH_3), 3.56 (t, $^3J_{H7\text{-}H6}$ = 6.5 Hz, 2H, H-7), 2.70 (qd, $^3J_{H4\text{-}H3/H5}$ = 7.5 Hz, $^3J_{H4\text{-}H2}$ = 1.7 Hz, 2H, H-4), 1.85 – 1.76 (m, 2H, H-6), 1.67 – 1.57 (m, 2H, H-5); **^{13}C NMR (101 MHz, $CDCl_3$):** δ 166.7 (C=O), 149.7 (C-3), 119.9 (C2), 51.0 (OCH_3), 44.7 (C-7), 32.0 (C-6), 28.0 (C-4), 26.1 (C-5). These data were in agreement with published literature.[298]

6.8.5 Methyl (*E*)-dec-2-enoate **119**

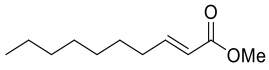

119, *E/Z* 94:6

Prepared as per Procedure D using octanol **28** (104.00 mg, 0.8 mmol, 1.0 equiv.) and methyl (triphenylphosphoranylidene)acetate **116** (0.53 g, 1.6 mmol, 2.0 equiv.). Reaction time: 23 h. Final ratio *E/Z* 94:6. Purification by column chromatography (Pet. Ether/Et_2O, 1:0, 8:2) afforded the product **119** as a white solid (129.00 mg, 0.7 mmol, 88 %).

R_f = 0.60 Pet. Ether/ Et_2O (1:1); **^{1}H NMR (400 MHz, $CDCl_3$):** δ 6.97 (dt, $^3J_{H3\text{-}H2}$ = 15.6 Hz, $^3J_{H3\text{-}H4}$ = 7.0 Hz, 1H, H-3), 5.82 (dt, $^3J_{H2\text{-}H3}$ = 15.6 Hz, $^4J_{H2\text{-}H4}$ = 1.6 Hz, 1H, H-2), 3.73 (s, 3H, OCH_3), 2.19 (qd, $^3J_{H4\text{-}H3/H5}$ = 7.2 Hz, $^4J_{H4\text{-}H2}$ = 1.6 Hz, 2H, H-4), 1.52 – 1.39 (m, 2H, H-5), 1.32 – 1.20 (m, 8H, CH_2), 0.90 – 0.86 (m, 3H, H-10); **^{13}C NMR (101 MHz, $CDCl_3$):** δ167.2 (C=O), 149.8 (C-3), 120.8 (C-2), 51.3 (OCH_3), 32.2 (C-4), 31.7 (CH_2), 29.1 (CH_2), 29.0 (CH_2), 28.0 (C-5), 22.6 (CH_2), 14.0 (C-10). These data were in agreement with published literature.[335]

6.8.6 Methyl (*E*)-undec-2-enoate **120**

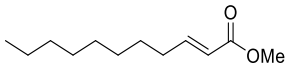

120, *E/Z* 88:12

Prepared as per Procedure D using nonanol **29** (58.00 mg, 0.4 mmol, 1.0 equiv.) and methyl (triphenylphosphoranylidene)acetate **116** (0.27 g, 0.8 mmol, 2.0 equiv.). Reaction time: 23 h. Final ratio *E/Z* 88:12. Purification by column chromatography (Pet. Ether/Et_2O, 1:0, 8:2) afforded the product **120** as a colourless oil (41.00 mg, 0.2 mmol, 52 %).

R_f = 0.60 Pet. Ether/ Et_2O (1:1); **^{1}H NMR (400 MHz, $CDCl_3$):** δ 6.97 (dt, $^3J_{H3\text{-}H2}$ = 15.6 Hz, $^3J_{H3\text{-}H4}$ = 7.0 Hz, 1H, H-3), 5.82 (dt, $^3J_{H2\text{-}H3}$ = 15.6 Hz, $^4J_{H2\text{-}H4}$ = 1.6 Hz, 1H, H-2), 3.72 (s, 3H, OCH_3), 2.19 (qd, $^3J_{H4\text{-}H3/H5}$ = 7.1 Hz, $^4J_{H4\text{-}H2}$ = 1.6 Hz, 2H, H-4), 1.54 – 1.38 (m, 2H, H-5), 1.37 – 1.19 (m, 10H, CH_2), 0.93 – 0.84 (m, 3H, CH_3, H-11); **^{13}C NMR (101 MHz, $CDCl_3$):** δ 167.2 (C=O), 149.8 (C-3), 120.8 (C-2), 51.3 (OCH_3), 32.2 (C-4), 31.8 (CH_2), 29.3 (CH_2), 29.2 (CH_2), 29.1 2 (CH_2), 28.0 (C-5), 22.6 (CH_2), 14.1 (C-11). These data were in agreement with published literature.[336] **HMRS** *m/z* (ESI$^+$) found $(M+NH_4)^+$ 216.1960, $C_{12}H_{22}O_2NH_4$ required 216.1958.

6.8.7 Methyl (*E*)-dodeca-2-enoate **121**

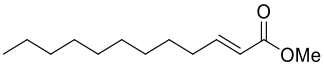

121, *E/Z* 86:14

Prepared as per Procedure D using decanol **30** (63.00 mg, 0.4 mmol, 1.0 equiv.) and methyl (triphenylphosphoranylidene)acetate **116** (0.20 g, 0.6 mmol, 1.5 equiv.). Reaction time: 22 h. Final ratio *E/Z* 86:14. Purification by column chromatography (Pet. Ether/Et_2O, 1:0, 8:2) afforded the product **121** as a colourless oil (13.00 mg, 0.1 mmol, 35 %).

R_f = 0.60 Pet. Ether/ Et_2O (1:1); **^{1}H NMR (400 MHz, $CDCl_3$):** δ 6.97 (dt, $^3J_{H3\text{-}H2}$ = 15.6 Hz, $^4J_{H3\text{-}H4}$ = 7.0 Hz, 1H, H-3), 5.82 (dt, $^3J_{H2\text{-}H3}$ = 15.6 Hz, $^4J_{H2\text{-}H4}$ = 1.6 Hz, 1H, H-2), 3.71 (s, 3H, OCH_3), 2.19 (qd, $^3J_{H4\text{-}H3/H5}$ = 7.2 Hz, $^4J_{H4\text{-}H2}$ = 1.6 Hz, 2H, H-4), 1.54 – 1.38 (m, 2H, H-5), 1.27 (m, 12H), 0.93 – 0.79 (m, 3H, CH_3, H-12);

^{13}C NMR (101 MHz, $CDCl_3$): δ 167.2 (C=O), 149.8 (C-3), 120.8 (C-2), 51.3 (OCH_3), 32.2 (C-4), 31.8 (CH_2), 29.4 (CH_2), 29.4 (CH_2), 29.3 (CH_2), 29.1 (CH_2), 28.0 (C-5), 22.6 (CH_2), 14.1 (C-12). These data were in agreement with published literature.[291] **HMRS** *m/z* (ESI$^+$) found $(M+H)^+$ 213.1850, $C_{13}H_{24}O_2Na^+$ required 213.1849.

6.8.8 Methyl (*E/Z*)-trideca-2-enoate **122**

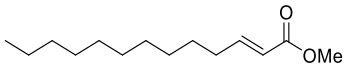

122, *E/Z* 93:7

Prepared as per Procedure C using undecanal **38** (170.00 mg, 1.0 mmol, 1.0 equiv.) and methyl (triphenylphosphoranylidene)acetate **116** (0.50 g, 1.5 mmol, 1.5 equiv.). Reaction time: 1.5 h. Final ratio *E/Z* 93:7. Purification by automated flash column chromatography afforded the product **122** as a white foam (156.00 mg, 0.7 mmol, 69 %).

R_f = 0.67 Hexane/EtOAc (6:4); **(*E*)-isomer: ^{1}H NMR (400 MHz, $CDCl_3$):** δ 6.97 (dt, $^3J_{H3\text{-}H2}$ = 15.6 Hz, $^4J_{H3\text{-}H4}$ = 7.0 Hz, 1H, H-3), 5.82 (dd, $^3J_{H2\text{-}H3}$ = 15.6 Hz, $^4J_{H2\text{-}H4}$ = 0.6 Hz, 1H, H-2), 3.72 (s, 3H, OCH_3), 2.19 (broad q, $^3J_{H4\text{-}H3/H5}$ = 7.2 Hz, 2H, H-4), 1.50 – 1.41 (m, 2H, H-5), 1.28-1.25 (m, 19H), 0.88 (t, $^3J_{H13\text{-}H12}$ = 6.7 Hz, 3H, CH_3, H-13); **^{13}C NMR (101 MHz, $CDCl_3$):** δ 167.1 (C=O), 149.8 (C-3), 120.7 (C-2), 51.2 (OCH_3), 32.2 (C-4), 31.8 (CH_2), 29.5 (CH_2), 29.4 (CH_2), 29.3 (CH_2), 29.2 (CH_2), 29.0 (CH_2), 28.0 (C-5), 22.6 (CH_2), 14.1 (C-13). These data were in agreement with published literature.[337] **(*Z*)-isomer: ^{1}H NMR (400 MHz, $CDCl_3$):** δ 6.23 (dt, $^3J_{H3\text{-}H2}$ = 11.5 Hz, $^3J_{H3\text{-}H4}$ = 7.5 Hz, 1H, H-3), 5.79 – 5.72 (m, 1H, H-2), 3.70 (s, 3H, OCH_3), 2.65 (qd, $^3J_{H4\text{-}H3/H5}$ = 7.4 Hz, $^4J_{H4\text{-}H2}$ = 1.7 Hz, 2H, H-4). **^{13}C NMR (101 MHz, $CDCl_3$):** δ 166.8 (C=O), 150.9 (C-3), 119.0 (C-2), 50.8 (OCH_3).

6.8.9 Methyl (*E/Z*)-dodeca-2-enoate **123**

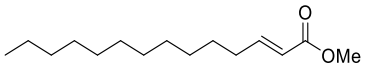

123, *E/Z* 92:8

Prepared as per Procedure C using dodecanal **39** (184 mg, 1.0 mmol, 1.0 equiv.) and methyl (triphenylphosphoranylidene)acetate (0.40 g, 1.2 mmol, 1.2 equiv.). Reaction time: 2 h. Crude ratio *E/Z* 92:8. Purification by automated flash column chromatography afforded the product **123** as a white foam (146.00 mg, 0.6 mmol, 61 %).

R_f = 0.75 Hexane/EtOAc (8:2); **(*E*)-isomer: ^{1}H NMR (400 MHz, $CDCl_3$):** δ 6.97 (dt, $^3J_{H3\text{-}H2}$ = 15.6 Hz, $^4J_{H3\text{-}H4}$ = 7.0 Hz, 1H, H-3), 5.82 (dt, $^3J_{H2\text{-}H3}$ = 15.6 Hz, $^4J_{H2\text{-}H4}$ = 1.5 Hz, 1H, H-2), 3.72 (s, 3H, OCH_3), 2.19 (qd, $^3J_{H4\text{-}H3/H5}$ = 7.2 Hz, $^4J_{H4\text{-}H2}$ = 1.4 Hz, 2H, H-4), 1.46–1.41 (m, 2H, H-5), 1.31-1.25 (m, 16H), 0.88 (t, $^3J_{H14\text{-}H13}$ = 6.8 Hz, 3H, CH_3, H-14); **^{13}C NMR (101 MHz, $CDCl_3$):** δ 167.1 (C=O), 149.7 (C-3), 120.7 (C-2), 51.2 (OCH_3), 32.1 (C-4), 31.8 (CH_2), 29.5 (CH_2), 29.5 (CH_2), 29.4 (CH_2), 29.3 (CH_2), 29.3 (CH_2), 29.1 (CH_2), 27.9 (C-5), 22.6 (CH_2), 14.0 (C-14). These data were in agreement with published literature.[335] **(*Z*)-isomer: ^{1}H NMR (400 MHz, $CDCl_3$):** δ 6.23 (dt, $^3J_{H3\text{-}H2}$ = 11.5 Hz, $^3J_{H3\text{-}H4}$ = 7.5 Hz, 1H, H-3), 5.76 (dt, $^3J_{H2\text{-}H3}$ = 11.5 Hz, $^4J_{H2\text{-}H4}$ = 1.8 Hz, 1H, H-2), 3.70 (s, 3H, OCH_3), 2.65 (qd, $^3J_{H4\text{-}H3}$ = 7.4 Hz, $^4J_{H4\text{-}H2}$ = 1.7 Hz, 2H, H-4); **^{13}C NMR (101 MHz, $CDCl_3$):** δ 166.8 (C=O), 151.0 (C-3), 119.1 (C-2), 50.9 (OCH_3).

6.8.10 Methyl (*E/Z*)-tetradeca-2-enoate **124**

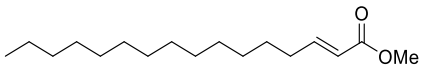

124, *E/Z* 9:1

Prepared as per Procedure C using tetradecanal **40** (212 mg, 1.0 mmol, 1.0 equiv.) and methyl (triphenylphosphoranylidene)acetate (0.52 g, 1.5 mmol, 1.5 equiv.). Reaction time: 2 h. Final ratio *E/Z* 9:1. Purification by automated flash column chromatography afforded the product **124** as a white foam (191.00 mg, 0.4 mmol, 40 %).

R_f = 0.75 Hexane/EtOAc (8:2); **(*E*)-isomer: ^{1}H NMR (400 MHz, $CDCl_3$):** δ 6.97 (dt, $^3J_{H3\text{-}H2}$ = 15.6 Hz, $^4J_{H3\text{-}H4}$ = 7.0 Hz, 1H, H-3), 5.82 (dt, $^3J_{H2\text{-}H3}$ = 15.6 Hz, $^4J_{H2\text{-}H4}$ = 1.6 Hz, 1H, H-2), 3.72 (s, 3H, OCH_3), 2.19 (qd, $^3J_{H4\text{-}H3/H5}$ = 7.2 Hz, $^4J_{H4\text{-}H2}$ = 1.5 Hz, 2H, H-4), 1.46–1.41 (m, 2H, H-5), 1.31-1.25 (m, 18H), 0.88 (t, $^3J_{H16\text{-}H15}$ = 6.8 Hz, 3H, CH_3, H-16); **^{13}C NMR (101 MHz, $CDCl_3$):** δ 167.1 (C=O), 149.7 (C-3), 120.7 (C-2), 51.3 (OCH_3), 32.2 (C-4), 31.9 (CH_2), 29.6 (CH_2), 29.6 (CH_2), 29.6 (CH_2), 29.5 (CH_2), 29.3 (CH_2), 29.3 (CH_2), 29.1 (CH_2), 27.9 (C-5), 22.6 (CH_2), 14.0 (C-16). These data were in agreement with published literature.[335] **(*Z*)-isomer: ^{1}H NMR (400 MHz, $CDCl_3$):** δ 6.23 (dt, $^3J_{H3\text{-}H2}$ = 11.5 Hz, $^3J_{H3\text{-}H4}$ = 7.5 Hz, 1H, H-3), 5.76 (dt, $^3J_{H2\text{-}H3}$ = 11.5 Hz, $^4J_{H2\text{-}H4}$ = 1.7 Hz, 1H, H-2), 3.70 (s, 3H, OCH_3), 2.65 (qd, $^3J_{H4\text{-}H3}$ = 7.5 Hz, $^4J_{H4\text{-}H2}$ = 1.7 Hz, 2H, H-4); **^{13}C NMR (101 MHz, $CDCl_3$):** δ 166.8 (C=O), 151.0 (C-3), 119.1 (C-2), 50.9 (OCH_3).

6.8.11 Methyl (*E*)-7-bromohept-2-enoate **127**

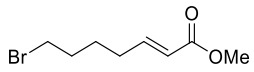

127, *E*/*Z* 99:1

Prepared as per Procedure D using 5-bromopentanol **86** (67.00 mg, 0.4 mmol, 1.0 equiv.) with methyl (triphenylphosphoranylidene)acetate **116** (0.27 g, 0.8 mmol, 2.0 equiv.). Reaction time: 5.5 h. Final ratio *E*/*Z* 99:1. Purification by column chromatography (Hexane/DCM, 1:0, 7:3, 3:2, 1:1, then DCM/MeOH; 8:2) afforded the product **127** as a colourless oil (75 mg, 0.3 mmol, 85 %).

R_f = 0.37 Hexane/DCM (1:1); **(*E*)-isomer: ^{1}H NMR (400 MHz, $CDCl_3$):** δ 6.95 (dt, $^3J_{H3\text{-}H2}$ = 15.7 Hz, $^3J_{H3\text{-}H4}$ = 6.9 Hz, 1H, H-3), 5.85 (dt, $^3J_{H2\text{-}H3}$ = 15.7 Hz, $^4J_{H2\text{-}H4}$ = 1.6 Hz, 1H, H-2), 3.73 (s, 3H, OCH_3), 3.41 (t, $^3J_{H7\text{-}H6}$ = 6.7 Hz, 2H, H-7), 2.25 (qd, $^3J_{H4\text{-}H3/5}$ = 7.2 Hz, $^4J_{H4\text{-}H2}$ = 1.6 Hz, 2H, H-4), 1.95 – 1.83 (m, 2H, H-6), 1.69 – 1.57 (m, 2H, H-5); **^{13}C NMR (101 MHz, $CDCl_3$):** δ 166.9 (C=O), 148.4 (C-3), 121.4 (C-2), 51.4 (OCH_3), 33.2 (C-7), 31.9 (C-6), 31.2 (C-4), 26.5 (C-5). **(Z)-isomer: ^{1}H NMR (400 MHz, $CDCl_3$):** δ 6.22 (dt, $^3J_{H3\text{-}H2}$ = 11.5 Hz, $^3J_{H3\text{-}H4}$ = 7.6 Hz, 1H, H-3), 5.81 (dt, $^3J_{H2\text{-}H3}$ = 11.5 Hz, $^4J_{H2\text{-}H4}$ = 1.7 Hz, 1H, H-2), 3.71 (s, 3H, OCH_3), 3.43 (t, $^3J_{H7\text{-}H6}$ = 6.7 Hz, 2H, H-7), 2.70 (qd, $^3J_{H4\text{-}H3/H5}$ = 7.5 Hz, $^4J_{H4\text{-}H2}$ = 1.7 Hz, 2H, H-4), 1.96 – 1.85 (m,

2H, H-6), 1.70 – 1.55 (m, 2H, H-5); **^{13}C NMR (101 MHz, $CDCl_3$):** δ 149.7 (C-3), 119.9 (C-2), 51.1 (OCH_3), 33.5 (C-7), 32.2 (C-6), 27.9 (C-4), 27.4 (C-5).

6.8.12 Methyl (*E*)-6-azido-hexa-2-enoate **128**

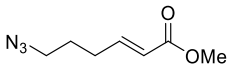

128, *E*/*Z* 97:3

Prepared as per Procedure D using 4-azidobutanol **87** (46.00 mg, 0.4 mmol, 1.0 equiv.) and methyl (triphenylphosphoranylidene)acetate **116** (0.27 g, 0.8 mmol, 2.0 equiv.). Reaction time: 5.5 h. Final ratio *E*/*Z* 97:3. Purification by column chromatography (Hexane/EtOAc, 7:3, 6:4, then DCM/MeOH 8:2) to afford product **128** as a yellow solid (35.00 mg, 0.2 mmol, 52 %).

R_f = 0.62 Hexane/EtOAc (1:1); **^{1}H NMR (400 MHz, $CDCl_3$):** δ 6.95 (dt, $^3J_{H3\text{-}H2}$ = 15.6 Hz, $^3J_{H3\text{-}H4}$ = 7.0 Hz, 1H, H-3), 5.84 (dt, $^3J_{H2\text{-}H3}$ = 15.6 Hz, $^4J_{H2\text{-}H4}$ = 1.6 Hz, 1H, H-2), 3.73 (s, 3H, OCH_3), 3.29 (t, $^3J_{H6\text{-}H5}$ = 6.5 Hz, 2H, H-6), 2.25 (qd, $^3J_{H4\text{-}H3/H5}$ = 7.1 Hz, $^4J_{H4\text{-}H2}$ = 1.6 Hz, 2H, H-4), 1.68 – 1.57 (m, 2H, H-5). **^{13}C NMR (101 MHz, $CDCl_3$):** δ 148.5 (C-3), 121.5 (C-2), 51.5 (OCH_3), 51.1 (C-6), 31.6 (C-4), 28.3 (C-5).

6.8.13 Methyl (*E*)-7-azido-hept-2-enoate **129**

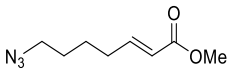

129, *E*/*Z* 99:1

Prepared as per Procedure D using 5-azidopentanol **88** (52.00 mg, 0.4 mmol, 1.0 equiv.) and methyl (triphenylphosphoranylidene)acetate **116** (0.27 g, 0.8 mmol, 2.0 equiv.). Reaction time: 5.5 h. Final ratio *E*/*Z* 99:1. Purification by column chromatography (Hexane/EtOAc, 7:3, then DCM/MeOH, 8:2) to afford the product **129** as a yellow oil (9.00 mg, 0.1 mmol, 13 %).

R_f = 0.62 Hexane/EtOAc (1:1); **^{1}H NMR (400 MHz, $CDCl_3$):** δ 7.00 – 6.88 (m, 1H, H-3), 5.84 (dt, $^3J_{H2\text{-}H3}$ = 15.6 Hz, $^4J_{H2\text{-}H4}$ = 1.6 Hz, 1H, H-2), 3.73 (s, 3H, OCH_3), 3.37 – 3.26 (m, 2H, H-7), 2.35 (td, $^3J_{H4\text{-}H3/5}$ = 7.5 Hz, $^4J_{H4\text{-}H2}$ = 1.7 Hz, 2H, H-4), 1.68 – 1.54 (m, 4H, H-5, H-6); **^{13}C NMR (101 MHz, $CDCl_3$):** δ167.2 (C=O),

149.8 (C-1), 121.5 (C-2), 51.5 (OCH_3), 51.1, 33.8 (C-7), 24.71 (C-4). **HMRS** *m/z* (ESI^+) found $(M+H)^+$ 184.1085, $C_8H_{14}N_3O_2^+$ required 184.1081.

6.8.14 Methyl (*E*)-6-chlorohex-2-enoate **130**

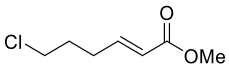

130, *E/Z* 99:1

Prepared as per Procedure D using 4-chlorobutanol **89** (108.00 mg, 1.0 mmol, 1.0 equiv.) with methyl (triphenylphosphoranylidene)acetate **116** (0.67 g, 2.0 mmol, 2.0 equiv.). Reaction time: 23 h. Final ratio *E/Z* 99:1. Purification by column chromatography (Hexane/DCM, 1:0, 8:2, 7:3, 1:1, then DCM/MeOH, 8:2) afforded the product **130** as a yellow oil (118.00 mg, 0.7 mmol, 73 %).

R_f = 0.47 Hexane/DCM (1:1); **(*E*)-isomer: ^{1}H NMR (400 MHz, $CDCl_3$):** δ 6.94 (dt, $^3J_{H3\text{-}H2}$ = 15.6 Hz, $^3J_{H3\text{-}H4}$ = 7.0 Hz, 1H, H-3), 5.88 (dt, $^3J_{H2\text{-}H3}$ = 15.7 Hz, $^4J_{H2\text{-}H4}$ = 1.6 Hz, 1H, H-2), 3.74 (s, 3H, OCH_3), 3.55 (t, $^3J_{H6\text{-}H5}$ = 6.4 Hz, 2H, H-6), 2.39 (qd, $^3J_{H4\text{-}H3/H5}$ = 7.2 Hz, $^4J_{H4\text{-}H2}$ = 1.6 Hz, 2H, H-4), 2.00 – 1.88 (m, 2H, H-5). **^{13}C NMR (101 MHz, $CDCl_3$):** δ 166.8 (C=O), 147.2 (C-3), 122.0 (C-2), 51.5 (OCH_3), 43.9 (C-6), 30.6 (C-5), 29.2 (C-4). These data were in agreement with published literature.[338] **(*Z*)-isomer: ^{1}H NMR (400 MHz, $CDCl_3$):** δ 6.22 (dt, $^3J_{H3\text{-}H2}$ = 11.5, $^3J_{H3\text{-}H4}$ = 7.6 Hz, 1H, H-3), 5.84 (dt, $^3J_{H2\text{-}H3}$ = 11.5 Hz, $^4J_{H2\text{-}H4}$ = 1.7 Hz, 1H, H-4), 3.72 (s, 3H, OCH_3), 3.56 (t, $^3J_{H6\text{-}H5}$ = 6.7 Hz, 2H, H-6), 2.81 (qd, $^3J_{H4\text{-}H3/H5}$ = 7.5, $^4J_{H4\text{-}H2}$ = 1.7 Hz, 2H, H-4), 2.00 – 1.88 (m, 2H, H-5). **^{13}C NMR (101 MHz, $CDCl_3$):** δ 166.6 (C=O), 148.9 (C-3), 120.5 (C-2), 51.1 (OCH_3), 44.3 (C-6), 31.9 (C-5), 26.4 (C-4). These data were in agreement with published literature.[338]

6.8.15 Methyl (*E*)-5-methylsulfanylpent-2-enoate **134**

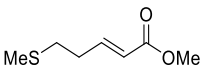

134, *E/Z* 87:13

Prepared as per Procedure D using 3-(methylthio)propanol **94** (42.00 mg, 0.4 mmol, 1.0 equiv.) with methyl (triphenylphosphoranylidene)acetate **116** (0.27 g, 0.8 mmol, 2.0 equiv.). Reaction time: 7 h.

Final ratio *E/Z* 87:13. Purification by column chromatography (toluene, 100 %) afforded the product **134** as a yellow oil (59.00 mg, 0.4 mmol, 92 %).

R_f = 0.40 Toluene/Acetone (8:2); **^{1}H NMR (400 MHz, $CDCl_3$):** δ 6.97 (dt, $^3J_{H3\text{-}H2}$ = 15.7 Hz, $^3J_{H3\text{-}H4}$ = 6.8 Hz, 1H, H-3), 5.89 (dt, $^3J_{H2\text{-}H3}$ = 15.7 Hz, $^4J_{H2\text{-}H4}$ = 1.5 Hz, 1H, H-2), 3.73 (s, 3H, OCH_3), 2.62 (m, 2H, H-5), 2.58 – 2.46 (m, 2H, H-4), 2.12 (s, 3H, SCH_3); **^{13}C NMR (101 MHz, $CDCl_3$):** δ 166.7 (C=O), 146.8 (C-1), 122.1 (C-0'), 51.4 (OCH_3), 32.4 (C-3), 31.8 (C-2), 15.5 (SCH_3). These data were in agreement with published literature.[339]

6.8.16 Methyl (*E*)-6-methylsulfanylhex-2-enaote **135**

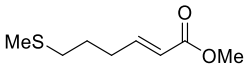

135, *E/Z* 87:13

Prepared as per Procedure D using 4-(methylthio)butanol **95** (48.00 mg, 0.4 mmol, 1.0 equiv.) with methyl (triphenylphosphoranylidene)acetate **116** (0.27 g, 0.8 mmol, 2.0 equiv.). Reaction time: 7 h. Final ratio *E/Z* 87:13. Purification by column chromatography (DCM, 100 %) afforded the product **135** as an orange oil (70.00 mg, 0.3 mmol, 71 %).

R_f = 0.40 Toluene/Acetone (8:2); **^{1}H NMR (400 MHz, $CDCl_3$):** δ 6.96 (dt, $^3J_{H3\text{-}H2}$ = 15.7 Hz, $^3J_{H3\text{-}H4}$ = 7.0 Hz, 1H, H-3), 5.86 (dt, $^3J_{H2\text{-}H3}$ = 15.7 Hz, $^3J_{H2\text{-}H4}$ = 1.6 Hz, 1H, H-2), 3.73 (s, 3H, OCH_3), 2.63 – 2.46 (m, 2H, H-6), 2.33 (dd, $^3J_{H4\text{-}H3/5}$ = 7.1 Hz, $^3J_{H4\text{-}H2}$ = 1.6 Hz, 2H, H-4), 2.09 (s, 3H, SCH_3), 1.88 – 1.66 (m, 2H, H-5); **^{13}C NMR (101 MHz, $CDCl_3$):** δ 166.7 (C=O), 148.3 (C-3), 121.5 (C-2), 51.4 (OCH_3), 33.4 (C-6), 30.9 (C-4), 27.2 (C-5), 15.4 (SCH_3).

6.8.17 (*E/Z*)-6-methylsulfanylhex-2-enenitrile **137**

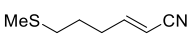

137, E/Z 51:49

Prepared as per Procedure E using 4-(methylthio)butanol **95** (96.00 mg, 0.8 mmol, 1.0 equiv.) with (cyanomethyl)triphenylphosphonium chloride **129** (0.98 g, 2.8 mmol, 7.0 equiv.) and 1.0 M NaOH

(6 mmol, 6 mL) at 5 h. Reaction time: 22 h. Final ratio *E/Z* 51:49. Purification by column chromatography (Hexane/DCM, 1:0, 8:2, 7:3, 6:4, 1:1, then DMC/MeOH, 8:2) afforded the desired product **137** as a yellow oil (45 mg, 0.3 mmol, 40 %).

R_f = 0.45 Hexane/EtOAc (7:3); **(*E*)-isomer: ^{1}H NMR (400 MHz, $CDCl_3$):** δ 6.72 (dt, $^3J_{H3\text{-}H2}$ = 16.3 Hz, $^3J_{H3\text{-}H4}$ = 7.0 Hz, 1H, H-3), 5.38 (dt, $^3J_{H2\text{-}H3}$ = 16.3 Hz, $^4J_{H2\text{-}H4}$ = 1.7 Hz, 1H, H-2), 2.60 – 2.47 (m, 2H, H-6), 2.41 – 2.31 (m, 2H, H-4), 2.11 (s, 3H, SC*H*$_3$), 1.85 – 1.70 (m, 2H, H-5); **^{13}C NMR (101 MHz, $CDCl_3$):** δ 154.8 (C-3), 153.9 (C-3), 117.3 (C≡N), 100.4 (C-2), 33.4 (C-6), 32.0 (C-4), 27.6 (C-5), 15.6 (SCH_3). **(*Z*)-isomer: ^{1}H NMR (400 MHz, $CDCl_3$):** δ 6.50 (dt, $^3J_{H3\text{-}H2}$ 10.9 Hz, $^3J_{H3\text{-}H4}$ = 7.7 Hz, 1H, H-3), 5.35 (dt, $^3J_{H2\text{-}H3}$ = 10.9 Hz, $^4J_{H2\text{-}H4}$ = 1.3 Hz, 1H, H-2), 2.60 – 2.47 (m, 4H, H-6, H-4), 2.41 – 2.31 (m, 2H, H-4), 2.10 (s, 3H, SCH_3), 1.85 – 1.70 (m, 2H, H-5); **^{13}C NMR (101 MHz, $CDCl_3$):** δ 154.8 (C-3), 153.9 (C-3), 115.8 (C≡N), 100.2 (C-2), 33.4 (C-6), 33.3 (C-4), 30.8 (C-4), 26.8 (C-5), 15.4 (SCH_3).

Chapter 7 - References

1 J. Guilbot, S. Kerverdo, A. Milius, R. Escola and F. Pomrehn, *Green Chemistry*, 2013, **15**, 3337.

2 V. S. Nagtode, C. Cardoza, H. K. A. Yasin, S. N. Mali, S. M. Tambe, P. Roy, K. Singh, A. Goel, P. D. Amin, B. R. Thorat, J. N. Cruz and A. P. Pratap, *ACS Omega*, 2023, **8**, 11674.

3 Investopedia, https://www.investopedia.com/terms/c/cagr.asp (accessed 01 October 2023).

4 R. A. Sheldon and J. M. Woodley, *Chem Rev*, 2018, **118**, 801.

5 J. Dambacher, W. Zhao, A. El-Batta, R. Anness, C. Jiang and M. Bergdahl, *Tetrahedron Lett*, 2005, **46**, 4473.

6 D. Balzer, *Nonionic Surfactants*, Taylor & Francis, 2000.

7 G. J. Galo and C. Sanchez, *New Journal of Chemistry*, 2000, **24**, 493.

8 M.-F. Gayral Chiral, S. Kervebo, J. Guilbot and H. Rolland, US Pat. 9 771 545 B2, 2011.

9 C. Amalric, J. Shen, J. Guilbot, H. Rolland, A. Gorce and S. Kerverdo, US Pat. 8 722 069 B2, 2010.

10 P. Johnson, A. Trybala, V. Starov and V. J. Pinfield, *Adv Colloid Interface Sci*, 2021, **288**, 102340.

11 Y. J. Ng, H. R. Lim, K. S. Khoo, K. W. Chew, D. J. C. Chan, M. Bilal, H. S. H. Munawaroh and P. L. Show, *Environ Res*, 2022, **212**, 113126.

12 T. Ivanković and J. Hrenović, *Archives of Industrial Hygiene and Toxicology*, 2010, **61**, 95.

13 J. W. Agger and B. Zeuner, *Curr Opin Biotechnol*, 2022, **78**, 102842.

14 T. Benvegnu, D. Plusquellec and L. Lemiègre, 'Surfactants from Renewable Sources: Synthesis and Applications', Elsevier, Polymers and Composites from Renewable Resources, 2008, 153..

15 J. R. Pinto, S. A. Monteiro e Silva, V. de S. S. Holsback and G. R. Leonardi, *J Cosmet Dermatol*, 2022, **21**, 4775.

16 A. M. Martins and J. M. Marto, *Sustain Chem Pharm*, 2023, **35**, 101178.

17 D. Geetha and R. Tyagi, *Tenside Surfactants Detergents*, 2012, **49**, 417.

18 M. S. Ortiz, J. G. Alvarado, F. Zambrano and R. Marquez, *J Surfactants Deterg*, 2022, **25**, 147.

19 N. S. Neta, J. A. Teixeira and L. R. Rodrigues, *Crit Rev Food Sci Nutr*, 2015, **55**, 595.

20 Procter and Gamble Chemical, https://www.pg.co.uk/ (accessed 01 October 2023).

21 L. Rodríguez-López, M. Rincón-Fontán, X. Vecino, J. M. Cruz and A. B. Moldes, *Tenside Surfactants Detergents*, 2018, **55**, 273.

22 K. Hill and O. Rhode, *Lipid - Fett*, 1999, **101**, 25.

23 A. B. Moldes, L. Rodríguez-López, M. Rincón-Fontán, A. López-Prieto, X. Vecino and J. M. Cruz, *Int J Mol Sci*, 2021, **22**, 2371.

24 R. S. Lanigan and T. A. Yamarik, *Int J Toxicol*, 2002, **21**, 93.

25 F. A. Andersen, *Int J Toxicol*, 2001, **20**, 27.

26 S. De, S. Malik, A. Ghosh, R. Saha and B. Saha, *RSC Adv*, 2015, **5**, 65757.

27 G. Stockburger, U.S. Pat. 4,297,290 A, 1981.

28 J. Ellis, J. Lewis and R. Beattie, U.S. Pat. 6 362 353, 2002.

29 H. E. Hoydonckx, D. E. De Vos, S. A. Chavan and P. A. Jacobs, *Top Catal*, 2004, **27**, 83.

30 H. Hass, F.Snell, W. York and L. Osipow, U.S. Pat. 2 893 990, 1955.

31 S. Bottle and I. D. Jenkins, *J. Chem. Soc., Chem. Commun.*, 1984, **0**, 385.

32 C. Chauvin and D. Plusquellec, *Tetrahedron Lett*, 1991, **32**, 3495.

33 K. Baczko, C. Nugier-Chauvin, J. Banoub, P. Thibault and D. Plusquellec, *Carbohydr Res*, 1995, **269**, 79.

34 P. Eichhorn and T. P. Knepper, *J Chromatogr A*, 1999, **854**, 221.

35 H. P. Wuff, P. A. Siracusa, P. E. Bator, B. A. Salka, M. W. Counts, R. A. Sleksejczyk, P. M. Jr. McCurry, R. S. McDaniel, W. G. Kozak, A. D. Urfer and G. Howell, US Pat. 5449763, 1995..

36 Earth Day 2021 CosmeticsDesign-Europe circular, sustainable beauty snapshot and brainstorm, https://www.cosmeticsdesign-europe.com/Article/2021/04/22/Earth-Day-2021-CosmeticsDesign-Europe-circular-sustainable-beauty-snapshot-and-brainstorm , (accessed 11 September 2023).

37 S. Yang, X. Wang, Y. Pan, Q. Zhan and L. E. Yvan, *Ind Eng Chem Res*, 2023, **62**, 8146.

38 M. Lotfi, A. H. Hasanpour, A. A. Moghadamnia and S. Kazemi, *Curr Neuropharmacol*, 2021, **19**, 1345.

39 Y. Cheng, Z. Shan, J. Zhou, Y. Bu, P. Li and S. Lu, *Chemosphere*, 2017, **175**, 219.

40 L. A. Bernal-Jácome, J. M. Izar-Landeta, R. Flores-Ramirez, K. X. Vargas-Berrones and J. M. i Farreras, *Res Sq*, 2023, 1–17.

41 S. M. Burkinshaw and O. Kabambe, *Dyes and Pigments*, 2011, **88**, 220.

42 M. B. Reddy, R. J. Looney, M. J. Utell, K. P. Plotzke and M. E. Andersen, *Toxicological Sciences*, 2007, **99**, 422.

43 M. A. Saleem, L. Pei, M. F. Saleem, S. Shahid and J. Wang, *J Clean Prod*, 2021, **279**, 123480.

44 Y. L. A. Tang, C. H. Lee, C. Y. Chan, Y. Wang and C.-W. Kan, *Journal of Natural Fibers*, 2023, **20**, 1.

45 M. M. Fiume, B. Heldreth, W. F. Bergfeld, D. V. Belsito, R. A. Hill, C. D. Klaassen, D. Liebler, J. G. Marks, R. C. Shank, T. J. Slaga, P. W. Snyder and F. A. Andersen, *Int J Toxicol*, 2013, **32**, 22S.

46 E. Fischer, *Berichte der deutschen chemischen Gesellschaft*, 1895, **28**, 1145.

47 E. Fischer, *Berichte der deutschen chemischen Gesellschaft*, 1893, **26**, 2400.

48 E. Fischer and L. Beensch, *Berichte der deutschen chemischen Gesellschaft*, 1894, **27**, 2478.

49 B. Roy and B. Mukhopadhyay, *Tetrahedron Lett*, 2007, **48**, 3783.

50 G. Guchhait and A. K. Misra, *Catal Commun*, 2011, **14**, 52.

51 M. Haese, K. Winterhalter, J. Jung and M. S. Schmidt, *Top Curr Chem*, 2022, **380**, 26.

52 K. K. De and T. E. Timell, *Carbohydr Res*, 1967, **4**, 177.

53 S. Y. Chin, S. Shahruddin, G. K. Chua, N. A. Samsudin, S. K. A. Mudalip, N. F. S. Ghazali, Z. Jemaat, S. F. Salleh, F. M. Said, N. Nadir, N. L. Ismail and S. H. Ng, *Ind Eng Chem Res*, 2023, **62**, 4210.

54 A. Karam, K. De Oliveira Vigier, S. Marinkovic, B. Estrine, C. Oldani and F. Jérôme, *ACS Catal*, 2017, **7**, 2990.

55 A. Karam, K. De Oliveira Vigier, S. Marinkovic, B. Estrine, C. Oldani and F. Jérôme, *ChemSusChem*, 2017, **10**, 3604.

56 J. Wang, Y. Xin, D. Fan and S. Chen, *Open Journal of Composite Materials*, 2015, **05**, 11.

57 B. M. de Roode, J. van Beek, A. van der Padt, M. C. R. Franssen and R. M. Boom, *Enzyme Microb Technol*, 2001, **29**, 513.

58 K. Wang, L. Zhao, T. Li, Q. Wang, Z. Ding and W. Dong, *Int J Mol Sci*, 2023, **24**, 3864.

59 R. A. Sheldon, *ACS Sustain Chem Eng*, 2018, **6**, 4464.

60 R. A. Sheldon, *Adv Synth Catal*, 2007, **349**, 1289.

61 S. Ali, W. Zafar, S. Shafiq and M. Manzoor, *International Journal of Scientific & Technology Research*, 2017, **6**, 64.

62 P. Bongartz, T. Karmainski, M. Meyer, J. Linkhorst, T. Tiso, L. M. Blank and M. Wessling, *Biotechnol Bioeng*, 2023, **120**, 1269.

63 C. F. Nising and F. von Nussbaum, *European J Org Chem*, 2022, **2022**, e202200252.

64 Y. Zhang, Y.-Q. Wu, N. Xu, Q. Zhao, H.-L. Yu and J.-H. Xu, *ACS Sustain Chem Eng*, 2019, **7**, 7218.

65 S. K. Ma, J. Gruber, C. Davis, L. Newman, D. Gray, A. Wang, J. Grate, G. W. Huisman and R. A. Sheldon, *Green Chem.*, 2010, **12**, 81.

66 J. Liang, J. Lalonde, B. Borup, V. Mitchell, E. Mundorff, N. Trinh, D. A. Kochrekar, R. Nair Cherat and G. G. Pai, *Org Process Res Dev*, 2010, **14**, 193.

67 E. Mundorff, E. de Vries, US. Pat. 8415126B2, 2013.

68 R. A. Sheldon and F. van Rantwijk, *Aust J Chem*, 2004, **57**, 281.

69 A. Godino, M. Amaranto, A. Manassero, F. Comba, M. A. Pérez, L. Simonella, M. Pernigotti and J. L. Barra, *J Biotechnol*, 2023, **363**, 1.

70 R. S. Heath, W. R. Birmingham, M. P. Thompson, A. Taglieber, L. Daviet and N. J. Turner, *ChemBioChem*, 2018, **20**, 276.

71 N. Jankowski, K. Koschorreck and V. B. Urlacher, *Appl Microbiol Biotechnol*, 2020, **104**, 9205.

72 T. P. de Almeida, M. M. C. H. van Schie, A. Ma, F. Tieves, S. H. H. Younes, E. Fernández-Fueyo, I. W. C. E. Arends, A. Riul and F. Hollmann, *Adv Synth Catal*, 2019, **361**, 2668.

73 M. Pickl, M. Fuchs, S. M. Glueck and K. Faber, *Appl Microbiol Biotechnol*, 2015, **99**, 6617.

74 J. D. de Oliveira, L. S. Carvalho, A. M. V. Gomes, L. R. Queiroz, B. S. Magalhães and N. S. Parachin, *Microb Cell Fact*, 2016, **15**, 1.

75 Y. Duan, P. Yao, X. Chen, X. Liu, R. Zhang, J. Feng, Q. Wu and D. Zhu, *J Mol Catal B Enzym*, 2015, **115**, 1.

76 M. Winkler, *Curr Opin Chem Biol*, 2018, **43**, 23.

77 R. S. Heath, R. E. Ruscoe and N. J. Turner, *Nat Prod Rep*, 2022, **39**, 335.

78 R. A. Sheldon, D. Brady and M. L. Bode, *Chem Sci*, 2020, **11**, 2587.

79 F. Berini, C. Casciello, G. L. Marcone and F. Marinelli, *FEMS Microbiol Lett*, 2017, **364**, 211.

80 M. Tuffin, D. Anderson, C. Heath and D. A. Cowan, *Biotechnol J*, 2009, **4**, 1671.

81 K. Rashamuse, V. Magomani, T. Ronneburg and D. Brady, *Appl Microbiol Biotechnol*, 2009, **83**, 491.

82 R. S. Heath, J. J. Sangster and N. J. Turner, *ChemBioChem*, 2022, **23**, 1.

83 R. S. Heath, M. Pontini, B. Bechi and N. J. Turner, *ChemCatChem*, 2014, **6**, 996.

84 R. S. Heath, W. R. Birmingham, M. P. Thompson, A. Taglieber, L. Daviet and N. J. Turner, *ChemBioChem*, 2018, **20**, 276.

85 D. Brady, S. Reddy, B. Mboniswa, L. H. Steenkamp, A. L. Rousseau, C. J. Parkinson, J. Chaplin, R. K. Mitra, T. Moutlana, S. F. Marais and N. S. Gardiner, *J Mol Catal B Enzym*, 2012, **75**, 1.

86 A. Krüger, C. Schäfers, C. Schröder and G. Antranikian, *N Biotechnol*, 2018, **40**, 144.

87 What Is Green Chemistry? - American Chemical Society, https://www.acs.org/greenchemistry/what-is-green-chemistry.html , (accessed 8 May 2023).

88 P. Anastas and N. Eghbali, *Chem. Soc. Rev.*, 2010, **39**, 301.

89 P. T. Anastas and J. C. Warner, *Green Chemistry: Theory and Practice*, Oxford University Press, 1998.

90 T. Drepper, T. Eggert, W. Hummel, C. Leggewie, M. Pohl, F. Rosenau, S. Wilhelm and K. E. Jaeger, *Biotechnol J*, 2006, **1**, 777.

91 M. Kordi, R. Salami, P. Bolouri, · Nasser Delangiz, · Behnam, A. Lajayer and E. D. Van Hullebusch, *Systems Microbiology and Biomanufacturing*, 2022, **2**, 413.

92 Cosmetics Market Size, Share and Industry Analysis 2023-2028, https://www.imarcgroup.com/cosmetics-market , (accessed 18 May 2023).

93 COSMETIC | English meaning - Cambridge Dictionary, https://dictionary.cambridge.org/dictionary/english/cosmetic , (accessed 12 May 2023).

94 D. Ribeaucourt, B. Bissaro, F. Lambert, M. Lafond and J.-G. Berrin, *Biotechnol Adv*, 2022, **56**, 107787.

95 A. P. Mattey, J. J. Sangster, J. I. Ramsden, C. Baldwin, W. R. Birmingham, R. S. Heath, A. Angelastro, N. J. Turner, S. C. Cosgrove and S. L. Flitsch, *RSC Adv*, 2020, **10**, 19501.

96 M. M. C. H. van Schie, T. Pedroso de Almeida, G. Laudadio, F. Tieves, E. Fernández-Fueyo, T. Noël, I. W. C. E. Arends and F. Hollmann, *Beilstein Journal of Organic Chemistry*, 2018, **14**, 697.

97 W. Finnigan, A. Thomas, H. Cromar, B. Gough, R. Snajdrova, J. P. Adams, J. A. Littlechild and N. J. Harmer, *ChemCatChem*, 2017, **9**, 1005.

98 E. Brenna, M. Crotti, M. De Pieri, F. G. Gatti, G. Manenti and D. Monti, *Adv Synth Catal*, 2018, **360**, 3677.

99 J.-P. Kanter, P. J. Honold, D. Luh, S. Heiles, B. Spengler, M. A. Fraatz, H. Zorn and A. K. Hammer, *J Agric Food Chem*, 2023, **71**, 8112.

100 A. J. C. Wahart, J. Staniland, G. J. Miller and S. C. Cosgrove, *R Soc Open Sci*, 2022, **9**, 211572.

101 J. Dong, E. Fernández-Fueyo, F. Hollmann, C. E. Paul, M. Pesic, S. Schmidt, Y. Wang, S. Younes and W. Zhang, *Angewandte Chemie*, 2018, **130**, 9380.

102 L. Martínez-Montero, V. Gotor, V. Gotor-Fernández and I. Lavandera, *Green Chemistry*, 2017, **19**, 474.

103 J. A. D. Cooper, W. Smith, M. Bacila and H. Medina, *Journal of Biological Chemistry*, 1959, **234**, 445.

104 D. Monti, G. Ottolina, G. Carrea and S. Riva, *Chem Rev*, 2011, **111**, 4111.

105 N. Ito, S. E. V. Phillips, C. Stevens, Z. B. Ogel, M. J. McPherson, J. N. Keen, K. D. S. Yadav and P. F. Knowles, *Nature*, 1991, **350**, 87.

106 B. Schilling and K. Lerch, *BBA - General Subjects*, 1995, **1243**, 529.

107 S. Fernando Castillo Pacheco, M. Jesus Moran, J. I. Santos, L. Salassa, F. López-Gallego, S. F. Castillo Pacheco, F. López-Gallego, M. Moran, L. Salassa, J. I. Santos SGIker-UPV and J. Mari Korta, *ChemRxiv*, 2023, 1.

108 D. Ouedraogo and G. Gadda, 'Flavoprotein Oxidases', in *Flavin-Based Catalysis*, Wiley, 2021, 225.

109 P. G. Ridge, Y. Zhang and V. N. Gladyshev, *PLoS One*, 2008, **3**, e1378.

110 F. P. Guengerich, *Journal of Biological Chemistry*, 2013, **288**, 13164.

111 Y. Wang, J. L. DuBois, B. Hedman, K. O. Hodgson and T. D. P. Stack, *Science (1979)*, 1998, **279**, 537.

112 J. W. Whittaker, *Chem Rev*, 2003, **103**, 2347.

113 M. M. Whittaker and J. W. Whittaker, *Biochemistry*, 2001, **40**, 7140.

114 L. Anghel, S. Rada and R.-V. Erhan, *Anal Lett*, 2023, 1.

115 M. Hammerstad and H.-P. Hersleth, *Arch Biochem Biophys*, 2021, **702**, 108826.

116 W. P. Dijkman, G. de Gonzalo, A. Mattevi and M. W. Fraaije, *Appl Microbiol Biotechnol*, 2013, **97**, 5177.

117 Fan and G. Gadda, *J Am Chem Soc*, 2005, **127**, 2067.

118 K. Rungsrisuriyachai and G. Gadda, *Biochemistry*, 2008, **47**, 6762.

119 D. Ribeaucourt, B. Bissaro, V. Guallar, M. Yemloul, M. Haon, S. Grisel, V. Alphand, H. Brumer, F. Lambert, J.-G. Berrin and M. Lafond, *ACS Sustain Chem Eng*, 2021, **9**, 4411.

120 J. I. Ramsden, R. S. Heath, S. R. Derrington, S. L. Montgomery, J. Mangas-Sanchez, K. R. Mulholland and N. J. Turner, *J Am Chem Soc*, 2019, **141**, 1201.

121 A. Basso and S. Serban, *Molecular Catalysis*, 2019, **479**, 110607.

122 D. Sánchez and M. L. Ferreira, *Biocatalyst Immobilization*, 2023, 203.

123 R. A. Sheldon, *Adv Synth Catal*, 2007, **349**, 1289.

124 D. R. Padrosa and F. Paradisi, *ChemBioChem*, 2023, **24**, e202200723.

125 *Enzyme immobilization for bioprocessing*, R. A. Rahman and S. M. Shaarani ed., Penerbit, 2022.

126 J. M. Bolivar, J. M. Woodley and R. Fernandez-Lafuente, *Chem Soc Rev*, 2022, **51**, 6251.

127 R. Fernandez-Lafuente, *Molecules*, 2023, **28**, 1373.

128 Y. R. Maghraby, R. M. El-Shabasy, A. H. Ibrahim, H. Mohamed and E.-S. Azzazy, *ACS Omega*, 2023, **8**, 5184.

129 O. Pauli, A. Ecker, A. Cruz-Izquierdo, A. Basso and S. Serban, *Catalysts*, 2022, **12**, 989.

130 M. P. Thompson, S. R. Derrington, R. S. Heath, J. L. Porter, J. Mangas-Sanchez, P. N. Devine, M. D. Truppo and N. J. Turner, *Tetrahedron*, 2019, **75**, 327.

131 C. Ottone, C. Bernal, N. Serna, A. Illanes and L. Wilson, *Appl Microbiol Biotechnol*, 2018, **102**, 237.

132 V. G. Tacias-Pascacio, E. García-Parra, G. Vela-Gutiérrez, J. J. Virgen-Ortiz, Á. Berenguer-Murcia, A. R. Alcántara and R. Fernandez-Lafuente, *Catalysts*, 2019, **9**, 1035.

133 B. Manickam, R. Sreedharan and M. Elumalai, ''Genipin'-The Natural Water Soluble Cross-linking Agent and Its Importance in the Modified Drug Delivery Systems: An Overview', in *Current Drug Delivery*, 2014, **11**, 139

134 S. Fujikawa, S. Nakamura and K. Koga, *Agric. Biol. Chem.*, 1988, **52**, 869.

135 A. Indurkar, A. Pandit, R. Jain and P. Dandekar, *J Biomater Appl*, 2021, **36**, 76.

136 F. A. Quiocho and F. M. Richards, *Proceedings of the National Academy of Sciences*, 1964, **52**, 833.

137 N. L. S. Clair and M. A. Navia, *J Am Chem Soc*, 1992, **114**, 7314.

138 L. Cao, F. Van Rantwijk and R. A. Sheldon, *Org Lett*, 2000, **2**, 1361.

139 S. Maury, P. Buisson, A. Perrard and A. C. Pierre, *J Mol Catal B Enzym*, 2005, **32**, 193.

140 K. Shortall, F. Otero, S. Bendl, T. Soulimane and E. Magner, *Langmuir*, 2022, **38**, 13382.

141 Z. Han, X. Fan, S. Yu, X. Li, S. Wang and L. Lu, *J Environ Chem Eng*, 2022, **10**, 108795.

142 E. Katchalski-Katzir and D. M. Kraemer, *J Mol Catal B Enzym*, 2000, **10**, 157.

143 O. Kirk and M. W. Christensen, *Org Process Res Dev*, 2002, **6**, 446.

144 A. Basso, M. S. Brown, A. Cruz-Izquierdo, C. A. Martinez and S. Serban, *Org Process Res Dev*, 2022, **26**, 2075.

145 K. Engelmark Cassimjee, M. Kadow, Y. Wikmark, M. Svedendahl Humble, M. L. Rothstein, D. M. Rothstein and J.-E. Bäckvall, *Chemical Communications*, 2014, **50**, 9134.

146 K. E. Cassimjee, R. Kourist, D. Lindberg, M. Wittrup Larsen, N. H. Thanh, M. Widersten, U. T. Bornscheuer and P. Berglund, *Biotechnol J*, 2011, **6**, 463.

147 S. A. Braham, E. H. Siar, S. Arana-Peña, H. Bavandi, D. Carballares, R. Morellon-Sterling, D. de Andrades, J. F. Kornecki and R. Fernandez-Lafuente, *Process Biochemistry*, 2021, **102**, 108.

148 X. Ma, Z. Chen, J. Han, Y. Zhou, Y. Mao, C. Li, L. Wang and Y. Wang, *New Journal of Chemistry*, 2022, **46**, 21615.

149 J. R. Guimarães, D. Carballares, J. Rocha-Martin, P. W. Tardioli and R. Fernandez-Lafuente, *Catalysts*, 2022, **12**, 1552.

150 E. Rembeza, A. Boverio, M. W. Fraaije and M. K. M. Engqvist, *ChemBioChem*, 2022, **23**, e202100510.

151 BRENDA, https://www.brenda-enzymes.org/ (accessed 3 September 2023).

152 G. Gadda, N. L. N. Powell and P. Menon, *Arch Biochem Biophys*, 2004, **430**, 264.

153 F. Salvi, Y. F. Wang, I. T. Weber and G. Gadda, *Acta Crystallogr D Biol Crystallogr*, 2014, **70**, 405.

154 W. B. Rizzo, *Biochimica et Biophysica Acta (BBA) - Molecular and Cell Biology of Lipids*, 2014, **1841**, 377.

155 M. D. Lloyd, K. D. E. Boardman, A. Smith, D. M. van den Brink, R. J. A. Wanders and M. D. Threadgill, *J Enzyme Inhib Med Chem*, 2007, **22**, 584.

156 D. L. Ebenezer, P. Fu, R. Ramchandran, A. W. Ha, V. Putherickal, T. Sudhadevi, A. Harijith, F. Schumacher, B. Kleuser and V. Natarajan, *Biochimica et Biophysica Acta (BBA) - Molecular and Cell Biology of Lipids*, 2020, **1865**, 158681.

157 D. Ribeaucourt, S. Saker, D. Navarro, B. Bissaro, E. Drula, L. O. Correia, M. Haon, S. Grisel, N. Lapalu, B. Henrissat, R. J. O'Connell, F. Lambert, M. Lafond and J.-G. Berrin, *Appl Environ Microbiol*, 2021, **87**, e0152621.

158 K. D. Bartle and P. Myers, *Trends in Analytical Chemistry*, 2002, **21**, 547.

159 R. Raju, T. Merl, M. K. Adam, E. Staykov, R. N. Ben, G. Bryant and B. L. Wilkinson, *Aust J Chem*, 2019, **72**, 637.

160 N. K. Korber and C. M. Pedersen, *Carbohydr Res*, 2022, **511**, 108497.

161 F. W. Studier, *Protein Expr Purif*, 2005, **41**, 207.

162 R. Re, N. Pellegrini, A. Proteggente, A. Pannala, M. Yang and C. Rice-Evans, *Free Radic Biol Med*, 1999, **26**, 1231.

163 S. M. Forget, F. R. Xia, J. E. Hein and H. Brumer, *Org Biomol Chem*, 2020, **18**, 2076.

164 A. P. Mattey, J. J. Sangster, J. I. Ramsden, C. Baldwin, W. R. Birmingham, R. S. Heath, A. Angelastro, N. J. Turner, S. C. Cosgrove and S. L. Flitsch, *RSC Adv*, 2020, **10**, 19501.

165 Purolite, 2014, 13.

166 EnginZyme™, .

167 J. Hausjell, J. Weissensteiner, C. Molitor, H. Halbwirth and O. Spadiut, *Microb Cell Fact*, 2018, **17**, 169.

168 S. H. Pan and B. A. Malcolm, *Biotechniques*, 2000, **29**, 1234.

169 Resins for Solid Phase Peptide Synthesis – Core Resins, https://www.peptide.com/resources/resins-for-solid-phase-peptide-synthesis-core-resins/, (accessed 5 July 2023).

170 L. A. Thompson and J. A. Ellman, *Chem Rev*, 1996, **96**, 555.

171 V. Martin, P. H. G. Egelund, H. Johansson, S. Thordal Le Quement, F. Wojcik and D. Sejer Pedersen, *RSC Adv*, 2020, **10**, 42457.

172 S. Kobayashi and Y. Aoki, *Tetrahedron Lett*, 1998, **39**, 7345.

173 Z. Hussain, E. Yousif, A. Ahmed and A. Altaie, *Org Med Chem Lett*, 2014, **4**, 1.

174 E. Raczuk, B. Dmochowska, J. Samaszko-Fiertek and J. Madaj, *Molecules*, 2022, **27**, 787.

175 H. Schiff, *Annalen der Chemie und Pharmacie*, 1864, **131**, 118.

176 W. Qin, S. Long, M. Panunzio and S. Biondi, *Molecules*, 2013, **18**, 12264.

177 G. C. Look, M. M. Murphy, D. A. Campbell and M. A. Gallop, *Tetrahedron Lett*, 1995, **36**, 2937.

178 J. Kalia and R. T. Raines, *Angewandte Chemie - International Edition*, 2008, **47**, 7523.

179 S. Ulrich, D. Boturyn, A. Marra, O. Renaudet and P. Dumy, *Chemistry - A European Journal*, 2014, **20**, 34.

180 A. Dirksen, T. M. Hackeng and P. E. Dawson, *Angewandte Chemie*, 2006, **118**, 7743.

181 S. Chowdhury, A. Rakshit, A. Acharjee, D. Kumar and B. Saha, *J Mol Liq*, 2022, **346**, 117118.

182 J.-F. Soulé, H. Miyamura and S. Kobayashi, *Chem. Commun.*, 2013, **49**, 355.

183 Y.-S. Lan, B.-S. Liao, Y.-H. Liu, S.-M. Peng and S.-T. Liu, *European J Org Chem*, 2013, **2013**, 5160.

184 H. Yuan, W.-J. Yoo, H. Miyamura and S. Kobayashi, *J Am Chem Soc*, 2012, **134**, 13970.

185 B. Gnanaprakasam, J. Zhang and D. Milstein, *Angewandte Chemie*, 2010, **122**, 1510.

186 L. Jiang, L. Jin, H. Tian, X. Yuan, X. Yu and Q. Xu, *Chemical Communications*, 2011, **47**, 10833.

187 Y. Shiraishi, M. Ikeda, D. Tsukamoto, S. Tanaka and T. Hirai, *Chemical Communications*, 2011, **47**, 4811.

188 C.-W. Wu, J.-G. Lee and W.-C. Lee, *Biotechnol. Appl. Biochem*, 1998, **27**, 225.

189 R. Ghosh and Z. F. Cui, *J Memb Sci*, 2000, **167**, 47.

190 R. Urbański, E. Góralska, H.-J. Bart and J. Szymanowski, *J Colloid Interface Sci*, 2002, **253**, 419.

191 T. Sokac, M. Gojun, A. Jurinjak, T. Sek, A. Sali and B. Zeli, *Renew Energy*, 2020, **159**, 642.

192 D. Abouelenein, A. M. Mustafa, S. Angeloni, G. Borsetta, S. Vittori, F. Maggi, G. Sagratini and G. Caprioli, *Molecules*, 2021, **26**, 4153.

193 A. Antoniewska, J. Rutkowska and M. Martinez Pineda, *Food Chem*, 2019, **286**, 376.

194 D. A. Heatherbell, R. E. Wroslstad and L. M. Libbey, *J Food Sci*, 1971, **36**, 219.

195 G. Borsotti and T. Pellizzon, U.S. Pat. 5 527 892A, 1996

196 K. Lokesh, C. West, J. CI. Kuylenstierna, J. Fan, V. Budarin, P. Priecel, J. A. Lopez-Sanchez and J. H. Clark, *J Clean Prod*, 2019, **209**, 283.

197 Rotating Bed Reactors - SpinChem, https://www.spinchem.com/rotating-bed-reactors/, (accessed 4 October 2023).

198 A. C. Vaucher and M. Reiher, *J Chem Inf Model*, 2016, **56**, 1470.

199 S. C. Cosgrove, G. J. Miller, A. Bornadel and B. Dominguez, *ACS Sustain Chem Eng*, 2023, **11**, 8556.

200 S. Stubbs, S. Yousaf and I. Khan, *DARU Journal of Pharmaceutical Sciences*, 2022, **30**, 407.

201 Y. Ran, F. Byrne, I. D. V. Ingram and M. North, *Chemistry - A European Journal*, 2019, **25**, 4951.

202 R. Santini, M. C. Griffith and M. Qi, *Tetrahedron Lett*, 1998, **39**, 8951.

203 V. K. Sarin, S. B. H. Kent and R. B. Merrifield, *J Am Chem Soc*, 1980, **102**, 5463.

204 J. K. Magtaan, M. Devocelle and F. Kelleher, *Journal of Peptide Science*, 2019, **25**, e3139.

205 C. Amadi-Kamalu, H. Clarke, M. McRobie, J. Mortimer, M. North, Y. Ran, A. Routledge, D. Sibbald, M. Tickias, K. Tse and H. Willway, *ChemistryOpen*, 2020, **9**, 431.

206 L. Ferrazzano, D. Corbisiero, G. Martelli, A. Tolomelli, A. Viola, A. Ricci and W. Cabri, *ACS Sustain Chem Eng*, 2019, **7**, 12867.

207 K. Wegner, D. Barnes, K. Manzor, A. Jardine and D. Moran, *Green Chem Lett Rev*, 2021, **14**, 153.

208 P. T. Anastas and R. L. Lankey, *Green Chemistry*, 2000, **2**, 289.

209 J. Pawlas and J. H. Rasmussen, *Green Chemistry*, 2019, **21**, 5990.

210 A. Kumar, A. Sharma, B. G. de la Torre and F. Albericio, *Green Chem Lett Rev*, 2021, **14**, 545.

211 E. Rojas-Escudero, A. L. Alarcón-Jiménez, P. Elizalde-Galván and F. Rojo-Callejas, *J Chromatogr A*, 2004, **1027**, 117.

212 C. Rumpel and M.-F. Dignac, *Soil Biol Biochem*, 2006, **38**, 1478.

213 A. I. Ruiz-Matute, O. Hernández-Hernández, S. Rodríguez-Sánchez, M. L. Sanz and I. Martínez-Castro, *Journal of Chromatography B*, 2011, **879**, 1226.

214 M. C. Bryan, C. Dalton, A. Díaz-Rodríguez, J. Doerfler, O. D. Engl, P. Ferguson, A. G. Molina, Z. S. Han, J. Hosford, G. P. Howell, M. Hutchby, W. Li, R. H. Munday, A. Navarro, M. Parmentier, J. Pawlas, P. F. Richardson, W. J. Smith, A. Steven, B. S. Takale, J. A. Terrett, D. S. Treitler and M. Zeng, *Org Process Res Dev*, 2022, **26**, 251.

215 D. J. C. Constable, P. J. Dunn, J. D. Hayler, G. R. Humphrey, J. L. Leazer, Jr., R. J. Linderman, K. Lorenz, J. Manley, B. A. Pearlman, A. Wells, A. Zaks and T. Y. Zhang, *Green Chem.*, 2007, **9**, 411.

216 M. C. Bryan, P. J. Dunn, D. Entwistle, F. Gallou, S. G. Koenig, J. D. Hayler, M. R. Hickey, S. Hughes, M. E. Kopach, G. Moine, P. Richardson, F. Roschangar, A. Steven and F. J. Weiberth, *Green Chemistry*, 2018, **20**, 5082.

217 J. Tadros, C. Dankers, J. R. Aldrich-Wright, A. Polyzos and C. P. Gordon, *European J Org Chem*, 2021, **2021**, 4184.

218 H. Choi, H. J. Shirley, P. A. Hume, M. A. Brimble and D. P. Furkert, *Angewandte Chemie*, 2017, **129**, 7528.

219 P. Metrangolo and G. Resnati, *Chemistry - A European Journal*, 2001, **7**, 2511.

220 J. A. Ippolito and D. W. Christianson, *Int J Biol Macromol*, 1992, **14**, 193.

221 A. Timmins and S. P. de Visser, 'Enzymatic Halogenases and Haloperoxidases', Elsevier, *Advances in Protein Chemistry and Structural Biology*, Academic Press Inc., 2015, **100**, 113.

222 S. Jiang, L. Zhang, D. Cui, Z. Yao, B. Gao, J. Lin and D. Wei, *Sci Rep*, 2016, **6**, 34750.

223 X. Xu, Y. Zhong, Q. Xing, Z. Gao, J. Gou and B. Yu, *Org Lett*, 2020, **22**, 5176.

224 D. J. Keavy, Y. Liu and G. W. Gribble, *Arkivoc*, 2020, **2019**, 368.

225 K. Antien, A. Lacambra, F. P. Cossío, S. Massip, D. Deffieux, L. Pouységu, P. A. Peixoto and S. Quideau, *Chemistry – A European Journal*, 2019, **25**, 11574.

226 N. M. Mozier, K. P. McConnell and J. L. Hoffman, *Journal of Biological Chemistry*, 1988, **263**, 4527.

227 A. S. Vangnai and D. J. Arp, *Microbiology (N Y)*, 2001, **147**, 745.

228 R. W. Bates and M. R. Dewey, *Org Lett*, 2009, **11**, 3706.

229 G. Wittig and W. Haag, *Chem Ber*, 1955, **88**, 1654.

230 G. Wittig and U. Schöllkopf, *Chem Ber*, 1954, **87**, 1318.

231 M. Mikolajczyk, S. Grzejszczak, W. Midura and A. Zatorski, *Synthesis* , 1975, **1975**, 278.

232 E. D'Incan and J. Seyden-Penne, *Synthesis*, 1975, **1975**, 516.

233 C. Piechucki, *Synthesis*, 1976, **1976**, 187.

234 G. MÄRKL and A. MERZ, *Synthesis,* 1973, **1973**, 295.

235 J. McNulty and D. McLeod, *Chemistry - A European Journal*, 2011, **17**, 8794.

236 P. Das and J. McNulty, *European J Org Chem*, 2010, **2010**, 3587.

237 H. Goetz, F. Nerdel and H. Michaelis, *Naturwissenschaften*, 1963, **50**, 496.

238 K. Jiang and Y.-C. Chen, *Tetrahedron Lett*, 2014, **55**, 2049.

239 J. Clayden, N. Greeves and S. Warren, *Organic Chemistry*, OUP Oxford, 2012.

240 Organic Chemistry Portal, https://www.organic-chemistry.org/namedreactions/wittig-reaction.shtm, (accessed 4 September 2023).

241 W. S. Wadsworth and W. D. Emmons, *J Am Chem Soc*, 1961, **83**, 1733.

242 M. Julia and J. M. Paris, *Tetrahedron Lett*, 1973, **14**, 4833.

243 M. Schlosser and K. F. Christmann, *Angewandte Chemie International Edition in English*, 1966, **5**, 126.

244 J. Wu, D. Zhang and S. Wei, *Synth Commun*, 2005, **35**, 1213.

245 J. Wu, D. Li and D. Zhang, *Synth Commun*, 2005, **35**, 2543.

246 D.-J. Dong, Y. Li, J.-Q. Wang and S.-K. Tian, *Chemical Communications*, 2011, **47**, 2158.

247 D.-J. Dong, H.-H. Li and S.-K. Tian, *J Am Chem Soc*, 2010, **132**, 5018.

248 R. W. Hoffmann, *Angewandte Chemie International Edition*, 2001, **40**, 1411.

249 E. Vedejs and M. J. Peterson, 'Stereochemistry and Mechanism in the Wittig Reaction', John Wiley & Sons Ltd, *Topics in Stereochemistry*, 1994, **21**, 1.

250 B. E. Maryanoff and A. B. Reitz, *Chem Rev*, 1989, **89**, 863.

251 T. Thiemann, S. Mataka, M. Tashiro, S. Sasaki and V. Vill, *J Chem Res*, 1997, 248.

252 F. Kazmierczak and P. Helquist, *J. Org. Chem*, 1989, **54**, 3988.

253 S. D. Rychnovsky and R. C. Hoye, *J. Am. Chem. Soc*, 1994, **116**, 47.

254 R. Broos, D. Tavernier and M. Anteunis, *J Chem Educ*, 1978, **55**, 813.

255 B. M. Butcher, R. J. Mathews and S. Middleton, *Aust J Chem*, 1973, **26**, 2067.

256 M. G. Russell and S. Warren, *J Chem Soc Perkin 1*, 2000, 505.

257 S. Hünig and I. Stemmler, *Tetrahedron Lett*, 1974, **15**, 3151.

258 M. Mikoajczyk, S. Grzejszczak, W. Midura and A. Zatorski, *Synthesis*, 1976, **1976**, 396.

259 C. Piechechi, *Synthesis*, 1974, **1974**, 869.

260 Y. Le Bigot, M. Delmas and A. Gaset, *Synth Commun*, 1982, **12**, 107.

261 M. Delmas, Y. Le Bigot and A. Gaset, *Tetrahedron Lett*, 1980, **21**, 4831.

262 M. Delmas, Y. Le Bigot, A. Gaset and J. P. Gorrichon, *Synth Commun*, 1981, **11**, 125.

263 T. Thiemann, M. Watanabe, Y. Tanaka and S. Mataka, *New J. Chem.*, 2004, **28**, 578.

264 V. P. Balema, J. W. Wiench, M. Pruski and V. K. Pecharsky, *J Am Chem Soc*, 2002, **124**, 6244.

265 P. Das, D. McLeod and J. McNulty, *Tetrahedron Lett*, 2011, **52**, 199.

266 R. Broos and M. Anteunis, *Synth Commun*, 1976, **6**, 53.

267 M. G. Russell and S. Warren, *Tetrahedron Lett*, 1998, **39**, 7995.

268 F. Sieber, P. Wentworth, J. D. Toker, A. D. Wentworth, W. A. Metz, N. N. Reed and K. D. Janda, *J Org Chem*, 1999, **64**, 5188.

269 C. Tanford, R. Breslow and D. Symp ; Rideout, *Adv Enzymol Relat Areas Mol Biol*, 1980, **110**, 7816.

270 M. Javaherian and P. Movaheditabar, *Journal of the Iranian Chemical Society*, 2023, **20**, 2103.

271 A. El-Batta, C. Jiang, W. Zhao, R. Anness, A. L. Cooksy and M. Bergdahl, *J Org Chem*, 2007, **72**, 5244.

272 M. J. B. Kelly, L. B. Fallot, J. L. Gustafson and B. M. Bergdahl, *J Chem Educ*, 2016, **93**, 1631.

273 G. G. Bai, F. Yuan, F. Q. Li, K. J. Mao, P. Zhou, J. W. Chen and X. Li, *Nat Prod Res*, 2015, **29**, 1481.

274 K. Mori, *Tetrahedron*, 2015, **71**, 5589.

275 D. Reiter, P. Frisch, T. Szilvási and S. Inoue, *J Am Chem Soc*, 2019, **141**, 16991.

276 D. I. Bugaenko and A. V. Karchava, *Adv Synth Catal*, 2023, **365**, 1893.

277 F.-H. Hu, L.-S. Wang and S.-F. Cai, *J Chem Eng Data*, 2009, **54**, 1382.

278 L.-J. Chen and D.-R. Hou, *Tetrahedron: Asymmetry*, 2008, **19**, 715.

279 *Fisher Scientific, '6-chloro-1-hexene', revision data 14-Feb-2020, https://www.fishersci.com/store/msds?partNumber=AAH5339606&productDescription=6-CHLORO-1-HEXENE%2C+97%25+5G&vendorId=VN00024248&countryCode=US&language=en (accessed 29 September 2023)*.

280 *Sigma-Aldrich, 'toluene', revision data 22-Aug-2023, https://www.sigmaaldrich.com/FR/en/sds/sial/244511 (accessed 05 October 2023)*

281 *Thermo Fisher Scientific, 'p-cresol', revision data 30-Jun-2022, https://www.fishersci.com/store/msds?partNumber=AC110591000&productDescription=P-*

CRESOL%2C+P.A.+100GR&vendorId=VN00032119&countryCode=US&language=en (accessed 05 October 2023).

282 *Sigma-Aldrich, 'methyl acrylate', revision data 04-Feb-2023, https://www.sigmaaldrich.com/FR/en/sds/ALDRICH/M27301 (accessed 05 October 2023).*

283 Sigma-Aldrich, 'Methyl (triphenylphosphoranylidene)acetate', revision 30-04-2022, https://www.sigmaaldrich.com/FR/en/sds/aldrich/157929 (accessed 05 October 2023).

284 K. Mori, *Tetrahedron*, 2015, **71**, 5589.

285 J. M. Concellón, H. Rodríguez-Solla, M. Huerta and J. A. Pérez-Andrés, *European J Org Chem*, 2002, **2002**, 1839.

286 I. Bonnard, M. Rolland, J. M. Salmon, E. Debiton, C. Barthomeuf and B. Banaigs, *J Med Chem*, 2007, **50**, 1266.

287 S. T. Kemme, T. Šmejkal and B. Breit, *Chemistry - A European Journal*, 2010, **16**, 3423.

288 I. Matsuda and Y. Izumi, *Tetrahedron Lett*, 1981, **22**, 1805.

289 A. Palanivel, S. Mubeen, T. Warner, N. Ahmed and D. L. J. Clive, *The Journal of Organic Chemistry,* 2019, **84**, 12542.

290 A. G. M. Barrett, J. Head, M. L. Smith, N. S. Stock, A. J. P. White and D. J. Williams, *J Org Chem*, 1999, **64**, 6005.

291 L. Li, J. C. Stimac and L. M. Geary, *Tetrahedron Lett*, 2017, **58**, 1379.

292 H. Chiba, H. Agematu, R. Kaneto, T. Terasawa, K. Sakai, K. Dobashi and T. Yoshioka, *The Journal of Antibiotics*, 1999, **52**, 695.

293 P. J. Mohr and B. N. Taylor, *CRC Handbook of Chemistry and Physics | Enhanced Reader*, CRC Press, 2005.

294 D. T. Witiak, K. Tomita, R. J. Patch and S. J. Enna, *J Med Chem*, 1981, **24**, 788.

295 B. Wu, K. Li and P. H. Toy, *Synlett*, 2012, **23**, 2564.

296 D. Enders, H. J. Scherer and J. Runsink, *Chem Ber*, 1993, **126**, 1929.

297 T. Fujita, T. Yamamoto, Y. Morita, H. Chen, Y. Shimizu and M. Kanai, *J Am Chem Soc*, 2018, **140**, 5899.

298 L.-J. Chen and D.-R. Hou, *Tetrahedron Asymmetry*, 2008, **19**, 715.

299 A. V. Malkov, N. Derrien, M. Barłóg and P. Kočovský, *Chemistry - A European Journal*, 2014, **20**, 4542.

300 N. Knouzi, M. Vaultier, L. Toupet and R. Carrie, *Tetrahedron Lett*, 1987, **28**, 1757.

301 J. M. Larsson, T. S. N. Zhao and K. J. Szabó, *Org Lett*, 2011, **13**, 1888.

302 L. Jaroskova, M. Bourgaux, I. Wenkin and L. Ghosez, *Tetrahedron Lett*, 1998, **39**, 3157.

303 N. Bacani, J. S. Barbay, S. C. Bembenek, M. Cai, C. Deckhut, J. P. Edwards, B. Ghosh, B. Hao, K. Kreutter, G. Li, M. Tichenor, J. D. Venable, J. Wei, J. J. M. Wiener, Y. Wu, Y. Zhu, F. Zhang, Z. Zhang, K. Xian, WIPO Pat. WO2017100668A1, 2017.

304 J. Wu and C. Yue, *Synth Commun*, 2006, **36**, 2939.

305 M. Grayson and P. T. Keough, *J Am Chem Soc*, 1960, **82**, 3919.

306 B. E. Maryanoff and A. B. Reitz, *Chem Rev*, 1989, **89**, 863.

307 R. Breslow, *Acc Chem Res*, 1991, **24**, 159.

308 K. Ando, M. Okumura and S. Nagaya, *Tetrahedron Lett*, 2013, **54**, 2026.

309 X. Huang, X. Li and N. Jiao, *Chem Sci*, 2015, **6**, 6355.

310 X.-D. An and S. Yu, *Org Lett*, 2015, **17**, 5064.

311 W.-Y. Fang and H.-L. Qin, *J Org Chem*, 2019, **84**, 5803.

312 Y. Chen, J. P. Romaire and T. R. Newhouse, *J Am Chem Soc*, 2015, **137**, 5875.

313 J. W. Cran, M. E. Krafft, K. A. Seibert, T. F. N. Haxell, J. A. Wright, C. Hirosawa and K. A. Abboud, *Tetrahedron*, 2011, **67**, 9922.

314 M. Monari, E. Montroni, A. Nitti, M. Lombardo, C. Trombini and A. Quintavalla, *Chemistry - A European Journal*, 2015, **21**, 11038.

315 T. Y. Zhang, J. C. O'Toole and J. M. Dunigan, *Tetrahedron Lett*, 1998, **39**, 1461.

316 J. Villieras, M. R. Et and B. Kirschleger, *Phosphorus and Sulfur and the Related Elements*, 1983, **14**, 385.

317 F. Texier-boullet, D. Villemin, M. Ricard, H. Moison and A. Foucaud, *Tetrahedron*, 1985, **41**, 1259.

318 R. A. Bunce and J. C. Allison, *Synth Commun*, 1999, **29**, 2175.

319 J. Bidange, C. Fischmeister, C. Bruneau, J.-L. Dubois and J.-L. Couturier, *Monatshefte für Chemie - Chemical Monthly*, 2015, **146**, 1107.

320 S. M. Rountree, S. F. R. Taylor, C. Hardacre, M. C. Lagunas and P. N. Davey, *Appl Catal A Gen*, 2014, **486**, 94.

321 W. Zhang, R. Zhang and R. He, *Tetrahedron Lett*, 2007, **48**, 4203–4205.

322 X. Miao, A. Blokhin, A. Pasynskii, S. Nefedov, S. N. Osipov, T. Roisnel, C. Bruneau and P. H. Dixneuf, *Organometallics*, 2010, **29**, 5257.

323 W. E. Crowe and D. R. Goldberg, *J Am Chem Soc*, 1995, **117**, 5162.

324 K. N. Ganesh, D. Zhang, S. J. Miller, K. Rossen, P. J. Chirik, M. C. Kozlowski, J. B. Zimmerman, B. W. Brooks, P. E. Savage, D. T. Allen and A. M. Voutchkova-Kostal, *Org Process Res Dev*, 2021, acs.oprd.1c00216.

325 L. J. Chen and D. R. Hou, *Tetrahedron Asymmetry*, 2008, **19**, 715.

326 M. M. Matin, S. C. Bhattacharjee, P. Chakraborty and M. S. Alam, *Carbohydr Res*, 2019, **485**, 107812.

327 J. Schmidt-Lassen and T. K. Lindhorst, *Medchemcomm*, 2014, **5**, 1218.

328 G. Milkereit, M. Morr, J. Thiem and V. Vill, *Chem Phys Lipids*, 2004, **127**, 47.

329 P. Džubák, S. Gurská, K. Bogdanová, D. Uhríková, N. Kanjaková, S. Combet, T. Klunda, M. Kolář, M. Hajdúch and M. Poláková, *Carbohydr Res*, 2020, **488**, 107905.

330 M. Tyagi and K. P. R. Kartha, *Carbohydr Res*, 2015, **413**, 85.

331 K. De Winter, L. Van Renterghem, K. Wuyts, H. Pelantová, V. Křen, W. Soetaert and T. Desmet, *Adv Synth Catal*, 2015, **357**, 1961.

332 X. Li, J. Turánek, P. Knötigová, H. Kudláčková, J. Mašek, D. B. Pennington, S. E. Rankin, B. L. Knutson and H.-J. Lehmler, *New Journal of Chemistry*, 2008, **32**, 2169.

333 J. Lee, S. Han, M. Kim and B.-S. Kim, *Macromolecules*, 2020, **53**, 355.

334 C.-W. Chang, M.-H. Lin, C.-K. Chan, K. Su, C.-H. Wu, W. Lo, S. Lam, Y.-T. Cheng, P.-H. Liao, C.-H. Wong and C.-C. Wang, *Angewandte Chemie International Edition*, 2021, **60**, 12413.

335 K. H. N. Tang, K. Uchida, K. Nishihara, M. Ito and T. Shibata, *Org Lett*, 2022, **24**, 1313.

336 A. Palanivel, S. Mubeen, T. Warner, N. Ahmed and D. L. J. Clive, *J Org Chem*, 2019, **84**, 12542.

337 U. S. Dakarapu, A. Bokka, P. Asgari, G. Trog, Y. Hua, H. H. Nguyen, N. Rahman and J. Jeon, *Org Lett*, 2015, **17**, 5792.

338 C. Schmidt and U. Kazmaier, *European J Org Chem*, 2008, **2008**, 887.

339 L. Jaroskova, M. Bourgaux, I. Wenkin and L. Ghosez, *Tetrahedron Lett*, 1998, **39**, 3157.

Chapter 8 - Appendix

8.1 Retention times of standards alkyl compounds

*Table 44 – GC-FID Methods and retention times for standard of alkyl alcohols **28-34**, alkyl aldehydes **35-41** and alkyl carboxylic acids **42-48**.*

Entry	Alcohol substrate	Method	Rt alcohol (min)	Rt aldehyde (min)	Rt carboxylic acid (min)
1	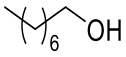	A	**28**, 4.1	**35**, 3.6	**42**, 4.9
2	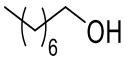	B	**28**, 7.3	**35**, 6.7	**42**, 8.3
3	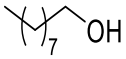	A	**29**, 4.8	**36**, 4.3	**43**, 5.6
4	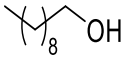	A	**30**, 5.6	**37**, 5.1	**44**, 6.2
5	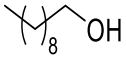	B	**30**,9.0	**37**, 8.5	**44**, 9.9
6	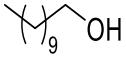	A	**31**, 6.2	**38**, 5.8	**45**, 6.8
7	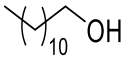	A	**32**, 6.9	**39**, 6.4	**46**,7.4
8	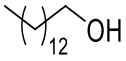	A	**33**, 8.1	**40**, 7.7	**47**, 8.1
9	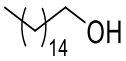	A	**34**, 9.8	**41**, n.a.	n.a.

Rt : retention time; n.a. : not available.
Method A (see supporting information)

Method B (see supporting information)

8.2 Plasmid sequences

8.2.1 pET21a-A0A075HNX4

TGATTGGACAACTGCACTGCTTGAGGCTGATGGTCAGGTGGGCGATTTTCCTGCAGCAGCTCTAGAACACC
ACCATCACCACCACCACCACCACCACTGAGATCCGGCTGCTAACAAAGCCCGAAAGGAAGCTGAGTTGGCT
GCTGCCACCGCTGAGCAATAACTAGCATAACCCCTTGGGGCCTCTAAACGGGTCTTGAGGGGTTTTTTGCT
GAAAGGAGGAACTATATCCGGATTGGCGAATGGGACGCGCCCTGTAGCGGCGCATTAAGCGCGGCGGGTG
TGGTGGTTACGCGCAGCGTGACCGCTACACTTGCCAGCGCCCTAGCGCCCGCTCCTTTCGCTTTCTTCCCTT
CCTTTCTCGCCACGTTCGCCGGCTTTCCCCGTCAAGCTCTAAATCGGGGGCTCCCTTTAGGGTTCCGATTTA
GTGCTTTACGGCACCTCGACCCCAAAAAACTTGATTAGGGTGATGGTTCACGTAGTGGGCCATCGCCCTGAT
AGACGGTTTTTCGCCCTTTGACGTTGGAGTCCACGTTCTTTAATAGTGGACTCTTGTTCCAAACTGGAACAA
CACTCAACCCTATCTCGGTCTATTCTTTTGATTTATAAGGGATTTTGCCGATTTCGGCCTATTGGTTAAAAAAT
GAGCTGATTTAACAAAAATTTAACGCGAATTTTAACAAAATATTAACGCTTACAATTTAGGTGGCACTTTTCG
GGGAAATGTGCGCGGAACCCCTATTTGTTTATTTTTCTAAATACATTCAAATATGTATCCGCTCATGAGACAAT
AACCCTGATAAATGCTTCAATAATATTGAAAAAGGAAGAGTATGAGTATTCAACATTTCCGTGTCGCCCTTATT
CCCTTTTTTGCGGCATTTTGCCTTCCTGTTTTTGCTCACCCAGAAACGCTGGTGAAAGTAAAAGATGCTGAA
GATCAGTTGGGTGCACGAGTGGGTTACATCGAACTGGATCTCAACAGCGGTAAGATCCTTGAGAGTTTTCG
CCCCGAAGAACGTTTTCCAATGATGAGCACTTTTAAAGTTCTGCTATGTGGCGCGGTATTATCCCGTATTGAC
GCCGGGCAAGAGCAACTCGGTCGCCGCATACACTATTCTCAGAATGACTTGGTTGAGTACTCACCAGTCAC
AGAAAAGCATCTTACGGATGGCATGACAGTAAGAGAATTATGCAGTGCTGCCATAACCATGAGTGATAACAC
TGCGGCCAACTTACTTCTGACAACGATCGGAGGACCGAAGGAGCTAACCGCTTTTTTGCACAACATGGGG
GATCATGTAACTCGCCTTGATCGTTGGGAACCGGAGCTGAATGAAGCCATACCAAACGACGAGCGTGACAC
CACGATGCCTGCAGCAATGGCAACAACGTTGCGCAAACTATTAACTGGCGAACTACTTACTCTAGCTTCCCG
GCAACAATTAATAGACTGGATGGAGGCGGATAAAGTTGCAGGACCACTTCTGCGCTCGGCCCTTCCGGCTG
GCTGGTTTATTGCTGATAAATCTGGAGCCGGTGAGCGTGGGTCTCGCGGTATCATTGCAGCACTGGGGCCA
GATGGTAAGCCCTCCCGTATCGTAGTTATCTACACGACGGGGAGTCAGGCAACTATGGATGAACGAAATAGA
CAGATCGCTGAGATAGGTGCCTCACTGATTAAGCATTGGTAACTGTCAGACCAAGTTTACTCATATATACTTTA
GATTGATTTAAAACTTCATTTTTAATTTAAAAGGATCTAGGTGAAGATCCTTTTTGATAATCTCATGACCAAAA
TCCCTTAACGTGAGTTTTCGTTCCACTGAGCGTCAGACCCCGTAGAAAAGATCAAAGGATCTTCTTGAGATC
CTTTTTTTCTGCGCGTAATCTGCTGCTTGCAAACAAAAAAACCACCGCTACCAGCGGTGGTTTGTTTGCCGG
ATCAAGAGCTACCAACTCTTTTTCCGAAGGTAACTGGCTTCAGCAGAGCGCAGATACCAAATACTGTCCTTC
TAGTGTAGCCGTAGTTAGGCCACCACTTCAAGAACTCTGTAGCACCGCCTACATACCTCGCTCTGCTAATCCT
GTTACCAGTGGCTGCTGCCAGTGGCGATAAGTCGTGTCTTACCGGGTTGGACTCAAGACGATAGTTACCGG
ATAAGGCGCAGCGGTCGGGCTGAACGGGGGGTTCGTGCACACAGCCCAGCTTGGAGCGAACGACCTACA
CCGAACTGAGATACCTACAGCGTGAGCTATGAGAAAGCGCCACGCTTCCCGAAGGGAGAAAGGCGGACA
GGTATCCGGTAAGCGGCAGGGTCGGAACAGGAGAGCGCACGAGGGAGCTTCCAGGGGGAAACGCCTGG
TATCTTTATAGTCCTGTCGGGTTTCGCCACCTCTGACTTGAGCGTCGATTTTTGTGATGCTCGTCAGGGGGGC
GGAGCCTATGGAAAAACGCCAGCAACGCGGCCTTTTTACGGTTCCTGGCCTTTTGCTGGCCTTTTGCTCAC
ATGTTCTTTCCTGCGTTATCCCCTGATTCTGTGGATAACCGTATTACCGCCTTTGAGTGAGCTGATACCGCTCG
CCGCAGCCGAACGACCGAGCGCAGCGAGTCAGTGAGCGAGGAAGCGGAAGAGCGCCTGATGCGGTATTT
TCTCCTTACGCATCTGTGCGGTATTTCACACCGCAATGGTGCACTCTCAGTACAATCTGCTCTGATGCCGCATA
GTTAAGCCAGTATACACTCCGCTATCGCTACGTGACTGGGTCATGGCTGCGCCCCGACACCCGCCAACACCC
GCTGACGCGCCCTGACGGGCTTGTCTGCTCCCGGCATCCGCTTACAGACAAGCTGTGACCGTCTCCGGGAG
CTGCATGTGTCAGAGGTTTTCACCGTCATCACCGAAACGCGCGAGGCAGCTGCGGTAAAGCTCATCAGCGT
GGTCGTGAAGCGATTCACAGATGTCTGCCTGTTCATCCGCGTCCAGCTCGTTGAGTTTCTCCAGAAGCGTTA
ATGTCTGGCTTCTGATAAAGCGGGCCATGTTAAGGGCGGTTTTTTCCTGTTTGGTCACTGATGCCTCCGTGT
AAGGGGGATTTCTGTTCATGGGGGTAATGATACCGATGAAACGAGAGAGGATGCTCACGATACGGGTTACT
GATGATGAACATGCCCGGTTACTGGAACGTTGTGAGGGTAAACAACTGGCGGTATGGATGCGGCGGGACC
AGAGAAAAATCACTCAGGGTCAATGCCAGCGCTTCGTTAATACAGATGTAGGTGTTCCACAGGGTAGCCAG
CAGCATCCTGCGATGCAGATCCGGAACATAATGGTGCAGGGCGCTGACTTCCGCGTTTCCAGACTTTACGA

AACACGGAAACCGAAGACCATTCATGTTGTTGCTCAGGTCGCAGACGTTTTGCAGCAGCAGTCGCTTCACG
TTCGCTCGCGTATCGGTGATTCATTCTGCTAACCAGTAAGGCAACCCCGCCAGCCTAGCCGGGTCCTCAACG
ACAGGAGCACGATCATGCGCACCCGTGGGGCCGCCATGCCGGCGATAATGGCCTGCTTCTCGCCGAAACGT
TTGGTGGCGGGACCAGTGACGAAGGCTTGAGCGAGGGCGTGCAAGATTCCGAATACCGCAAGCGACAGG
CCGATCATCGTCGCGCTCCAGCGAAAGCGGTCCTCGCCGAAAATGACCCAGAGCGCTGCCGGCACCTGTCC
TACGAGTTGCATGATAAAGAAGACAGTCATAAGTGCGGCGACGATAGTCATGCCCCGCGCCCACCGGAAGG
AGCTGACTGGGTTGAAGGCTCTCAAGGGCATCGGTCGAGATCCCGGTGCCTAATGAGTGAGCTAACTTACA
TTAATTGCGTTGCGCTCACTGCCCGCTTTCCAGTCGGGAAACCTGTCGTGCCAGCTGCATTAATGAATCGGC
CAACGCGCGGGGAGAGGCGGTTTGCGTATTGGGCGCCAGGGTGGTTTTTCTTTTCACCAGTGAGACGGGC
AACAGCTGATTGCCCTTCACCGCCTGGCCCTGAGAGAGTTGCAGCAAGCGGTCCACGCTGGTTTGCCCCAG
CAGGCGAAAATCCTGTTTGATGGTGGTTAACGGCGGGATATAACATGAGCTGTCTTCGGTATCATCGTATCCC
ACTACCGAGATATCCGCACCAACGCGCAGCCCGGACTCGGTAATGGCGCGCATTGCGCCCAGCGCCATCTG
ATCGTTGGCAACCAGCATCGCAGTGGGAACGATGCCCTCATTCAGCATTTGCATGGTTTGTTGAAAACCGG
ACATGGCACTCCAGTCGCCTTCCCGTTCCGCTATCGGCTGAATTTGATTGCGAGTGAGATATTTATGCCAGCC
AGCCAGACGCAGACGCGCCGAGACAGAACTTAATGGGCCCGCTAACAGCGCGATTTGCTGGTGACCCAAT
GCGACCAGATGCTCCACGCCCAGTCGCGTACCGTCTTCATGGGAGAAAATAATACTGTTGATGGGTGTCTGG
TCAGAGACATCAAGAAATAACGCCGGAACATTAGTGCAGGCAGCTTCCACAGCAATGGCATCCTGGTCATC
CAGCGGATAGTTAATGATCAGCCCACTGACGCGTTGCGCGAGAAGATTGTGCACCGCCGCTTTACAGGCTT
CGACGCCGCTTCGTTCTACCATCGACACCACCACGCTGGCACCCAGTTGATCGGCGCGAGATTTAATCGCCG
CGACAATTTGCGACGGCGCGTGCAGGGCCAGACTGGAGGTGGCAACGCCAATCAGCAACGACTGTTTGCC
CGCCAGTTGTTGTGCCACGCGGTTGGGAATGTAATTCAGCTCCGCCATCGCCGCTTCCACTTTTTCCCGCGT
TTTCGCAGAAACGTGGCTGGCCTGGTTCACCACGCGGGAAACGGTCTGATAAGAGACACCGGCATACTCTG
CGACATCGTATAACGTTACTGGTTTCACATTCACCACCCTGAATTGACTCTCTTCCGGGCGCTATCATGCCATA
CCGCGAAAGGTTTTGCGCCATTCGATGGTGTCCGGGATCTCGACGCTCTCCCTTATGCGACTCCTGCATTAG
GAAGCAGCCCAGTAGTAGGTTGAGGCCGTTGAGCACCGCCGCCGCAAGGAATGGTGCATGCAAGGAGAT
GGCGCCCAACAGTCCCCCGGCCACGGGGCCTGCCACCATACCCACGCCGAAACAAGCGCTCATGAGCCCG
AAGTGGCGAGCCCGATCTTCCCCATCGGTGATGTCGGCGATATAGGCGCCAGCAACCGCACCTGTGGCGCC
GGTGATGCCGGCCACGATGCGTCCGGCGTAGAGGATCGAGATCTCGATCCCGCGAAATTAATACGACTCAC
TATAGGGGAATTGTGAGCGGATAACAATTCCCCTCTAGAAATAATTTTGTTTAACTTTAAGAAGGAGATATAC
ATATGGCACAAGGCGCCCAGAGGAAGAATTTCGGCCACAATCAGATCCTTAGACCTTCTGCAGCTTATACAC
CGGTTGATGAACAAGAGGTACTCCAGATCTTGGATCGACACAGAGGACAGAGGATACGAGCTGTGGGACG
ATTGCATTCCTGGTCCGAGGCAGTTACCGGTGATGGTGTACTTTTGGACTTACAGAGACTAAATGATGTCAG
ACTGCAGTCGGACGGTGACCAACTGGTCGCAACGGTGGGCGCTGGTTGTCAGATTAAAAGACTTTTGAAG
GAGTTGAATCGTGAAGGAGCAACCTTACACTCTCTGGGTCTCATCACAGCTCAGACTATTGCCGGAGCTATT
TCCACAGGTACACATGGATCCGGACGTAACTCCATGTCTCATTACGTTGTTGGTGTGCGATTGGCATGTTACG
ATGCTTCGACAGGTCAGGCTATTATCGAGGAGTTGTCTGCAGGAGAACCTCTTCAGGCTGCCAGATGCAGT
TTAGGTTCCTTGGGCATCATACTGGCAGTAAGAATTCGTTGTCGAGAACAATACAACGTACAGGAGCATTTC
ACGGAGTCACGAAGGCTGTTAGACGTTATGGACGCTGAGGCTCCTTTTCCACTTCAACAGTTTTACTTGTTG
CCGTGGAGATGGAGTTACTTTATCCAGCACAGAAGAGAGGACGATAGGCCAAGATCGAGGCTAGCTAGAC
TATATAGATTGTACTGGTTGGGAACTATGGATTATGGTTTGATATTACAGATCTTGTTTCTTGAGAGAGTCGCC
CGATCAAGAAGATTAATCAGACTGGCTTTCAGACGTATCATTCCTGCTTTCTTGATTAGAAATTGGAGAGTTA
CTGACCGTTCGTCTTCCATGCTTGTCATGAGACATGACGCTTTCAGGCACATCGAAATTGAGTTGTTTGTAAG
AAGAGACCAACTCGCAGACGCATTGGGATTTACCCAAGAAGTAATTAAGATTGCTGGTGGTCGTGAATCCG
CATTGAGTGCTGACAATCAGAGAAGAATCGAGGAGCTCGGTATGCAAGAGGCCCTAGCTGGTTTGCATGAC
CAGTATTGTCATCACTTCCCAATCTGCGTTCGTAGAGTTTTGCCGGACGACACCCTAATAAGCATGGCTTCCG
GTGCTGGCGAAGATTGGTACGCTTTGTCTTTCATTTCATACGCCAAACCGGCAAGACGTGCCGGGTTCTCTC
TTTTCGCCAGTTTCATGGCTAGATCAATGTCGAGACTTTTCCACGCTAGGCCCCATTGGGGAAAGGTTTGTC
CATTGGAAGCCGATGAGCTAACTAGTTTGTATCCACGTTTCGATGCCTTTAGGACTGTTTGTAATACACTAGA
CCCACAGGGTGTTTTCCAAAA

8.2.2 Choline oxidase AcCO6

TGGCGAATGGGACGCGCCCTGTAGCGGCGCATTAAGCGCGGCGGGTGTGGTGGTTACGCGCAGCGTGACC
GCTACACTTGCCAGCGCCCTAGCGCCCGCTCCTTTCGCTTTCTTCCCTTCCTTTCTCGCCACGTTCGCCGGCT
TTCCCCGTCAAGCTCTAAATCGGGGGCTCCCTTTAGGGTTCCGATTTAGTGCTTTACGGCACCTCGACCCCA
AAAAACTTGATTAGGGTGATGGTTCACGTAGTGGGCCATCGCCCTGATAGACGGTTTTTCGCCCTTTGACGT
TGGAGTCCACGTTCTTTAATAGTGGACTCTTGTTCCAAACTGGAACAACACTCAACCCTATCTCGGTCTATTC
TTTTGATTTATAAGGGATTTTGCCGATTTCGGCCTATTGGTTAAAAAATGAGCTGATTTAACAAAAATTTAAC
GCGAATTTTAACAAAATATTAACGTTTACAATTTCAGGTGGCACTTTTCGGGGAAATGTGCGCGGAACCCCT
ATTTGTTTATTTTTCTAAATACATTCAAATATGTATCCGCTCATGAATTAATTCTTAGAAAAACTCATCGAGCATC
AAATGAAACTGCAATTTATTCATATCAGGATTATCAATACCATATTTTTGAAAAAGCCGTTTCTGTAATGAAGG
AGAAAACTCACCGAGGCAGTTCCATAGGATGGCAAGATCCTGGTATCGGTCTGCGATTCCGACTCGTCCAA
CATCAATACAACCTATTAATTTCCCCTCGTCAAAAATAAGGTTATCAAGTGAGAAATCACCATGAGTGACGAC
TGAATCCGGTGAGAATGGCAAAAGTTTATGCATTTCTTTCCAGACTTGTTCAACAGGCCAGCCATTACGCTC
GTCATCAAAATCACTCGCATCAACCAAACCGTTATTCATTCGTGATTGCGCCTGAGCGAGACGAAATACGCG
ATCGCTGTTAAAAGGACAATTACAAACAGGAATCGAATGCAACCGGCGCAGGAACACTGCCAGCGCATCAA
CAATATTTTCACCTGAATCAGGATATTCTTCTAATACCTGGAATGCTGTTTTCCCGGGGATCGCAGTGGTGAG
TAACCATGCATCATCAGGAGTACGGATAAAATGCTTGATGGTCGGAAGAGGCATAAATTCCGTCAGCCAGTT
TAGTCTGACCATCTCATCTGTAACATCATTGGCAACGCTACCTTTGCCATGTTTCAGAAACAACTCTGGCGCA
TCGGGCTTCCCATACAATCGATAGATTGTCGCACCTGATTGCCCGACATTATCGCGAGCCCATTTATACCCATA
TAAATCAGCATCCATGTTGGAATTTAATCGCGGCCTAGAGCAAGACGTTTCCCGTTGAATATGGCTCATAACA
CCCCTTGTATTACTGTTTATGTAAGCAGACAGTTTTATTGTTCATGACCAAAATCCCTTAACGTGAGTTTTCGT
TCCACTGAGCGTCAGACCCCGTAGAAAAGATCAAAGGATCTTCTTGAGATCCTTTTTTTCTGCGCGTAATCT
GCTGCTTGCAAACAAAAAAACCACCGCTACCAGCGGTGGTTTGTTTGCCGGATCAAGAGCTACCAACTCTT
TTTCCGAAGGTAACTGGCTTCAGCAGAGCGCAGATACCAAATACTGTCCTTCTAGTGTAGCCGTAGTTAGGC
CACCACTTCAAGAACTCTGTAGCACCGCCTACATACCTCGCTCTGCTAATCCTGTTACCAGTGGCTGCTGCCA
GTGGCGATAAGTCGTGTCTTACCGGGTTGGACTCAAGACGATAGTTACCGGATAAGGCGCAGCGGTCGGG
CTGAACGGGGGGTTCGTGCACACAGCCCAGCTTGGAGCGAACGACCTACACCGAACTGAGATACCTACAG
CGTGAGCTATGAGAAAGCGCCACGCTTCCCGAAGGGAGAAAGGCGGACAGGTATCCGGTAAGCGGCAGG
GTCGGAACAGGAGAGCGCACGAGGGAGCTTCCAGGGGGAAACGCCTGGTATCTTTATAGTCCTGTCGGGT
TTCGCCACCTCTGACTTGAGCGTCGATTTTTGTGATGCTCGTCAGGGGGGCGGAGCCTATGGAAAAACGCC
AGCAACGCGGCCTTTTTACGGTTCCTGGCCTTTTGCTGGCCTTTTGCTCACATGTTCTTTCCTGCGTTATCCC
CTGATTCTGTGGATAACCGTATTACCGCCTTTGAGTGAGCTGATACCGCTCGCCGCAGCCGAACGACCGAGC
GCAGCGAGTCAGTGAGCGAGGAAGCGGAAGAGCGCCTGATGCGGTATTTTCTCCTTACGCATCTGTGCGG
TATTTCACACCGCATATATGGTGCACTCTCAGTACAATCTGCTCTGATGCCGCATAGTTAAGCCAGTATACACT
CCGCTATCGCTACGTGACTGGGTCATGGCTGCGCCCCGACACCCGCCAACACCCGCTGACGCGCCCTGACG
GGCTTGTCTGCTCCCGGCATCCGCTTACAGACAAGCTGTGACCGTCTCCGGGAGCTGCATGTGTCAGAGGT
TTTCACCGTCATCACCGAAACGCGCGAGGCAGCTGCGGTAAAGCTCATCAGCGTGGTCGTGAAGCGATTCA
CAGATGTCTGCCTGTTCATCCGCGTCCAGCTCGTTGAGTTTCTCCAGAAGCGTTAATGTCTGGCTTCTGATAA
AGCGGGCCATGTTAAGGGCGGTTTTTTCCTGTTTGGTCACTGATGCCTCCGTGTAAGGGGGATTTCTGTTCA
TGGGGGTAATGATACCGATGAAACGAGAGAGGATGCTCACGATACGGGTTACTGATGATGAACATGCCCGG
TTACTGGAACGTTGTGAGGGTAAACAACTGGCGGTATGGATGCGGCGGGACCAGAGAAAAATCACTCAGG
GTCAATGCCAGCGCTTCGTTAATACAGATGTAGGTGTTCCACAGGGTAGCCAGCAGCATCCTGCGATGCAGA
TCCGGAACATAATGGTGCAGGGCGCTGACTTCCGCGTTTCCAGACTTTACGAAACACGGAAACCGAAGACC
ATTCATGTTGTTGCTCAGGTCGCAGACGTTTTGCAGCAGCAGTCGCTTCACGTTCGCTCGCGTATCGGTGAT
TCATTCTGCTAACCAGTAAGGCAACCCCGCCAGCCTAGCCGGGTCCTCAACGACAGGAGCACGATCATGCG
CACCCGTGGGGCCGCCATGCCGGCGATAATGGCCTGCTTCTCGCCGAAACGTTTGGTGGCGGGACCAGTG
ACGAAGGCTTGAGCGAGGGCGTGCAAGATTCCGAATACCGCAAGCGACAGGCCGATCATCGTCGCGCTCC
AGCGAAAGCGGTCCTCGCCGAAAATGACCCAGAGCGCTGCCGGCACCTGTCCTACGAGTTGCATGATAAA
GAAGACAGTCATAAGTGCGGCGACGATAGTCATGCCCCGCGCCCACCGGAAGGAGCTGACTGGGTTGAAG
GCTCTCAAGGGCATCGGTCGAGATCCCGGTGCCTAATGAGTGAGCTAACTTACATTAATTGCGTTGCGCTCA

CTGCCCGCTTTCCAGTCGGGAAACCTGTCGTGCCAGCTGCATTAATGAATCGGCCAACGCGCGGGGAGAG
GCGGTTTGCGTATTGGGCGCCAGGGTGGTTTTTCTTTTCACCAGTGAGACGGGCAACAGCTGATTGCCCTT
CACCGCCTGGCCCTGAGAGAGTTGCAGCAAGCGGTCCACGCTGGTTTGCCCCAGCAGGCGAAAATCCTGT
TTGATGGTGGTTAACGGCGGGATATAACATGAGCTGTCTTCGGTATCGTCGTATCCCACTACCGAGATATCCG
CACCAACGCGCAGCCCGGACTCGGTAATGGCGCGCATTGCGCCCAGCGCCATCTGATCGTTGGCAACCAGC
ATCGCAGTGGGAACGATGCCCTCATTCAGCATTTGCATGGTTTGTTGAAAACCGGACATGGCACTCCAGTCG
CCTTCCCGTTCCGCTATCGGCTGAATTTGATTGCGAGTGAGATATTTATGCCAGCCAGCCAGACGCAGACGC
GCCGAGACAGAACTTAATGGGCCCGCTAACAGCGCGATTTGCTGGTGACCCAATGCGACCAGATGCTCCAC
GCCCAGTCGCGTACCGTCTTCATGGGAGAAAATAATACTGTTGATGGGTGTCTGGTCAGAGACATCAAGAA
ATAACGCCGGAACATTAGTGCAGGCAGCTTCCACAGCAATGGCATCCTGGTCATCCAGCGGATAGTTAATGA
TCAGCCCACTGACGCGTTGCGCGAGAAGATTGTGCACCGCCGCTTTACAGGCTTCGACGCCGCTTCGTTCT
ACCATCGACACCACCACGCTGGCACCCAGTTGATCGGCGCGAGATTTAATCGCCGCGACAATTTGCGACGG
CGCGTGCAGGGCCAGACTGGAGGTGGCAACGCCAATCAGCAACGACTGTTTGCCCGCCAGTTGTTGTGCC
ACGCGGTTGGGAATGTAATTCAGCTCCGCCATCGCCGCTTCCACTTTTTCCCGCGTTTTCGCAGAAACGTGG
CTGGCCTGGTTCACCACGCGGGAAACGGTCTGATAAGAGACACCGGCATACTCTGCGACATCGTATAACGT
TACTGGTTTCACATTCACCACCCTGAATTGACTCTCTTCCGGGCGCTATCATGCCATACCGCGAAAGGTTTTG
CGCCATTCGATGGTGTCCGGGATCTCGACGCTCTCCCTTATGCGACTCCTGCATTAGGAAGCAGCCCAGTAG
TAGGTTGAGGCCGTTGAGCACCGCCGCCGCAAGGAATGGTGCATGCAAGGAGATGGCGCCCAACAGTCCC
CCGGCCACGGGGCCTGCCACCATACCCACGCCGAAACAAGCGCTCATGAGCCCGAAGTGGCGAGCCCGAT
CTTCCCCATCGGTGATGTCGGCGATATAGGCGCCAGCAACCGCACCTGTGGCGCCGGTGATGCCGGCCACG
ATGCGTCCGGCGTAGAGGATCGAGATCTCGATCCCGCGAAATTAATACGACTCACTATAGGGGAATTGTGAG
CGGATAACAATTCCCCTCTAGAAATAATTTTGTTTAACTTTAAGAAGGAGATATACCATGGGCAGCAGCCATC
ATCATCATCATCACAGCAGCGGCCTGGTGCCGCGCGGCAGCCATATGCACATCGATAACATCGAAAATCTGA
GCGATCGCGGTTTTGATTATGTTGTTATTGGTGGTGGTAGTGCCGGTGCAGCAGTTGCAGCACGTCTGAGC
GAAGATCCGGATGTTAGCGTTGCACTGGTTGAAGCAGGTCCGGATGATCGTAATATTCCGGAAATTCTGCAG
CTGGATCGTTGGATGGAACTGCTGGAAAGCGGTTATGATTGGGATTATCCGATTGAACCGCAAGAAAATGG
CAATAGCTTTATGCGTCATGCACGTGCCAAAGTTATGGGTGGTTGTAGCAGCCATAATGCATGTATTGCATTT
TGGGCACCGCGTGAAGATCTGGATGAATGGGAAAGCAAATATGGTGCCACCGGTTGGAATGCAGCAAATG
CATGGCCTCTGTATAAACGTCTGGAAACCAATCAGGATGCAGGTCCTGATGCACCGCATCATGGTGATAGCG
GTCCGGTTCATCTGATGAATGTTCCGCCTGCAGATCCGAGCGGTGTTGCACTGCTGGATGCATGTGAAGAG
GCAGGTATTCCGCGTGCACGTTTTAATACCGGCACCACCGTTGTTAATGGTGCAAACTTTTTTCAGATTAACC
GTCGTGGTGATGGCACCCGTAGCAGCAGCAGCGTTAGCTATATTCATCCGATTATTGAACGCGATAACTTTAC
CCTGCTGACCGGTCTGCGTGCCCGTCAGCTGGTTTTTGATGCAGATAAACGTTGTACCGGTGTTGAAGTTGT
GGGTGGTGCACGTGGTCGTACCCATCGTCTGACCGCACGTCATGAAGTTATTCTGAGTACCGGTGCAATTGA
TAGCCCGAAACTGCTGATGCTGAGCGGTATTGGTCCGGCAGAACATCTGGCACAGCATGGTATTGAAGTTC
TGGTTGATAGTCCGGGTGTTGGTGAAAATCTGCAGGATCATCCTGAAGGTGTTGTTCAGTTTGAAGCAAAA
CAGCCGATGGTTCAGACCAGCACCCAGTGGTGGGAAATTGGTATTTTTACCCCGACCGAAGATGGTCTGGA
TCGTCCGGATCTGATGATGCACTATGGTAGCACTCCGCGTGATCGCAATACCCTGCGTCATGGTTATCCGACC
ACCGAAAATGGTTTTAGCCTGACCCCGAATGTTACCCATGCACGTAGCCGTGGCACCGTTCGTCTGCGTAGT
CGTGATTTTCGTGATAAACCGATGGTTGATCCGCGTTATTTTACCGATCCGGAAGGTCATGATATGCGTGTTAT
GGTTGCGGGTATTCGTAAAGCACGTGAAATTGCAGCACAGCCTGCAATGAGCGCATGGACCGGTCGTGAA
CTGTCACCGGGTGTGGGTGCACAGACCGATGAAGAACTGCAGGATTATATTCGCAAAACCCATAACACCGT
TTATCATCCGGTTGGTACAGTTCGTATGGGTGCAGATGATGATGGTATGAGTCCGCTGGATGCCCGTCTGCGT
GTTAAAGGTGTTACAGGTCTGCGCGTTGCAGATGCAAGCGTTATGCCGGAACATGTTACCGTTAATCCGAAC
ATTACCGTGATGATGATTGGTGAACGTTGTGCCGATCTGATTAAAGCAGATTATGCCGGTGCCGATGCACTG
GAAGAAAAAGAACTGACCACCAGTTTTGCCTAACTCGAGCACCACCACCACCACCACTGAGATCCGGCTGC
TAACAAAGCCCGAAAGGAAGCTGAGTTGGCTGCTGCCACCGCTGAGCAATAACTAGCATAACCCCTTGGG
GCCTCTAAACGGGTCTTGAGGGGTTTTTTGCTGAAAGGAGGAACTATATCCGGAT

8.3 Protein sequences

All DNA sequences are given in the 5’ - 3’ direction, beginning with the 5’ restriction site and ending with the 3’ restriction site. The coding sequence for the protein is shown with red text. All amino acid sequences are given in the N-terminal to C-terminal direction showing the expressed protein sequence without the periplasmic signal peptide (if appropriate).

8.3.1 pET21a-A0A075HNX4

8.3.1.1 DNA insert sequence

ATGGCACAAGGCGCCCAGAGGAAGAATTTCGGCCACAATCAGATCCTTAGACCTTCTGCAGCTTATACACC

GGTTGATGAACAAGAGGTACTCCAGATCTTGGATCGACACAGAGGACAGAGGATACGAGCTGTGGGACGA

TTGCATTCCTGGTCCGAGGCAGTTACCGGTGATGGTGTACTTTTGGACTTACAGAGACTAAATGATGTCAGA

CTGCAGTCGGACGGTGACCAACTGGTCGCAACGGTGGGCGCTGGTTGTCAGATTAAAAGACTTTTGAAGG

AGTTGAATCGTGAAGGAGCAACCTTACACTCTCTGGGTCTCATCACAGCTCAGACTATTGCCGGAGCTATTT

CCACAGGTACACATGGATCCGGACGTAACTCCATGTCTCATTACGTTGTTGGTGTGCGATTGGCATGTTACGA

TGCTTCGACAGGTCAGGCTATTATCGAGGAGTTGTCTGCAGGAGAACCTCTTCAGGCTGCCAGATGCAGTT

TAGGTTCCTTGGGCATCATACTGGCAGTAAGAATTCGTTGTCGAGAACAATACAACGTACAGGAGCATTTCA

CGGAGTCACGAAGGCTGTTAGACGTTATGGACGCTGAGGCTCCTTTTCCACTTCAACAGTTTTACTTGTTGC

CGTGGAGATGGAGTTACTTTATCCAGCACAGAAGAGAGGACGATAGGCCAAGATCGAGGCTAGCTAGACT

ATATAGATTGTACTGGTTGGGAACTATGGATTATGGTTTGATATTACAGATCTTGTTTCTTGAGAGAGTCGCCC

GATCAAGAAGATTAATCAGACTGGCTTTCAGACGTATCATTCCTGCTTTCTTGATTAGAAATTGGAGAGTTAC

TGACCGTTCGTCTTCCATGCTTGTCATGAGACATGACGCTTTCAGGCACATCGAAATTGAGTTGTTTGTAAG

AAGAGACCAACTCGCAGACGCATTGGGATTTACCCAAGAAGTAATTAAGATTGCTGGTGGTCGTGAATCCG

CATTGAGTGCTGACAATCAGAGAAGAATCGAGGAGCTCGGTATGCAAGAGGCCCTAGCTGGTTTGCATGAC

CAGTATTGTCATCACTTCCCAATCTGCGTTCGTAGAGTTTTGCCGGACGACACCCTAATAAGCATGGCTTCCG

GTGCTGGCGAAGATTGGTACGCTTTGTCTTTCATTTCATACGCCAAACCGGCAAGACGTGCCGGGTTCTCTC

TTTTCGCCAGTTTCATGGCTAGATCAATGTCGAGACTTTTCCACGCTAGGCCCCATTGGGGAAAGGTTTGTC

CATTGGAAGCCGATGAGCTAACTAGTTTGTATCCACGTTTCGATGCCTTTAGGACTGTTTGTAATACACTAGA

CCCACAGGGTGTTTTCCAAAATGATTGGACAACTGCACTGCTTGAGGCTGATGGTCAGGTGGGCGATTTTC

CTGCAGCAGCTCTAGAAC

8.3.1.2 Expressed amino acid sequence

MAQGAQRKNFGHNQILRPSAAYTPVDEQEVLQILDRHRGQRIRAVGRLHSWSEAVTGDGVLLDLQRLNDVRL

QSDGDQLVATVGAGCQIKRLLKELNREGATLHSLGLITAQTIAGAISTGTHGSGRNSMSHYVVGVRLACYDAST

GQAIIEELSAGEPLQAARCSLGSLGIILAVRIRCREQYNVQEHFTESRRLLDVMDAEAPFPLQQFYLLPWRWSYFI

QHRREDDRPRSRLARLYRLYWLGTMDYGLILQILFLERVARSRRLIRLAFRRIIPAFLIRNWRVTDRSSSMLVMRH

DAFRHIEIELFVRRDQLADALGFTQEVIKIAGGRESALSADNQRRIEELGMQEALAGLHDQYCHHFPICVRRVLP

DDTLISMASGAGEDWYALSFISYAKPARRAGFSLFASFMARSMSRLFHARPHWGKVCPLEADELTSLYPRFDAF

RTVCNTLDPQGVFQNDWTTALLEADGQVGDFPAAALEHHHHHHHHHH

8.3.2 Choline oxidase AcCO6

8.3.2.1 DNA insert sequence

ATGCACATCGATAACATCGAAAATCTGAGCGATCGCGGTTTTGATTATGTTGTTATTGGTGGTGGTAGTGCCG

GTGCAGCAGTTGCAGCACGTCTGAGCGAAGATCCGGATGTTAGCGTTGCACTGGTTGAAGCAGGTCCGGA

TGATCGTAATATTCCGGAAATTCTGCAGCTGGATCGTTGGATGGAACTGCTGGAAAGCGGTTATGATTGGGA

TTATCCGATTGAACCGCAAGAAAATGGCAATAGCTTTATGCGTCATGCACGTGCCAAAGTTATGGGTGGTTG

TAGCAGCCATAATgcaTGTATTGCATTTTGGGCACCGCGTGAAGATCTGGATGAATGGGAAAGCAAATATGGT

GCCACCGGTTGGAATGCAGCAAATGCATGGCCTCTGTATAAACGTCTGGAAACCAATCAGGATGCAGGTCC

TGATGCACCGCATCATGGTGATAGCGGTCCGGTTCATCTGATGAATGTTCCGCCTGCAGATCCGAGCGGTGT

TGCACTGCTGGATGCATGTGAAGAGGCAGGTATTCCGCGTGCACGTTTTAATACCGGCACCACCGTTGTTAA

TGGTGCAAACTTTTTTCAGATTAACCGTCGTGGTGATGGCACCCGTAGCAGCAGCAGCGTTAGCTATATTCA

TCCGATTATTGAACGCGATAACTTTACCCTGCTGACCGGTCTGCGTGCCCGTCAGCTGGTTTTTGATGCAGAT

AAACGTTGTACCGGTGTTGAAGTTGTGGgTGGTGCAcgTGGTCGTACCCATCGTCTGACCGCACGTCATGAA

GTTATTCTGAGTACCGGTGCAATTGATAGCCCGAAACTGCTGATGCTGAGCGGTATTGGTCCGGCAGAACAT

CTGGCACAGCATGGTATTGAAGTTCTGGTTGATAGTCCGGGTGTTGGTGAAAATCTGCAGGATCATCCTGAA

GGTGTTGTTCAGTTTGAAGCAAAACAGCCGATGGTTCAGACCAGCACCCAGTGGTGGGAAATTGGTATTTT

TACCCCGACCGAAGATGGTCTGGATCGTCCGGATCTGATGATGCAcTATGGTAGCactCCGcgtGATcgcAATAC

CCTGCGTCATGGTTATCCGACCACCGAAAATGGTTTTAGCCTGACCCCGAATGTTACCCATGCACGTAGCCGT

GGCACCGTTCGTCTGCGTAGTCGTGATTTTCGTGATAAACCGATGGTTGATCCGCGTTATTTTACCGATCCGG

AAGGTCATGATATGCGTGTTATGGTTGCGGGTATTCGTAAAGCACGTGAAATTGCAGCACAGCCTGCAATGA

GCGCATGGACCGGTCGTGAACTGTCACCGGGTGTGGGTGCACAGACCGATGAAGAACTGCAGGATTATATT

CGCAAAACCCATAACACCGTTTATCATCCGGTTGGTACAGTTCGTATGGGTGCAGATGATGATGGTATGAGTC

CGCTGGATGCCCGTCTGCGTGTTAAAGGTGTTACAGGTCTGCGCGTTGCAGATGCAAGCGTTATGCCGGAA

CATGTTACCGTTAATCCGAACATTACCGTGATGATGATTGGTGAACGTTGTGCCGATCTGATTAAAGCAGATT

ATGCCGGTGCCGATGCACTGGAAGAAAAAGAACTGACCACCAGTTTTGCCTAA

8.3.2.2 Expressed amino acid sequence

MHIDNIENLSDRGFDYVVIGGGSAGAAVAARLSEDPDVSVALVEAGPDDRNIPEILQLDRWMELLESGYDWD

YPIEPQENGNSFMRHARAKVMGGCSSHNACIAFWAPREDLDEWESKYGATGWNAANAWPLYKRLETNQD

AGPDAPHHGDSGPVHLMNVPPADPSGVALLDACEEAGIPRARFNTGTTVVNGANFFQINRRGDGTRSSSSVS

YIHPIIERDNFTLLTGLRARQLVFDADKRCTGVEVVGGARGRTHRLTARHEVILSTGAIDSPKLLMLSGIGPAEHLA

QHGIEVLVDSPGVGENLQDHPEGVVQFEAKQPMVQTSTQWWEIGIFTPTEDGLDRPDLMMHYGSTPRDRN

TLRHGYPTTENGFSLTPNVTHARSRGTVRLRSRDFRDKPMVDPRYFTDPEGHDMRVMVAGIRKAREIAAQPA

MSAWTGRELSPGVGAQTDEELQDYIRKTHNTVYHPVGTVRMGADDDGMSPLDARLRVKGVTGLRVADASV

MPEHVTVNPNITVMMIGERCADLIKADYAGADALEEKELTTSFA

8.4 GC-FID traces for alkyl compounds C_8 and C_{10} with GC-FID method A

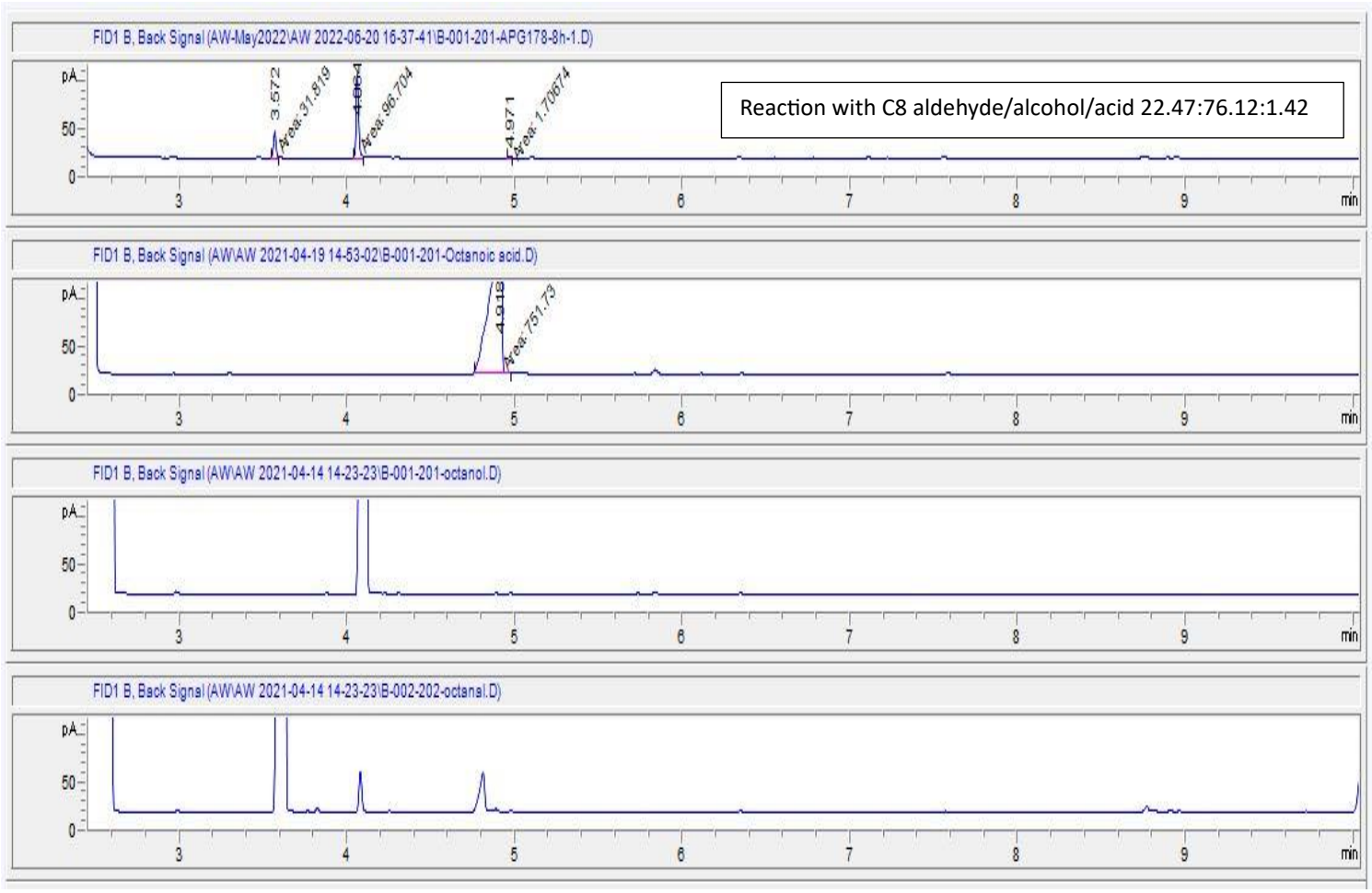

*Figure 37 – Top to bottom: biotransformation with AcCO6 CFE of octanol **28**, standard of octanoic acid **42**, standard of octanol **28**, standard of octanal **35**.*

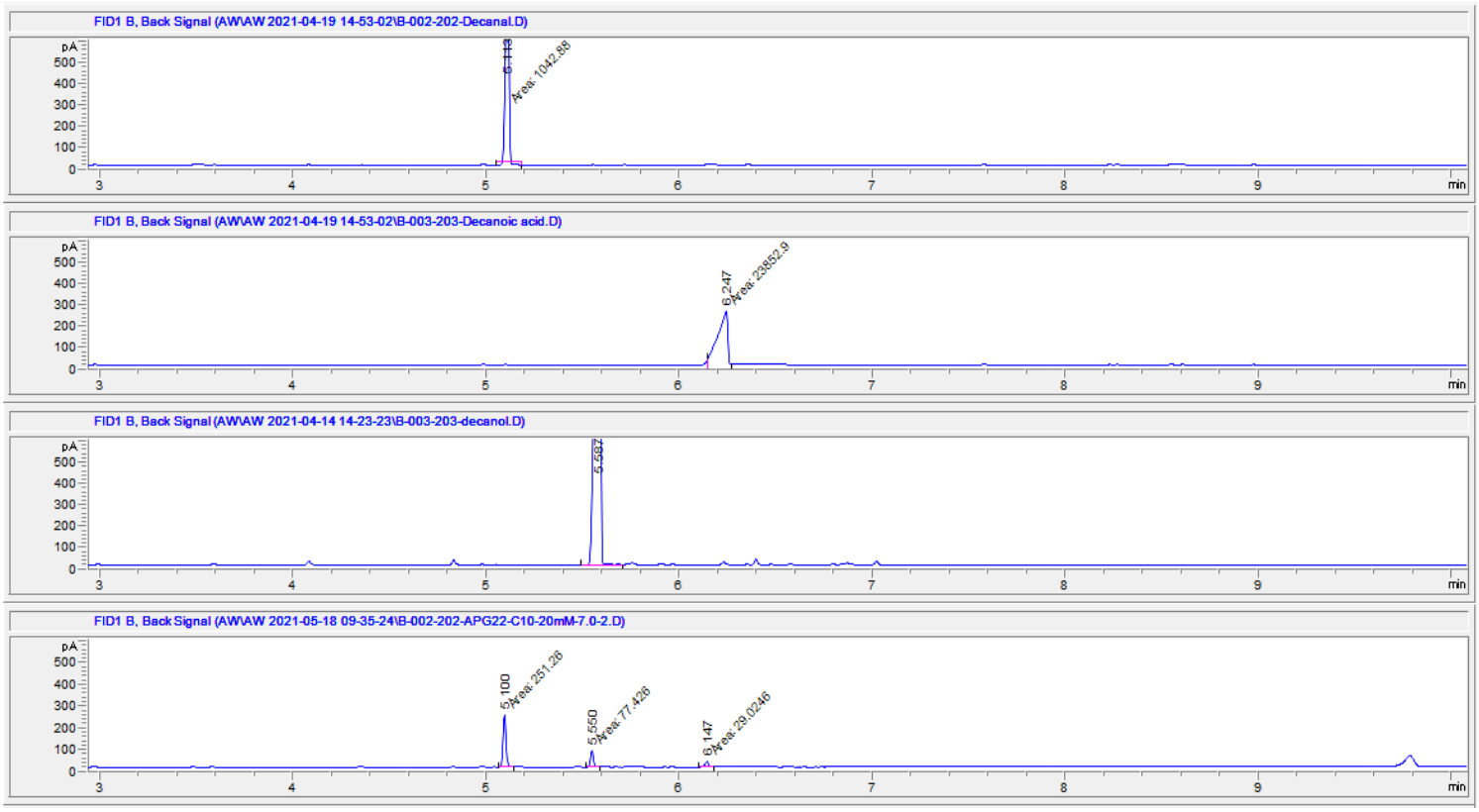

*Figure 38 - Top to bottom: standard of decanal **37**, standard of decanoic acid **44**, standard of decanol **30**, biotransformation with AcCO6 CFE of decanol **30**.*